

Design of Overhead VMS Structures for Fatigue Loads

By

Fouad H. Fouad and Ian E. Hosch
Department of Civil, Construction, and Environmental Engineering
The University of Alabama at Birmingham
Birmingham, Alabama

Prepared by

UTCA

University Transportation Center for Alabama
The University of Alabama, The University of Alabama at Birmingham, and
The University of Alabama in Huntsville

UTCA Report Number 09203
July 31, 2011

Technical Report Documentation Page

1. Report No. (FHWA/CA/OR-) 09203	2. Government Accession No.	3. Recipient's Catalog No.	
4. Title and Subtitle Design of Overhead VMS Structures for Fatigue Loads		5. Report Date: July 31, 2011	
		6. Performing Organization Code	
7. Author(s) Fouad H. Fouad and Ian E. Hosch		8. Performing Organization Report No. UTCA Report #09203	
9. Performing Organization Name and Address Civil, Construction, and Environmental Engineering The University of Alabama at Birmingham 1075 13th Street South Birmingham, AL 35294-4440		10. Work Unit No. (TRAIS)	
		11. Contract or Grant No. GR 21710	
12. Sponsoring Agency Name and Address University Transportation Center for Alabama Civil, Construction, and Environmental Engineering The University of Alabama; Box 870205 Tuscaloosa, AL 35487-0206		13. Type of Report and Period Covered Final Report: 1/1/2009 – 12/31/2011	
		14. Sponsoring Agency Code	
15. Supplementary Notes			
16. Abstract <p>The 2001 edition of the American Association of State Highway and Transportation Officials (AASHTO) <i>Standard Specifications for Structural Supports for Highway Signs, Luminaires and Traffic Signals</i> has been revised in its entirety through a major research project conducted under the auspices of the National Cooperative Highway Research Program (NCHRP 17-10). A major part of the revision includes updated provisions and criteria for extreme wind loads and new provisions and criteria on fatigue design. These provisions differ considerably from those in previous editions of the specifications.</p> <p>The impact of the fatigue criteria on the design of highway overhead variable message sign (VMS) support structures has not been evaluated and is not currently being implemented by the Alabama Department of Transportation (ALDOT). The main goal of the proposed work was to conduct an experimental program to develop realistic loading criteria for the use in fatigue design of bridge-type overhead VMS support structures. The study addressed fatigue loading related to natural wind and truck-induced wind gusts. An efficient step-by-step design methodology was formulated and made available from the established fatigue loading. The data analyses involved fundamental principles related to Structural Dynamics. Design examples with associated commentary are provided that describe the methodology and application of the fatigue loading criteria developed from this study. Recommendations for fatigue design of overhead VMS support structures were made.</p>			
17. Key Word(s) VMS structures, fatigue		18. Distribution Statement	
19. Security Classif. (of this report) unclassified	20. Security Classif. (of this page) unclassified	21. No. of Pages 263	22. Price

Contents

Contents	iii
Tables	xii
Figures.....	xv
Executive Summary	xxi
1.0 Introduction.....	22
Report Overview	22
Problem Statement	22
Project Objectives.....	22
Specific Objectives.....	23
Project Tasks	23
2.0 Literature Review.....	26
Overview	26
Research Paper Breakdown.....	26
Research Review	27
DeSantis and Haig (1996)	27
Davenport (1961)	29
Kaczinski et al. (1998).....	30
Fouad et al. (1997-1998)	30
Dexter and Ricker (2002).....	31
Cook et al. (1996).....	32
Creamer et al. (1979).....	32
McLean et al. (2004)	32
3.0 Fatigue Provisions of the AASHTO <i>Supports Specifications</i>	34
Overview	34
Fatigue Load due to Natural Wind Gust	34

Infinite-Life Approach	34
Predicting the Environment.....	35
Structural Excitation.....	38
Design Fatigue Equation for Natural Wind Gust.....	38
Fatigue Load due to Truck-Induced Wind Gust.....	39
4.0 Highway Overhead Bridge-Type VMS Support Structure	41
Overview	41
Bridge-Type VMS Support Structure.....	41
Geometric Properties	41
Material Properties	42
5.0 Experimental Instrumentation.....	44
Overview	44
Strain Gauges	44
Upright Member	44
Truss Chord Member.....	46
Anemometers.....	46
Accelerometers	50
Data Acquisition System	53
6.0 Experimental Testing Procedure.....	55
Overview	55
Natural Wind Gust.....	55
Pre-Determined Sample Size.....	55
Test Procedure	56
Truck-Induced Wind Gust.....	56
Test Procedure	56
7.0 Experimental Data Collection Samples	58
Overview	58
Test Schedule	58

Natural Wind Gust.....	58
Sample Size	58
Usable Data Collection.....	61
Truck-Induced Wind Gust.....	63
Sample Size	63
8.0 Operational Modal Analysis	65
Overview	65
Modal Data Utilization.....	65
Systemizing the Degrees-of-Freedom	65
Modal Analysis Test Setup.....	66
Spectral Analysis	69
Natural Wind Gust.....	69
Truck-Induced Wind Gust.....	74
Critical Damping Percentage.....	76
9.0 Experimental Calculation of the Fatigue Load due to Natural Wind Gust.....	80
Overview	80
Fatigue Load Calculation Approach.....	80
Structural Excitation.....	81
Reduction of Structural Excitation Experimental Data.....	81
Averaging Time.....	82
Transformation from Compass Bearings to Polar Bearings.....	82
Wind Directionality Unit Vector	82
Structural Response.....	83
Data Offsetting	83
Strain Ranges.....	88
Wind Pressure Back-Calculation.....	88
Theoretical Structural Analysis	89
Exposed Area Breakdown	90
Exposed Area Segmentation	92
Height Coefficient	92

Drag Coefficient	94
Finite Element Analysis Loading Input.....	95
Finite Element Analysis Solution.....	96
Stress and Strain Finite Elements.....	97
Wind Pressure Calculation	99
Theoretical Unit Strain	99
Pressure Ratio.....	99
Wind Velocity vs. Wind Pressure	100
Infinite-Life Approach	102
10.0 Experimental Calculation of the Fatigue Load due to Truck-Induced Wind Gust	104
Overview	104
Fatigue Load Calculation Approach.....	104
Structural Excitation.....	105
Structural Response	106
Acceleration Ranges.....	106
Transient Events.....	107
Truck-Induced Wind Pressure Back-Calculation.....	109
Effective Mass	110
Exposed Area Breakdown	111
Vertical Component	112
Horizontal Component	112
Effective Area Breakdown	113
Drag Coefficient.....	113
Effective Area Calculation	114
Wind Pressure Calculation	114
Predicting the Maximum Wind Pressure.....	116
Trendline of the Upper Limit	118
11.0 Theoretical Calculation of the Fatigue Load due to Natural Wind Gust	121
Overview	121
Specific Objectives of the Theoretical Program.....	121

Significance of the Theoretical Program	122
Methodology	123
Structural Excitation.....	124
Davenport Excitation Model	124
Infinite-Life Approach	128
Experimentally Collected Wind Data Excitation Model.....	129
Wind Velocity Power Density Spectrum	129
Approximation of the Experimental Wind Velocity Power Density Spectrum	131
Comparison between the Davenport and the Experimental Excitation Models.....	134
Structural Response	135
Response Power Density Spectrum.....	135
Root Mean Square	137
Vibration Response Spectrum	137
Natural Frequency	139
Critical Damping Percentage.....	140
Peak-to-Peak Stress Range	141
Fatigue Load Vibration Response Spectrum.....	143
12.0 Theoretical Calculation of the Fatigue Load due to Truck-Induced Wind Gust	146
Overview	146
Research Significance	146
Methodology	148
Structural Excitation.....	148
Structural Response.....	151
Shock Response Spectrum	153
Natural Frequency	155
Fatigue Load Shock Response Spectrum	156
13.0 Discussion of the Results and Comparisons between the	
Theoretical and Experimental Programs.....	158
Overview	158
Fatigue Load due to Natural Wind Gust	158

Theoretical Calculation	158
Experimental Calculation	159
Comparison of the Results	160
Discussion of the Comparison.....	161
Fatigue Load due to Truck-Induced Wind Gust.....	162
Theoretical Calculation	162
Comparison of the Results	165
Discussion of the Comparison.....	165
14.0 Finite Element Analysis.....	167
Overview	167
Model Development	167
Geometry	167
Element Type	170
Material Definition	170
Loading Designations.....	171
Fatigue Loading Input for Natural Wind Gust.....	171
Fatigue Loading Input for Truck-Induced Wind Gust	172
Vertical Component	173
Horizontal Component	174
Solution	174
Combined Loading Analysis	176
Discussion of the Results	180
Natural Wind Gust.....	180
Truck-Induced Wind Gust.....	180
Maximum Horizontal Loading.....	1181
15.0 Proposed Fatigue Provisions.....	182
Overview	182
Design Fatigue Load due to Natural Wind Gust	182
General Fatigue Design Equation for Natural Wind Gust	182
Detailed Fatigue Design Equation for Natural Wind Gust.....	183

Natural Frequency	184
Critical Damping Percentage.....	184
Fatigue Design Procedure	185
Design Fatigue Load due to Truck-Induced Wind Gust	187
General Fatigue Design Equation for Truck-Induced Wind Gust.....	188
Vertical Component	188
Horizontal Component	188
Detailed Fatigue Design Equation for Truck-Induced Wind Gust.....	189
Natural Frequency	189
Fatigue Design Procedure	190
16.0 Design Fatigue Load Example Calculations.....	193
Overview	193
Fatigue Provisions of the AASHTO <i>Supports Specifications</i>	193
Natural Wind Gust.....	193
Truck-Induced Wind Gust.....	194
Design Case Scenarios	194
Design Fatigue Load due to Natural Wind Gust	196
Discussion of the Results	199
Design Fatigue Load due to Truck-Induced Wind Gust	199
Discussion of the Results	204
17.0 Summary and Conclusions	205
Overview	205
Project Summary	206
Highway Overhead Support Structure Specimen.....	206
Structural Instrumentation.....	206
Testing Procedure.....	206
Data Collection Samples	207
Operational Modal Analysis.....	207
Design Fatigue Load due to Natural Wind Gust	207
Design Fatigue Load due to Truck-Induced Wind Gust	208

Comparisons between the Theoretical and Experimental Programs	208
Finite Element Analysis	209
Design Examples and Comparisons with the <i>Supports Specifications</i>	209
Project Conclusions	209
Structural Instrumentation	209
Testing Procedure	209
Operational Modal Analysis	210
Experimental Calculation of the Fatigue Load due to Natural Wind Gust	210
Experimental Calculation of the Fatigue Load due to Truck-Induced Wind Gust	210
Theoretical Calculation of the Fatigue Load due to Natural Wind Gust	211
Theoretical Calculation of the Fatigue Load due to Truck-Induced Wind Gust	211
Comparison between the Theoretical and Experimental Results	212
Fatigue Load due to Natural Wind Gust	212
Fatigue Load due to Truck-Induced Wind Gust	212
Finite Element Analysis	212
Proposed Fatigue Provisions	213
Design Fatigue Equation due to Natural Wind Gust	213
General Equation	213
Detailed Equation	213
Design Fatigue Load due to Truck-Induced Wind Gust	216
General Equation for the Vertical Component	216
General Equation for the Horizontal Component	217
Detailed Equation	217
Design Fatigue Load Examples and Comparisons with the AASHTO Supports Specifications	220
Fatigue Load due to Natural Wind Gust	220
Fatigue Load due to Truck-Induced Wind Gust	220
18.0 Future Investigations and Research	221
Overview	221
Operational Modal Analysis of Highway Overhead Sign Support Structures	221
Fatigue Design of Bridge-Type Sign Support Structures	222

Fatigue Design of Anchor Bolt Connections of Highway Overhead Support Structures	222
Applications of the Vibration Response Spectrum for Traffic Signals, Luminaires, and High Mast Support Structures	223
Design of Highway Overhead Support Structures to Mitigate Fatigue Stresses.....	223
19.0 References.....	225
Appendix A: Shop Drawings of the Tested Bridge-Type VMS Support Structure.....	231
Appendix B: Instrumentation Layout of the Bridge-Type VMS Support Structure.....	238
Appendix C: Finite Element Analysis Results for Optimal Placement of the Upright Strain Gauges on the Bridge-Type VMS Support Structure.....	243
Appendix D: Radar Speed Gun used to Measure Truck Speed for Truck-Induced Gust Testing on the Bridge-Type VMS Support Structure	256
Appendix E: Truck-Induced Wind Gust Data Collection for the Bridge-Type VMS Support Structure.....	259

List of Tables

Number		Page
2-1	Terrain Coefficients developed for the wind velocity power density spectrum (Davenport 1961)	30
3-1	Terrain Coefficients developed for the wind velocity power density spectrum (Davenport 1961)	35
4-1	Primary dimensions of the bridge-type VMS support structure	42
4-2	Primary member sizes of the bridge-type VMS support structure.....	42
4-3	Material properties of the bridge-type VMS support structure.....	43
7-1	Test schedule for natural wind and truck-induced wind gusts	58
7-2	Descriptive statistics of the wind velocity raw data collected	60
7-3	Descriptive statistics of the wind velocity usable data collection.....	62
7-4	Truck types measured during the truck-induced wind gusts data collection	63
7-5	Distribution of samples of the truck-induced wind gusts data collection	64
8-1	Descriptive statistics of the time history used for the natural wind gusts operational frequency analysis	70
8-2	First three modal frequencies and shapes showing the largest average amplitudes of vibration	73
8-3	Modal damping results of the horizontal and vertical modes of vibration	79
9-1	Drag coefficients used for the members of the support structure	94
9-2	Relevant stress and strain equations used for combined loading analysis	98
10-1	Total mass of the bridge-type VMS support structure for vibration in the vertical and horizontal directions	111
10-2	Breakdown of the exposed areas for the evaluation of the truck-induced wind gust	113
10-3	Drag coefficients used in the evaluation of the truck-induced wind gust	114
10-4	Effective area used in the evaluation of the vertical component of the truck-induced wind gust	114
10-5	Effective area used in the evaluation of the horizontal component of the truck-induced wind gust	114
10-6	Upper limit of the truck-induced wind gust pressure.....	116

Number		Page
11-1	Terrain Coefficients developed for the wind velocity power density spectrum (Davenport 1961)	125
13-1	Structural dynamic properties required to determine the fatigue load due to natural wind gust	159
13-2	Comparison of the theoretical and experimental fatigue load due to natural wind gust	160
13-3	Structural dynamic properties to determine the fatigue load due to truck-induced wind gust	163
13-4	Comparison of the theoretical and experimental fatigue load due to truck-induced wind gust	165
14-1	Material property definitions for the FEA model	171
14-2	Fatigue loads due to natural wind gust.....	172
14-3	Fatigue loads due to natural wind gust used for the FEA input for each of the exposed members	172
14-4	Fatigue loads due to truck-induced wind gust.....	173
14-5	Fatigue loads of the vertical component of the truck-induced wind gust used for the FEA input	174
14-6	Fatigue loads of the horizontal component of the truck-induced wind gust used for the FEA input	174
14-7	Relevant stress equations used for the combined loading analysis of the FEA results	176
14-8	FEA results of the combined loading analysis for fatigue loading due to natural wind gust.....	177
14-9	FEA results of the combined loading analysis for fatigue loading due to truck-induced wind gust.....	177
14-10	Maximum stresses and locations from the FEA results for natural wind gust.....	180
14-11	Maximum stresses and locations from the FEA results for truck-induced wind gust	180
14-12	Controlling fatigue loads at the connection details	181
15-1	Conservative estimates of the natural frequency and critical damping percentages	185
16-1	Bridge-type VMS support structure design cases	195
16-2	Design case results with the evaluation of the design fatigue load due to natural wind gust.....	196
16-3	Design case results with the evaluation of the vertical component	200

Number		Page
16-4	Design case results with the evaluation of the horizontal component	200
17-1	Conservative estimates of the natural frequency and critical damping percentages	214

List of Figures

Number		Page
2-1	Research paper breakdown used to organize the reviewed literature	27
2-2	Referenced papers in the research breakdown spreadsheet	28
4-1	Picture of the bridge-type VMS support structure selected for field measurement	41
5-1	Strain gauge locations on the northbound lane upright with cross sectional views	45
5-2	Uncovered uni-axial strain gauges attached to the upright post at location 1	45
5-3	Protected uni-axial strain gauges attached to the upright post at location 2	46
5-4	Strain gauge locations on the bottom truss chord member with cross sectional view	47
5-5	Uncovered uni-axial strain gauges attached to the truss chord member at location 3	48
5-6	WindSonic ultra-sonic wind and direction sensor used to measure the wind dynamic behavior	48
5-7	Anemometer locations and identification placed 4 ft (1.22 m) above the upright	49
5-8	Pictures of the anemometers and extension placed 4 ft (1.22 m) above the upright	49
5-9	Anemometer wind display in compass bearings showing the North identification	50
5-10	Accelerometer locations, identifications, and vibratory direction of measurement	51
5-11	Accelerometer 1L measuring the upright in the longitudinal direction normal to traffic	52
5-12	Attachment of the 2V and 3H accelerometer to the rounded members	52
5-13	Accelerometer 4H measuring the horizontal direction parallel to traffic.....	53
5-14	ALDOT van parked next to the structure with fed wiring from the instrumentation.....	54
5-15	The data acquisition system inside the ALDOT van parked next to the structure.....	54

Number		Page
6-1	Radar speed gun used to measure the speed of passing semi-trailers	57
7-1	Histogram of the wind velocity showing the distribution of the raw data collection	59
7-2	Wind rose diagram of the raw data showing the wind velocity distribution of direction.....	60
7-3	Histogram of the usable wind velocity data collection	61
7-4	Wind rose diagram of the usable wind direction data collection	62
8-1	Accelerometer locations, identifications, and vibratory direction of measurement	67
8-2	Accelerometer 1L measuring the upright in the longitudinal direction normal to traffic	68
8-3	Accelerometers 2V & 3H measuring the horizontal and vertical directions of the span.....	68
8-4	Accelerometer 4H to measure the horizontal direction parallel to traffic.....	69
8-5	Frequency analysis of the support structure from natural wind gust	71
8-6	Mode 1 modal shape of vibration in the longitudinal direction perpendicular to traffic	72
8-7	Mode 2 modal shape of vibration in the horizontal direction parallel to traffic ...	72
8-8	Mode 3 modal shape of vibration in the vertical direction parallel to the direction of gravity	73
8-9	Frequency analysis of the strain gage data collected on post 1 of the uprights	74
8-10	Structural response to the truck events obtained from the accelerometer data	75
8-11	Frequency analysis of the support structure to truck-induced wind gust.....	75
8-12	Typical truck transient event experimentally obtained from the accelerometers	76
8-13	Exponential decay of the transient truck event	77
8-14	Trendline of extracted peak amplitudes used for the determination of the rate of decay	78
9-1	Coordinate system used to develop the wind directionality unit vector	83
9-2	Filtered strain values in 0.5 mph wind velocity intervals used for the data offsetting procedure	85
9-3	Transformed regressor for the linearization process used in the data offsetting procedure.....	85

Number		Page
9-4	Parabolic curve fit obtained from the linear transformation showing the y-intercept.....	86
9-5	Parabolic trendline with the y-intercept offset	86
9-6	Trendline projection to the 90 mph (40.2 m/s) wind velocity.....	87
9-7	Peak-to-peak range of the experimentally collected strain gauge data	88
9-8	Area breakdown of the front face of the bridge-type VMS support structure	91
9-9	Area breakdown of the East side face of the bridge-type VMS support structure.....	91
9-10	Area breakdown of the West side face of the bridge-type VMS support structure.....	92
9-11	Height coefficient stepped profile based on the provisions of the <i>Supports Specifications</i>	93
9-12	Segmented exposed areas corresponding to the stepped profile of the height coefficient, K_z	94
9-13	Wind directionality of the loading input ranging from 45° to 135° onto the front face	96
9-14	Internal unit axial reaction versus wind directionality at the location of SG-4	97
9-15	Typical stress element formed from the combined loading analysis	98
9-16	Internal unit microstrain versus wind directionality at the location of SG-4.....	99
9-17	Wind velocity vs. wind pressure for the strain gauges located on the uprights	101
9-18	Transformed trendline of the wind velocity vs. wind pressure relationship	101
9-19	Wind velocity vs. wind pressure trendline for the strain gauges located on the uprights.....	102
9-20	Equivalent static wind load equal to 7.03 psf (337 Pa) at the fatigue wind velocity	103
10-1	Accelerometer locations, identifications, and vibratory direction of measurement	107
10-2	Truck event for the horizontal (3H), vertical (2V), and longitudinal (1L) acceleration response	108
10-3	Maximum peak-to-peak accelerometer ranges measured from the all truck wind events.....	109
10-4	Underneath exposed area used in the evaluation of the vertical component	112
10-5	Front exposed area used in the evaluation of the horizontal component	113
10-6	Vertical truck-induced wind pressure versus truck speed.....	115

Number		Page
10-7	Vertical truck-induced wind pressure versus truck speed.....	115
10-8	Upper limit for the vertical component of the truck-induced wind gust.....	117
10-9	Upper limit for the horizontal component of the truck-induced wind gust.....	117
10-10	Transformed regressor for the linearization process.....	118
10-11	Parabolic curve fit obtained from the linear transformation for the vertical component.....	119
10-12	Parabolic curve fit obtained from the linear transformation for the horizontal component.....	119
11-1	Highway overhead support structures with different configurations, sizes and shapes.....	123
11-2	Wind velocity PDS for an annual mean wind velocity equal to 11 mph (5 m/s).....	126
11-3	Wind pressure PDS for an annual mean wind velocity equal to 11 mph (5 m/s).....	127
11-4	Wind pressure PDS of the fatigue wind velocity equal to 38 mph (17 m/s).....	129
11-5	Experimental wind velocity PDS.....	131
11-6	Logarithmic transformation of the average wind velocity PDS curvature.....	132
11-7	Best fit line for approximating the average wind velocity PDS curvature.....	133
11-8	Theoretical plot of the experimental average wind velocity PDS of the best fit line process.....	133
11-9	Comparison between the Davenport excitation model and the experimental excitation model.....	134
11-10	Response to wind pressure excitation PDS for 2.0% damping and 2.0 Hz natural frequency.....	136
11-11	Dynamic response models of n SDOF systems to common excitation input.....	138
11-12	VRS wind pressure RMS for a structure with 2.0% damping and natural frequency of 2.0 Hz.....	138
11-13	Horizontal vibratory motion in the direction of the wind loading.....	139
11-14	VRS wind pressure RMS with a critical damping percentage equal to 0.5%.....	140
11-15	Response to wind pressure excitation PDS for 0.5% damping and 2.0 Hz natural frequency.....	141
11-16	Peak-to-peak VRS for a support structure with 2.0 Hz natural frequency and 2.0% damping.....	143
11-17	Fatigue load VRS using the Davenport excitation model.....	144

Number		Page
11-18	VRS plot showing increasing pressure ranges with decreasing critical damping percentages	145
12-1	Highway overhead support structures with different configurations, sizes and shapes	147
12-2	Vertical truck-induced wind gust impulses	150
12-3	Horizontal truck-induced wind gust impulses	150
12-4	Structural response time history due to the vertical Control impulse	152
12-5	Dynamic response models of n SDOF systems to common excitation input	153
12-6	SRS for the vertical component of the truck-induced wind gust	154
12-7	SRS for the horizontal component of the truck-induced wind gust	154
12-8	Vertical vibratory motion in the direction of loading	155
13-1	VRS for 0.361% damping, 2.81 frequency, and 11 mph (5 m/s) annual mean wind velocity	160
13-2	Comparison of the experimental and theoretical fatigue load due to natural wind gust	161
13-3	Vertical shock response spectrum used to determine the truck-induced wind pressure	164
13-4	Horizontal shock response spectrum used to determine the truck-induced wind pressure	164
13-5	Comparison of the experimental and theoretical fatigue load due to truck-induced wind gust	165
14-1	Basic geometry of the FEA model	168
14-2	Sign-to-truss connection of the FEA model	168
14-3	Truss-to-post connection of the FEA model	169
14-4	Fixed-end connection of the uprights for the FEA model	170
14-5	Base plate-to-support post connection used in the evaluation of the FEA solution results	175
14-6	Base plate-to-support post connection used in the evaluation of the FEA solution results	176
14-7	Typical stress element formed from the combined loading analysis of the FEA results	177
14-8	Graphical representation of the FEA results for fatigue loading due to natural wind gust	178

Number		Page
14-9	Graphical representation of the FEA results for fatigue due to truck-induced wind gust	179
15-1	Fatigue load VRS for a critical damping percentage equal to 1.5%	186
15-2	Fatigue load VRS for a critical damping percentage equal to 0.35%	186
15-3	VRS plot of critical damping percentages ranging from 1.0% to 0.1%	187
15-4	SRS for the vertical component of the truck-induced wind gust	191
15-5	SRS for the horizontal component of the truck-induced wind gust	191
16-1	Horizontal vibratory motion in the direction of loading	195
16-2	Vertical vibratory motion in the direction of loading	196
16-3	VRS of structure 1 design case scenario	197
16-4	VRS of structure 2 design case scenario	197
16-5	VRS of structure 3 design case scenario	198
16-6	Comparisons between the fatigue load due to natural wind calculation approaches	198
16-7	Vertical SRS of Structure 1 design case scenario	200
16-8	Vertical SRS of Structure 2 design case scenario	201
16-9	Vertical SRS of Structure 3 design case scenario	201
16-10	Horizontal SRS of Structure 1 design case scenario	202
16-11	Horizontal SRS of Structure 2 design case scenario	202
16-12	Horizontal SRS of Structure 3 design case scenario	203
16-13	Comparisons between the vertical component calculation approaches	203
16-14	Comparisons between the horizontal component calculation approaches	204
17-1	Fatigue load VRS for a critical damping percentage equal to 1.5%	215
17-2	Fatigue load VRS for a critical damping percentage equal to 0.35%	215
17-3	VRS plot of critical damping percentages ranging from 1.0% to 0.1%	216
17-4	SRS for the vertical component of the truck-induced wind gust	218
17-5	SRS for the horizontal component of the truck-induced wind gust	219

Executive Summary

The 2001 edition of the American Association of State Highway and Transportation Officials (AASHTO) *Standard Specifications for Structural Supports for Highway Signs, Luminaires and Traffic Signals* has been revised in its entirety through a major research project conducted under the auspices of the National Cooperative Highway Research Program (NCHRP 17-10). A major part of the revision includes updated provisions and criteria for extreme wind loads and new provisions and criteria on fatigue design. These provisions differ considerably from those in previous editions of the specifications.

The impact of the fatigue criteria on the design of highway overhead variable message sign (VMS) support structures has not been evaluated and is not currently being implemented by the Alabama Department of Transportation (ALDOT). The main goal of the proposed work was to conduct an experimental program to develop realistic loading criteria for the use in fatigue design of bridge-type overhead VMS support structures. The study addressed fatigue loading related to natural wind and truck-induced wind gusts. An efficient step-by-step design methodology was formulated and made available from the established fatigue loading. The data analyses involved fundamental principles related to Structural Dynamics. Design examples with associated commentary are provided that describe the methodology and application of the fatigue loading criteria developed from this study. Recommendations for fatigue design of overhead VMS support structures were made.

Section 1

Introduction

Report Overview

The goal of Project No. 09203 focused on evaluating the fatigue loading for highway overhead bridge-type variable message sign (VMS) support structures. The information contained in this report covers the instrumentation and experimentation of the support structure under wind-induced fatigue loads. A literature review is also provided describing past work accomplished on this subject. Design fatigue loads were developed through theoretical and experimental processes and are presented in this report. Design examples on the application of the developed methodology are provided.

The project was performed in collaboration with the Alabama Department of Transportation (ALDOT). The ALDOT research team and the UAB research team worked together for successful completion of the project objectives. The instrumentation and testing were performed by the ALDOT team with consultation from UAB. The UAB team performed all data analysis, reports, and presentations.

Problem Statement

There currently exists an area within the literature where there is a partial absence of information concerning cantilever-type overhead variable message sign (VMS) support structures subjected to fatigue loading. The use of cantilevered structures to support VMSs has not been commonly implemented by state DOTs due to their high risk failure when subjected to natural wind and truck induced wind gusts. To alleviate this susceptibility, bridge-type support structures have been used in their place. However, relevant information and research on bridge-type VMS support structures is also limited and often times incomplete. Moreover, the 2001 edition of the *AASHTO Standard Specifications for Structural Supports for Highway Signs, Luminaires and Traffic Signals* (hereafter referred to as the *Supports Specifications*) addresses fatigue loading onto cantilever-type sign support structures, but does not carry provisions related to VMS support structures, nor does it address bridge-type structures used for supporting signs or VMSs. A study is needed to investigate these issues in order to design VMS support structures that are safe yet efficient within the transportation system.

Project Objective

The main objective of the proposed project is to perform an **experimental** study that will evaluate the performance of *bridge-type* overhead variable message sign (VMS) structures

subjected to wind induced fatigue loads. Fatigue loading for these structures will be determined from the experimental data. A step-by-step fatigue design procedure will be formulated since the topic is not addressed by the current AASHTO 2001 *Supports Specifications*. This information will be used to provide an improved and more realistic design method for VMS support structures. This was accomplished by executing the following objectives:

1. Perform experimental and theoretical studies to evaluate the performance of bridge-type VMS highway support structures subjected to wind induced fatigue loads. The loading under consideration included two major wind events:
 - Natural Wind Gust, and
 - Truck-Induced Wind Gust.
2. Use this information to develop fatigue design loads to provide an improved and more reliable design method, and
3. Compare the developed criteria with the *Supports Specifications (AASHTO 2009)*, and propose new fatigue design equations based on the developed methodology.

Specific Objectives

Specific objectives of the project are numerated as follows:

1. Complete a detailed fatigue loading theoretical analysis and develop an accurate fatigue design model to account for the variety of sign support structures in design.
2. Instrument one bridge-type VMS support structure and take field measurements under varying natural wind and truck induced wind gust fatigue loading conditions.
3. Develop design fatigue load criteria for bridge-type VMS support structure from the experimental measurements.
4. Compare the experimental fatigue load criteria to the results and conclusions of the theoretical program.
5. Create finite element models to analyze the stresses generated from the developed fatigue loads and the *Supports Specifications* and compare.
6. Perform fatigue load calculations in accordance with the *Supports Specifications* and assess the “accuracy” of *Supports Specifications* fatigue provisions with the developed fatigue loading criteria.
7. Propose design recommendations as to fatigue load considerations for bridge-type VMS support structures based on the developed loading criteria.

Project Tasks

The specific objectives for this project were accomplished through the following tasks. More detail on each task is provided in the sections of this report.

Task 1: Literature Review

An extensive review of research performed on fatigue of highway overhead support structures was conducted. The most recent studies on the subject were reviewed and noted. Other aspects of study that were indirectly related to this project were also reviewed and entailed applications and theories were evaluated.

Task 2: Evaluation of the Current AASHTO *Supports Specifications*

The current fatigue provisions in the AASHTO *Supports Specifications* were reviewed and evaluated. Studies that were used in the development of the fatigue provisions were evaluated.

Task 3: Analytical Studies

The analytical studies with this project involved two areas:

1. Development of a theoretical model to determine the fatigue load due to natural wind and truck-induced wind gusts. The model addressed the variety of support structures, each with different sizes, shapes, configurations, and material properties.
2. Perform finite element analysis (FEA) using the SAP2000 (Creamer, *et al.* 1979) computer software package to analyze the stresses and behavior of the structure to the developed fatigue loading and the *Supports Specifications*.

Task 4: Site Selection

An already constructed bridge-type VMS support structure was chosen for field testing based on such parameters as span length, wind characteristics, and accessibility. The structure located on I-65 Southbound near Alabaster Exit 312 was selected.

Task 5: Sign Structure Instrumentation

The support structure was instrumented with strain gauges, accelerometers, and anemometers. Electric strain gages, accelerometers, and anemometers were used for the field testing. A data acquisition system was used to manage and record data. It was placed in a van and driven to the sites.

Task 6: Structural Testing

The support structure was tested under the following loading conditions:

- Natural wind gust, and
- Truck induced wind gust.

The natural wind data was taken over an extended time period in an effort to capture the structural behavior to predominant natural wind gusts. Random truck data were recorded for the truck-induced wind gust experimentation involving a variety of truck types traveling at various speeds

Task 7: Experimental Data Reduction

Three major studies were performed with the experimentally collected data:

1. *Operational Modal Analysis*—to determine structural dynamic characteristics of the structure such as modal frequencies, modal shapes, and damping properties during operation.
2. *Fatigue Load due to Natural Wind Gust*—to determine the fatigue load from naturally occurring wind gusts. A design equation was developed from the data analysis.
3. *Fatigue Load due to Truck-Induced Wind Gust*—to determine the fatigue load from passing semi-trailer vehicles underneath the sign structure. A design equation was developed from the data analysis.

Task 8: Design Recommendations

Design fatigue load recommendations for natural wind and truck-induced gusts were developed after the completion of Task 7. The comparison of the analytical results to the experimental data was utilized and fatigue design criteria were developed that encompassed the results of these efforts.

Task 9: Design Examples

The effect of the proposed provisions was assessed and explained by performing fatigue load calculations for design. The examples compared fatigue loads using the fatigue provisions of *Supports Specifications* and the fatigue loads according to the proposed guidelines of this study of both experimental and theoretical means. The comparisons addressed the “accuracy” of *Supports Specifications* fatigue provisions for cantilever-type sign structures.

Task 10: Project Report

A report summarizing Tasks 1 through 9 was prepared.

Section 2

Literature Review

Overview

An extensive literature review was performed on fatigue of overhead highway sign and VMS support structures. A spreadsheet was developed to categorize the reviewed studies by breaking down the research into important areas of interests. Interests included recommendations for future research, vibration analysis, and instrumentation of support structures. The cataloging helped to develop and systemize the research program. Also provided in the literature review are descriptions of the most relevant studies that played a crucial role in the development progress of the fatigue provisions of the *Supports Specifications*, as well as other projects that were considered important to the research and the developed methodology of this project.

Research Paper Breakdown

Various research papers and documentations on highway overhead support structures were reviewed before developing the research program. Important aspects that had relevancy to this project were identified during the review process. Each of the literature documents reviewed were tagged and categorized regarding the predetermined interests of this study. A spreadsheet was created that helped to label the reviewed studies with respect to the tagged aspects. Figure 2-1 displays the spreadsheet showing the properties of interests for this project and the color coded categorizing method. The numbers at the top of the spreadsheet reference the papers (Figure 2-2) from which the color coded categories were indentified. When reference to a particular subject was needed during the project execution, the spreadsheet was utilized by first referring to the legend with respect to the property of interest, and then identifying the documentation that contained information on the subject. This process helped to allow the research to perform smoothly and efficiently.

Many aspects that were considered important by the researchers were not found in the literature and were therefore excluded from the spreadsheet. Some aspects were dropped from the spreadsheet because of relevancy as the research progressed, whereas other aspects were added which resulted in the breakdown shown in the Figure 2-1.

The research paper breakdown served as a useful tool during the development of the research program. Relevant information on gathered literature documents was easily and quickly identified to extract information. The breakdown also helped to identify areas where research is needed or is lacking. Only the most prominent papers as they related to the research performed with this project was included in the breakdown. A complete list of reviewed papers is provided in the **Section 19: References**.

Property of Interest	Referenced Papers																			
	1	2	3	4	5	6	7	8	9	10	11	12	13	14	15	16	17	18	19	20
Cantilever-Type Highway Sign Support Structure																				
Cantilever-Type VMS Support Structure	Δ																			
Bridge-Type Highway Sign Support Structure																				
Bridge-Type VMS Support Structure	Δ																			
High Mast Structure																				
Traffic Signal Structure																				
Luminare Structure																				
Strain Guage Transducers																				
Anemometer Transducers																				
Accelerometer Transducers																				
Pressure Transducers																				
Galloping																				
Vortex Shedding																				
Anchor Bolt Study																				
Natural Wind Gusts: Fatigue Loading																				
Natural Wind Gusts: Fatigue Resistance																				
Truck-Induced Wind Gusts: Fatigue Loading	Δ																			
Truck-Induced Wind Gusts: Fatigue Resistance																				
Horizontal Loading for Truck Gust	Δ																			
Suction Pressure for Truck Gust	Δ																			
Variation in Truck Type																				
Spectral Analysis																				
Natural Frequencies of Support Structures																				
Damping of Support Structures																				
Modal Shapes of Support Structures																				
Steel Structure																				
Aluminum Structure																				
Design Example																				





Legend	
	Involved Experimental Program
	Involved Analytical Program
	Involved Experimental & Analytical Programs
	Includes Equation

Figure 2-1. Research paper breakdown used to organize the reviewed literature

Research Review

A description of the reviewed studies that played a crucial role in the development of the fatigue provisions in the *Supports Specifications* are listed as follows. Other projects included in the literature review were considered important to the research and are described.

DeSantis and Haig (1996)

The fatigue provisions for truck-induced wind gust in the *Supports Specifications* were initially based on this study. The research focused on a cantilever-type overhead variable message sign support structure. The structure failed because of fatigue loading for which prompted the study. After the structure was replaced, large deflections were observed because of wind gust created from passing trucks. In the analysis, the researchers assumed that the velocity of the wind gusts onto the structure was equal in magnitude to the speed of the truck in addition to a gust factor

equal to 1.3 to account for head winds. The wind pressure was calculated using the fundamental fluid mechanics relationship between wind force and the square of the wind velocity. The resulting wind pressure was doubled to account for the upward deflection of the sign plus the downward deflection because of the pull of gravity. The concluded value represented a pressure range to be used for fatigue design, and is shown in Eq. 2-1.

Referenced Papers	
1	Cook, Ronald A., Bloomquist, D., Agosta, A.M., Taylor, K.F., <i>Wind Load Data for Variable Message Signs</i> . Report Number 0728-9488. Florida Department of Transportation, Research Management Center, April, 1996.
2	Azzam, D., <i>Fatigue Behavior of Highway Welded Aluminum Light Pole Support Structures</i> . Dissertation, University of Adron, May 2006.
3	Creamer, B. M., Frank, K. H., Klingner, R. E., <i>Fatigue Loading on Cantilever Sign Support Structures from Truck Wind Gusts</i> . Research Report Number 209-1F. Texas State Department of Highways and Public Transportation, Transportation Planning Division, April, 1979.
4	Dexter, R. J., Ricker, M. J., <i>Fatigue-Resistant Design of Cantilevered Signal, Signs, and Light Supports</i> . NCHRP Report 469. The Transportation Research Board, Washington D.C. 2002
5	Zalewski, B., Huckelbridge, A., <i>Dynamic Load Environment of Bridge-Mounted Sign Support Structures</i> . Report No. S/T/SS/05-002. Ohio Department of Transportation, Office of Research and Development, September 2005.
6	Foutch, D.A., Kim, T.W., LaFave, J.M., Rice, J.A. <i>Evaluation of Aluminum Highway Sign Truss Designs and Standards for Wind and Truck Gust Loadings</i> . Research Report NO. 153. Illinois Department of Transportation, Bureau of materials and Physical Research, December 2006.
7	Ginal, S. <i>Fatigue Performance of Full-Span Support Structures Considering Truck-Induced Gust and Natural Wind Pressures</i> . Thesis, Marquette University, December 2003.
8	Kaczinski, M.R., Dexter,R.J., and VanDien, J.P. <i>Fatigue Resistant Design of Cantilevered Sign, Signal and Light Supports</i> . NCHRP Report 412. Transportation Research Board. Washington D.C. 1998.
9	South, S.M. <i>Fatigue Analysis of Overhead Sign and Signal Structures</i> . Report No. 115. Illinois Department of Transportation, Bureau of Materials and Physical Research. May 1994.
10	Fouad, F.H., Calvert, E.A., and Nunez, E. <i>Structural Supports for Highway Signs, Luminaires, and Traffic Signals</i> . NCHRP Report 411, Transportation Research Board, Washington D.C. 1998.
11	Edwards, J.A., and Bingham, W.L. <i>Deflection Criteria for Wind Induced Vibrations in Cantilever Highway Sign Structures</i> . Report No. FHWA/NC/84-001, Center for Transportation Engineering Studies, North Carolina State University,
12	DeSantis, P.V., and Haig, P.E., <i>Unanticipated Loading Causes Highway Sign Failure</i> . Proceedings of ANSYS Convention, 1996.
13	Albert, M.N., Manuel, L., Frank, K.H., and Wood, S.L., <i>Field Testing of Cantilevered Traffic Signal Structures under Truck-Induced Gust Loads</i> . Report No. FHWA/TX-08/0-4586-2, Center for Transportation Research, University of Texas at Austin, 2007.
14	Cali, P., and Covert, E.E., <i>On the Loads on Overhead Sign Structures in Still Air by Truck Induced Gusts</i> . Wright Brothers Facility Report 8-97, Massachusetts Institute of Technology.
15	Ramy, A.S., <i>Fatigue Resistant Design of Non-Cantilevered Sign Support Structures</i> . Thesis, University of Alabama at Birmingham, 2000.
16	Fisher, J.W., Nussbaumer, A., Keating, P.B., and Yen, B.T., <i>Resistance of Welded Details Under Variable Amplitude Long-Life Fatigue Loading</i> . NCHRP Report 354, The Transportation Research Board, Washington D.C., 1993.
17	Irwin, H.P., and Peeters, M. <i>An Investigation of the Aerodynamic Stability of Slender Sign Bridges</i> . Calgary. LTR-LA-246, national Research Council Canada-Aeronautical Establishment, 1980.
18	McDonald, J.R., Mehta, K.C., Oler, W., and Pulipaka, N., <i>Wind Load Effects on Signs, Luminaires and Traffic Signal Structures</i> . Texas Department of Transportation Report No. 1303-1F, Wind Engineering Research Center-Texas Tech University, Lubbock, TX, 1995.
19	Gilani, A.S., Chavez, J.W., and Whittaker, A.S., <i>Fatigue-Life Evaluation of Changeable Message Sign Structures, Volume 1 - As Built Structures</i> . Report No. UCB/EERC-97/10, Earthquake Engineering Research Center, University of California, Berkeley, CA, 1997.
20	Kashar, L., Nester, M.R., Johns, J.W., Hariri, M., and Freizner, S., <i>Analysis of the Catastrophic Failure of the Support Structure of a Changeable Message Sign</i> . Structural Engineering in the 21st Century, Proceedings of the 1999 Structures Congress, New Orleans, LA, 1115-118, 1999.

Figure 2-2. Referenced papers in the research breakdown spreadsheet

$$P_{TG} = 36.6C_d \text{ (psf)} \quad [\text{Eq. 2-1}]$$

where

P_{TG} = design fatigue pressure load due to truck - induced wind gust

C_d = drag coefficient

The researchers performed a FEA model of the structure using the software package ANSYS. The cantilevered end of the structure was observed in the field to deflect about 1 ft (0.305 m) in length after exposed to wind gust from passing trucks. Experimentation was not performed to validate the tip deflection other than visual observation. To help verify the observations, the researchers back-calculated the wind pressure that would theoretically produce a 1 ft (0.305 m) deflection, and inputted the pressure into the ANSYS program of the modeled structure. The results matched the wind pressure calculated from Eq. 2.1 and was concluded as the appropriate design load based on this comparison (DeSantis, *et al.* 1998).

Davenport (1961)

Davenport's research was not focused on overhead sign support structures but rather focused on wind velocity. His research has provided an accurate model for simulating wind velocity behavior. The model was used in the development of the fatigue provisions for natural wind gust in the *Supports Specifications*. It simulated the randomness along with the gustiness and turbulence commonly associated with wind velocity. The model was developed in the form of a power density spectrum generally used for predicting randomly occurring events. The power density spectrum was created using experimentally measured wind velocity time histories gathered from sites located around the world. An empirical formulation was developed as a function of the annual mean wind velocity, and is shown in Eq. 2-2. Terrain coefficients were also identified the formulation process, and are shown in Table 2-1 (Davenport 1961).

$$S_v(f) = \frac{4\kappa\bar{V}_{10}^2 x^2}{f(1+x^2)^{\frac{4}{3}}} \quad [\text{Eqn. 2-2}]$$

where

$S_v(f)$ = wind velocity power spectral density at any height

f = frequency

\bar{V}_{10} = mean wind velocity at a standard height of 10 meters above ground level

κ = surface drag coefficient (Table 2 - 1)

$x = \frac{1200f}{\bar{V}_{10}^2}$ with $\frac{f}{\bar{V}_{10}^2}$ in cycles per meter.

Table 2-1. Terrain Coefficients developed for the wind velocity power density spectrum (Davenport 1961)

Type of Surface	κ	α
Open unobstructed country (e.g., prairie-type grassland, arctic tundra, desert)	0.005	0.15
Country broken by low clustered obstructions such as trees and houses (below 10 m high)	0.015 - 0.020	0.27 – 0.31
Heavily built-up urban centers with tall buildings	0.050	0.43

Kaczinski et al. (1998)

The research performed by Kaczinski reported in NCHRP Report 412 formed the framework of the fatigue provisions for galloping, vortex shedding, natural wind gust, and truck-induced wind gusts in the *Supports Specifications*. The majority of his work related to natural wind and truck-induced wind gusts was entirely theoretical. By using the research performed by DeSantis and Haig, the fatigue provisions for the truck-induced gust were created. Equation 2-1 was recommended as the appropriate pressure load to use for truck-induced wind gusts.

Davenport’s wind velocity power density spectrum was used to create the fatigue provisions for natural wind gust. The velocity spectrum was transformed into a wind force spectrum. The spectrum was applied as input into an FEA program to generate a stress response spectrum for four particular overhead sign support structures. The stress spectrum was formed at different locations in the modeled structure and compared. The fatigue load was then developed using the infinite-life approach. Equation 2-3 was developed from the results and was recommended as the appropriate pressure load to use for natural wind gust.

$$P_{NW} = 5.2C_d I_F \text{ (psf)} \quad \text{[Eq. 2-3]}$$

where

P_{NW} = design fatigue pressure load due to natural wind gusts

C_d = drag coefficient

I_F = importance factor

Report 412 also focused on developing S-N curves (stress vs. number of cycles) for anchor bolt connection details. The results were used to create the constant-amplitude fatigue thresholds currently available in the *Supports Specifications*. Recommendations for anchor bolt design and structural analysis were provided. In addition, Report 412 introduced “Importance Factors” to be used with the *Supports Specifications*. Fatigue design examples are provided for different types of supports structures including overhead sign, traffic signals, and luminaires. The examples provided a thorough design procedure using the proposed fatigue design equations. Stresses at critical details were calculated and compared to the fatigue thresholds (Kaczinski, *et al.* 1998).

Fouad et al. (1997-1998)

The research by Fouad et al in NCHRP project 17-10 and 17-10(2) looked at fatigue design of sign support structures. The research was compiled into a specification based on the Allowable

Stress Design (ASD) methodology, the basis of which the current *Supports Specifications* were formed. The impact of the new specifications was analyzed with significant conclusions. The research brought together important fatigue concerns such as galloping, vortex shedding, natural wind, and truck-induced gusts. Many design examples were made which provided the framework for engineers to use for fatigue evaluations. The work performed by Fouad et al compiled all relevant information on fatigue of sign support structures into a single stand-alone document. It now resides as a well established document for fatigue design that is specific to sign support structures, from which helped to propel future enhancements and innovations to fatigue design of these structures. The researchers also provided valuable information on transforming the specification into a Load and Resistance Factor Design (LRFD) methodology in the future. The focus was to first develop a much needed stand-alone specification using the ASD method, and then upgrade to LRFD in the future (Fouad, *et al.* 1997 - 2005).

Dexter and Ricker (2002)

The research performed by Dexter and Ricker reported in NCHRP Report 469 formed the framework of the current *Supports Specifications*. Their research involved experimental and analytical programs. They concluded that the fatigue provisions for natural wind gusts in the *Supports Specifications* were accurate. However, the truck-induced gusts were highly conservative as compared to their experimentally determined values. A reduction in the truck provisions were recommended by Eq. 2-4. The reduction did not reflect the experimental values gathered in the report because they were significantly less the fatigue provisions, and it was believed the committee would not accept them. The authors were also concerned with the type of structures used in the analysis. The fatigue load was determined from analysis on variable message signs which are significantly heavier than conventional signs. The reduction of the fatigue design equation for truck-induced gusts shown as Eq. 2-4 was recommended.

$$P_{TG} = 18.8C_dI_f \text{ (psf)} \tag{Eq. 2-4}$$

where

P_{TG} = design fatigue pressure load due to truck - induced wind gust

C_d = drag coefficient

I_F = importance factor

Report 469 also provided a reduction to the fatigue load to accommodate for height of the structure above the ground. They recommended a linear reduction in wind pressure starting from 19.7 ft (6.00 m) above ground level to zero at approximately 32.8 ft (10.0 m) above ground level. A recommended area on the support structure to apply the truck load was also provided. It was proposed to apply a uniformly distributed load to the 12 ft (3.66 m) area of the structure that produces the maximum stress range. This was recommended as opposed to applying the load to portions of the structure that is not directly above the traffic lane (Dexter, *et al.* 2002).

Cook et al. (1996)

The research performed by Cook et al is identified in this review because of its relevancy to fatigue design due to truck-induced gusts. Their research determined the truck-induced wind gusts through direct measurement of wind pressure. Pressure transducers were placed on a bridge spanning a highway to measure the wind pressure from passing trucks. Importantly, the bridge was extremely rigid so that the measured values were not influenced by the type of structure. Twenty-three loading events were measured and recorded.

The results provided a clear view of the wind behavior created from passing trucks. It revealed a biaxial loading event with a vertically applied pressure and a horizontally applied pressure. A suction event was also recorded as the truck passed underneath the structure. The results indicated a ramped loading impulse. Variation of the truck-induced with respect to height above ground level was also measured. A 10% pressure reduction per foot above 17 ft (5.18 m) above ground level was found (Cook, *et al.* 1996).

Creamer et al. (1979)

The work performed by Creamer et al was very influential for future research. Their research focused on fatigue induced loading due truck wind gusts. Where Cook's determined the truck wind pressure directly using pressure transducers, Creamer's work determined the truck wind pressure indirectly. They measured strain variations at critical locations of a cantilevered structure because of truck wind gusts, and back calculated for wind pressure. A ramped impulse function was developed and inputted into a FEA model of the tested structure. The loading simulation produced similar strains on the structure as measured experimentally (Creamer, *et al.* 1979).

McLean et al. (2004)

The work performed by McLean et al evaluated the performance of two bridge-type VMS support structures. The structures were located in Birmingham, Alabama and Mobile, Alabama. Each structure had very similar configurations and material properties but with different span lengths. The Birmingham structure had a span length of 145 ft (44.2 m) and the Mobile structure had a span length of 89 ft (27 m).

The project evaluated the fatigue stresses induced onto the structures due to wind-induced loading. The fatigue life of each structure was estimated using the latest methodologies. Stresses at critical locations were compared to the endurance limit of the detailed as specified in the *Supports Specifications*. Finite element analysis (FEA) was utilized for the structural analysis tasks of the project. Stresses cycles were experimentally measured and compared to the stress ranges produced by the fatigue provisions in the *Supports Specifications*.

The conclusions of the project indicated that the stresses generated from natural wind gust induced the most severe stresses. The stresses on the Birmingham structure were found to be profound, and it was estimated that premature fatigue damage is expected. This conclusion

proved the *Supports Specifications* to underestimate the fatigue loading for this particular. In contrast, the Mobile structure was found to have an infinite-life (McLean, *et al.* 2004).

Section 3

Fatigue Provisions of the AASHTO *Supports Specifications*

Overview

An overview of the development of the natural wind and truck-induced wind gusts fatigue provisions within the AASHTO *Standards Specifications* is provided. A complete understanding of the developed fatigue provisions was obtained before addressing their accuracy with the fatigue criteria developed with this project. The provisions for natural wind in the *Supports Specifications* were formed indirectly through theoretical calculations. They were developed using the infinite-life approach to fatigue design. Spectral analysis formed the framework of the development procedure. The truck-induced wind gust fatigue provisions were developed through theoretical and experimental observations.

Fatigue Load due to Natural Wind Gust

Infinite-Life Approach

The method used to develop the natural wind provisions was based on spectral analysis in collaboration with the infinite-life approach to fatigue design. The provisions are adequate within certain limitations, as they were formed using four particular categorized structural types, each of which were chosen to represent the population of the category selected. The structural response of two overhead signal support structures, one cantilever-type overhead sign support structure, and one luminaire support structure to natural wind excitation were analyzed, the transmitted stresses of each were averaged, and the code was developed from the averaged results (Kaczinski, *et al.* 1998).

The AASHTO fatigue code was based on the constant amplitude fatigue limit (CAFL). Tests to developed plots of the stress vs. the number of cycles (S-N curves) for common connection details were used to determine this value. Fatigue stress ranges that occurred below the CAFL were estimated to have an infinite life. Stresses ranges at critical locations such as welded or bolted connections must be under the CAFL to be in compliance with the code. Changes in the design must be made if they are not to lower the fatigue stresses to fall below the CAFL.

The CAFL tests were based on constant amplitude, whereas amplitudes that occur because of natural wind are random with variable amplitudes. To account for variable amplitude loading, the infinite-life approach adopted the findings of the National Cooperative Highway Research Program NCHRP Report 354 where variable amplitude fatigue tests were performed on a variety of full scale connection details. From the results, it was determined that failure would still occur if the variable amplitudes exceeded the CAFL of the connection detail 0.05% of the time.

However, if the CAFL was exceeded 0.01% of the time, the specimen was said to have an infinite life (Fisher, *et al.* 1993). In view of the results, the infinite-life approach involved estimating the stress ranges that would occur onto the structure with a 0.01% exceedence probability, including dynamic amplification. These ranges were referred to as the fatigue limit-state load ranges. The structure was designed such that the limit-state stress ranges did not exceed the CAFL of the detail in question.

Predicting the Environment

The first step in determining the fatigue limit-state load ranges to develop the AASHTO fatigue provisions was to estimate the natural wind gust structural excitation. This involved predicting the natural wind environment for which the structure is to be exposed. This was done using a spectral analysis. Simulating the natural wind force can be difficult because of the randomness, turbulence and gustiness of natural wind velocity. A static load that represents the natural wind force can be easily calculated, as well as a dynamic load in terms of a periodic wave such as a sine wave. This type of examination does not account for the gustiness and turbulent nature of the wind itself. In most cases, a gust factor is used to account for the random nature of wind excitation, specifically for structural capacity predictions. A. G. Davenport developed a wind velocity power spectral density (PSD) curve (Davenport 1961) shown in Eq. 3-1 that simulated the turbulent nature of wind velocity.

$$S_v(f) = \frac{4\kappa\bar{V}_{10}^2 x^2}{f(1+x^2)^3} \quad [\text{Eq. 3-1}]$$

where

$S_v(f)$ = wind velocity power spectral density at any height

f = frequency

\bar{V}_{10} = mean wind velocity at a standard height of 10 meters above ground level

κ = surface drag coefficient (Table 3-1)

$x = \frac{1200f}{\bar{V}_{10}^2}$ with $\frac{f}{\bar{V}_{10}^2}$ in cycles per meter.

Table 3-1. Terrain Coefficients developed for the wind velocity power density spectrum (Davenport 1961)

Type of Surface	κ	α
Open unobstructed country (e.g., prairie-type grassland, arctic tundra, desert)	0.005	0.15
Country broken by low clustered obstructions such as trees and houses (below 10 m high)	0.015 - 0.020	0.27 - 0.31
Heavily built-up urban centers with tall buildings	0.050	0.43

Random excitation is best analyzed over a frequency spectrum. PSD curves are commonly used for dynamic loading analysis, but more specifically suited to random vibration. In random excitations, there are no periodic systems within the excitation that can be analyzed at specific

frequencies because the excitation is applied randomly over a spectrum of frequencies. To account for this, the natural wind fatigue analysis involved an examination of the total energy, or power, in the random excitation over a frequency band. A typical PSD curve is plotted with the ordinate in units of the parameter (force, acceleration, velocity, displacement, etc.) squared divided by the bandwidth (e.g., N²/Hz), and the abscissa in units of frequency (Hz). The peaks on a PSD curve identify the frequency range(s) at which the majority of the energy lies within the particular excitation. The area under a PSD curve is equal to the mean square value, and the square root of this area is equal to the RMS value: a value of which plays an important role in determining the magnitude of loads that are transmitted onto a structure from vibration (Harris 1996, Irvine Oct. 2000).

Davenport developed his wind velocity PSD curve from at least 70 experimental wind velocity data collections from various locations around the world. His intention was to develop a model which simulated the turbulence and gustiness of wind velocity. He developed Eq. 3-1 from the 70 experimental data collections. The equation is a function of wind velocity frequency with respect to a mean wind velocity at a specified height.

Once the behavior of the wind velocity environment was estimated, the PSD was transformed into a wind force PSD by using principles related to fluid mechanics. An induced natural wind gust force onto a structure, referred to as drag, is proportional to wind velocity squared, as shown by the Eq. 3-2.

$$F_D = \frac{1}{2} \rho C_d A V^2 \quad [\text{Eq. 3-2}]$$

where

F_D = drag force

ρ = density of air = $1.22 \frac{\text{kg}}{\text{m}^3}$

C_d = drag coefficient

A = area of exposed surface

V = wind velocity at any height.

By utilizing the proportionality between drag pressure and wind velocity, and accounting for the turbulent wind velocity and its variance about the mean wind velocity, a wind pressure PSD was developed from Davenport's wind velocity PSD shown in Eq. 3-3.

$$S_F(f) = \rho^2 C_d^2 A^2 V^2 S_v(f) \quad [\text{Eq. 3-3}]$$

The PSD function accounts for the gustiness and turbulence of wind velocity over a spectrum of frequencies, based on an averaged wind velocity taken at a specified height above ground level. Since most support structure are at or around 32.8 ft (10.0 m) in height, the PSD curve was well

suited for these types of structures. Yet, the PSD can be used at any particular height by using the power law profile for approximating variation in wind velocity with height, as shown in Eq. 3-4:

$$V = \bar{V}_{10} \alpha z^\alpha \quad [\text{Eq. 3-4}]$$

where

V = wind velocity at height z

α = surface coefficient in Table 3-1

z = height above ground.

In this case, where the objective was concentrated on formulating a design code for fatigue wind, the wind velocity variable in the pressure PSD equation was taken at the standard height of 32.8 ft (10.0 m) above ground level, and kept uniform across the exposed façade. The purpose of which was to provide a simplified design equation for commercial use. Some conservative formulation exists as the wind velocity typically increases from the ground level upwards (Davenport 1961).

Once the natural wind environment was estimated, the next step was to apply the PSD to the infinite-life approach in determining the limit-state stress ranges. Since the force spectrum was based primarily on the annual mean wind velocity, the wind velocity that was exceeded 0.01% of the time was found and referred to as the limit-state wind velocity. The force spectrum was calculated using the limit-state wind velocity and used to calculate the structural response to determine the limit-state stress range.

Wind velocity is random in nature, but it can be predicted through statistical relationships. It has been found through many experiments that the magnitude of the wind velocity vector will follow a Rayleigh distribution (Dexter, *et al.* 2002, Kaczinski, *et al.* 1998, Liu 1991). By using the Rayleigh distribution, the 0.01% exceedence probability can be found through the relationship in Eq. 3-5 based on the annual mean wind velocity.

$$P_E(v) = e^{-\frac{\pi v^2}{4\bar{V}^2}} \quad [\text{Eq. 3-5}]$$

where

$P_E(v)$ = probability

v = wind velocity corresponding to the probability

\bar{V} = mean wind velocity.

An analysis was conducted to determine which annual mean wind velocity to use in Eq. 3-5 to determine the limit-state wind velocity (wind velocity with a 0.01% exceedence probability). The annual mean wind velocities of major U.S. cities were analyzed. It was found that an annual mean wind velocity of 11 mph (5 m/s) was exceeded in only 19% of the U.S. cities analyzed and

was therefore chosen. By plugging in 11 mph in Eq. 3.5, and solving for the wind velocity corresponding to the 0.01% probability, a limit-state wind velocity was found to be equal to 37 mph (17 m/s). The force spectrum was then formed using the limit-state wind velocity and was used as the natural wind velocity prediction model for structural excitation.

Structural Excitation

Once the excitation was determined, the spectral density of the response was calculated. This was done through finite element analysis for the signal, sign, and luminaire support structures. Each structure had different dynamic characteristics such as natural frequency and critical damping percentages, all of which are based on the size, shape, and material of the structure. The response PSD was calculated in units of stress squared divided by Hz. The area underneath the response PSD curve is equal to the variance of the response about the mean. The square root of the area is equal to the root mean square (RMS). If the mean is equal to zero, then the RMS is equal to the standard deviation. Since the response curves of support structures are predominately controlled by a single frequency of vibration, the developed response PSD curves were narrow-banded at the natural frequency of the structures. Therefore, the stress range was calculated as a constant amplitude in the form of a sinusoid. For any sinusoid, the peak stress amplitude is equal to the square root of two times the RMS (assuming a zero mean for analysis purposes). The stress amplitude was then multiplied by two to account for a peak-to-peak stress range. The RMS was determined from the response PSD for each structure, and the effective stress range was calculated using Eq. 3-6

$$S_r^{eff} = 2.8\sigma_{rms} \quad [\text{Eq. 3-6}]$$

where

S_r^{eff} = effective stress range or limit - state stress range

σ_{rms} = RMS of the response

Design Fatigue Equation for Natural Wind Gust

The fatigue provisions for natural wind in the *Supports Specifications* were developed based on four particular categorized structural types. The structural response of one overhead signal support structure, one cantilever-type overhead sign support structure, and two luminaire support structures to natural wind excitation were analyzed. The transmitted stresses of each structure were averaged, and the fatigue provisions were developed from the averaged results (Kaczinski, *et al.* 1998).

The transmitted stresses were calculated using Eq. 3-3 through Eq. 3-6 with the specific natural frequencies of each structure and the fatigue wind equal to 37 mph (17 m/s) used in the equations. The resulting effect stress range calculated from Eq. 3-6 was then used for a back calculation procedure using finite element analysis (FEA). The required uniformly applied wind pressure that would produce the effective stress range was determined from the back calculation.

The drag coefficients and exposed areas were normalized during the calculation in order to account for the different member sizes.

The back calculation resulted in uniformly distributed wind pressures ranging from 3.6 to 6.3 psf (170 to 300 Pa) for the four specific structural types. Critical damping percentages ranging from 1% to 2% were used. An average was taken of the wind pressure results and used for the finalized code fatigue provisions. The fatigue equation for natural wind gusts shown as Eq. 3-7 was produced. The equation is multiplied by the drag coefficient, importance factor, and a wind factor to account member sizes, structural importance, and for other annual mean wind velocities existing in different areas of the country.

$$P_{NW} = 5.2C_d I_F \left(\frac{\bar{v}}{11} \right)^2 \quad [\text{Eq. 3-7}]$$

where

P_{NW} = design fatigue load due to natural wind, psf (Pa)

C_d = drag coefficient

I_F = importance factor

\bar{v} = annual mean wind velocity other than 11 mph (5 m/s)

Fatigue Load due to Truck-Induced Wind Gust

The truck-induced gust fatigue provision was developed as an impulse loading occurring over a finite length of time. The loading was created when semi-trailer trucks passed underneath the structure causing the structure to vibrate. The vibration generated stresses in the structure that can potentially accumulate fatigue damage over time.

The *Supports Specifications* design equations for truck-induced gusts was originally developed from the work performed by Desantis and Haig (1996), and later revised from the work presented in NCHRP Report 469 (Dexter, *et al.* 2002). It assumes that the wind loading onto the structure was equivalent to the speed of the passing truck, plus a gust factor of 1.3 to account for head wind. For instance, a truck traveling at 65 mph (105 kph) would produce a 65 mph (105 kph) wind onto the structure. The result was an 18.3 psf (876 Pa) magnitude static pressure. The code only accounted for a vertical force applied upward (ground up) onto the structure.

Assuming that the upward motion of the structure resulting from the truck gust was equivalent to a proceeding downward motion, the 18.3 psf (876 Pa) was doubled to account for a peak-to-peak range equaling 36.6 psf (1,760 Pa).

NCHRP Report 469 investigated the fatigue load due to truck gusts performed by researchers on VMS cantilever structures. The research indicated that the current code was too conservative based on their conclusions. A reduction of the loading was recommended by the following equation:

$$P_{TG} = 18.8C_d I_F \left(\frac{V}{65} \right)^2 \quad [\text{Eq. 3.8}]$$

where

P_{TG} = design fatigue load due to truck gust, psf (Pa)

C_d = drag coefficient

I_F = importance factor

V = truck speed, mph (m/s)

The reduction was determined based on experimental evidence from VMS structures. Strain measurements on a cantilevered VMS support structure were recorded during random truck events. An equivalent static load was calculated that would produce the same strain range measured experimentally. The resulting load was to be applied vertically to all horizontal areas (underside of the structure) along a 12 ft length (3.7 m), or equal to the width of a travel lane. A reduction in the load with respect to height of the structure above ground level was also permitted. It was discovered the pressure load decreased linearly with height, with the maximum occurring at 19.7 ft (6 m) above ground level to zero at 32.8 ft (10 m).

Section 4

Highway Overhead Bridge-Type VMS Support Structure for Field Measurement

Overview

A description of the bridge-type VMS support structure selected for field measurement is presented. The major geometric and material properties are provided for reference. The shop drawings of the structure are provided in Appendix A of this report.

Bridge-Type VMS Support Structure

A four chord truss bridge-type highway overhead VMS support structure was chosen for analysis. The structure was located on highway I-65 Northbound near Alabaster, AL. A picture of the structure is shown in Figure 4-1.



Figure 4-1. Picture of the bridge-type VMS support structure selected for field measurement

Geometric Properties

The bridge structure spanned two lanes of highway. The full span was 71 ft (22 m) from support to support. The bottom of the VMS sign reached 20 ft (6.1 m) above the roadway with the top of the structure reaching 29 ft (8.8 m). Primary dimensions of the structure are listed in Table 4-1, and member sizes are provided in Table 4-2.

Table 4-1. Primary dimensions of the bridge-type VMS support structure

Parameter	Value
Bridge Span	71 ft
VMS height above roadway	20 ft
Height of Upright	29 ft
Anchor Bolts	Four 1 1/4 in Diameter Bolts per Upright
Base Plate	15.5 in x 15.5 in x 1 in
VMS Location	17 ft – 10 1/4 in from Northbound Upright
VMS Width	31 ft – 8 in
VMS Height	9 ft – 4 3/16 in
VMS Depth	3 ft
VMS Sign Area	296.05 ft ²

1 ft = 0.3048 m

1 in = 25.4 mm

Material Properties

The uprights and truss sections were made of API-5L-X52 steel pipe. All plates were structure steel ASTM A572 Gr. 50. The anchor bolts were AASHTO M314-90 Gr. 55. The W-shape and T-shape sections used for the VMS-to-truss connections were made of A572 Gr. 50 steel. The concrete pile foundation was conventional concrete with #9 size rebar Gr. 60. All of the primary material properties of the designations given are listed in Table 4-3.

Table 4-2. Primary member sizes of the bridge-type VMS support structure

Member	Diameter	Thickness
Vertical Uprights	8.625 in	0.25 in
Upright Diagonal Struts	1.9 in	0.2 in
Upright Horizontal Struts	1.9 in	0.2 in
Chords	3.5 in	0.216 in
Truss Vertical Diagonal Struts	1.9 in	0.145 in
Truss Vertical Struts	1.315 in	0.133 in
Truss Horizontal Diagonal Struts	1.66 in	0.14 in
Truss Horizontal Struts	1.315 in	0.133 in
Truss Internal Diagonal Struts	1.315 in	0.133 in

1 in = 25.4 mm

Table 4-3. Material properties of the bridge-type VMS support structure

Material	Members	Material Designation	Modulus of Elasticity (psi)	Yield Stress (psi)	Tensile Stress (psi)
Steel Pipe	Truss, Uprights	API-5L-X52	29,000,000	52,000	66,000
Steel Plate	Truss and Base Plates	ASTM A572 Gr. 50	29,000,000	50,000	65,000
Steel rod	Anchor Bolts	AASHTO M314-90 Gr. 55	29,000,000	55,000	75,000
Concrete	Pile Foundation	4,000 psi Compressive Strength	3,600,000	NA	NA
Rebar	Pile Reinforcement	ASTM A706 Gr. 60	29,000,000	60,000	80,000

1 psi = 6,891.2 Pa
 NA = not applicable

Section 5

Experimental Instrumentation

Overview

A detailed description of the instrumentation program for the bridge-type VMS support structures is provided. The structure was instrumented with electric strain gauges to determine stresses at critical locations. Accelerometers were mounted on the structure to determine structural dynamic behavior, and anemometers were attached to measure wind velocity vectors (magnitude and direction). Each transducer provided time history streamlines that were collected simultaneously using a data acquisition system. A list of all strain gauge identifications and their locations are provided in Appendix B.

Strain Gauges

Uni-axial strain gauges were used to measure the strain response of the structure. They were placed on the structure where strains were most critical, and especially applicable to determining the causative fatigue load from wind-induced loading. The instrumented locations included the uprights and truss chord on the northbound side of the structure.

Upright Member

Eight uni-gauges were placed on the upright members. Four gauges on each post were attached. They were placed to measure strain along the longitudinal axis. Finite element analysis (FEA) was conducted on the structure to determine the most effective location to place the gauges. In order to avoid bending moments with only normal stresses existing, it was determined from the FEA that a location 8 ft – 6 in (2.4 m – 152 mm) above the base plate would be the optimal position. Results from the FEA for determining the most effective location for the strain gauges are provided in Appendix C. A detailed description of the FEA model for the support structure in terms of its development and solution is provided in **Section 14: Finite Element Analysis**.

The gauges were placed on each post of the northbound lane upright. They were placed at 90° around the post circumference. The locations of the gauges are shown in Figure 5-1. One gauge was slightly altered because of conduit interference. A picture of the upright gauges at location 1 is shown in Figure 5-2. A protective coating and tape were used to cover the gauges from the environment. A picture of the finished attachment is shown in Figure 5-3 at location 2.

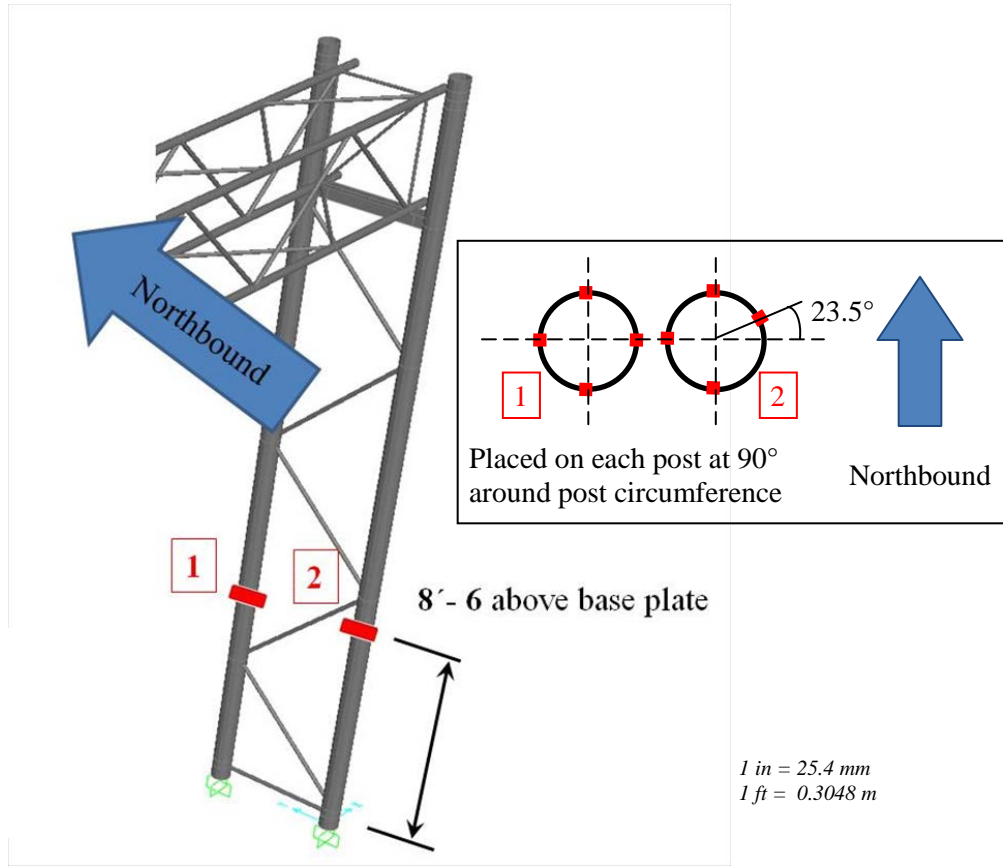


Figure 5-1. Strain gauge locations on the northbound lane upright with cross sectional views



Figure 5-2. Uncovered uni-axial strain gauges attached to the upright post at location 1



Figure 5-3. Protected uni-axial strain gauges attached to the upright post at location 2

Truss Chord Member

Four uni-axial strain gauges were attached on the truss chord member. The bottom chord facing the northbound traffic was instrumented. The gauges were located 22 in (559 mm) out from the first vertical strut of the truss. They were placed to measure strain along the longitudinal axis of the chord member. The locations are illustrated in Figure 5-4. A picture of the uncovered gauges is shown in Figure 5-5. The gauges were covered with a protective coating and tape to guard against the environmental conditions using the same procedure as the upright gauges.

Anemometers

Anemometers were used to measure wind velocity and direction for natural wind events. The WindSonic ultra-sonic wind and direction sensor was used for this application (see Figure 5-6). The anemometer calculated speed and direction by measuring the time needed for generated sound pulses to travel from one transducer to the other within the air gaseous medium. Two anemometers were required for wind measurements. They were placed 4 ft (1.22 m) above the upright using a steel extension that was fabricated to fit the structure. This was to avoid any effects for wind dynamics (turbulence, vortices, etc.) caused by the structure.

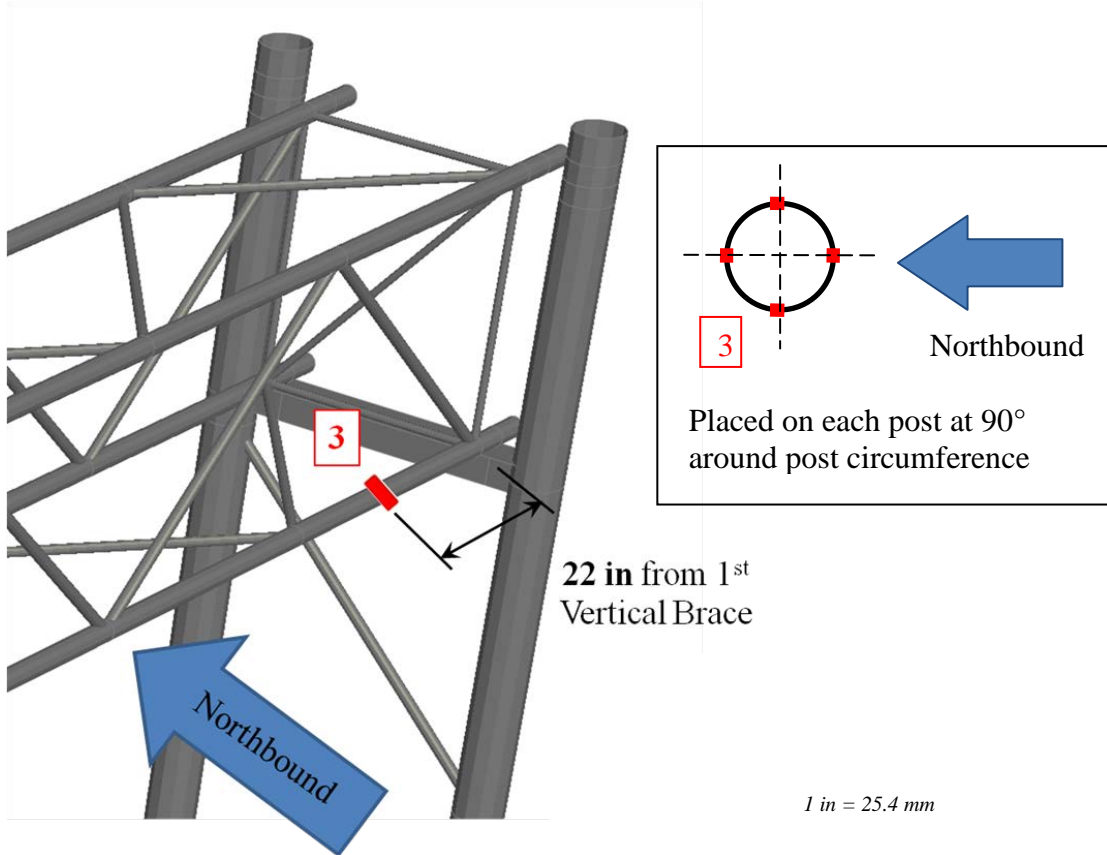


Figure 5-4. Strain gauge locations on the bottom truss chord member with cross sectional view

Two anemometers were used for redundancy as well as for providing differing measurement planes: AN-2 measured the vertical plane whereas AN-1 measured the horizontal plane. A detailing of this layout is shown in Figure 5-7, and a picture of the anemometers is shown in Figure 5-8. Each anemometer provided wind velocity and direction angle measured from an identified North direction, as indicated in the anemometer wind display shown in Figure 5-9. For all anemometers, the North compass on the instrument was directed normal to the back façade of the structure the direction of traffic. A list of the anemometers identification and locations are provided in Appendix B, along with a schematic detailing their locations.



Figure 5-5. Uncovered uni-axial strain gauges attached to the truss chord member at location 3



Figure 5-6. WindSonic ultra-sonic wind and direction sensor used to measure the wind dynamic behavior

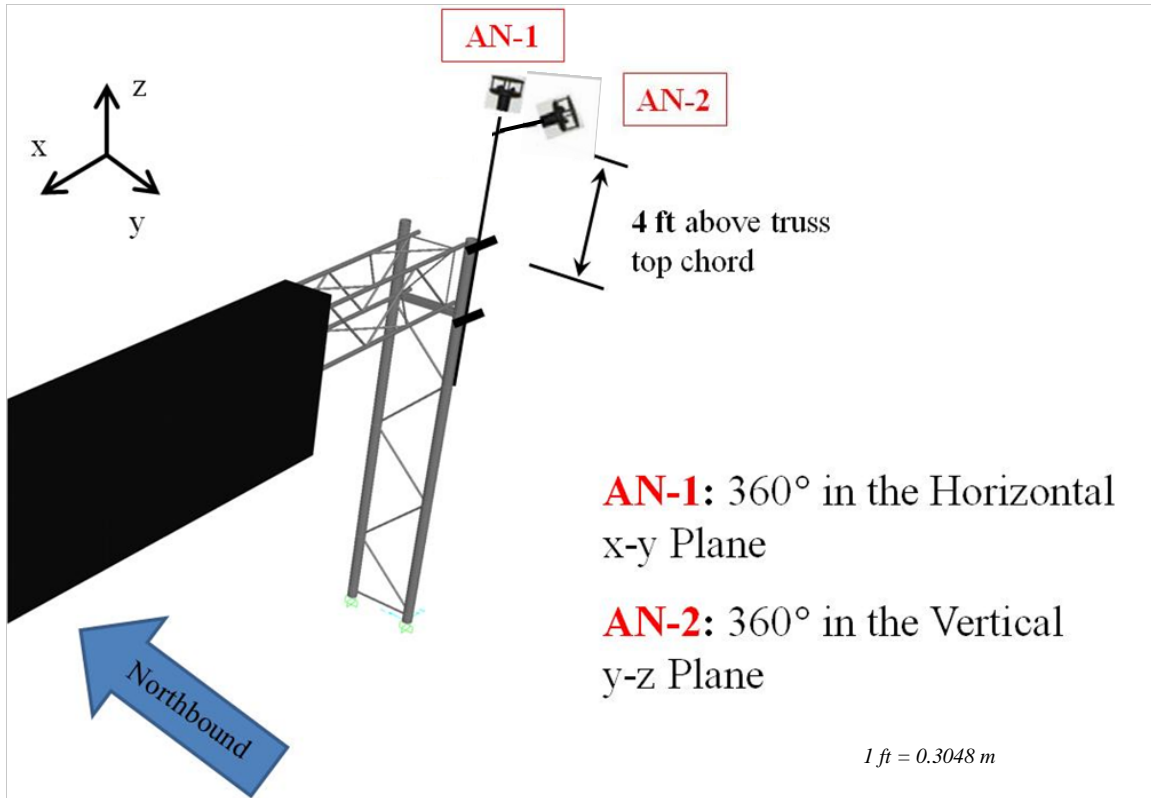


Figure 5-7. Anemometer locations and identification placed 4 ft (1.22 m) above the upright



Figure 5-8. Pictures of the anemometers and extension placed 4 ft (1.22 m) above the upright

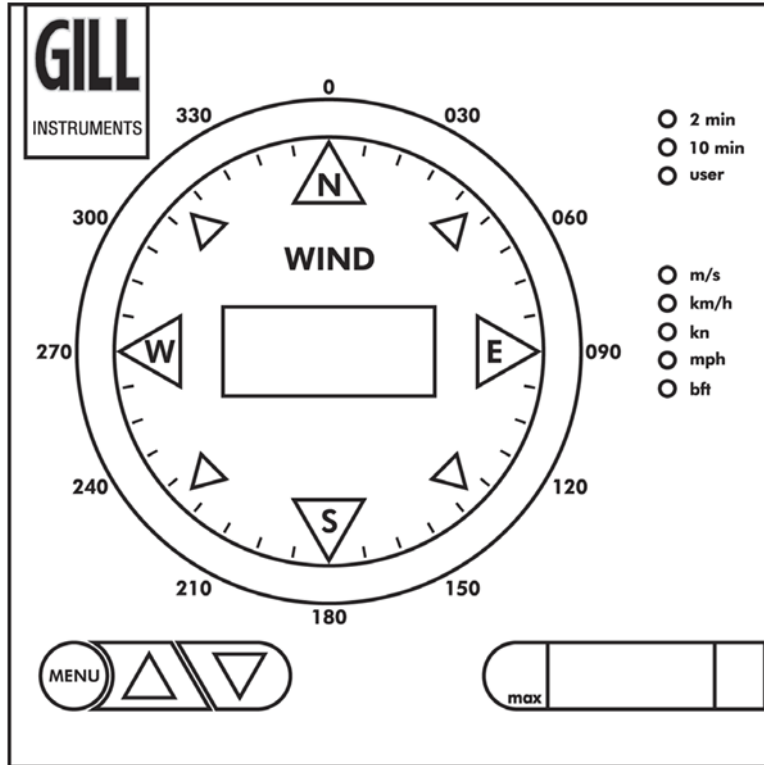


Figure 5-9. Anemometer wind display in compass bearings showing the North identification

Accelerometers

Accelerometers were used to obtain the acceleration response of the structure. They were of piezoelectric type that uses a piezoelectric crystal mounted to a small mass from which the voltage output is converted to acceleration. Each accelerometer had a maximum capacity of 96.5 ft/sec^2 (3 G). The data was used to determine major dynamic characteristics of the structure such as:

- Natural frequencies and periods,
- Modal shapes, and
- Critical damping percentages

The locations of the accelerometers were strategically chosen. A combined total of four unidirectional accelerometers were required for the structure in order to obtain accurate measurements of vibration for all structural degrees-of-freedom in translation. Accelerometer locations and identification are shown in Figure 5-10.

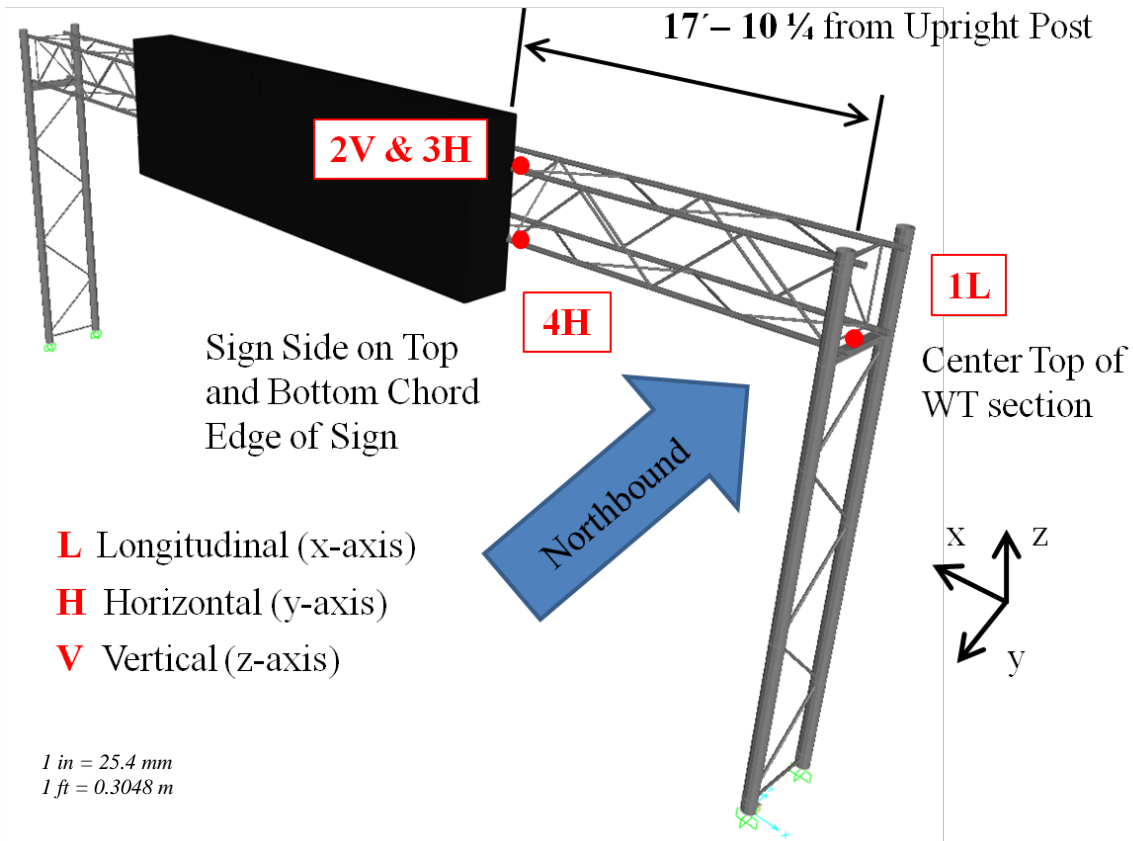


Figure 5-10. Accelerometer locations, identifications, and vibratory direction of measurement

One accelerometer was placed at location 1L (see Figure 5-11) to measure the longitudinal acceleration in the direction normal to the northbound traffic of the upright member. Two accelerometers were placed at location 2V and 3H to measure the vertical and horizontal directions (Figure 5-12). One accelerometer was placed at location 4H to measure the horizontal direction for identifying torsion behavior of the truss (Figure 5-13).

The accelerometers were attached to the structure by screwing the accelerometers to a mounting box, which was securely glued to a notched steel plate and tightly strapped to the round steel pipe members using hose clamps. A picture of the instrument attachment to the chord member of the box truss is shown in Figure 5-12 as an example.



Figure 5-11. Accelerometer 1L measuring the upright in the longitudinal direction normal to traffic

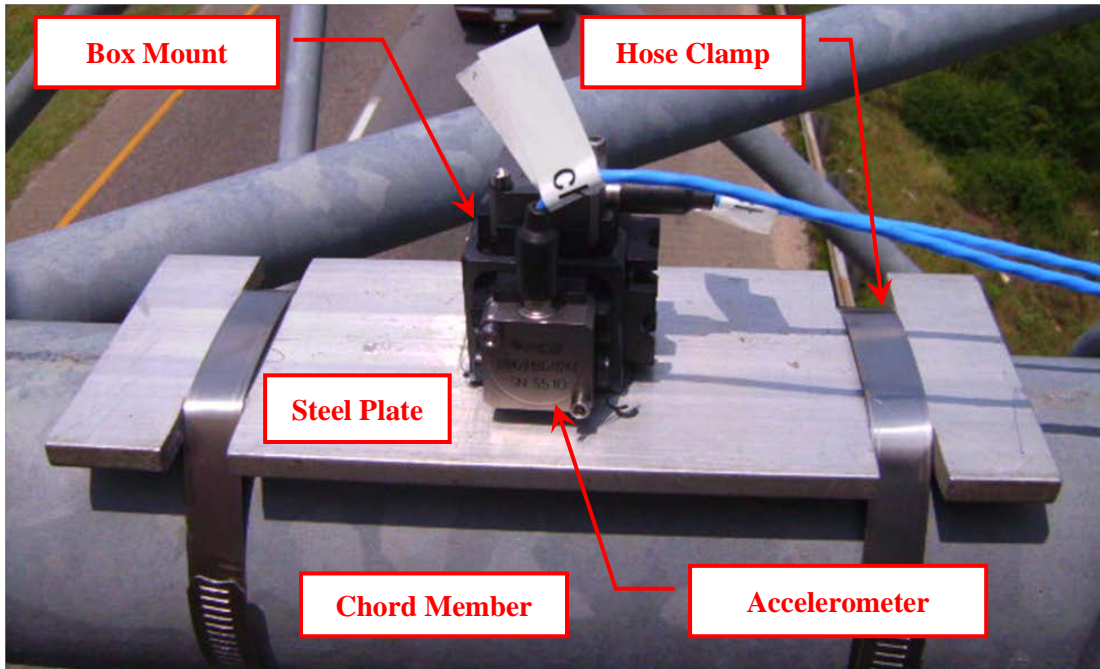


Figure 5-12. Attachment of the 2V and 3H accelerometer to the rounded members

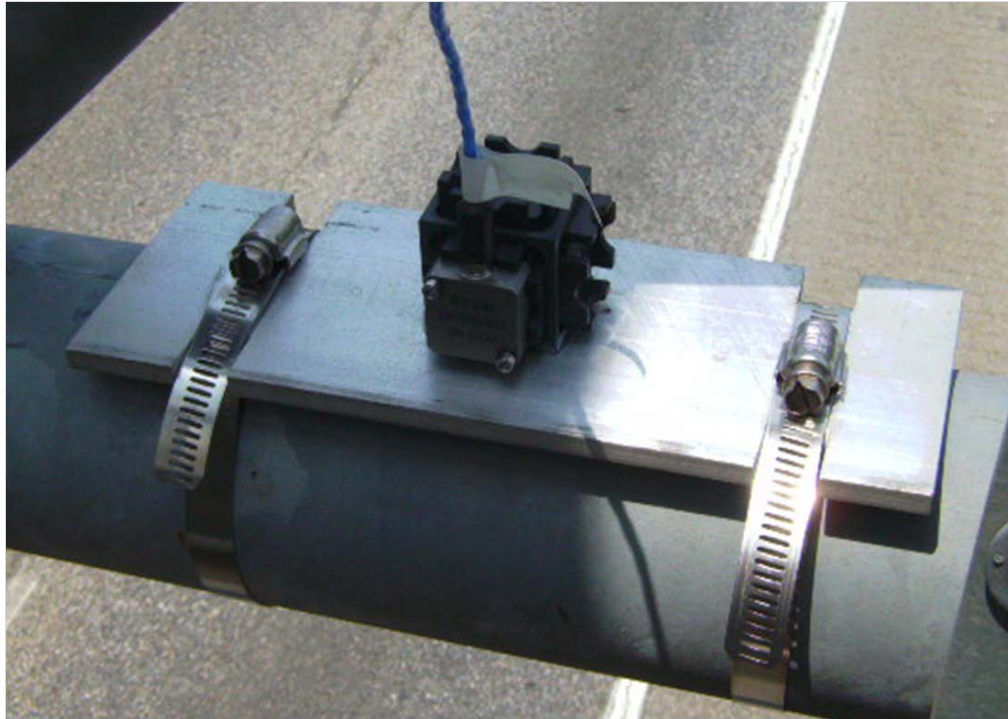


Figure 5-13. Accelerometer 4H measuring the horizontal direction parallel to traffic

Data Acquisition System

All instrumentation was wired into a data acquisition system. The data was converted into engineering units by the data acquisition system, filtered, and stored onto the hard drive of a portable computer. Data was then saved onto Maxwell CD-R data storage disks to be distributed after testing. A white van was used to hold the data acquisition system and computer during testing. It was driven to and parked next to the support structure on the side of the highway for testing. A typical test setup with the van and all instrumentation wiring fed through a side hole in the van and hooked to the acquisition system is shown in Figure 5-14. A close up of the data acquisition system and computer is shown in Figure 5-15.

The data acquisition was capable for collecting all data from instrumentation simultaneously, which was required for the fatigue tests. The maximum number of channels used was as follows:

- Strain Gauges: 12 channels
- Anemometers: 4 channels
- Accelerometers: 4 channels
- Total Channels = 20

Data were collected at 60 samples per second for all instrumentation, which was at least six times greater than the highest structural natural frequency to avoid aliasing and other related errors. A digital low-pass Butterworth filter was used and set at 20 Hz to filter out unwanted high frequencies from the collected data.



Figure 5-14. ALDOT van parked next to the structure with fed wiring from the instrumentation



Figure 5-15. The data acquisition system inside the ALDOT van parked next to the structure

Section 6 Experimental Testing Procedure

Overview

The bridge-type VMS support structure was tested under two predominant fatigue loading events:

- a) Natural wind gust, and
- b) Truck-induced wind gust.

A detailed description of the testing procedures performed to capture the fatigue load for the two wind events are provided.

Natural Wind Gust

The natural wind data was taken over an extended time period in order to capture the predominant natural wind gusts. Wind data from the National Weather Service in the form of the annual mean wind velocity for the area was determined to help schedule appropriate testing days between ALDOT and the UAB research team.

Pre-Determined Sample Size

At least 32 hours of wind velocity data was desired for data collection. The collected data was distributed between the following sampling intervals:

- 0 to 10 mph (0 – 4.47 m/s): low wind
- 10 to 20 mph (4.47 – 8.94 m/s): medium wind (fatigue wind)
- 20 to 30 mph (8.94 – 13.4 m/s): high wind.

A 20 to 30 mph (8.94 – 13.4 m/s) wind velocity was considered as high wind. The wind velocity having a 0.01% exceedence probability in accordance to the infinite-life approach of the *Supports Specifications* was 38 mph (17 m/s). Capturing this wind was considered probable, and likely during sampling of the categorized “high wind” label; however such conditions warranted extreme weather that may be unsuitable for field testing because of safety issues. The intention was to capture the vibration behavior of the sign support structure in response to vibratory induced wind velocities, typically above 10 mph (4.47 m/s), and form a relationship between wind velocity and structural response stress ranges. Low wind data was wanted in order to establish a wind velocity limit in which structural vibration was excited.

Test Procedure

On the scheduled testing day, ALDOT drove the data acquisition van to the site and began attaching wiring from the instrumentation to the van. This took typically one hour. The testing began after instrumentation was operated and all transducers checked for accuracy. All instrumentation was measured simultaneously at 60 samples per second. Data recording intervals were set at no smaller than 45 minutes each, therefore allowing for a continuous 45 minute long recorded streamline. Anemometers AN-1 and AN-2 were used to measure the ambient wind velocity and direction during testing. All strain gauges and accelerometers were used to measure the structural response. Data was saved onto a CD for storage and distribution, and later used for determining the fatigue load due to natural wind back in the lab.

After data collection was finished for the scheduled event, all wiring was disconnected from the data acquisition system. Instrumentation connections were then stored properly next to the structure for future testing, and ALDOT researchers left with the data acquisition van. This procedure continued for each scheduled day.

Truck-Induced Wind Gust

A random experimentation process was used to measure truck gusts. Trucks were randomly chosen as they passed under the structure and all information was recorded. Wind gusts created from trucks representative of the following list were recorded.

- Truck cab only
- Truck cab with wind guard
- Cab + trailer
- Cab with wind guard+ trailer
- Dumpster truck (full)
- Dumpster truck (empty).

Test Procedure

The tests were conducted using electronic and manual processes. The data acquisition system measured the vibration of the structure and stored the information in terms of acceleration versus time. The time when data sampling began was manually recorded as the start time. Two researchers were positioned next to the highway and slightly obscured from the view of the truck drivers. One researcher measured the speed of the passing semi-trailers using a handheld and cordless Bushnell Speedster II Radar Speed Gun. Specifications of the radar gun that were provided by the manufacturer are provided in Appendix D.

The truck speed was captured at the instant the semi-trailer passed underneath the support structure. An example picture of the speed monitoring using the radar gun is shown in Figure 6-

1. The other researcher recorded the time the semi-trailer passed, the speed captured from the radar gun, the lane used by the vehicle, and the type of semi-trailer (i.e., box trailer, tanker, flatbed, etc.).

The semi-trailers were randomly selected by the researchers based on their type, occupied lane, and presumed speed. All times of passing semi-trailers coincided with the start time of the data acquisition system. The truck-induced wind gusts were later isolated from the data time history record according to the passing time that was recorded in the field.



Figure 6-1. Radar speed gun used to measure the speed of passing semi-trailers

Section 7 Experimental Data Collection Samples

Overview

A summary of the samples obtained during the experimental data collection for bridge-type VMS support structure is presented. The samples for natural wind gusts were filtered for wind velocities greater than 9 mph (4 m/s) and directed onto the front face of the support structure. This was characterized as usable data. Descriptive statistics, histograms, and wind rose diagrams are provided for the raw and usable data samples. All accelerations and strains used to develop the fatigue load due to natural wind gusts were based on the usable data collection presented in this section. The data samples for truck-induced wind gusts are provided and represent the range of semi-trailers using the highway system. A summary and descriptive statistics of this data is provided.

Test Schedule

Test days were schedule based on meteorological data. Days were scheduled between ALDOT and UAB at least one week in advance. Table 7-1 provides a listing of the days when testing occurred for natural wind gusts and truck-induced wind gusts.

Table 7-1. Test schedule for natural wind and truck-induced wind gusts

Runs	Date	Hours Collected
1-4	8/26/2010	3
5-21	9/3/2010	12.75
22-26*	12/2/2010	3.75
27-31	2/2/2011	3.75

** Indicates testing for truck-induced wind gusts was performed on this day*

Natural Wind Gust

Sample Size

A total of 23.25 hours of data were collected. The average wind velocity measured was equal to 5.22 mph (2.33 m/s) with the maximum velocity equal to 28 mph (13 m/s). A histogram of the collected wind velocity data is shown in Figure 7-1. A wind rose diagram of the wind direction is shown in Figure 7-2. The vertical axis of the histogram and of the wind rose diagram in Figure 7-

1 and Figure 7-2 represents the occurrence frequencies. Descriptive statistics of the raw data sample is provided in Table 7-2.

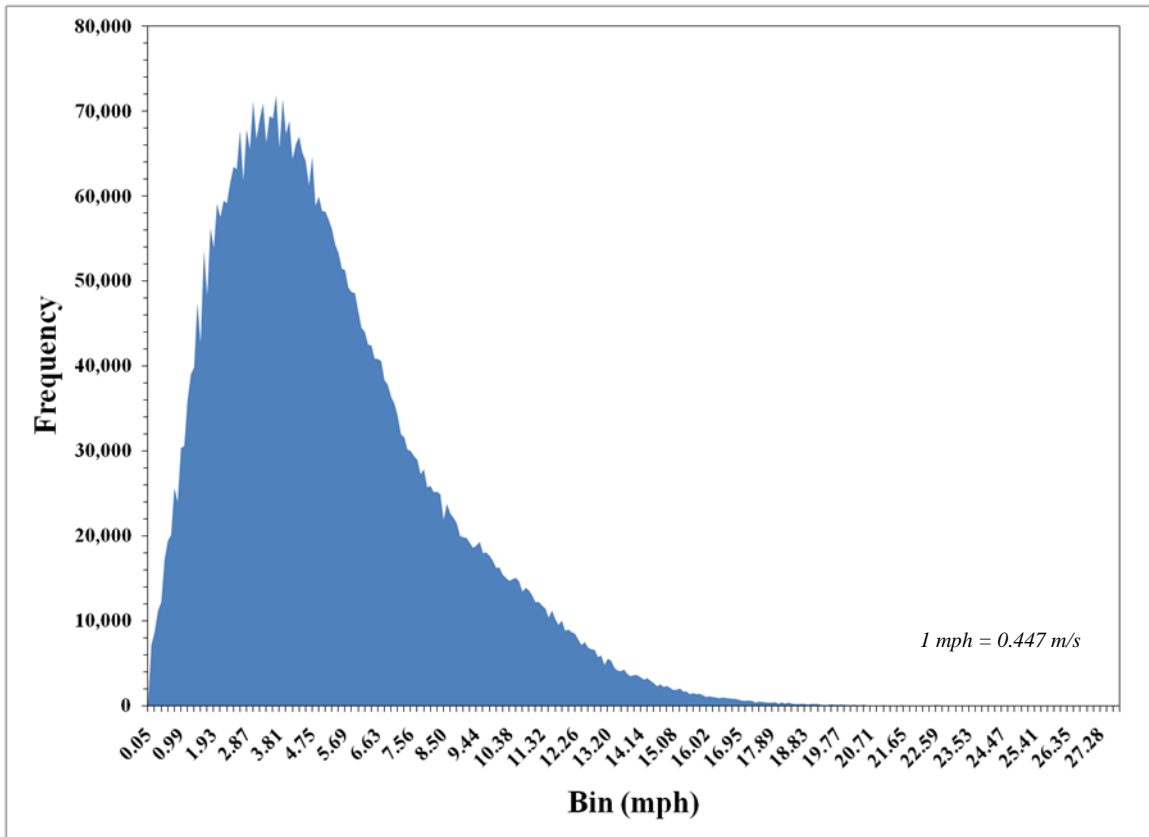
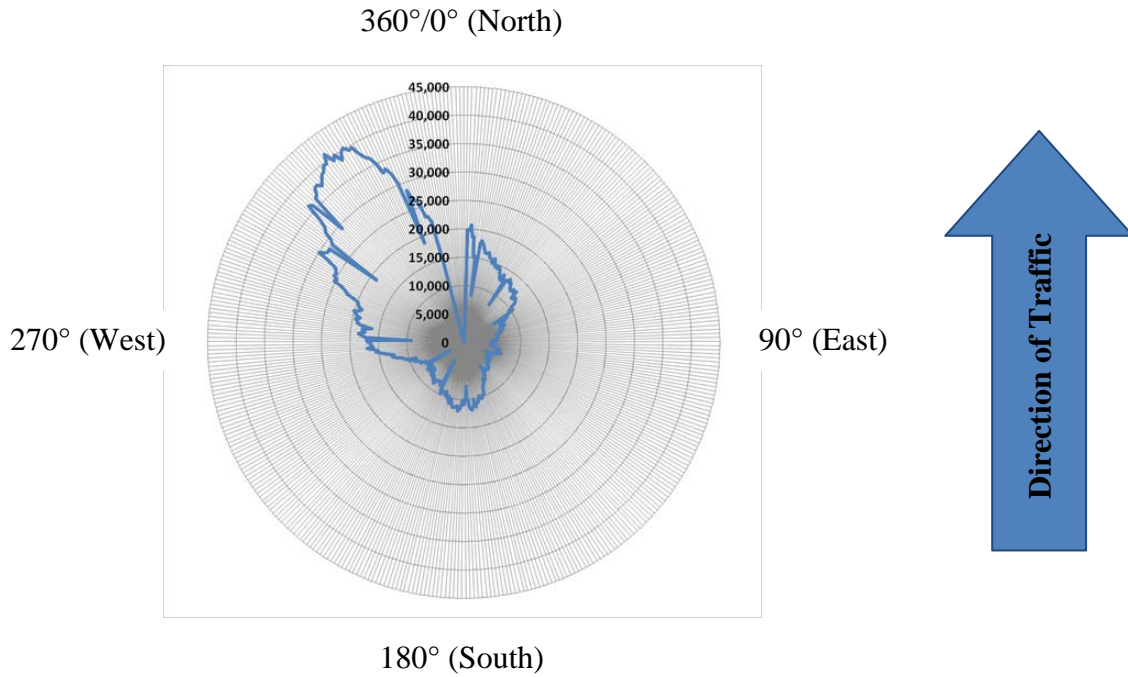


Figure 7-1. Histogram of the wind velocity showing the distribution of the raw data collection

Back Face of VMS



Front Face of VMS

Figure 7-2. Wind rose diagram of the raw data showing the wind velocity distribution of direction

Table 7-2. Descriptive statistics of the wind velocity raw data collected

Statistic	Wind Velocity (mph)	Wind Direction (degree)
Mean	5.22	219.72
Median	4.60	264.61
Std. Dev.	3.16	117.96
Variance	9.98	13,915.09
Range	27.80	359.85
Minimum	0.05	0.15
Maximum	27.85	360.00
Count	4,977,474 samples	

1 mph = 0.447 m/s

The total data collection contains 4,977,474 wind samples for a sampling frequency of 60 Hz. There were matching acceleration and strain gage samples for each wind velocity sample. This equals to a total of 59,729,699 structural response samples that correspond to each of the wind samples collected.

Usable Data Collected

The data collected from the anemometers were used to distinguish between usable and discarded data to apply for wind pressure back-calculation. Data was considered usable if it complied with the following criteria:

- Wind velocity was greater than 9 mph (4 m/s), and
- Wind velocity was directed onto the front face of the structure.

The data was broken down into wind velocity and direction. It was discovered from the collected structural response data that significant structural vibration was only induced with wind velocities greater than 9 mph (4 m/s). Only wind velocities directed onto the front of the structure were used for evaluation because the drag coefficients used in the wind pressure calculation were developed based on this type of exposure.

A histogram of the usable wind velocity data based on the criteria is shown in Figure 7-3. The wind rose diagram of the usable wind direction is provided in Figure 7-4. The filtering resulted in a total of 66,357 wind samples. This corresponds to 796,284 acceleration and strain gage samples that were used to determine the fatigue load due to natural wind gusts. A list of the descriptive statistics of the usable data sample is provided in Table 7-3.

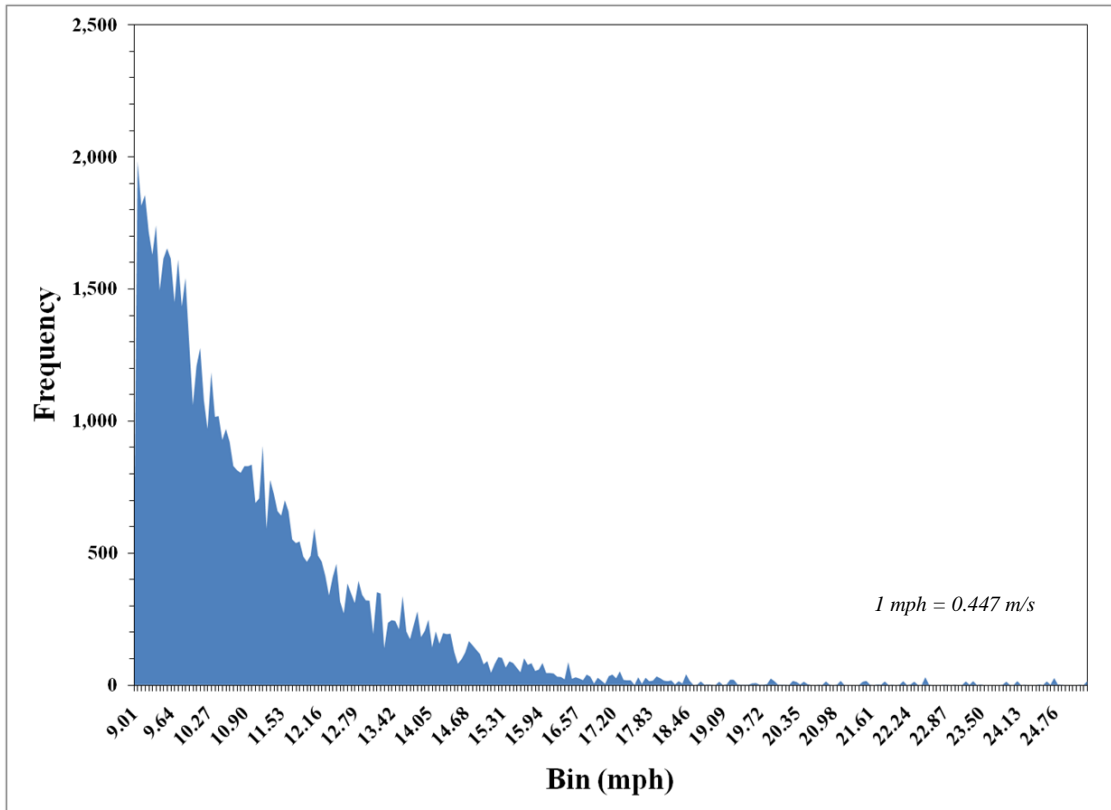


Figure 7-3. Histogram of the usable wind velocity data collection

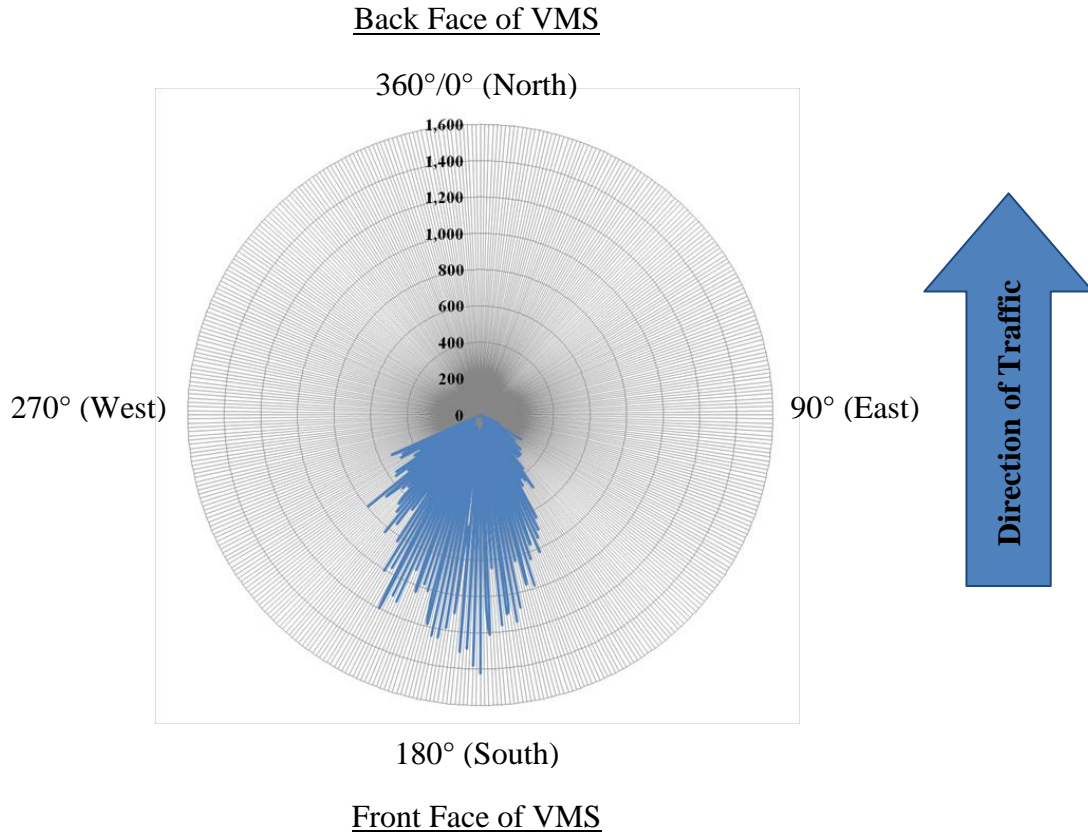


FIGURE 7-4. Wind rose diagram of the usable wind direction data collection

Table 7-3. Descriptive statistics of the wind velocity usable data collection

Statistic	Wind Velocity (mph)	Wind Direction (degree)
Mean	10.99	185.28
Median	10.42	185.13
Std. Dev.	1.93	19.65
Variance	3.74	386.22
Range	16.33	90.00
Minimum	9.00	135.00
Maximum	25.33	225.00
Count	66,357 samples	







1 mph = 0.447 m/s

Truck-Induced Wind Gust

Sample Size

A total of 157 truck-induced wind gusts events were recorded. The truck speed, occupied lane, and structural response were collected for each event. The collection data is provided in Appendix J for reference. The structural responses to several semi-trailer truck types were collected. A list of the truck types measured along with a picture representing the type is provided in Table 7-4.

Table 7-4. Truck types measured during the truck-induced wind gusts data collection

Identification	Description	Picture
1	Cab Only	
2	Typical Deflector	
3	No Deflector	
4	Tandem	
5	Flat Bed	
6	Tanker	

Sample Distribution

The distribution of samples with respect to truck speed and truck type of the truck-induced wind gusts data collection is provided in Table 7-5. The most popular truck type was observed to be the typical deflector type 2. The majority of all truck types measured were traveling between 60 mph (27 m/s) to 70 mph (31 m/s).

TABLE 7-5. Distribution of samples of the truck-induced wind gusts data collection

Truck Type	Number of Samples						Row Totals
	50-55 mph	55-60 mph	60-65 mph	65-70 mph	70-75 mph	75-80 mph	
1	0	0	4	1	1	0	6
2	3	7	36	38	14	3	101
3	0	2	5	3	5	0	15
4	0	0	1	2	0	0	3
5	0	1	7	7	2	2	19
6	0	2	3	5	1	0	11
Other	1	0	0	1	0	0	2
<i>Col. Totals</i>	4	12	56	57	23	5	157

1 mph = 0.447 m/s

Section 8

Operational Modal Analysis

Overview

Operational modal analyses of the experimentally tested bridge-type VMS support structure was conducted from the experimentally collected data. The measurements obtained from accelerometers were used for the study. Important dynamic properties were gathered from the analysis to understand the behavior of these structures to the dynamic loading environments and to be used in the development of the fatigue loads due to natural wind and truck-induced wind gusts.

Modal Data Utilization

The data obtained from the modal analysis were utilized to understand the dynamic behavior of the structural system. The major parameters that were obtained from the modal analysis were as follows:

- Identify modal frequencies and periods of vibration,
- Determine modal damping,
- Obtain modal shapes, and
- Predict structural response to dynamic excitation.

The investigation of the bulleted parameters were necessary to devise and develop the fatigue loading due to natural wind and truck-induced wind gusts for both the experimental and theoretical programs of study associated with this project.

Systemizing the Degrees-of-Freedom

The number of measured degrees of freedom was chosen to represent the dynamic behavior of the structural system. They were chosen based on the expected modal shapes of the system. Four dynamic vibratory shapes were identified as crucial dynamic behavior that governs the vibratory movement of the structure as it relates to the wind-induced fatigue loading:

1. Longitudinal displacement of the uprights along the x -axis direction.
2. Vertical displacement of the truss span along the z -axis direction.
3. Horizontal displacement of the truss along the y -axis direction.

4. Torsion displacement of the truss about the longitudinal x -axis because of the off-centered weight of the VMS.

The placements of the accelerometers were identified based on the four assumed vibratory responses and are shown in Figure 8-1. The associated degrees of freedom and their alignment were defined as follows:

- 1L: $1x$,
- 2V: $2z$
- 3H & 4H: $3y$

The total number of degrees of freedom was three.

Modal Analysis Test Setup

Accelerometers were used to obtain the acceleration response of the structure. They were of the piezoelectric type that uses a piezoelectric crystal mounted to a small mass from which the voltage output is converted to acceleration. Each accelerometer had a maximum capacity of 96.5 ft/sec^2 (3 G). The locations of the accelerometers were strategically chosen, as the accelerometer only gave the natural frequency of the member upon which it rests. A combined total of four unidirectional accelerometers were required. They were placed at particular locations to measure each possible degree of freedom in vibration direction. Accelerometer locations are shown in Figure 8-1.

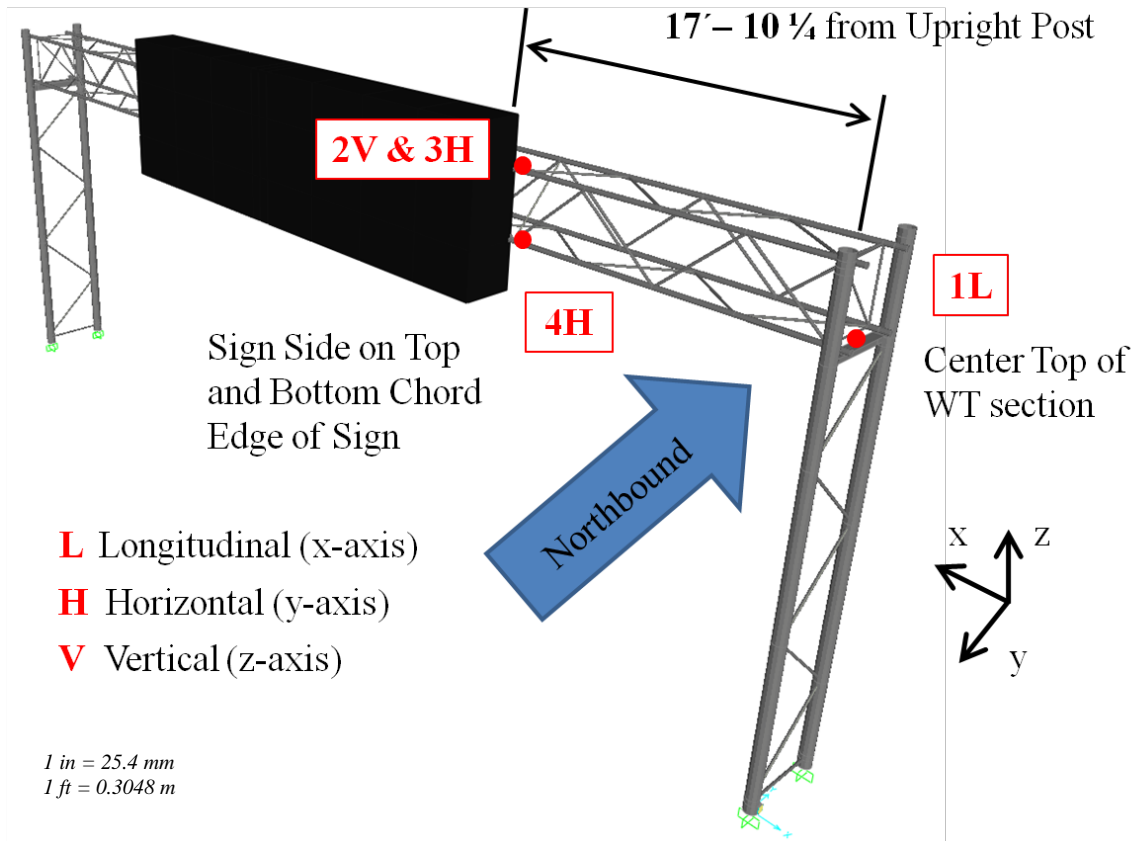


Figure 8-1. Accelerometer locations, identifications, and vibratory direction of measurement

A description of the accelerometer locations in reference to Figure 8-1, and the strategic reasoning for their placement were as follows:

1L

One accelerometer was placed at this location to measure the longitudinal acceleration along the x -axis direction. A picture of this location is shown in Figure 8-2.

2V & 3H

Two accelerometers were placed at this location. Accelerometer 2V measured the vertical acceleration of the truss along the z -axis direction. Accelerometer 3H measured the horizontal acceleration of the truss along the y -axis direction. A picture of this location is shown in Figure 8-3.

4H

One accelerometer was placed at this location. It was used to measure the horizontal acceleration of the truss along the y -axis direction. The data obtained was compared to

accelerometer 3H to ascertain possible torsion of the truss because of the off-centered weight of the VMS. A picture of this location is shown in Figure 8-4.



Figure 8-2. Accelerometer 1L measuring the upright in the longitudinal direction normal to traffic

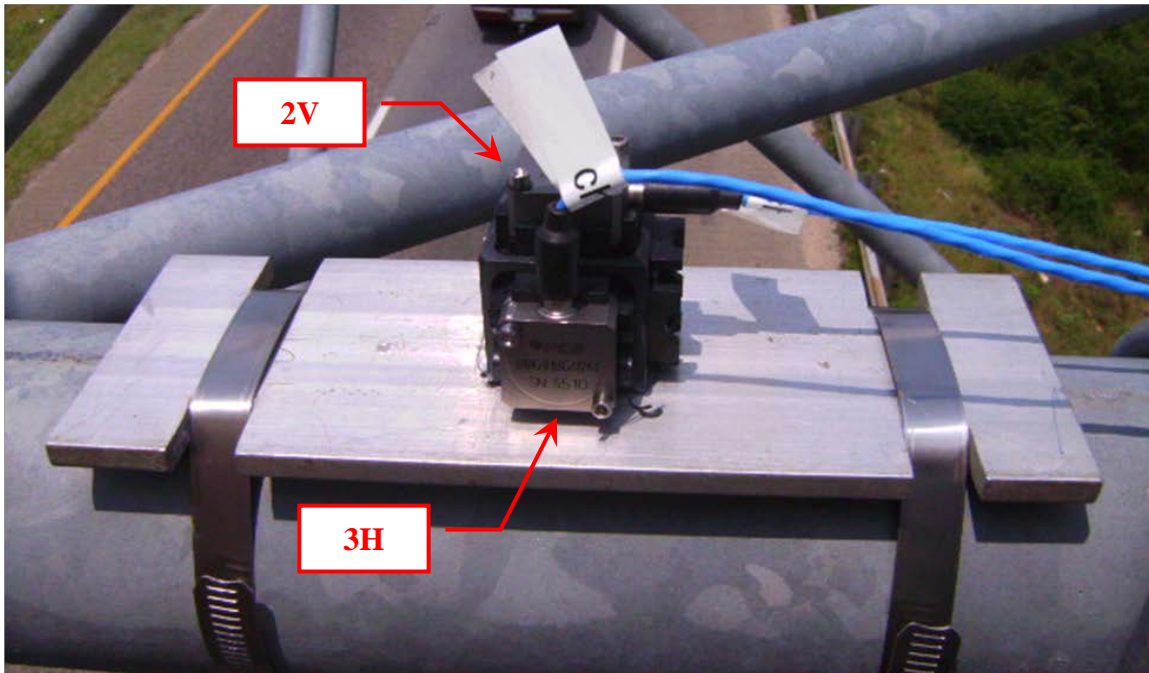


Figure 8-3. Accelerometers 2V & 3H measuring the horizontal and vertical directions of the span

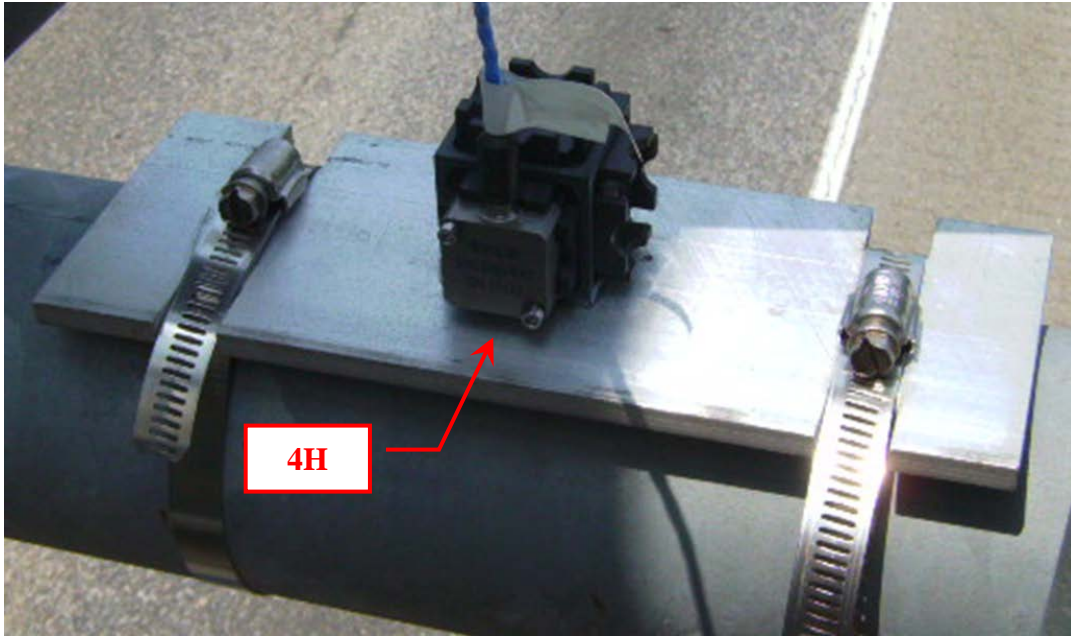


Figure 8-4. Accelerometer 4H to measure the horizontal direction parallel to traffic

Spectral Analysis

A spectral analysis was conducted to determine the vibration characteristics of the support structure. The accelerometer instrumentation was used for the analysis. The instruments were placed strategically on the structure to measure all translational degrees-of-freedom. The measurements were made during operation of the structure. Analysis of the collected data provided the frequency at which the structures vibrated and the directions of vibration. This information was used to determine the design fatigue load due to natural wind and truck-induced wind gusts.

Natural Wind Gust

The operation frequency response of the support structure to natural wind gusts was evaluated. The accelerometer time history data collected in the field was used for the analysis because the data indicates not only the frequency of vibration but also the direction. The data collected from each accelerometer were used in the analysis. The collected time duration used was 45 minutes. The event was representative a random vibration occurrence, and assumed as a continuous function. In order for completeness and accurate representation of the dynamic behavior of the structural system, the chosen event must excite all major natural frequencies. The data collection sample with a high predominant wind speed was used for the evaluation. This was to ensure a representation with all of the modes of vibration exited. Another important aspect of the time history used for the analysis was a significant variation of the wind direction as to apply wind pressure at all angles on the structure. The descriptive statistics of the wind velocity time history used for the analysis is listed in Table 8-1.

Table 8-1. Descriptive statistics of the time history used for the natural wind gusts operational frequency analysis

Descriptive Statistic	Wind Velocity (mph)	Wind Direction (degree)
Mean	5.21	192.74
Median	4.78	192.20
Mode	3.22	182.18
Standard Deviation	3.09	58.59
Sample Variance	9.56	3,433.09
Range	25.31	384.78
Minimum	0.02	0.00
Maximum	25.33	360.00
Count	162,001	162,001

1 mph = 0.447 m/s

The time domain of the natural wind time history was transformed into a frequency domain using the Fourier transform (shown as Eq. 8-1). Hanning windows were used to ensure the signal begins and ends at zero.

$$X(f) = \int_{-\infty}^{\infty} x(t)e^{-j2\pi ft} dt \quad [\text{Eq. 8-1}]$$

where

$X(f)$ = fourier transform

$x(t)$ = continous time series

$j = \sqrt{-1}$

f = frequency where $-\infty < f < \infty$

t = time

The spectral plot of the transformed event is shown in Figure 8-5. The plot indicates a significant broadband spectrum around the lower frequencies, which is evident of the background turbulence effect of the wind pressure. Since natural wind is highly turbulent and predominantly occurring at frequencies less than 0.1 Hz, a broadband response spectrum is produced. An extremely narrowband spectrum is located at the natural frequencies of the structural system, which is evident of the structural resonance effect. This describes the resonant response of the structure at each mode of vibration that was exited during the wind event. Therefore, the response of the structure is a combination of the background turbulence and the resonant vibration.

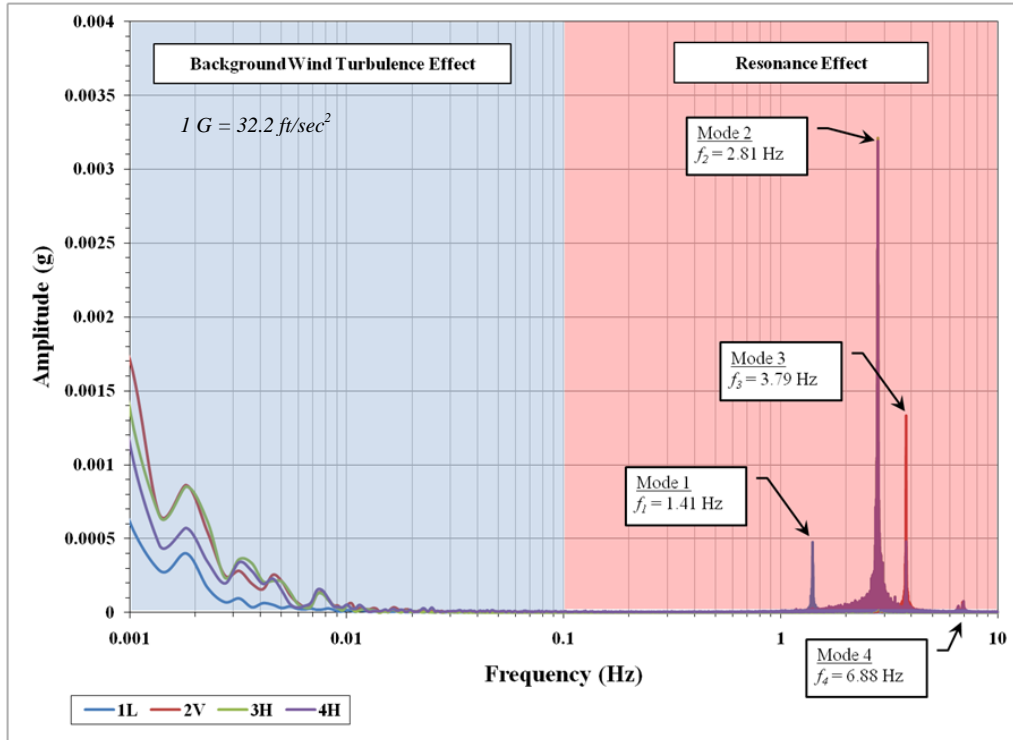


Figure 8-5. Frequency analysis of the support structure from natural wind gust

The modal shapes of vibration can be obtained from the frequency analysis plot in Figure 8-5. Each accelerometer was placed strategically on the structure to measure vibration directions as it relates to the translational degrees-of-freedom of the structure. Although many other modes of vibration exist, only the first three major modal shapes showing the largest average amplitudes are significant. Modes 1 through 3 are provided in Figure 8-6, Figure 8-7, and Figure 8-8, respectively. A listing of the modes, frequencies, and shapes are provided in Table 8-2.

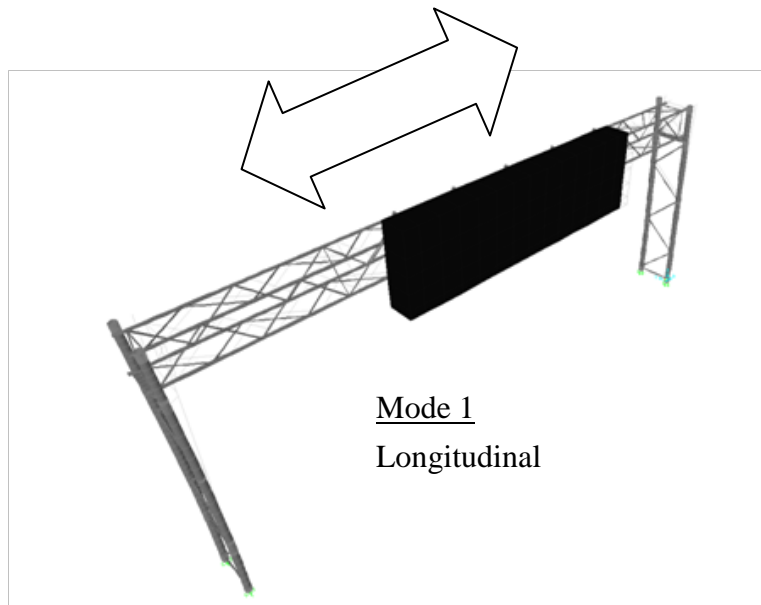


Figure 8-6. Mode 1 modal shape of vibration in the longitudinal direction perpendicular to traffic

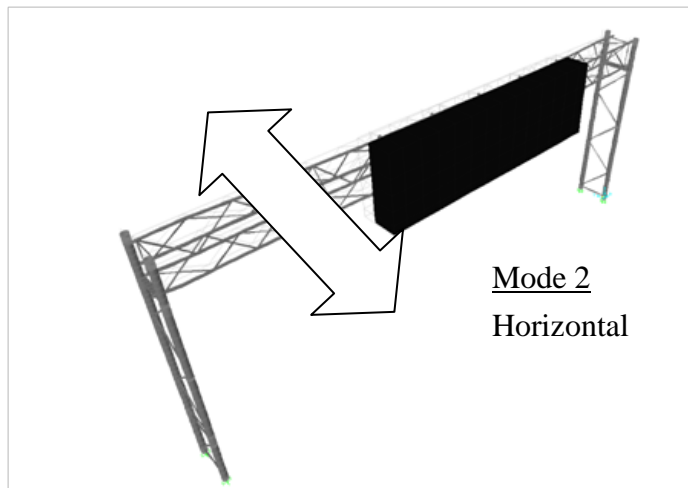


Figure 8-7. Mode 2 modal shape of vibration in the horizontal direction parallel to traffic

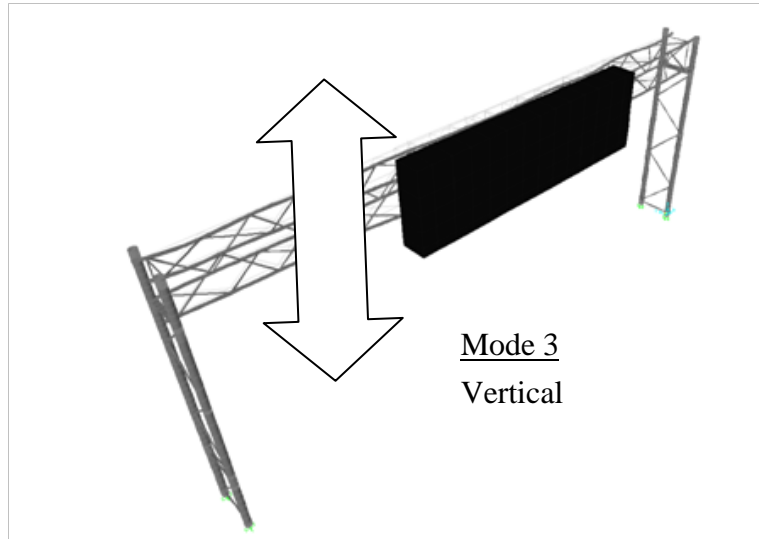


Figure 8-8. Mode 3 modal shape of vibration in the vertical direction parallel to the direction of gravity

Table 8-2. First three modal frequencies and shapes showing the largest average amplitudes of vibration

Mode	Frequency	Shape
1	1.41 Hz	Longitudinal
2	2.81 Hz	Horizontal
3	3.79 Hz	Vertical

The foremost mode of vibration that produced the largest average amplitude was mode 2 at 2.81 Hz. This was in the horizontal direction parallel to the direction of traffic. The average amplitude was greater than twice that of the amplitude of the next largest mode: mode 3. This indicates that although other modes of vibration exist simultaneously, the horizontal modal shape controlled the majority of vibration. This is especially evident in the frequency analysis of the time history data collected from the strain gages. The Fourier transform of the strain gages on the post 1 of the uprights for the same time history used for the frequency analysis with the accelerometers is shown in Figure 8-9. The most prominent average amplitude shown in the plot is of mode 2, indicating large amplitudes of vibration occurring at this frequency due to natural wind gusts.

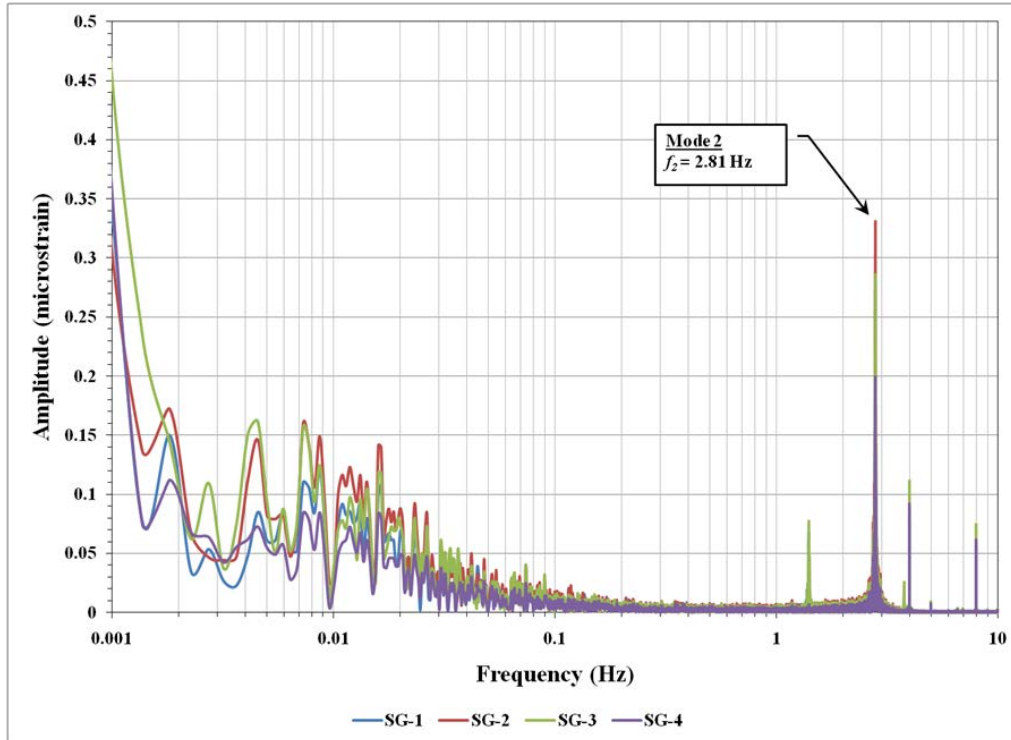


Figure 8-9. Frequency analysis of the strain gage data collected on post 1 of the uprights

Truck-Induced Wind Gust

The dynamic behavior of the bridge-type VMS support structure when subjected to truck-induced wind gusts was investigated. In particular, the investigation was conducted to ascertain the predominant mode of vibration and direction of the structure in response to passing trucks. The analysis involved calculating the Fourier transform of the time history response data collected during truck events.

A typical time history of the truck-induced wind gust event is shown in Figure 8-10. The data was collected for the most common truck type using the highway system. This corresponds to type 2 with a box trailer and wind guard. The figure demonstrates the time history collected from each accelerometer on the support structure. It is evident from the figure that the largest vibration amplitude was in the horizontal direction measured by accelerometer 3H. The Fourier transform of the time history is provided in Figure 8-11. Although other modes of vibration exist, it is clearly evident that the majority of vibration is of mode 2 in the horizontal direction parallel to the direction of traffic. The average amplitude of mode 2 is 3.5 times greater than the average amplitude of the vertical mode 3.

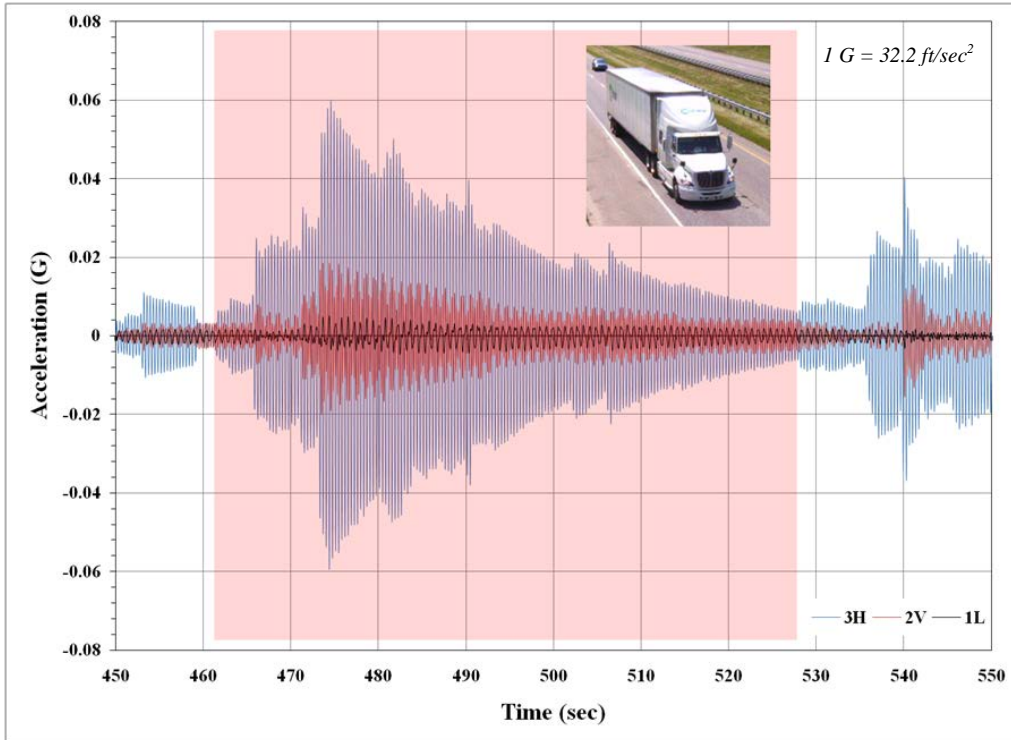


Figure 8-10. Structural response to the truck events obtained from the accelerometer data

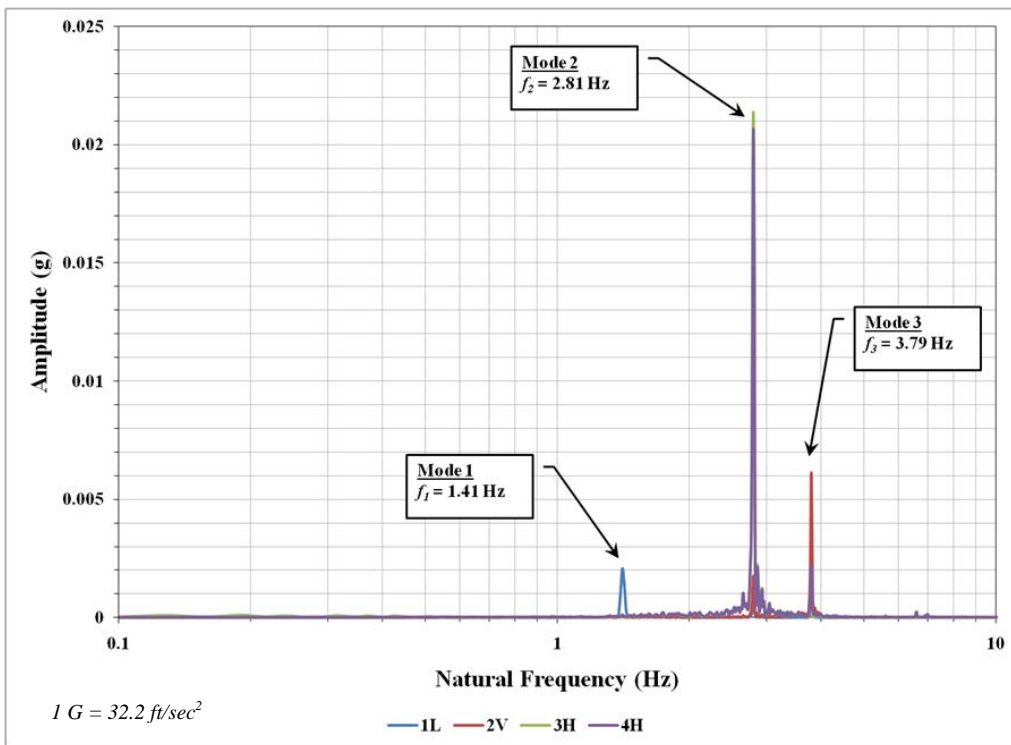


Figure 8-11. Frequency analysis of the support structure to truck-induced wind gust

Critical Damping Percentage

A modal damping analysis was performed from the experimentally collected accelerometer data. The analysis was conducted in order to determine the damping ratio, ζ , of the structure for further fatigue analysis in this project. Only the damping values of the second (horizontal vibration) and third (vertical vibration) major vibratory modes were considered most significant because of their amplitudes of vibration as compared to other vibratory modes. The damping ratio was used in developing a dynamic model of the structure to simulate the response to wind loading events, and to determine the fatigue load based on the dynamic characteristics.

The transient events used in the damping analysis were the measured structural response from the truck-induced wind gust experimentation. The truck tests were performed on a relatively low wind day as to not have external effects from natural wind gusts. The result was a noticeable transient event as seen from the response data.

There are many ways to calculate the modal damping of the structure. An understanding of the forced excitation was developed before the damping calculations were made. An experimentally measured transient event was isolated and plotted on amplitude versus time graph. An example of a typical truck transient event measured by the accelerometers, and used for this analysis, is shown in Figure 8-12.

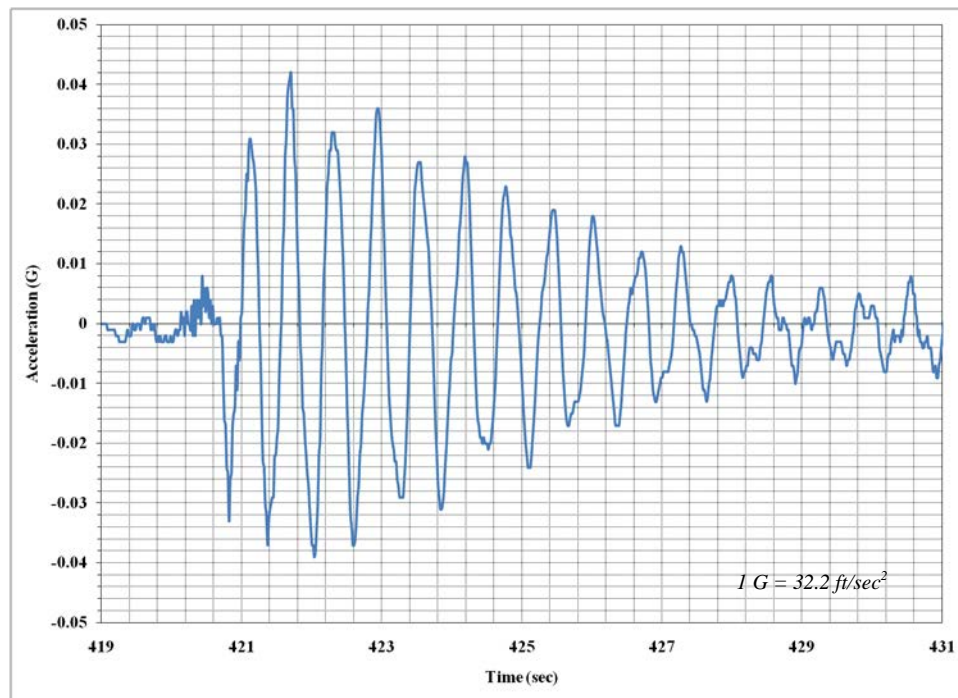


Figure 8-12. Typical truck transient event experimentally obtained from the accelerometers

The event depicted in Figure 8-12 was representative of a free vibration system of oscillatory motion. The displacement of the response was estimated mathematically as an underdamped,

periodic dynamic system. The expression shown in Eq. 8-2 is a representation of the exponential decay in amplitude with time in conjunction with the periodic motion of the modal frequency:

$$x(t) = A_0 e^{-\xi \omega_n t} \cos(\omega_d t - \varphi_0) \quad [\text{Eq. 8-2}]$$

where

$x(t)$ = amplitude as a function of time (G)

A_0 = initial amplitude (G)

ξ = damping ratio

ω_n = natural frequency (rad/sec)

ω_d = damped frequency (rad/sec)

t = time (sec)

φ_0 = initial phase (rad)

The exponential expression in Eq. 8-2 (shown as Eq. 8-3) is representative of the exponential decay of the amplitude peaks with increasing time. The cosine expression represents the periodic motion of the system. In relation to the measured transient event, Eq. 8-3 (and Eq. 8-2) is better described in Figure 8-13.

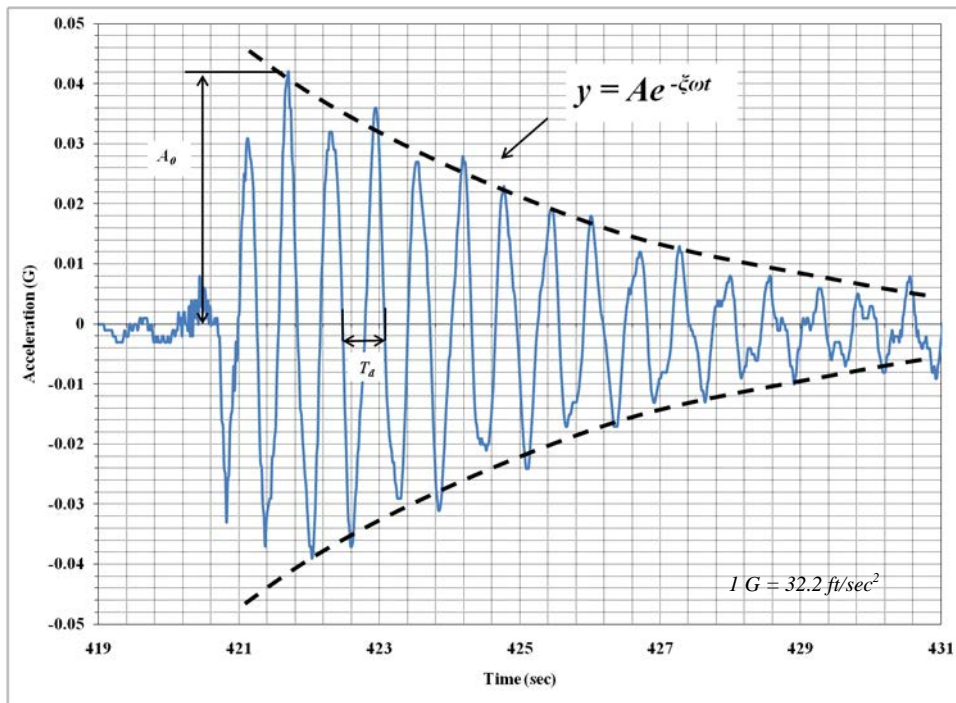


Figure 8-13. Exponential decay of the transient truck event

$$y = Ae^{-\xi\omega t}$$

[Eq. 8-3]

where

y = amplitude as a function of time of the exponential expression (G)

A = initial amplitude of the exponential expression (G)

ξ = damping ratio

ω = natural frequency (rad/sec)

t = time (sec)

A regression analysis was done to determine the damping ratio. The positive peak amplitudes of each wavelength was extracted from the time history graphs and plotted separately. The time was equalized to start from zero so that the amplitude, A_0 , could be realized. An example of the resulting plot is shown in Figure 8-14. A trendline was fitted to the plotted peaks and the equation of the trendline was extracted. The exponent of the trendline equation was set equal to the absolute value exponent of Eq. 8-3. By knowing the natural frequency of the structure, ω , the damping ratio, ξ , was calculated. A sequence of the calculation events, using the trendline equation in Figure 8-14 as an example, is shown in the following system of equations:

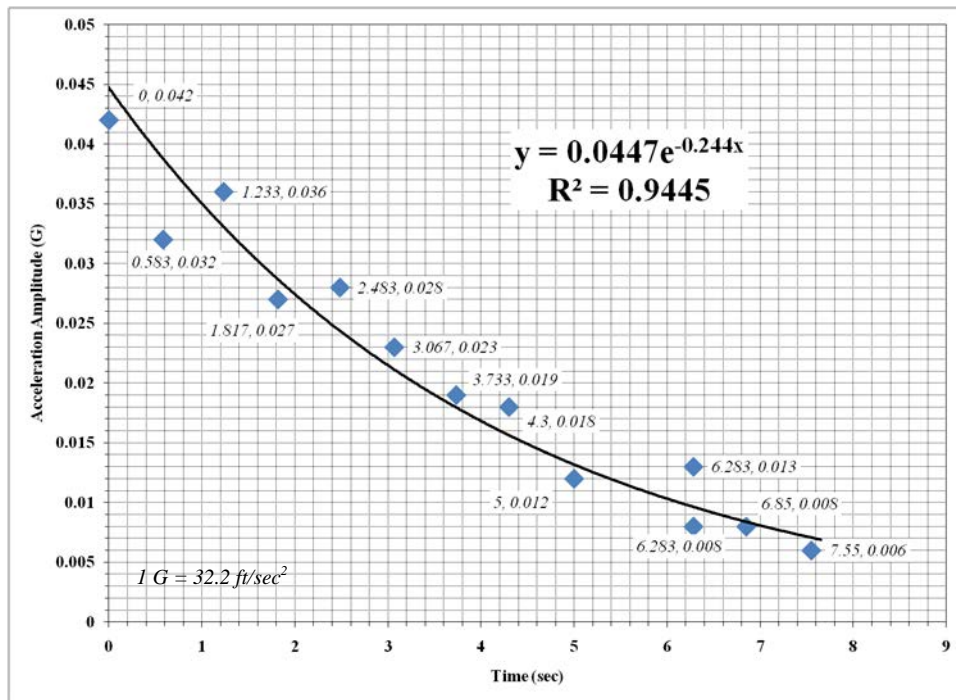


Figure 8-14. Trendline of extracted peak amplitudes used for the determination of the rate of decay

$$y = Ae^{-\xi\omega t} = 0.0447e^{-0.244x} \quad [\text{Eq. 8-4}]$$

where

$$A = 0.0447 \text{ G}$$

$$-\xi\omega t = -0.244x$$

$$t = x$$

and with

$$\omega = 1.61 \text{ Hz} = 10.116 \text{ rad/sec (Mode 1)}$$

therefore

$$-\xi\omega t = -0.244x$$

$$\xi = \frac{0.244}{10.116} = 0.02412 = 2.41\% \quad [\text{Eq. 8-5}]$$

This process was performed for the upper positive peaks and lower negative peaks for each transient truck event measured. The results of the modal damping analysis for the horizontal and vertical modal shapes are listed in Table 8-3. The larger damping value for mode 2 was attributed to an additional aerodynamic damping of the sign as it vibrated horizontally.

Table 8-3. Modal damping results of the horizontal and vertical modes of vibration

Mode	Shape	Damping Value from Loading Events					Average
		1	2	3	4	5	
2	Horizontal	0.374%	0.340%	0.345%	0.391%	0.357%	0.361%
3	Vertical	0.113%	0.097%	0.118%	0.157%	0.109%	0.119%

Section 9

Experimental Calculation of the Fatigue Load due to Natural Wind Gust

Overview

The experimental methodology and calculation of the fatigue load due to natural wind are presented in this section. Only collected data with wind velocity greater than 9 mph (4 m/s) and directed onto the front face of the structure were used. A three second average was used for data reduction in order to be applicable with the drag coefficients specified in the *Supports Specifications*. The fatigue load was based on an upper to lower peak-to-peak stress range and representative of an equivalent static wind load that would produce equivalent stress ranges as the dynamic loading environment.

The analysis procedure of the experimentally collected data was divided into two distinct components:

- Structural excitation, and
- Structural response.

The measurements obtained from the anemometers were used to evaluate the excitation component. The measurements made from the accelerometers and strain gauges were used to evaluate the structural response component.

Fatigue Load Calculation Approach

The equivalent static wind load approach was used in determining the fatigue load due to natural wind. The same approach was performed on both support structures analyzed with this project. The excitation and response of the structure was measured experimentally. The behavior was dynamic in nature. An equivalent static wind load was back-calculated from the measured response values that would produce the same dynamic response of the structure in terms of the maximum peak-to-peak stress ranges.

The experimental data collected was analyzed in the same fashion as the development of the natural wind fatigue provisions in the *Supports Specifications*, except for using experimental data in place of theoretical values. This was done precisely in order to develop a strong comparison of the experimental data collected with this project and the fatigue load generated from the data to the fatigue load specified in the fatigue provisions of the *Supports Specifications*. The comparison was used to assess the accuracy of the *Supports Specifications*.

Wind directionality unit vectors were formed from the experimentally obtained wind data. Peak-to-peak stress ranges were determined from the experimentally obtained strain gauge data. These processes are detailed in the **Structural Excitation** and **Structural Response** subsections. A stress element was formed using a combined loading analysis through theoretical structural analysis procedures as a function of wind directionality. Finite element analysis (FEA) was utilized for the structural analysis to develop the stress element. The stress element was then used in the back-calculation procedure to determine the equivalent static wind load that would produce the same peak-to-peak stress range determined experimentally. This process is detailed in the **Wind Pressure Back Calculation** section. The back-calculated wind pressure was set with its corresponding average wind velocity for each three second interval. The data was then filtered at 1 mph (0.447 m/s) intervals to develop a wind speed versus wind pressure plot. The infinite-life approach was performed to determine the wind pressure at the fatigue wind.

A general description of the methodology and evaluation of the experimental data went as follows:

1. Wind velocity directionality unit vectors were developed to describe natural wind loading orientations,
2. Maximum peak-to-peak stress ranges were determined,
3. Equivalent static wind pressures were back-calculated using the stress ranges and loading unit vectors,
4. The pressures were categorized to their corresponding wind velocities and plotted,
5. The wind velocity corresponding to a 0.01% probability of exceedence was determined, and
6. The pressure corresponding to the 0.01% exceedence probability was extracted from the plot.

Structural Excitation

The structural excitation was developed using the experimentally collected anemometer data. The data was in the form of wind velocity and direction. The data was averaged every three seconds in order to be applicable with the drag coefficients specified in the *Supports Specifications*. Three dimensional wind velocity unit vectors were developed from the collected data. The unit vectors provided the orientation of the wind loading on structure to further develop free body diagrams and structural analysis for the wind pressure back-calculation.

Reduction of Structural Excitation Experimental Data

The collected excitation data determined as usable was further reduced for analysis. Usable data represented wind velocity greater than 9 mph (4 m/s) and directed onto the front face of the structure. The direction of the wind velocity vector was transformed from the compass bearings used for experimental measurement, to polar bearings for data analysis. A wind directionality

unit vector was developed to use in the back-calculation for determining the equivalent static wind load.

Averaging Time The data streamlines were averaged every three seconds in order to be in compliance with the drag coefficients and height coefficients available in the *Supports Specifications* for wind loading analysis. It was representative of an instantaneous value.

Transformation from Compass Bearings to Polar Bearings The magnitude and direction of the wind velocity vector was broken down into North (Y component) and East/West (X component) components. The North direction was oriented in the direction opposite of the front face of the structure, in the direction traffic. This was done to avoid the cross-over issue from 360° to 0°, since the data collected that was usable was oriented on the front face of the structure. The data was transformed from compass bearings to polar bearings. An average of the components for every three seconds was taken. The wind velocity vector was then formed for each three second window.

Wind Directionality Unit Vector A wind directionality unit vector was formed after the excitation was transformed from compass bearings to polar bearings. The unit vector was developed into Cartesian coordinates (\underline{i} , \underline{j} , \underline{k}). This was done in order describe mathematically where the wind velocity, and subsequent wind pressure load, was directed for back-calculation of the equivalent static wind load. Using the polar coordinates, the unit vector was calculated by the following system of equations:

$$\begin{aligned}\underline{\lambda} &= (\lambda_x \underline{i} + \lambda_y \underline{j} + \lambda_z \underline{k}) \\ &= \left[\left(\frac{V_x}{V} \right) \underline{i} + \left(\frac{V_y}{V} \right) \underline{j} + \left(\frac{V_z}{V} \right) \underline{k} \right] \\ &= [(\cos \beta \cos \alpha) \underline{i} + (\cos \beta \sin \alpha) \underline{j} + (\sin \beta) \underline{k}]\end{aligned}\quad [\text{Eq. 9-1}]$$

where

$\underline{\lambda}$ = wind directionality unit vector

α = wind orientation along the horizontal plane (xy - plane) measured from AN - 1

β = wind orientation along the vertical plane (zy - plane) measured from AN - 2

A schematic of the coordinate system for the unit vector directionality is shown in Figure 9-1.

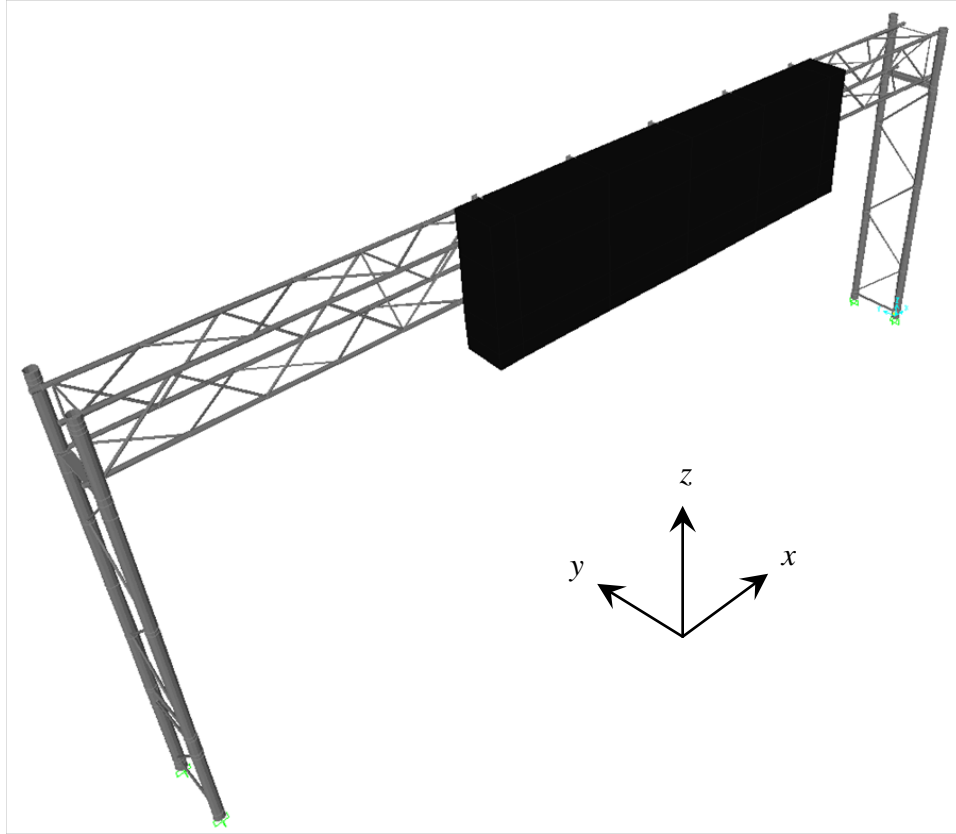


Figure 9-1. Coordinate system used to develop the wind directionality unit vector

A wind velocity directionality unit vector was formed for each three second averaging window for all usable data collected. The unit vector represented the direction of the structural excitation with respect to the coordinate system shown in Figure 9-1. The magnitude of the wind velocity was proportional to the magnitude of the wind pressure to be back-calculated from the measured structural response.

Structural Response

The structural response analysis involved the strain gauge data corresponding to the usable wind data (data was measured simultaneously in the field). The same three second averaging window of the structural excitation was used for the analysis. The major outcome was to determine the experimentally measured stress ranges from the measured structural excitation to back-calculate the equivalent static wind load and subsequent calculation of the fatigue load.

Data Offsetting

The first step involved the offsetting procedure to generate the true strain time history from the collected raw data. Wind velocity occurs randomly in nature and cannot be controlled manually.

For this reason, the zeroing of the gauges before testing in the field was not representative of a true no-strain condition. The structure was continually vibrating because of the wind velocity presence, and the zeroing of the scales occurred during backward and sometimes forward vibratory movement which was unavoidable. The solution was to perform an offsetting procedure on the collected data to offset the strain value to be representative of a non-vibratory state.

Important for this process was the simultaneous collection of strain and wind velocity data. The strain data collected during each run was filtered with respect to its corresponding collected wind velocity. This was done in +/- 0.5 mph (0.224 m/s) wind velocity magnitude intervals. The strain values that occurred during each interval were determined and averaged together. The values were plotted on a wind velocity versus strain diagram (see Figure 9-2). For example, all strain values occurring during a 3.5 to 4.5 mph (1.56 to 2.01 m/s) interval were averaged and plotted as a 4 mph (1.79 m/s) data point. The data formed a parabola, which adhered to the fluid mechanics relationship between wind force and the square of wind velocity.

A regression analysis was performed to determine a best fit line of the plotted data. This was done through a transformation regressor linearization process. The independent variable (wind velocity on the abscissa axis) was squared. It was plotted versus its corresponding averaged strain (see Figure 9-3). The linearization of the data proved the purely parabolic nature of the data. A best fit line was then constructed as a linear predictor. The intercept of the trendline on the ordinate axis indicated the strain value to offset. For example, the offset for the data run presented in Figure 9-3 was 1.1501 microstrain. This means that when the strain gauges were zeroed during the testing procedure, the structure was vibrating because of the continuous wind excitation, and at the moment of zeroing an approximate magnitude of 1.1501 microstrain was induced onto the structure. This is evident from Figure 9-3 at the zero squared wind velocity point.

Returning to Figure 9-2, a line was plotted to fit the data based on the information gathered from the transformation (Figure 9-3). As shown in Figure 9-3, the slope of the trendline was the slope of the parabola, and the y-intercept of the trendline was the y-intercept of the parabola. Plotting a line on Figure 9-2 using the transformation regressor values is shown in Figure 9-4. Once the trendline was produced for the parabolic data, the offset (1.1501 for the example data sample in Figure 9-4) was subtracted from the trendline to produce an accurate zeroed time history. The offset plot is shown in Figure 9-5. As a side note, the plot in Figure 9-5 can be used to project strain values for higher wind velocities than that used for fatigue analysis. For instance, Figure 9-6 shows the plot projected to a 90 mph (40.2 m/s) wind, which is used for capacity calculations and design.

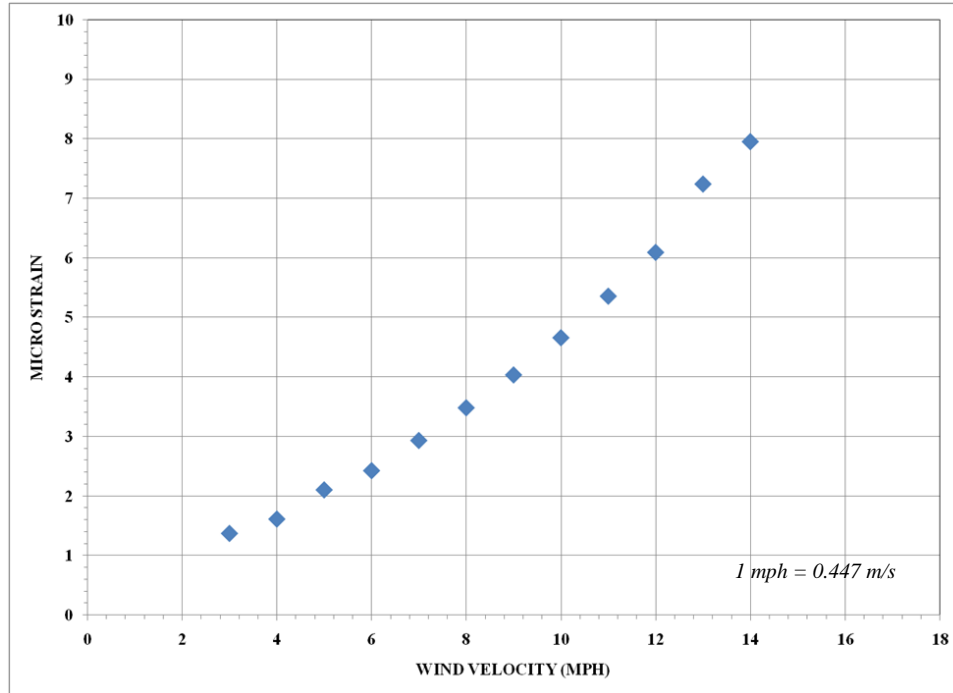


Figure 9-2. Filtered strain values in 0.5 mph wind velocity intervals used for the data offsetting procedure

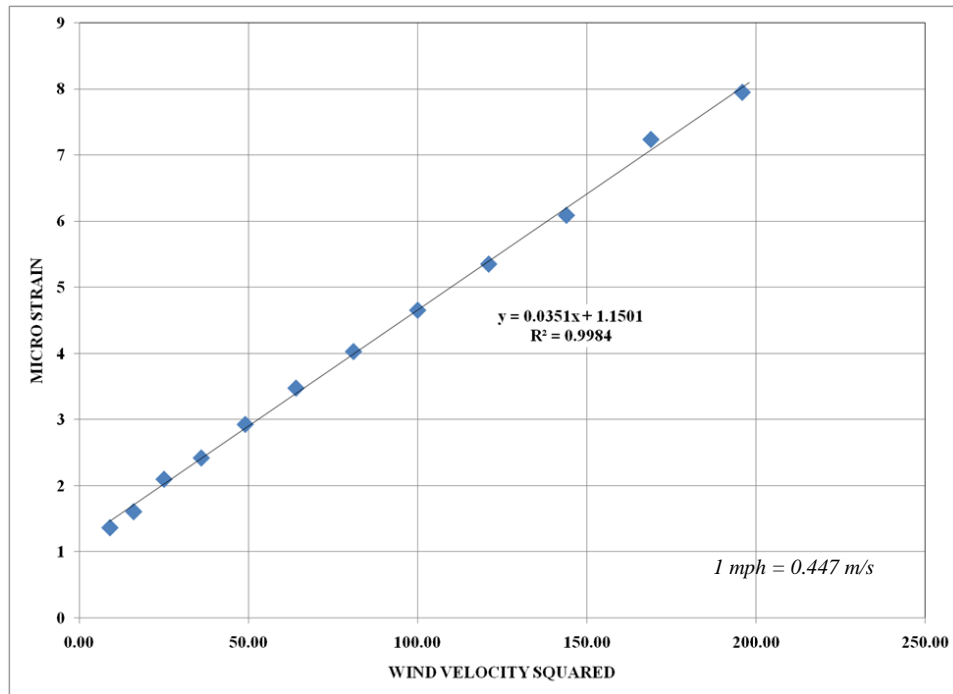


Figure 9-3. Transformed regressor for the linearization process used in the data offsetting procedure

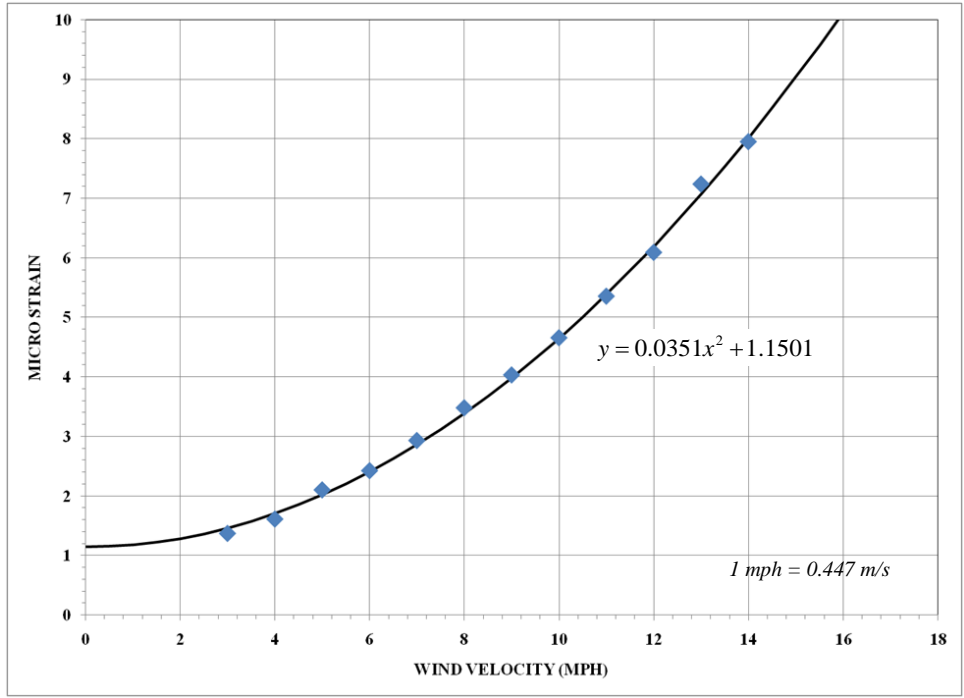


Figure 9-4. Parabolic curve fit obtained from the linear transformation showing the y-intercept

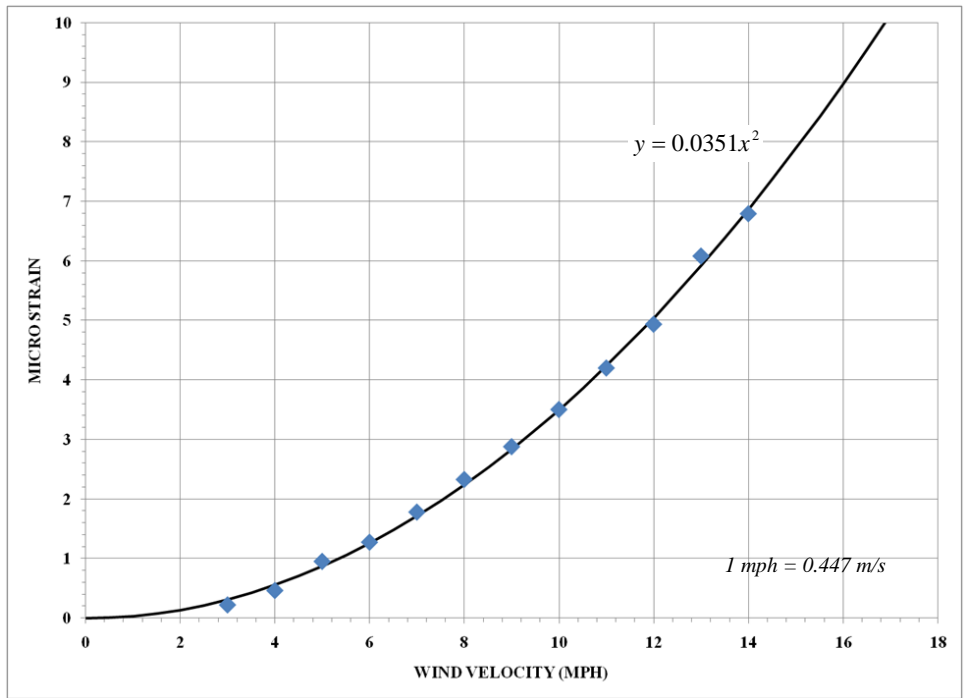


Figure 9-5. Parabolic trendline with the y-intercept offset

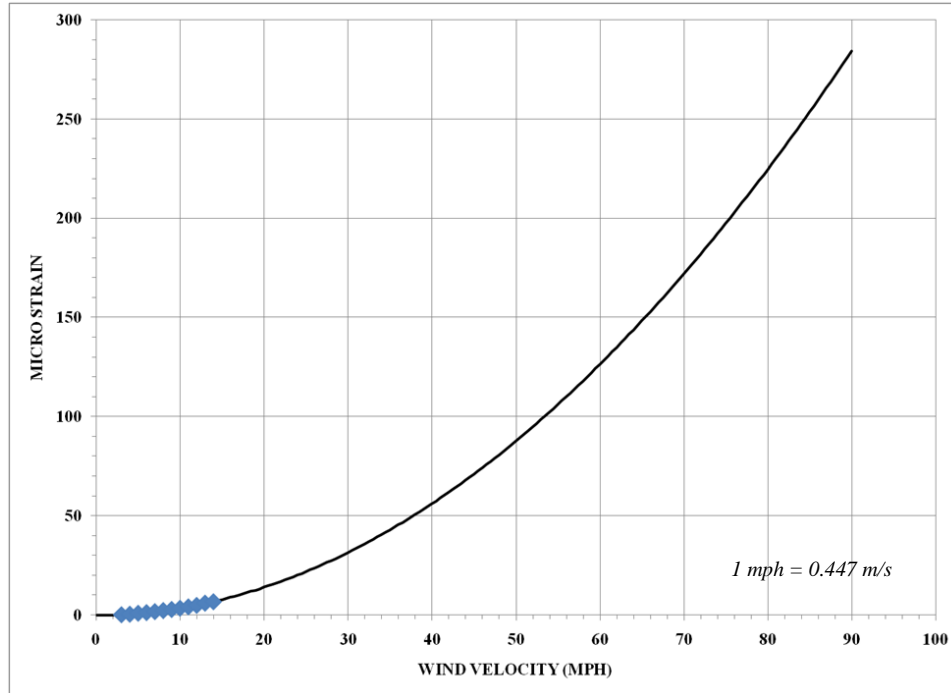


Figure 9-6. Trendline projection to the 90 mph (40.2 m/s) wind velocity

A systemized procedure of the offsetting process used for this project is numerated as follows:

1. Filter the collected strain data in +/- 0.5 mph (0.224 m/s) intervals corresponding to the wind data collection,
2. Strain values from each interval were averaged,
3. Averaged strain values versus the wind velocity interval were plotted to test correspondence with force and wind velocity as a parabola,
4. The data was transformed into a linear plot by squaring the independent variable (wind velocity),
5. The transformed wind data was plotted with its corresponding averaged strain to test the linearization process,
6. A regression was performed on the transformed data to generate a linear best fit trendline,
7. The trendline was projected to determine its intercept with the ordinate axis, and
8. The intercept value was subtracted from the raw strain data time history streamline to produce the true strain time history.

The offsetting procedure described was done for each strain gauge time history of the data collection. It produced the true strain values to account for zeroing the instrumentation during wind velocity excitation. To lessen the magnitude of the offset, the ALDOT team was encouraged to zero the instrumentation and begin data collection when the wind velocity was

relatively low. Since zeroing at exactly a zero wind velocity was practically impossible, the offset procedure was implemented to all data.

Strain Ranges

The next step was analyzing the offset data to determine the strain range. The offset data was averaged every three seconds. The maximum and minimum values within each three second window were determined and subtracted from each other. The result was the maximum peak-to-peak range within each three second window. Other parameters such as the standard deviation and peak-to-standard deviation ratio were determined for each three second window for behavioral purposes. An example of a typical peak-to-peak range calculation, represented in a plotted streamline, is shown in Figure 9-7.

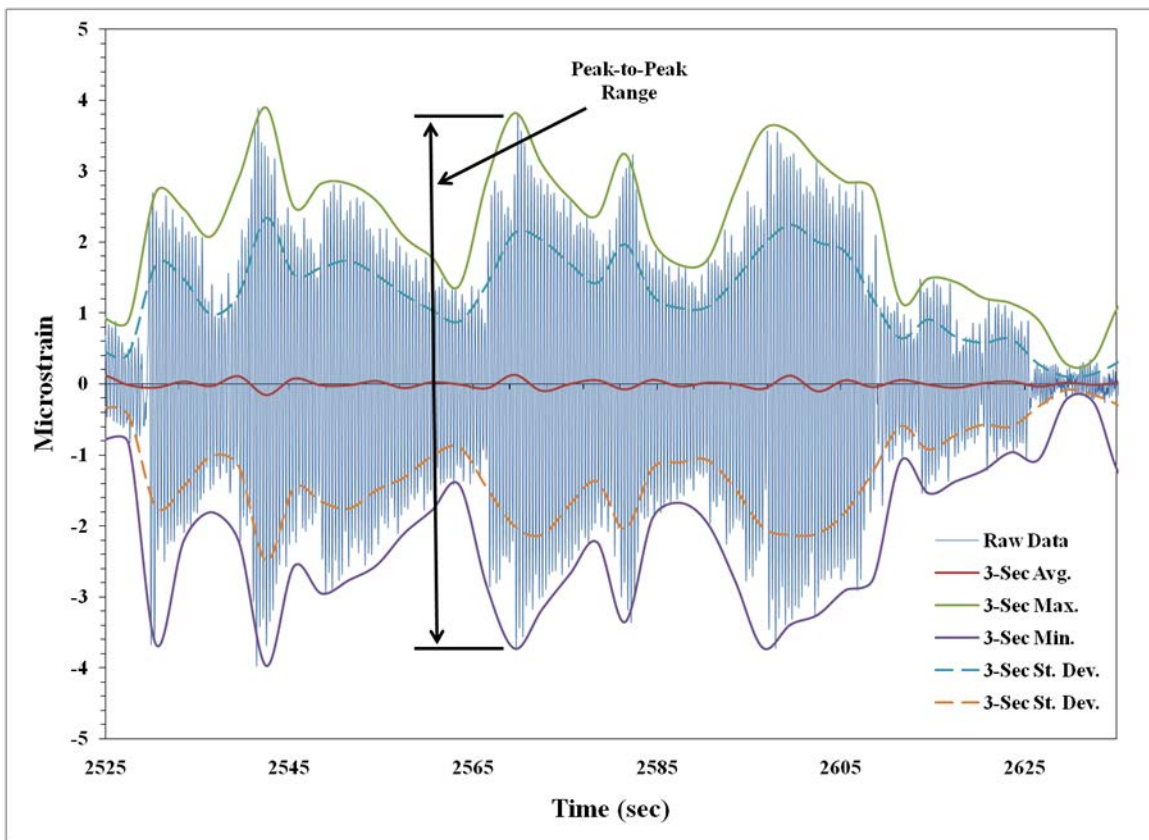


Figure 9-7. Peak-to-peak range of the experimentally collected strain gauge data

Wind Pressure Back-Calculation

The equivalent static wind load that would produce the same peak-to-peak stress range determined experimentally was back-calculated. An example of the stress range is shown in

Figure 9-7. The three second ranges and wind directionality unit vectors were used for this calculation. Three measures formed the basis of the back-calculation procedure:

- 1st. A theoretical structural analysis was conducted to develop a relationship between the excitation and the response of the structure as a function of the wind direction. Equations representing stress and strain finite elements as a function of wind directionality and based on a unit wind pressure load were developed at each strain gauge location.
- 2nd. The experimentally obtained wind directionality unit vectors that were developed in the **Structural Excitation** subsection were applied to the equations to determine the theoretical response of the structure as it relates to the direction of the wind measured experimentally.
- 3rd. A ratio was developed that relates the theoretical response from the unit pressure load to the experimentally obtained peak-to-peak strain ranges that were determined in the **Structural Response** subsection from a variable wind pressure. The wind pressure was solved and the back-calculation procedure was completed.

The process was performed for each strain gauge and three second interval resulting in an instantaneous wind pressure based on the wind direction and the structural response of the structure. Since the wind pressure that was back-calculated represents the peak-to-peak stress range determined from the response, all structural dynamics and response amplification were included in the calculation.

Theoretical Structural Analysis

Finite element analysis (FEA) was used to conduct the theoretical structural analysis for the support structure. A model was developed based on the shop drawings of the structure and was used to determine the internal reactions at the strain gauged locations. A detailing of the FEA model is provided in **Section 14: Finite Element Analysis**. A picture of the model is shown in Figure 9-1.

The exposed areas of the structure in relationship to the data determined as usable were compiled. Drag and height coefficients provided by the *Supports Specifications*, which were developed using three second wind averages in previous studies, were determined for each member exposed to wind and used in the FEA. Stress and strain elements were formed in a combined loading analysis from the results of the FEA. The wind pressure magnitude was then solved to conclude the back calculation. A list of the major steps with this process is numerated as follows:

1. Determine the exposed areas of the structure for the limitations set for filtering the collected data as usable.
2. Further segment the exposed areas to account for the height coefficients that differ with increasing height.

3. Determine the drag coefficients for each member of the exposed areas. This included the truss members, uprights, struts, and VMS.
4. Develop the loading input for the FEA model. Apply the loading in all directions within the limitation set for filtering the collected data as usable. Apply as a 1 psf (47.9 Pa) unit load multiplied by the height coefficient and drag coefficient corresponding to the particular member and height above ground level. For the pipe members, apply the FEA load as a uniformly distributed load per foot. For the VMS, apply as an area load.
5. Run the FEA solution and determine the internal response reactions versus the load direction (angle) at the locations of the strain gauges.
6. Develop stress and strain elements versus wind directionality plots for each strain gauge using a combined loading analysis. Construct equations of the strain as a function of the wind directionality through regression analysis on the developed plots.
7. Calculate the FEA strain, ϵ_{FEA} , using the developed functions for each three second interval of the wind directionality vectors obtained experimentally.
8. Set up the ratio, $1/\epsilon_{FEA} = P/\epsilon_{Exp}$, to determine the wind pressure for each three second interval (ϵ_{Exp} represents the experimental maximum three second interval peak-to-peak ranges).

Exposed Area Breakdown The front and the sides of the structure were exposed to wind pressure from the wind data determined as usable. Each face was divided into individual segments for structural analysis. The segmented division depended on the type of member exposed. The front face of the structure contained three segments, front sign, front truss, and front uprights. The side of the structure was segmented into two areas: East side face and the West side face. An illustration of the exposed areas to wind pressure used for the structural analysis is shown in Figure 9-8 through Figure 9-10. The exposed area segments were further broken down into additional segmentation to account in the variation of wind pressure with height (detailed in the next section).

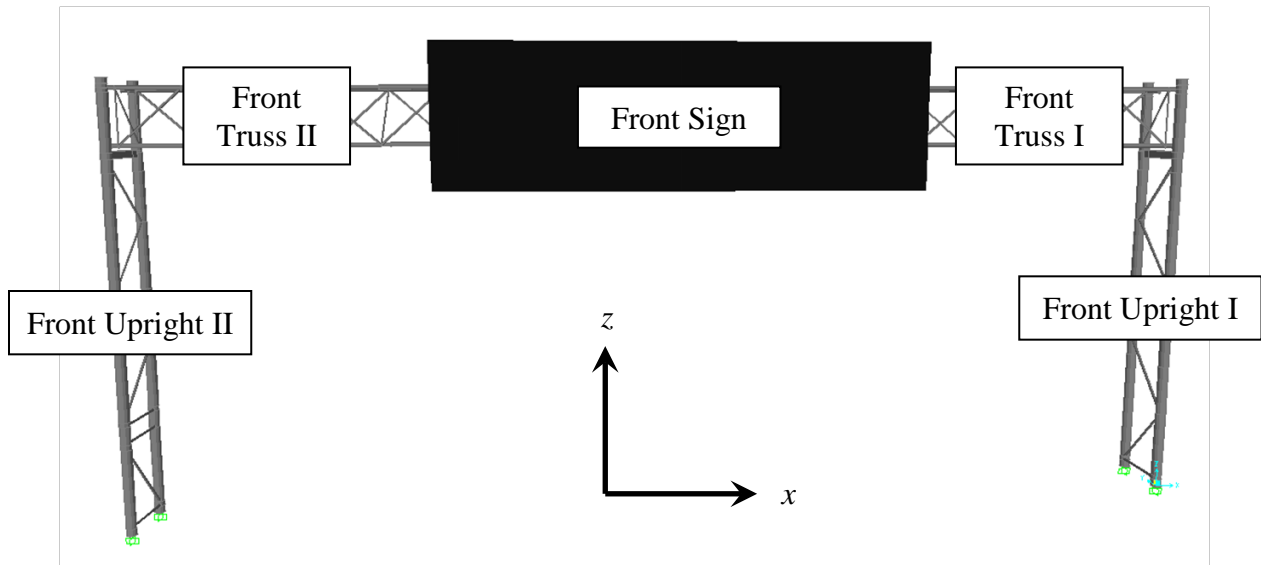


Figure 9-8. Area breakdown of the front face of the bridge-type VMS support structure

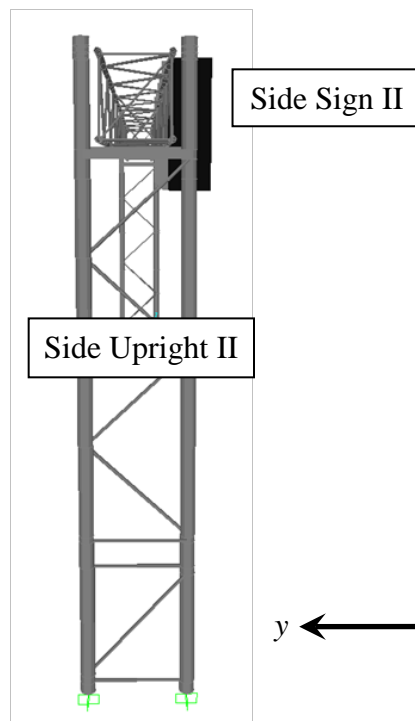


Figure 9-9. Area breakdown of the East side face of the bridge-type VMS support structure

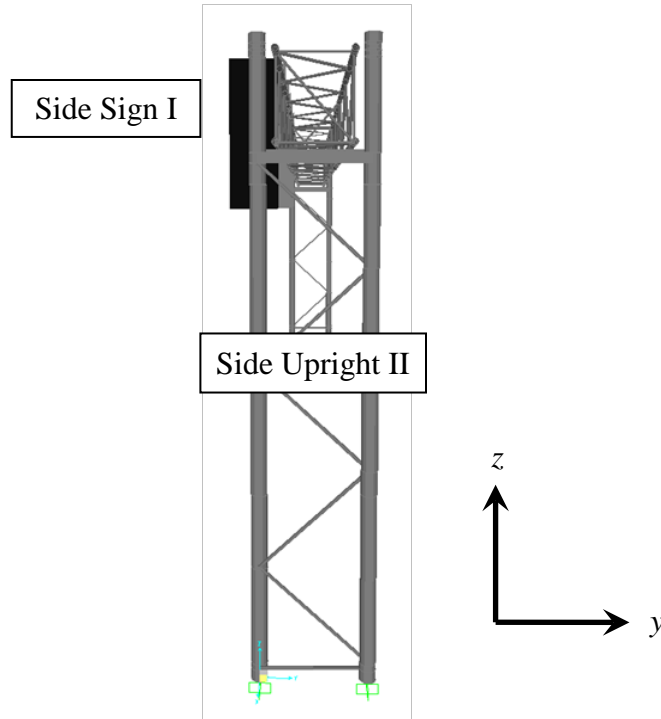


Figure 9-10. Area breakdown of the West side face of the bridge-type VMS support structure

Exposed Area Segmentation The exposed areas were further segmented to account for the changing values associated with the height coefficient. The height coefficient changes with increasing height from the ground level. A value was obtained for each member at the specified levels that correspond to separate coefficients.

Height Coefficient. All height coefficients were calculated based on Table 3-5 of the *Supports Specifications*. Exposure condition C (open terrain with scattered obstructions) was used for the calculation. The height coefficient represents a change in turbulence of wind pressure, becoming less turbulent and more stable as the height above ground level increases. The coefficient used in the *Supports Specifications* was defined using the power law of the wind velocity profile with respect to height above ground level shown in Eq. 9-2. The curved profile with height defined by Eq. 9-2 was simplified into a stepped profile by the *Supports Specifications* and is shown in Figure 9-11. This profile, as it applies to the bridge-type VMS support structure, is shown in Figure 9-12, demonstrating the height coefficient assigned to the members at each of the levels of the specified stepped profile.

$$v_w = v_{10} \left(\frac{h}{h_{10}} \right)^\alpha \quad [\text{Eq. 9-2}]$$

where

v_w = wind velocity

v_{10} = wind velocity at a reference height of 32.8 ft (10 m); normalized at 1.0

h = height above ground level

h_{10} = reference height of 32.8 ft (10 m)

α = terrain constant equal to 0.16 for neutral air above flat open coast.

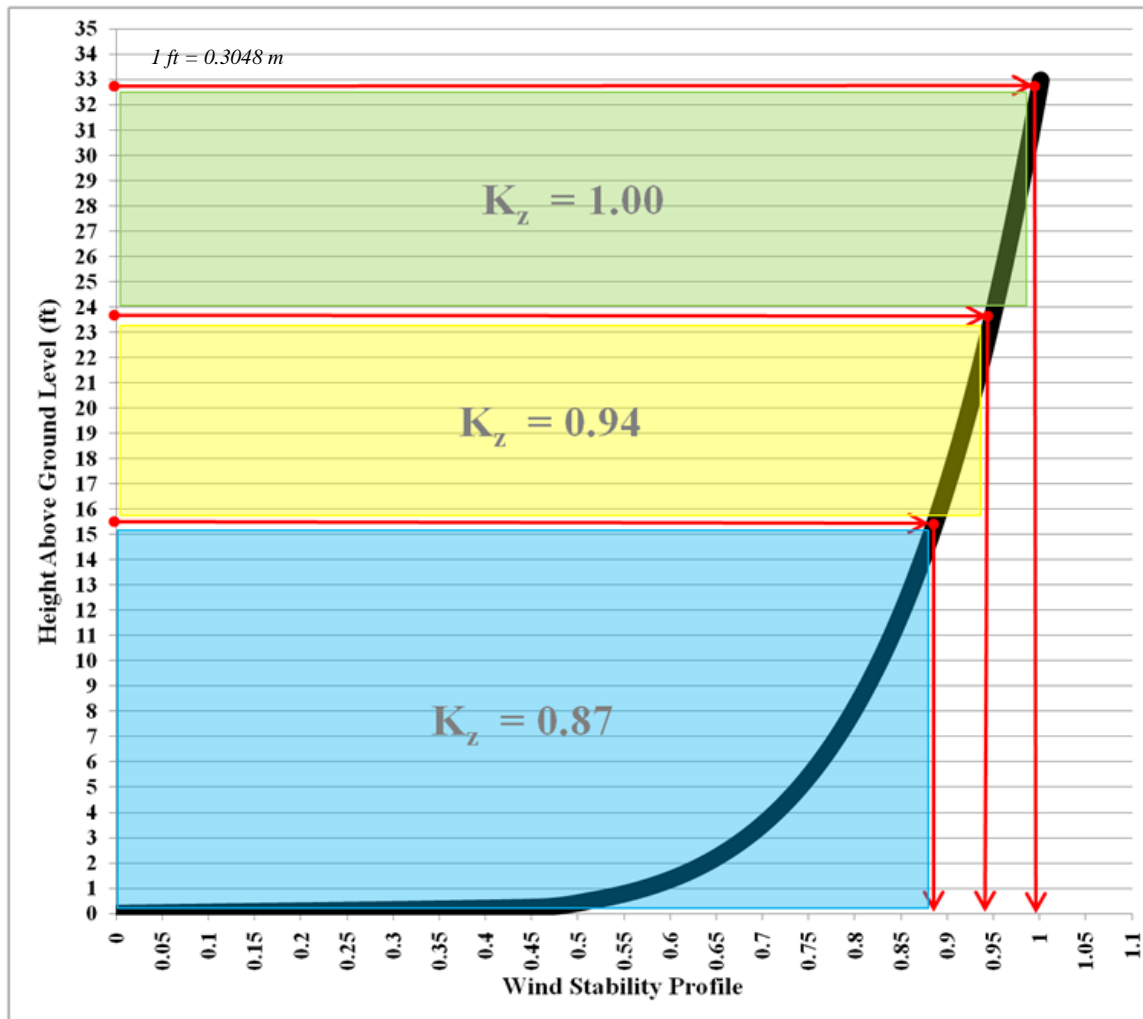


Figure 9-11. Height coefficient stepped profile based on the provisions of the *Supports Specifications*

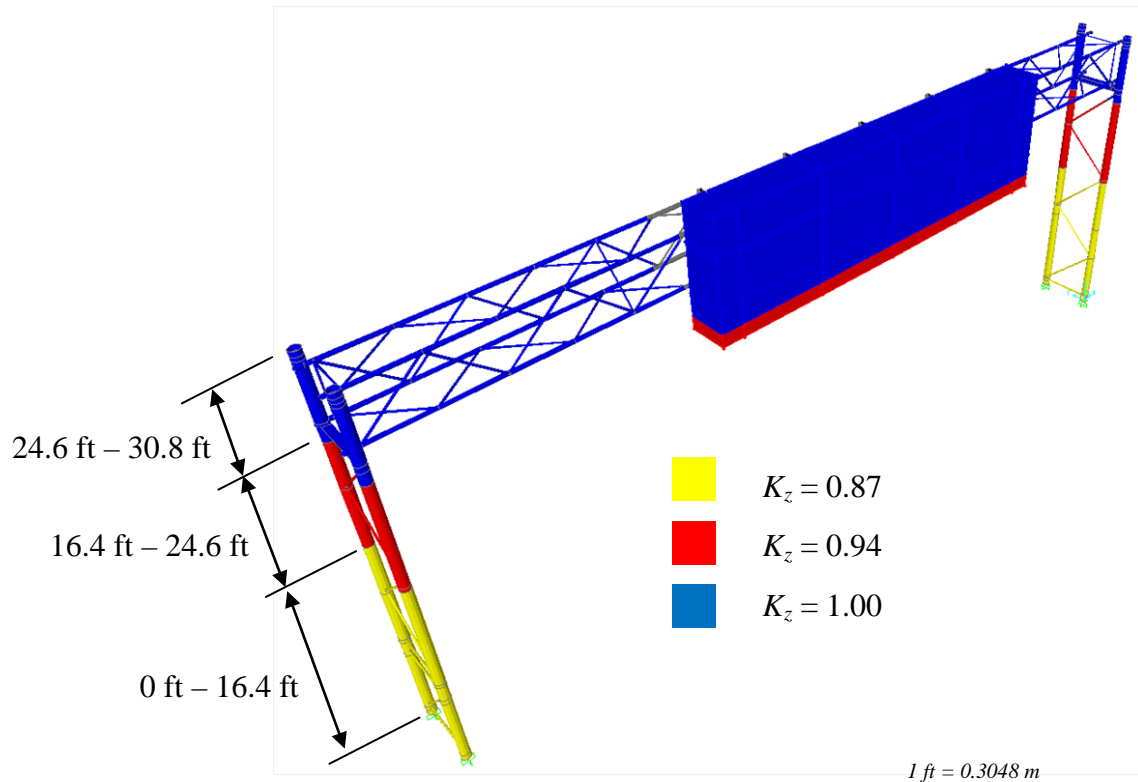


Figure 9-12. Segmented exposed areas corresponding to the stepped profile of the height coefficient, K_z

Drag Coefficient All drag coefficients were calculated using Table 3-6 of the *Supports Specifications*. Fifty year design life was used in the calculation with a velocity conversion factor equal to 1.00 (no conversion needed). The results are listed in Table 9-1. A value of 1.2 was used the chord members to account for the effect of two members in front of the other on the horizontal plane because angled wind directions would otherwise not be applied, 1.1 was used for all web members and upright posts, and 1.7 was used for the VMS sign.

Table 9-1. Drag coefficients used for the members of the support structure

Member	Exposed Area	Drag Coefficient, C_d
Upright Posts	Front & Side Upright I & II	1.1
Upright Horizontal Struts	Side Upright I & II	1.1
Upright Diagonal Struts	Side Upright I & II	1.1
WT Sections (WT6X13)	Side Upright I & II	1.7
Truss Horizontal Struts	Side Upright I & II	1.1
Truss Internal Diagonals	Side Upright I & II	1.1
Truss Vertical Struts	Front Truss I & II	1.1
Truss Vertical Diagonals	Front Truss I & II	1.1
Truss Chords	Front Truss I & II	1.2
VMS	Front Sign & Side Sign I & II	1.7

Finite Element Analysis Loading Input The load was inputted into the FEA software as uniformly distributed loads per length for all pipe members, and area pressure loads for the VMS. A 1 psf (47.9 Pa) unity wind pressure load was used and multiplied by the drag and height coefficients assigned to the members. This was referred to as the effective load. It was applied at all angles ranging from 45° to 135° as shown in Figure 9-13 to account for the wind directionality. A generalized equation used to calculate the effective load for the pipe members is shown as Eq. 9-3 and for the VMS as Eq. 9-4.

$$\omega = \underline{\lambda}[P(C_d K_z)\phi] \quad [\text{Eq. 9-3}]$$

$$\Omega = \underline{\lambda}[P(C_d K_z)] \quad [\text{Eq. 9-4}]$$

where

ω = uniformly distributed load applied to the pipe members, lb/ft (N/m)

Ω = uniformly distributed load applied to the VMS, psf (Pa)

$\underline{\lambda}$ = wind directionality unit vector

P = unit wind pressure, 1 psf (47.9 Pa)

C_d = drag coefficient

K_z = height coefficient

ϕ = pipe diameter, ft (m)

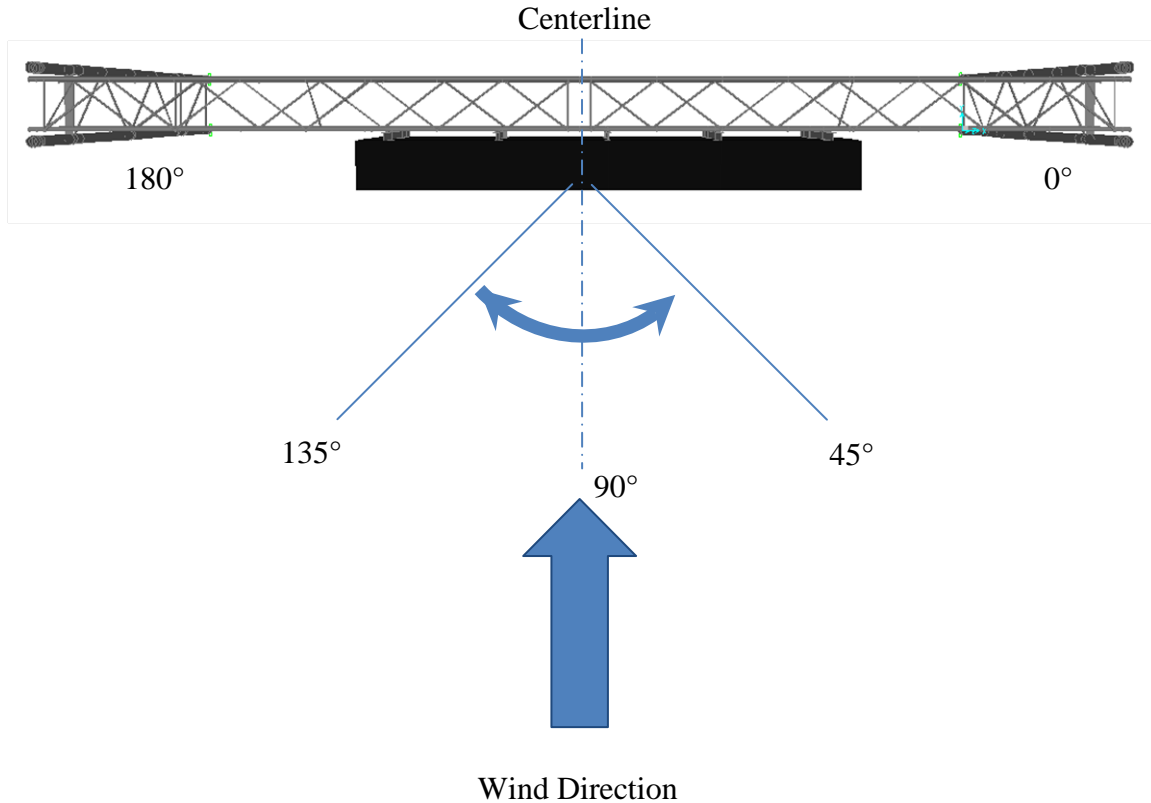


Figure 9-13. Wind directionality of the loading input ranging from 45° to 135° onto the front face

Finite Element Analysis Solution A $P-\Delta$ analysis and linear-static solution was conducted by the FEA program. The $P-\Delta$ analysis was solved first to obtain the stiffness of the structure that accounted for the dead load and the offsetting weight of the VMS. The stiffness determined from the $P-\Delta$ analysis was then used in the linear-static solution for the loading scenarios. Importantly, the loading inputted into the FEA program was representative a unit load.

Internal reactions obtained at the strain gauged locations were extracted from the linear-static solution. This included all moment and axial forces. The moments were considerably small at these locations, which was the basis for the positioning of the strain gauges to simplify the structural analysis. Plots were made of the internal reaction versus the wind directionality. An example of these plots is shown in Figure 9-14 for the strain gauge labeled as SG-4 located on the North post of the upright. The plot shows the internal unit axial reaction at this location. It is evident from the plot that the axial reaction is in compression, which should be the case with the wind applied to the front of the structure, and the reaction reaches its maximum at 90° when the wind was applied exactly perpendicularly to the front face.

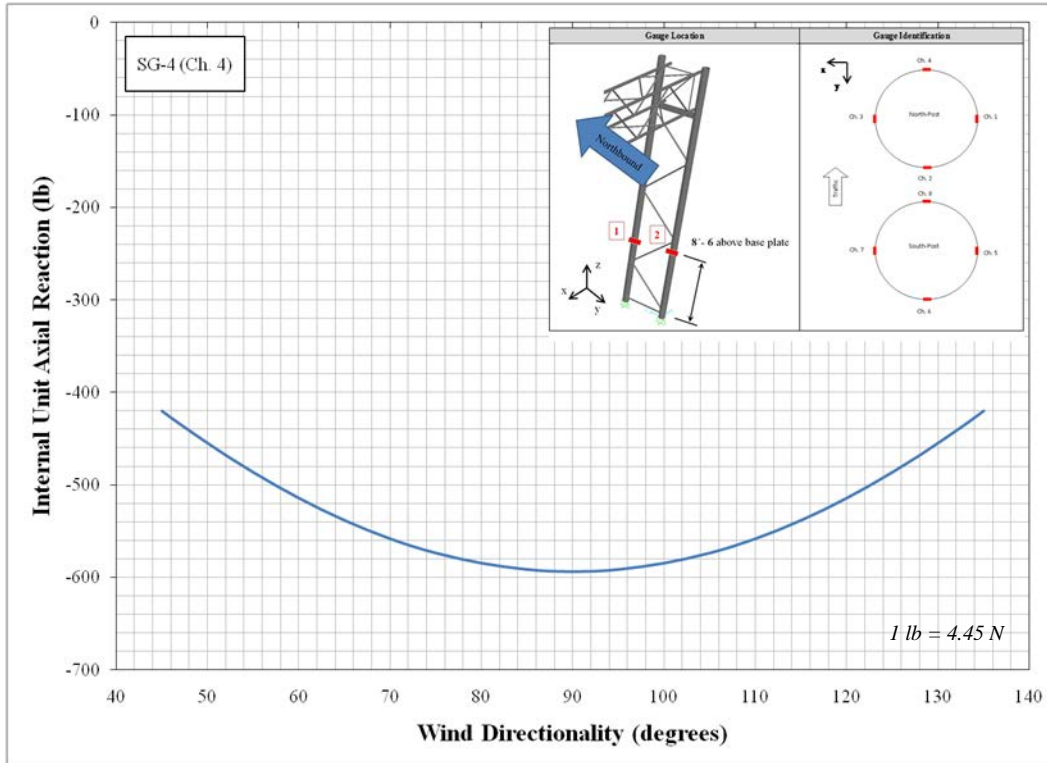


FIGURE 9-14. Internal unit axial reaction versus wind directionality at the location of SG-4

Stress and Strain Finite Elements Stress and strain finite elements were developed at each strain gauge locations. Plots similar to Figure 9-14 were constructed for each gauge and unit internal reactions. A combined loading analysis was conducted using the reactions to form finite stress elements (see Figure 9-15) at the gauged locations. The equations listed in Table 9-2 were used for this calculation. The stress elements were representative of the reaction because of the unit loading. The unit stress elements were further transformed into unit strain elements by using the modulus of elasticity of the structural members. Plots were constructed of the unit strain element versus the wind directionality. An example plot for the SG-4 example is provided in Figure 9-16. A regression was performed on the plots and an equation of the unit strain as a function of the wind directionality was formed. An example of the developed functions is shown in Figure 9-16.

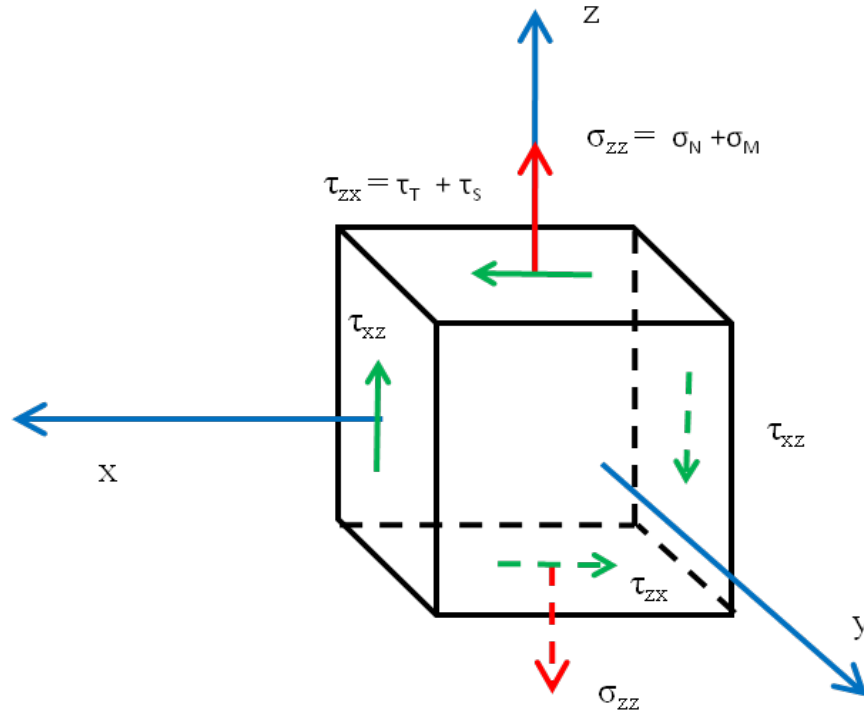


Figure 9-15. Typical stress element formed from the combined loading analysis

Table 9-2. Relevant stress and strain equations used for combined loading analysis

Stress	Stress Equation	Strain Equations
Normal	$\sigma_N = \frac{F_z}{A}$	$\epsilon_N = \frac{\sigma_N}{E}$
Torsion	$\tau_T = \frac{M_z \rho}{J_{ZZ}}$	$\gamma_T = \frac{\tau_T}{G}$
Unsymmetrical Bending	$\sigma_M = -\frac{M_x y}{I_{XX}} + \frac{M_y x}{I_{YY}}$	$\epsilon_M = \frac{\sigma_M}{E}$
Transverse Shear*	$\tau_s = \frac{FQ}{It} = \frac{2F}{A}$	$\gamma_s = \frac{\tau}{G}$

*for maximum transverse shear stress at neutral axis for thin walled pipes

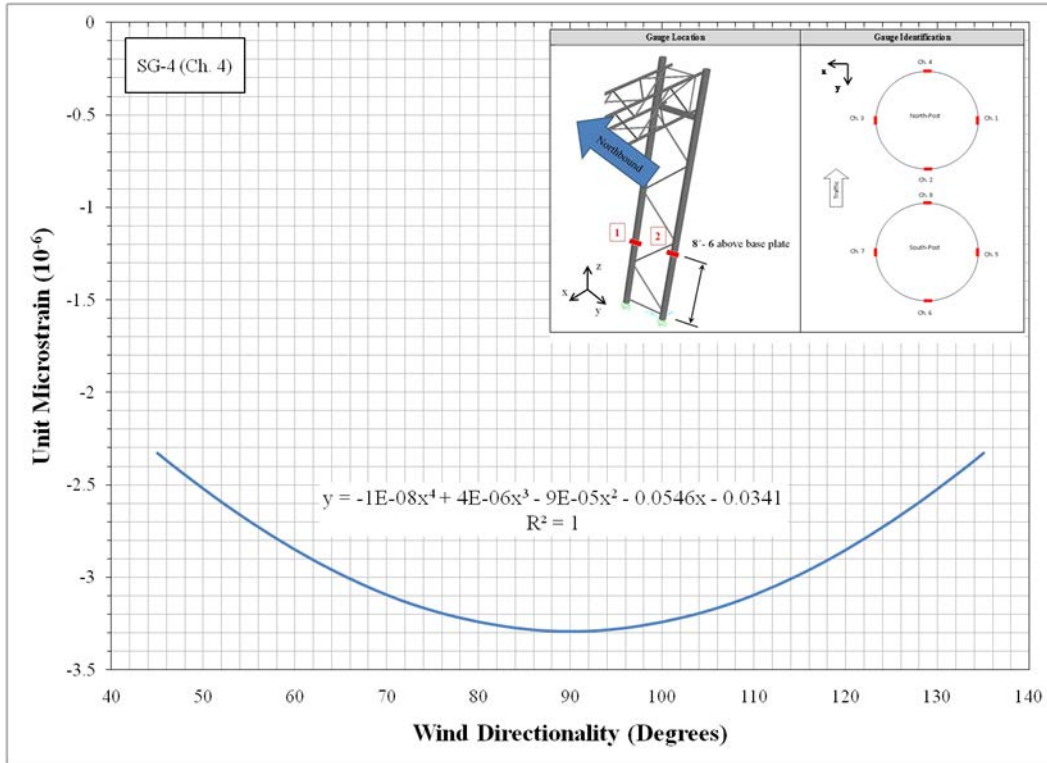


Figure 9-16. Internal unit microstrain versus wind directionality at the location of SG-4

Wind Pressure Calculation

Theoretical Unit Strain The theoretical unit strain based on the three second average wind directionality unit vectors formed from the experimentally obtained data (see subsection **Structural Excitation** for details) was calculated. The equations of the unit microstrain as a function of the wind directionality developed from the FEA were used for this analysis. The experimental wind directionality was plugged into the developed functions and the strain was calculated. The result of the calculation was representative of the theoretical unit strain based on the wind directions obtained from the experimental data. This process was done with the usable data collected experimentally for each strain gauge.

Pressure Ratio A ratio was set up to calculate the wind pressure using the theoretical unit strain and the peak-to-peak strain ranges collected experimentally. The wind pressure calculated from the ratio represented the equivalent static wind load in the form of a uniformly distributed load that would produce the peak-to-peak strain range. Knowing that the theoretical unit strain was developed based on a unit loading and the wind directionality unit vectors, the following ratio can be used to back-calculate the equivalent static wind load for each experimentally measured wind direction:

$$\frac{1 \text{ psf}}{\varepsilon_{FEA}} = \frac{P}{\varepsilon_{Exp}} \quad [\text{Eq. 9-5}]$$

Solving for the equivalent static wind load, P , provides the following relationship:

$$P = (1 \text{ psf}) \left(\frac{\varepsilon_{Exp}}{\varepsilon_{FEA}} \right)$$

where

P = equivalent static wind pressure, psf (Pa)

ε_{FEA} = theoretical unit strain

ε_{Exp} = experimental peak - to - peak strain range

The result is the maximum wind pressure occurring within each three second interval. It represents the equivalent static wind load that would produce the maximum three second peak-to-peak strain range measured experimentally.

Wind Velocity vs. Wind Pressure

The maximum wind pressure magnitude, P , occurring within each three second interval was calculated for all strain gauges located on the North and South uprights. The calculation was performed using Eq. 9-5. The calculated wind pressures were plotted versus their corresponding average three second wind velocity (average wind for the three second duration) and are shown in Figure 9-17.

A profound curve can be seen from the figure, characteristic to a parabola which coincides with the fundamental fluid mechanics relationship of proportionality between pressure and the velocity squared. The spread observed at higher velocities was because of the limited number of data points measured at that velocity range. A regression analysis was performed to determine a trendline of the plotted data to simulate the parabolic curve. This was done through a transformation regressor linearization process similar to the process performed for the offsetting procedure. An average was taken of the data points for all gauges at each wind velocity interval. The independent variable (wind velocity on the abscissa axis) was squared and was plotted versus its corresponding wind pressure magnitude (see Figure 9-18).

The linearization of the transformed wind velocity vs. wind pressure plot proved the parabolic nature of the data. A best fit line was then constructed as a linear predictor to acquire a linear equation of the transformed data. Reversing the transformation, and using the best fit line equation, a parabolic trendline of the data was produced and is shown in Figure 9.35. The slope of the developed trendline was equal to 0.0048, with a y-intercept equal to 0.0958.

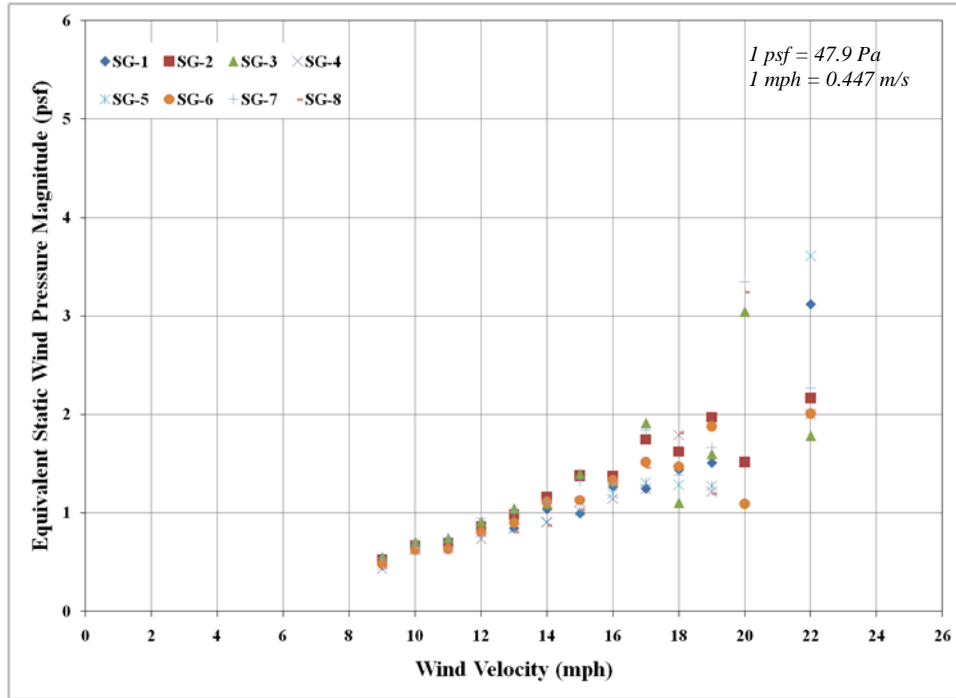


Figure 9-17. Wind velocity vs. wind pressure for the strain gauges located on the uprights

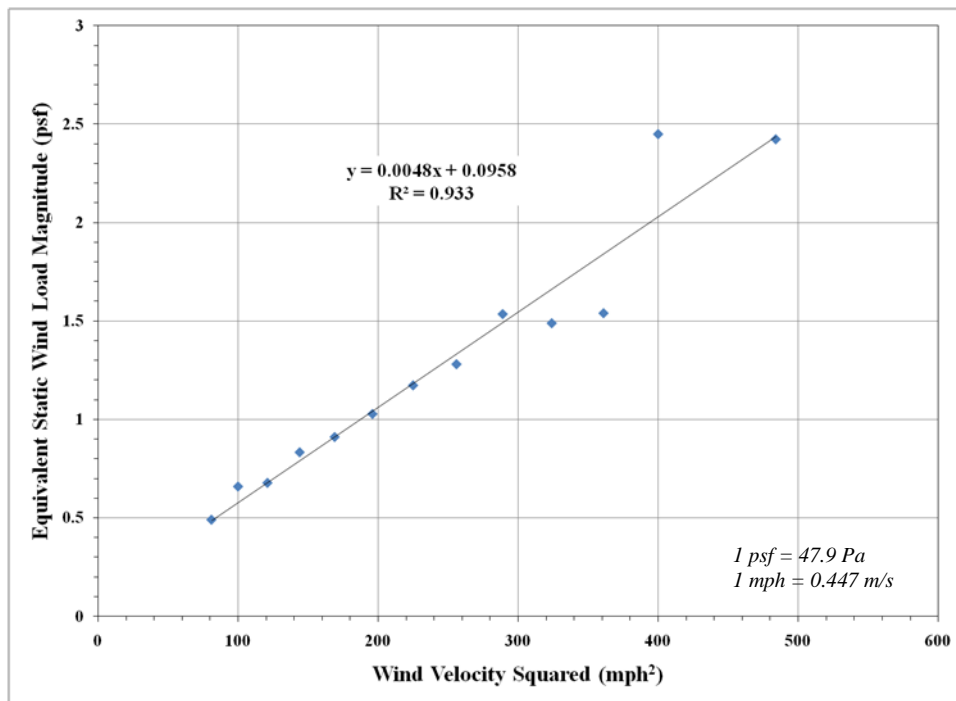


Figure 9-18. Transformed trendline of the wind velocity vs. wind pressure relationship

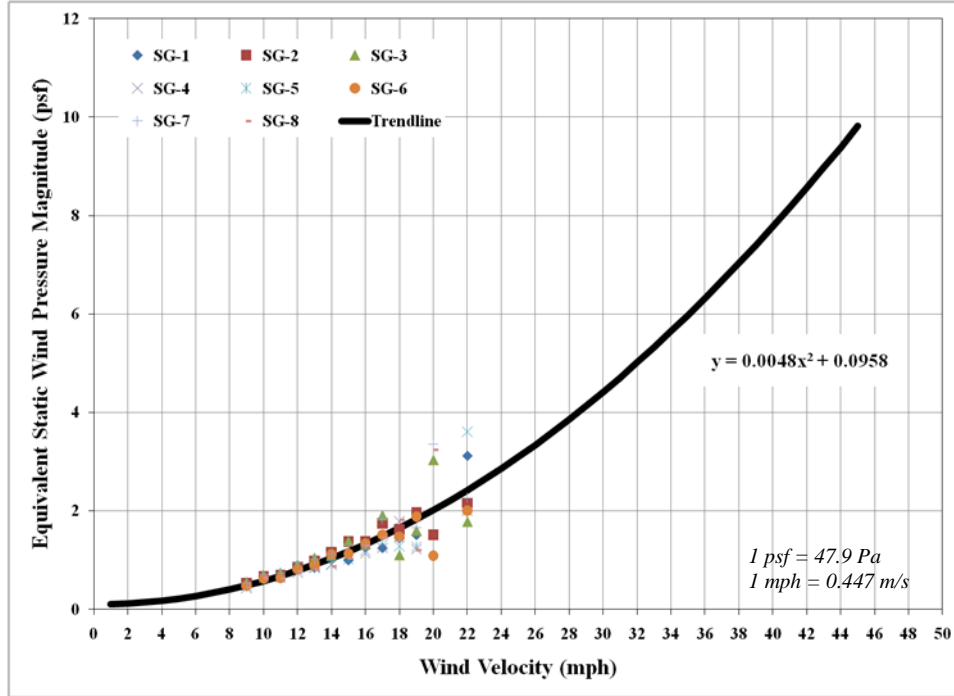


Figure 9-19. Wind velocity vs. wind pressure trendline for the strain gauges located on the uprights

Infinite-Life Approach

The infinite-life approach was used in the same fashion as the *Supports Specifications*. The wind velocity that was exceeded only 0.01% of the time was calculated using a Rayleigh distribution density function shown as Eq. 9-6, and was referred to as the fatigue wind velocity (also referred to as the limit-state wind velocity in the *Supports Specifications*). Using the same annual mean wind velocity equal to 11 mph (5 m/s) as the *Supports Specifications*, the fatigue wind velocity calculated with Eq. 9-6 was found to be 38.0 mph (17 m/s). The equivalent static wind pressure corresponding to the fatigue wind velocity using the trendline developed from the data collected from this project is shown in Figure 9-20, and is found to be equal to 7.03 psf (337 Pa).

$$P_E(v) = e^{\frac{-\pi v^2}{4\bar{v}^2}} \quad [\text{Eq. 9-6}]$$

where

$P_E(v)$ = probability

v = wind velocity

\bar{v} = mean wind velocity.

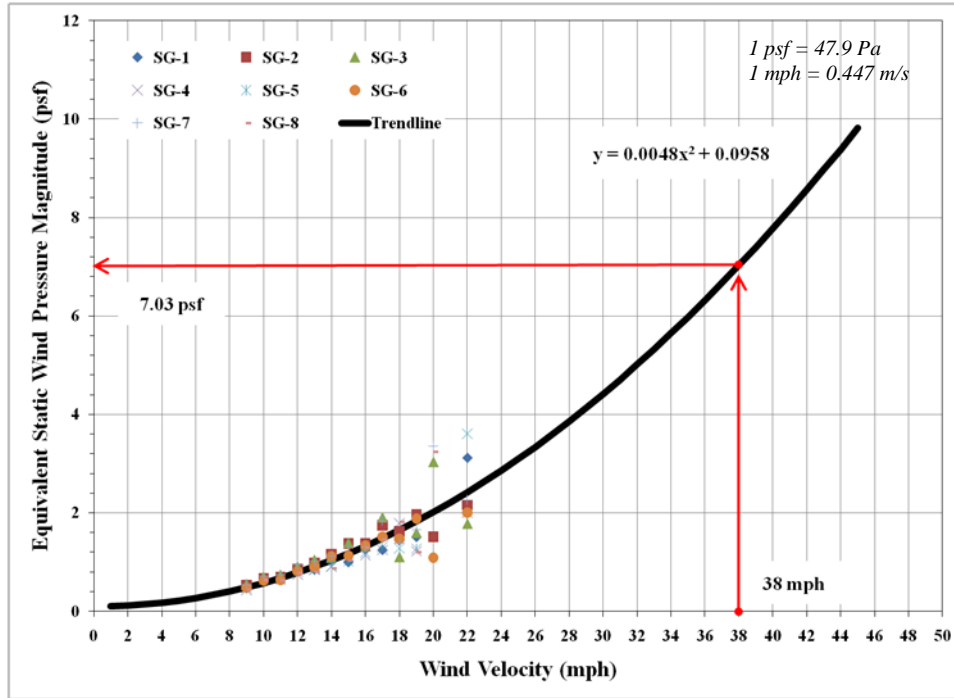


Figure 9-20. Equivalent static wind load equal to 7.03 psf (337 Pa) at the fatigue wind velocity

It was concluded from the results of this project that the fatigue load due to natural wind gust determined from experimental data collected and the analysis procedures conducted was equal to 7.03 psf (337 Pa) for the bridge-type VMS support structure.

Section 10

Experimental Calculation of the Fatigue Load due to Truck-Induced Wind Gust

Overview

A detailed description on the processes and results of determining the fatigue load due to truck-induced wind gust is presented. The fatigue load for the bridge-type VMS support structure was determined from the experimental data collection. A detailed description of the sample sizes and data collected with the support structure for the truck-induced wind gust fatigue load evaluation is provided in **Section 7: Experimental Data Collection Samples**.

The method for data reduction is presented, along with an analysis of the results. A fatigue load due to truck-induced wind gusts was determined in the horizontal and vertical directions. The horizontal component was directed onto the vertical face of the structure and parallel to the direction of the traffic. The vertical component was directed upwards onto the underneath portion of the structure and perpendicular to the direction of traffic. Only data collected on days with relatively low wind velocity was used, specifically less than 9 mph (4 m/s). This was done in order to avoid, as much as possible, structural effects created from natural wind gust.

Fatigue Load Calculation Approach

Projects that focused on analyzing the fatigue load due to truck-induced gusts have been gathered and reported in NCHRP Report No. 469 (Dexter, *et al.* 2002) which comprised the basis of the current *Supports Specifications* fatigue provisions for truck-induced gusts. The conclusions reported in Report 469 were based on experimental evaluation of cantilever-type VMS support structures, and not cantilever-type sign or bridge-type VMS support structures. Yet, many indirect observations related to truck gusts on support structures were made during in Report 469. Most importantly, these observations were made independent to the type of structure in the analysis. These observations were used in this project are summarized as follows:

- The fatigue wind pressure for the vertical component of the truck gust was applied onto the underneath exposed area of the structure,
- The exposed area underneath the structure was equal to 12 ft (3.7 m) in length,
- The exposed area was located directly above the traffic lane used by the truck, and
- The gust was assumed maximum at the bottom of the sign and decreased to zero in a linear proportionality with height at 32.8 ft (10 m) above the roadway.

Report 469 concluded that the full strength of the vertically applied truck gusts pressure equal to 18.8 psf (900 Pa) was produced on the underneath exposed area of the structure at 19.7 ft (6 m) or less above the roadway. The pressure decreased linearly to zero at a height of 32.8 ft (10 m) above the roadway. The pressure load applied in the horizontal direction was found to be insignificant compared to the fatigue load due to natural wind, and was excluded from the results and conclusions of Report 469. The underneath exposed area to truck gusts was determined to cover 12 ft (3.7 m) in length or the length of the traffic lane, whichever was greater. The provisions indicated that the truck gust pressure should be applied over the exposed length located where the force would create the worst-case scenario (largest moment arm). In particular, it was specified for most cases to be the outermost 12 ft (3.7 m) length of cantilever-type support structures (Dexter, *et al.* 2002).

The objective of the truck gust tests performed in this project was to evaluate the accuracy of the truck gust provisions in the *Supports Specifications* as applied to bridge-type VMS support structures. Therefore, many of the specifics reported in Report 469 and later used in the *Supports Specifications* were applied in the evaluation of the truck gusts on the supports structure for this project. These observations had no influence, or were influenced in their discovery, by the structural response of the structure tested when the observations were made for Report 469, making them independent on the type of support structure. In view of this, these observations were assumed as factual, and were used in the evaluation of the fatigue due to truck-induced wind gusts for this project.

The truck-induced wind gusts experimentation was based on randomly selecting semi-trailers as they passed underneath the structure to use for measurement as the structural excitation. A radar gun was used to measure the speed of the trucks, and the time they passed underneath the structure was recorded so that the records from the data acquisition system could be isolated in the laboratory for analysis. The accelerometers were used primarily for the analysis of the structural response. This was because they provided specific measurements related to the direction of the wind-induced vibrations. The strain gauges were not used for this analysis because of the configuration of the structure in relation to problems that arise when isolating strains generated from the horizontal and vertical components of the truck gust.

The truck-induced wind gust load was developed as a uniformly distributed pressure load that can be applied for the fatigue design and analysis of these structures. A horizontal and vertical component to the fatigue load was determined from the collected data. The loads represented the maximum peak-to-peak vibratory response of the structure, which included the dynamic amplification of the structure in response to the generated truck impulses.

Structural Excitation

A total of 157 truck-induced wind gusts events were recorded. The truck speed, occupied lane, and structural response were collected for each event. The collection data is provided in Appendix E for reference. The measured truck speeds ranged from 50 mph (22 m/s) to 80 mph (36 m/s). The structural responses to several semi-trailer truck types were collected. This

included standard semi-trailers with and without wind guards, tankers, cab only, and flat bed trucks. The most popular truck was the standard semi-trailer with a wind guard on the top of the cab.

Structural Response

The measurements made from the accelerometers comprised the majority of the structural response for the bridge structure. The accelerometers located on the overhead truss span were used, which were in proximity to the lanes used by the trucks. Acceleration measurements were made in the horizontal and vertical vibratory directions. The analysis of the data involved the responses to vertically and horizontally applied pressure onto the exposed horizontal area on the underneath section of the structure and the vertical area on the front face of the structure. The exposed areas were 12 ft (3.7 m) in length located directly above the traffic lane used by the trucks, which was in collaboration with NCHRP Report No. 469 (Dexter, *et al.* 2002). The analysis involved a back-calculation from the accelerometer measurements to determine the forces generated from the truck-induced wind gusts, from which the wind pressures were determined.

Acceleration Ranges

The truck-induced gust pressure was back-calculated from a peak-to-peak acceleration ranges determined from the accelerometer measurements. A schematic depicting the location of the gauges is shown in Figure 10-1. Accelerometers 2V, 3H and 4H were used in for the analysis. The vertical component of the truck-induced wind gust was measured using accelerometer 2V, and the horizontal component was measured using accelerometers 3H and 4H. Two accelerometers were used to measure this direction to evaluated possible torsion of the overhead truss span because of both the horizontal and vertical component of the truck gust.

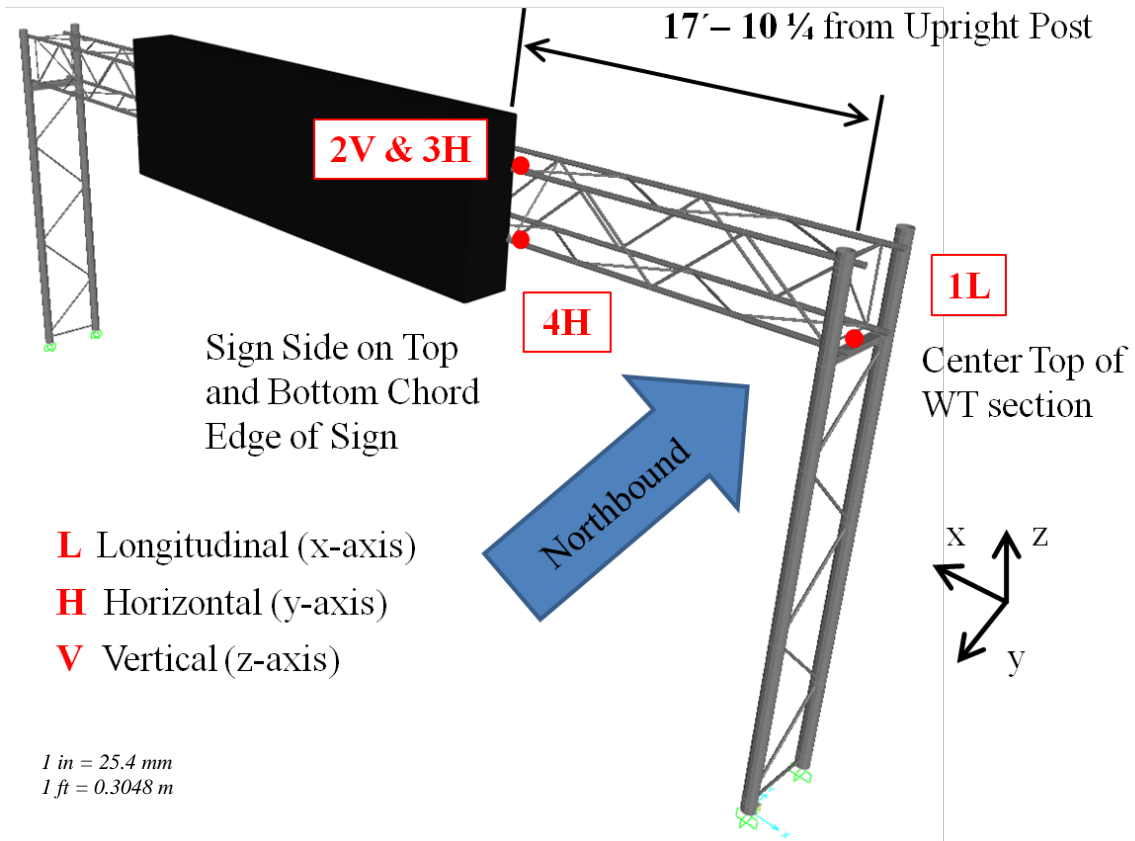


Figure 10-1. Accelerometer locations, identifications, and vibratory direction of measurement

Transient Events A typical transient event of a truck-induced wind gust as measured by the accelerometers is shown in Figure 10-2. It is evident in the figure that vibration occurs in both the vertical and horizontal directions. As the structure accelerates, it creates a displacement which causes fatigue stresses on the structure. The load was based on the maximum peak-to-peak amplitude range for the vertical and horizontal components. The horizontal vibration was observed to be the largest with all the truck events measured and evaluated. However, it is important to note the exposed area of the structure was also largest with the horizontal loading than with the vertical loading.

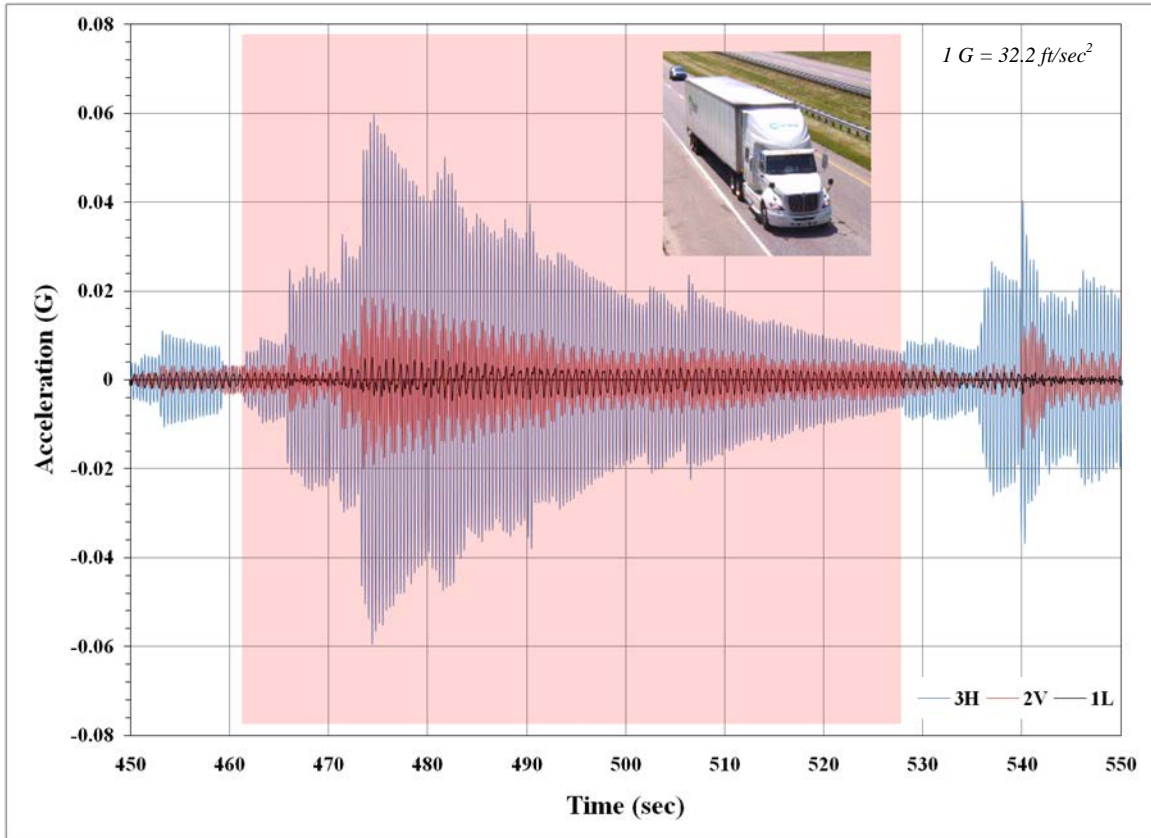


Figure 10-2. Truck event for the horizontal (3H), vertical (2V), and longitudinal (1L) acceleration response

The length of the transient event was inconsequential for determining the fatigue load. Because of the nature of the load, its repetition, and randomness, the fatigue load must represent the maximum peak-to-peak stress range of the structural response that is generated from the acceleration. As long as the endurance limit of the detail is greater than the maximum measured peak-to-peak range, then significant fatigue deterioration due to truck gust is avoided during the lifespan of the structure. Details of the peak-to-peak ranges measured by the vertical and horizontal accelerometers are provided in Figure 10-3 showing the ranges versus the speed of the truck for all events measured.

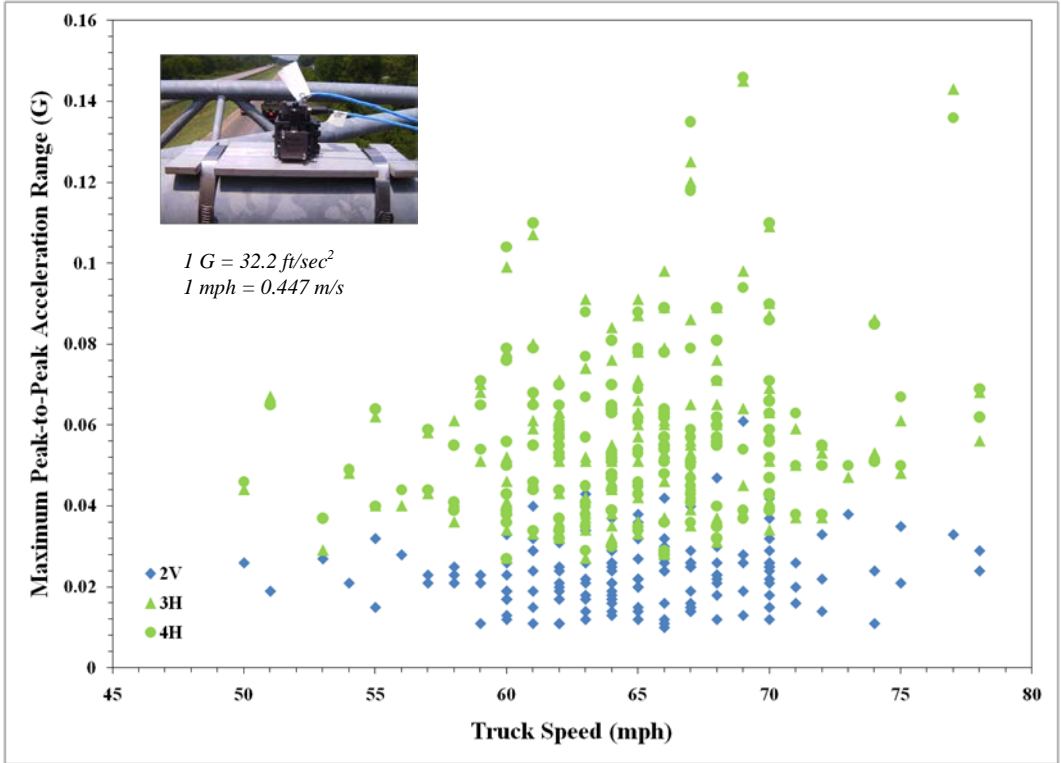


Figure 10-3. Maximum peak-to-peak accelerometer ranges measured from the all truck wind events

Truck-Induced Wind Pressure Back-Calculation

A back-calculation procedure was used to determine an equivalent static wind pressure that could be applied to the structure to produce an equivalent acceleration range as the experimentally measured values. The force generated from the acceleration ranges depicted in Figure 10-3 was determined using Newton's second law of motion shown in Eq. 10-1.

$$F = ma \quad [\text{Eq. 10-1}]$$

where

F = force, lb (N)

m = mass, slug (kg)

a = acceleration, $\frac{\text{ft}}{\text{sec}^2}$ (G)

The effective mass was used which represented the structural members and the VMS as a lumped mass at the center of the structure. The acceleration ranges were multiplied by the effective mass to determine the force. This was done for accelerometers measuring the vertical and horizontal directions. The force represented an equivalent static force that would produce an

equivalent acceleration range as measured by the accelerometers. The static force was then divided by the effective area for the vertical and horizontal truck gust components to produce the equivalent static wind pressure.

Effective Mass

The mass of the bridge-type VMS support structure was calculated separately for the vibration in the vertical and horizontal directions. An effective mass was used to lump at the center of the structure the distributed mass of the pipe members that made up the truss and uprights. The mass of the VMS was modeled as a discrete mass at the center. The total mass was therefore the effective mass of the pipe members plus the discrete mass of the VMS.

For the vertical vibration, only the mass of the VMS and the pipe members that made up the truss were used for the calculation. The VMS was placed as a discrete mass at the center of the structure. The effective mass, $m_{t,eff}$, of the distributed mass of the truss pipe members was calculated using the first term in Eq. 10-2. The term was developed on the assumption that the vibration of the truss span acts as a simply support beam based on the U-bolt connection details of the truss to the uprights. The total mass was therefore the effective mass of the truss members plus the discrete mass of the VMS at the center of the structure. The calculation results are provided in Table 10-1. Specific details on the derivation of Eq. 10-2 are provided in Appendix F of reference Irvine (2004).

$$\begin{aligned} m_T &= m_{t,eff} + m_{VMS} \\ &= \frac{48\rho L}{\pi^4} + \frac{W_{vms}}{g} \end{aligned} \quad \text{[Eq. 10-2]}$$

where

m_T = total mass, slug (kg)

$m_{t,eff}$ = effective mass of the truss pipe members, slug (kg)

m_{VMS} = mass of the VMS, slug (kg)

ρ = mass density per unit length, slug/in (kg, mm)

L = length of the mass member, in (mm)

W_{VMS} = weight of the VMS structure, lb (N)

g = acceleration of gravity, $386 \frac{\text{in}}{\text{sec}^2} \left(9.81 \frac{\text{m}}{\text{sec}^2} \right)$

For the horizontal vibration, the mass of the VMS, and the distributed mass of the pipe members that made up the truss and uprights were used for the calculation. The VMS was placed as a discrete mass at the center of the structure. The effective mass, $m_{t,eff}$, of the distributed mass of the truss pipe members was calculated using the first term in Eq. 10-3. The effective mass, $m_{up,eff}$, of the distributed mass of upright pipe members was calculated using the second term in Eq. 10-

3. The $m_{t,eff}$ term was developed on the assumption that the vibration of the truss span acts as a simply support beam based on the U-bolt connection details of the truss to the uprights. The $m_{up,eff}$ was developed on the assumption that the uprights act as cantilevers with fixed end supports. The effective mass term lumps the distributed mass of the upright members to the end of the cantilever system. The total mass is therefore equal to the effective mass of the truss pipe members, plus the effective mass of the upright pipe members, plus the discrete mass of the VMS. Specific details on the derivation of Eq. 10-3 are provided in Appendices B, C, and F of reference Irvine (2004).

$$\begin{aligned}
 m_T &= m_{t,eff} + m_{up,eff} + m_{VMS} \\
 &= \frac{48\rho L}{\pi^4} + 0.2235\rho L + \frac{W_{vms}}{g}
 \end{aligned}
 \tag{Eq. 10-3}$$

where

m_T = total mass, slug (kg)

$m_{t,eff}$ = effective mass of the truss pipe members, slug (kg)

$m_{up,eff}$ = effective mass of the upright pipe members, slug (kg)

m_{VMS} = mass of the VMS, slug (kg)

ρ = mass density per unit length, slug/in (kg, mm)

L = length of the mass member, in (mm)

W_{VMS} = weight of the VMS structure, lb (N)

g = acceleration of gravity, $386 \frac{\text{in}}{\text{sec}^2} \left(9.81 \frac{\text{m}}{\text{sec}^2} \right)$

Table 10-1. Total mass of the bridge-type VMS support structure for vibration in the vertical and horizontal directions

Vibration Direction	Total Mass, m_T (slug)
Vertical	177.7999
Horizontal	207.9231

1 slug = 14.6 kg

A total weight of the VMS sign equal to 3,900 lb (17,349 N) was assumed for the VMS. This number was determined from shop drawings of the VMS structure provided to the research team. The specific weight of steel equal to 0.284 lb/in³ [7.71 (10⁻⁵) N/mm³] was used for the mass density per length of the steel pipe members.

Exposed Area Breakdown

The areas on the structure that were exposed to the vertical and horizontal components of the truck-induced wind gust were determined. This involved the underneath portion of the truss span

and VMS for the vertical component, and the front portion of the VMS for the horizontal component.

Vertical Component The wind pressure was applied onto the area located on the underneath portion of the truss span, in compliance with the research collected in NCHRP Report 469 (Dexter, *et al.* 2002) and used in the *Supports Specifications*. The exposed underneath area equaled 12 ft (3.7 m) in length. It was located directly above the traffic lanes used by the truck, as shown in Figure 10-4. The area included the bottom portion of the VMS and the truss span including the chords and struts. The exposed areas for each lane were essentially the same. The exposed area of the VMS was approximately 20 ft (6.1 m) above the roadway, whereas the exposed area of the truss span was 22.927 ft (6.9881 m) above the roadway. Assuming the wind pressure decreases linearly to zero at approximately 32.8 ft (10.0 m) above the roadway, the pressure on the bottom of the VMS will be greater than the pressure at the location of the truss area that is 2.927 ft (0.892 m) higher. To account for this, and knowing that the wind pressure is proportional to the exposed area, the truss area was multiplied by a factor equal to 0.775 to account for the lessened wind pressure at this location in relation to the maximum pressure at the bottom of the VMS. A breakdown of the exposed areas used in the analysis is provided in Table 10-2.

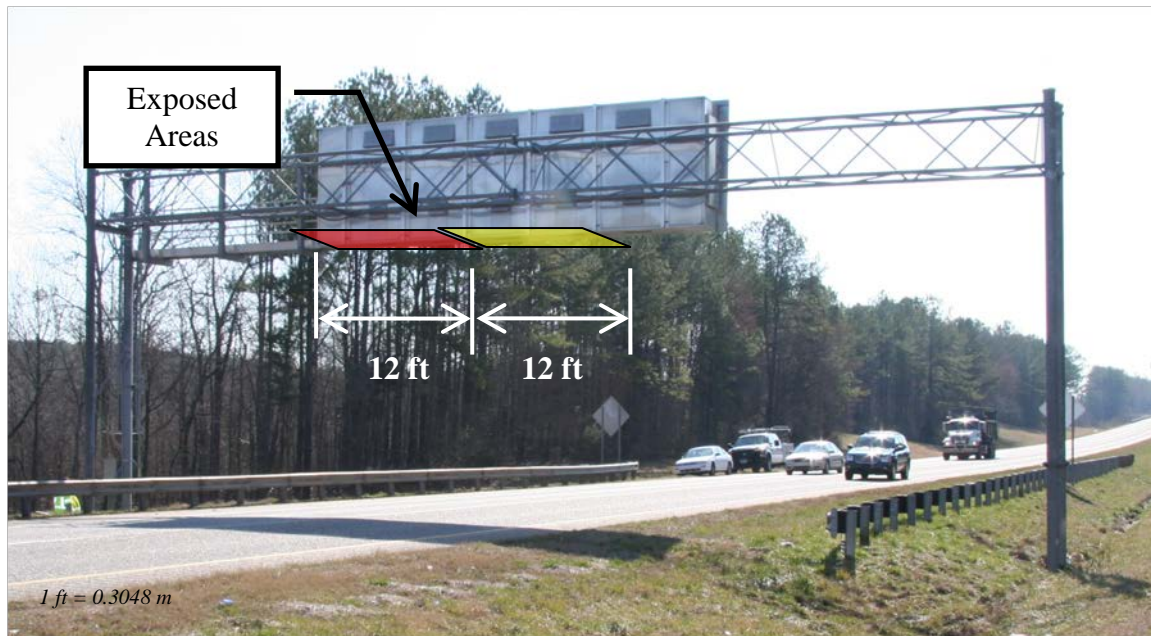


Figure 10-4. Underneath exposed area used in the evaluation of the vertical component

Horizontal Component The wind pressure was applied onto the area located on the front face of the VMS. It was applied on a portion of the sign in compliance with the research collected in NCHRP Report 469 (Dexter, *et al.* 2002) and used in the *Supports Specifications*. The exposed area equaled 12 ft (3.7 m) in length. Accordingly, the pressure was maximum at the bottom of the VMS located at 20 ft (6.1 m) above the roadway, and decreased linearly to zero at 32.8 ft (10.0 m) above the roadway. The height of the VMS was only 9.349 ft (2.850 m) and therefore

the full height of the VMS was exposed to the wind pressure. As a result, the load had the form of a trapezoid. To account for this, and knowing that the wind pressure is proportional to the exposed area, the area that was initially exposed to a uniformly distributed load was multiplied by a factor of 0.635. The factor was determined using the slope of the linear decrease of the wind pressure and the height of the VMS. The area was located directly above the traffic lane used by the truck as shown in Figure 10-5 at the same location used for the vertical component. A breakdown of the exposed area used in the analysis is listed in Table 10-2.

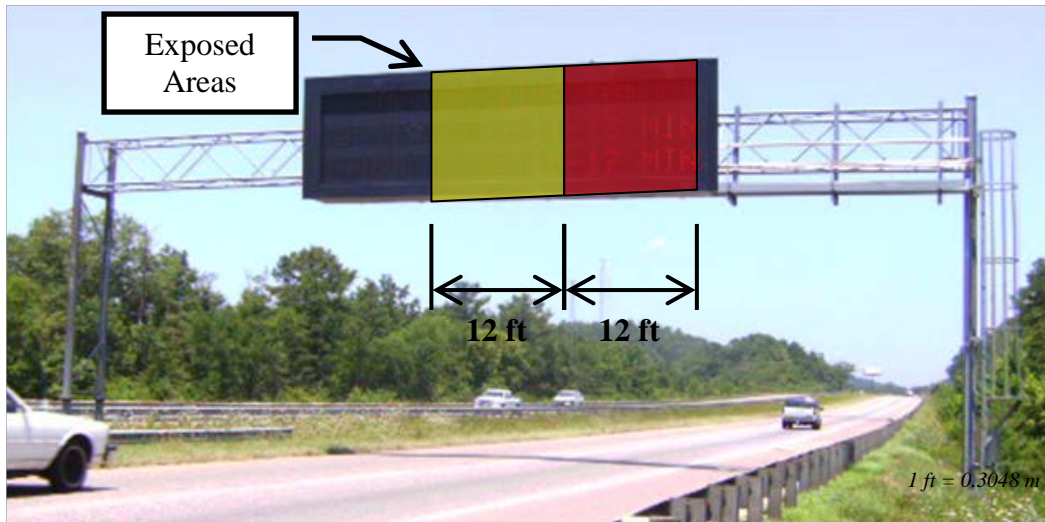


Figure 10-5. Front exposed area used in the evaluation of the horizontal component

TABLE 10-2. Breakdown of the exposed areas for the evaluation of the truck-induced wind gust

Component	Segment	Members	Label	Area (in ²)	Total Area (in ²)
Vertical	Bottom Truss	Chords	A ₁	781.200	6,293.634
		Horizontal Diagonal Strut	A ₂	248.942	
		Horizontal Strut	A ₃	79.492	
	VMS	Underneath Panel	A ₄	5,184	
Horizontal	VMS	Front Panel	A ₅	10,255.284	10,255.284

1 in² = 6.45 cm²

Effective Area Breakdown

The effective areas were calculated of the exposed areas listed in Table 10-2 for the vertical and horizontal components of the truck gust. The effective area represented the exposed area multiplied by the drag coefficient of the members that made up the particular area.

Drag Coefficient All drag coefficients were calculated using Table 3-6 of the *Supports Specifications*. Fifty year design life was used in the calculation with a velocity conversion factor

equal to 1.00 (no conversion needed). The worst case scenario was applied by maximizing the wind speed and member diameter. A maximum wind speed of 70 mph (31.293 m/s) was used, assuming the wind gust equals the speed of the truck, and the largest diameter member equal to 3.5 in (88.9 mm). The results of the drag coefficient calculation are listed in Table 10-3.

Table 10-3. Drag coefficients used in the evaluation of the truck-induced wind gust

Segment	Members	Label	Drag Coefficient, C_d
Bottom Truss	Chords	A_1	1.10
	Horizontal Diagonal Strut	A_2	1.10
	Horizontal Strut	A_3	1.10
VMS	Underneath Panel	A_4	1.70
VMS	Front Panel	A_5	1.70

Effective Area Calculation The effective area was defined as the exposed area of the segment multiplied by the drag coefficient of the members that make up the area segment. The results of the calculation are listed in Table 10-4 for the vertical component and Table 10-5 for the horizontal component of the truck gust.

Table 10-4. Effective area used in the evaluation of the vertical component of the truck-induced wind gust

Segment	Location	Label	Area (in ²)	Drag Coefficient C_d	Effective Area, $A_{e,i}$ (in ²)
Bottom Truss	Chord	A_1	781.200	1.10	859.320
	Horizontal Diagonal Strut	A_2	248.942	1.10	273.836
	Horizontal Strut	A_3	79.492	1.10	87.441
VMS	Underneath Panel	A_4	5,184	1.70	8,812.8
Total Effective Area =					10,033.397

$1 \text{ in}^2 = 6.45 \text{ cm}^2$

Table 10-5. Effective area used in the evaluation of the horizontal component of the truck-induced wind gust

Segment	Location	Label	Area (in ²)	Drag Coefficient, C_d	Effective Area, $A_{e,i}$ (in ²)
VMS	Front Panel	A_4	10,255.284	1.70	17,433.983

$1 \text{ in}^2 = 6.45 \text{ cm}^2$

Wind Pressure Calculation

The truck-induced wind gust was calculated using the acceleration ranges, effective mass, and the effective areas. Equation 10-1 was used to calculate the wind force. The force was then divided by the effective areas to determine the wind pressure. This was done for the vertical and horizontal components of the truck-induced wind gust. The resulting calculation for each accelerometer and all truck events recorded is provided in Figure 10-6 for the vertical component, and Figure 10-7 for the horizontal component of the truck-induced wind gust.

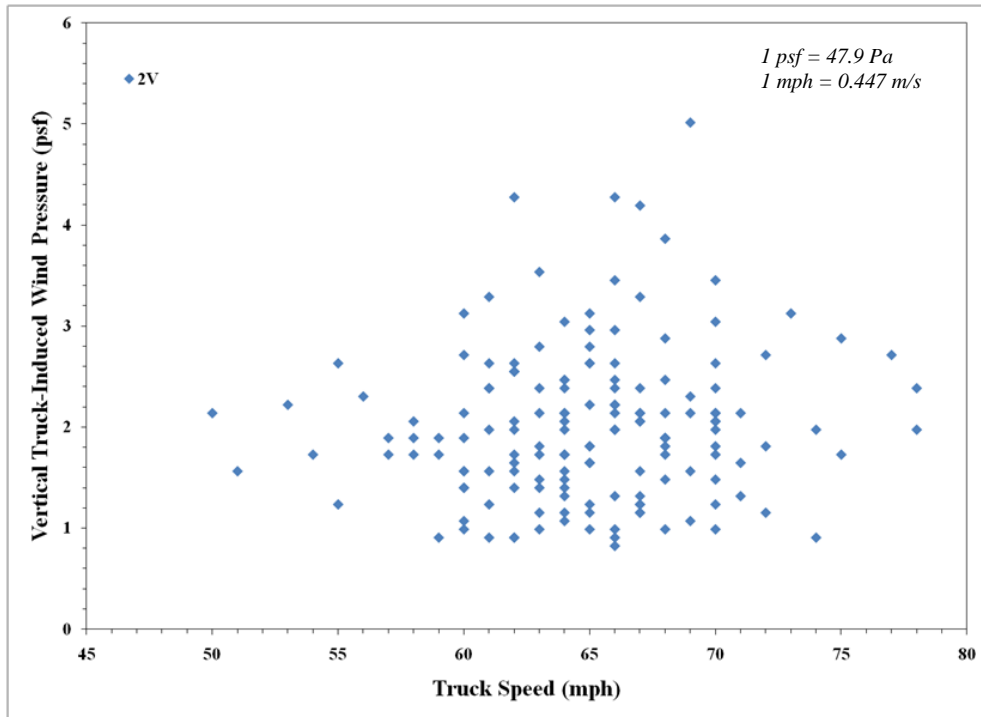


Figure 10-6. Vertical truck-induced wind pressure versus truck speed

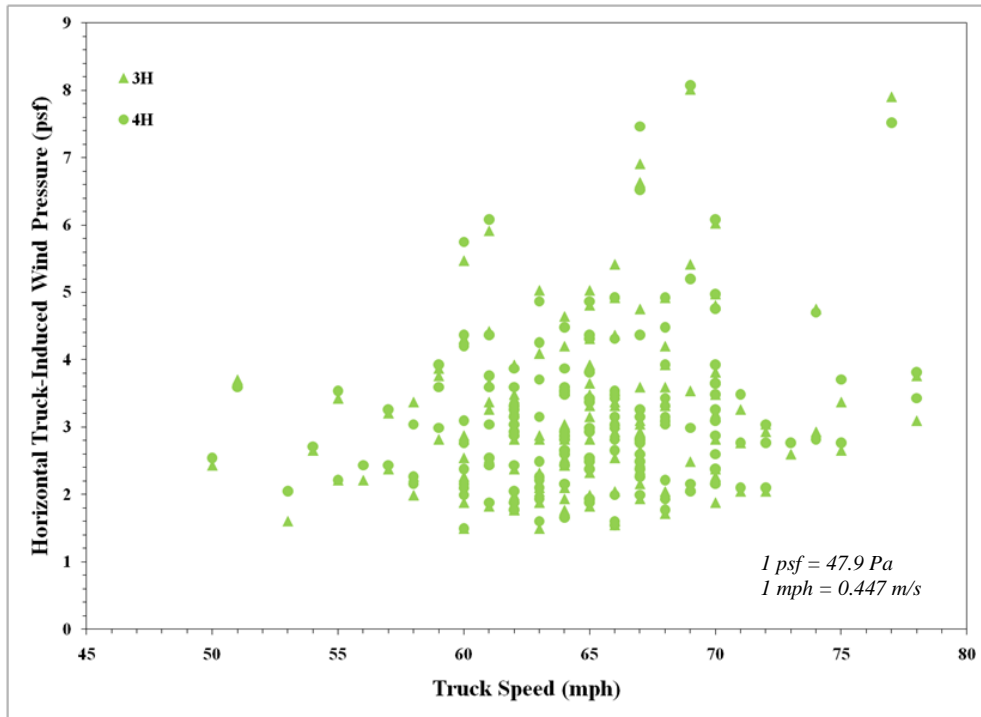


Figure 10-7. Vertical truck-induced wind pressure versus truck speed

Predicting the Maximum Wind Pressure

The maximum truck-induced wind gust was determined using an envelopment procedure. The P(95/50) Upper Limit Tolerance Approach [P(95/50) rule] was used for this analysis (Harris 1996). It was developed as a prediction model representative of the exposure environment resulting from the truck-induced wind gusts defined at a 95% confidence level that the maximum value of wind pressure will be equal to or below the upper limit at least 50% of the time. The upper limit for the P(95/50) rule was calculated using Eq. 10-4:

$$\text{Upper Limit} = \bar{x} + k\sigma \quad [\text{Eq. 10-4}]$$

where

\bar{x} = average of data samples

k = normal tolerance factor

σ = standard deviation of the data samples

The tolerance factor, k , was obtained from reference Harris (1996) with the confidence coefficient gamma factor, γ , taken as 50%, and the minimum probability beta factor, β , taken as 95%. The values were developed assuming the data samples follow a normal distribution.

The back-calculated truck-induced wind gust pressures were filtered according to the their corresponding truck speeds and allocated into 5 mph (2.24 m/s) truck speed intervals. The average pressure, standard deviation, number of samples, and normal tolerance factor was calculated for each interval. The upper limit was then calculated using Eq. 10-4 to determine the maximum values. The results of the calculation are provided in Table 10-6 for the vertical and horizontal components. A plot of the upper limit against the data samples is provided in Figure 10-8 for the vertical component, and Figure 10-9 for the horizontal component.

Table 10-6. Upper limit of the truck-induced wind gust pressure

Truck Speed Interval (mph)	Average Speed of Interval (mph)	Truck-Induced Wind Gust Upper Limit (psf)	
		Vertical Component	Horizontal Component
50-55	52	2.491	4.182
55-60	57	2.605	4.031
60-65	62	3.101	4.643
65-70	67	3.583	5.590
70-75	71	3.125	5.034
75-80	77	3.196	7.956

1 psf = 47.9 Pa

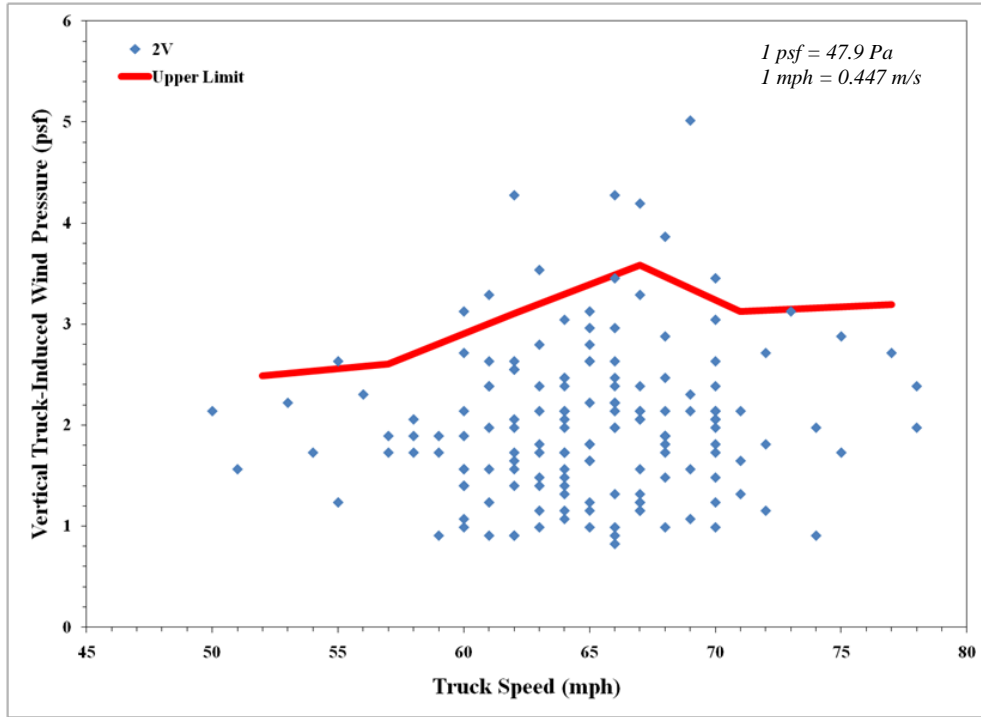


Figure 10-8. Upper limit for the vertical component of the truck-induced wind gust

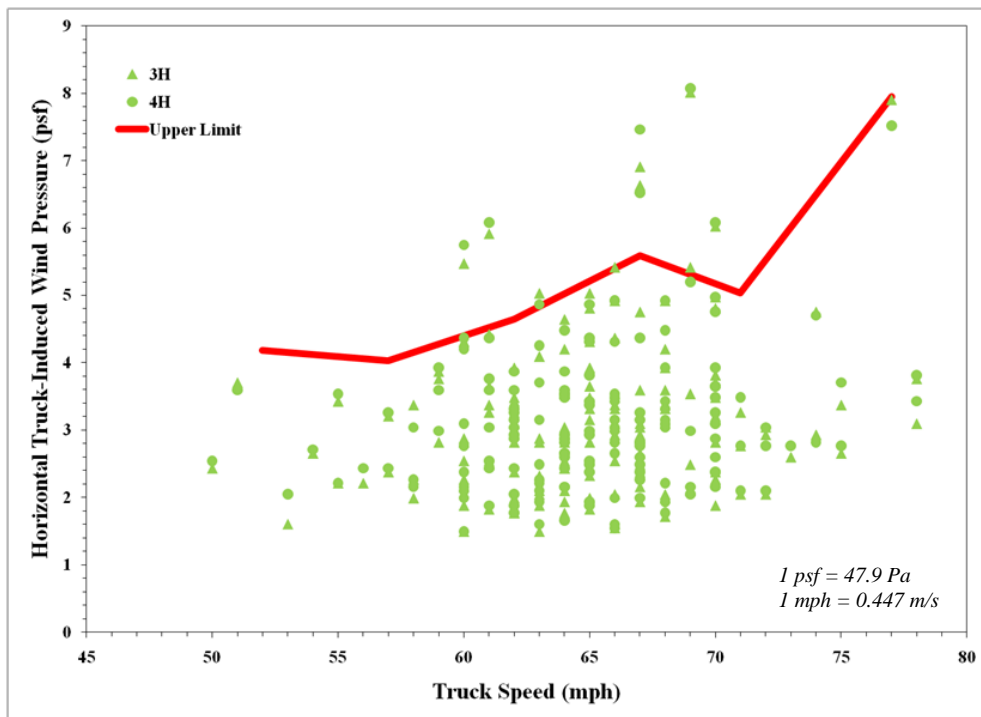


Figure 10-9. Upper limit for the horizontal component of the truck-induced wind gust

Trendline of the Upper Limit

A regression analysis was performed to determine a best fit trendline of the upper limit values of the vertical and horizontal components of the truck gust. This was done through a transformation regressor linearization process. It was assumed that the data adhered to the fluid mechanics relationship between wind force and the square of wind velocity. The independent variable (truck speed on the abscissa axis) was squared. It was plotted versus its corresponding wind pressure (see Figure 10-10). A best fit line was then constructed as a linear predictor and was plotted to fit the data based on the information gathered from the transformation. The slope of the trendline was the slope of the parabola, and the y-intercept of the trendline was the y-intercept of the parabola.

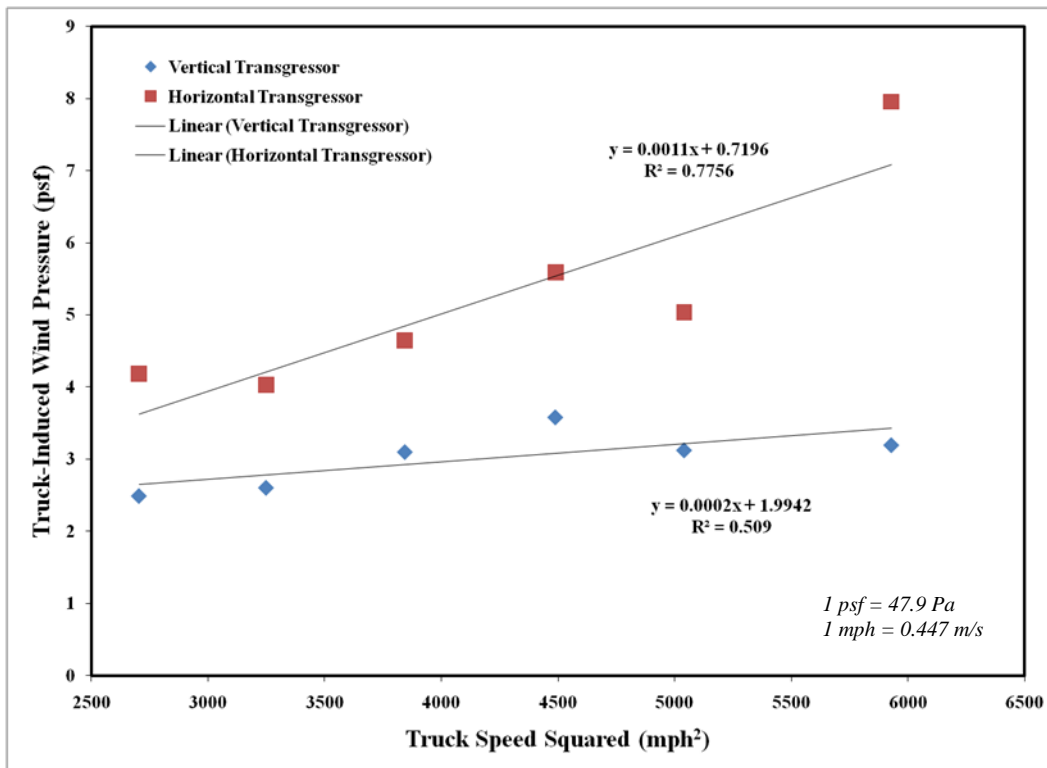


Figure 10-10. Transformed regressor for the linearization process

The equations of the transformed regressor were used to plot the parabolic trendline of the upper limit envelopment data. The plots are shown in Figure 10-11 for the vertical component, and Figure 10-12 for the horizontal component. The truck-induced wind gust wind pressure can be approximated for any truck speed using the equations of the trendline.

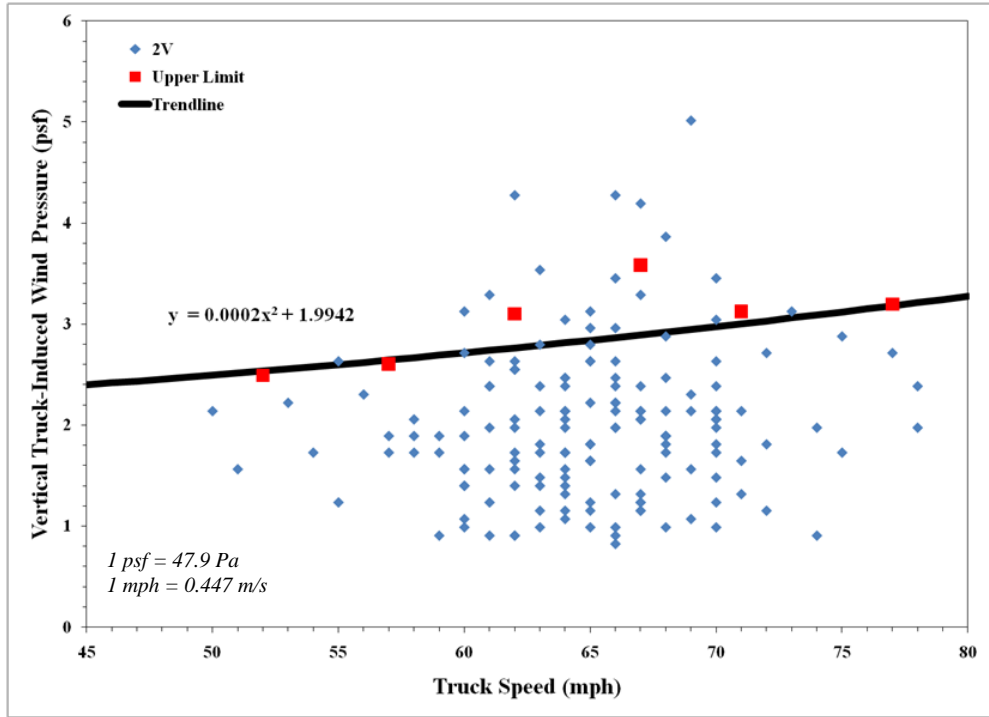


Figure 10-11. Parabolic curve fit obtained from the linear transformation for the vertical component

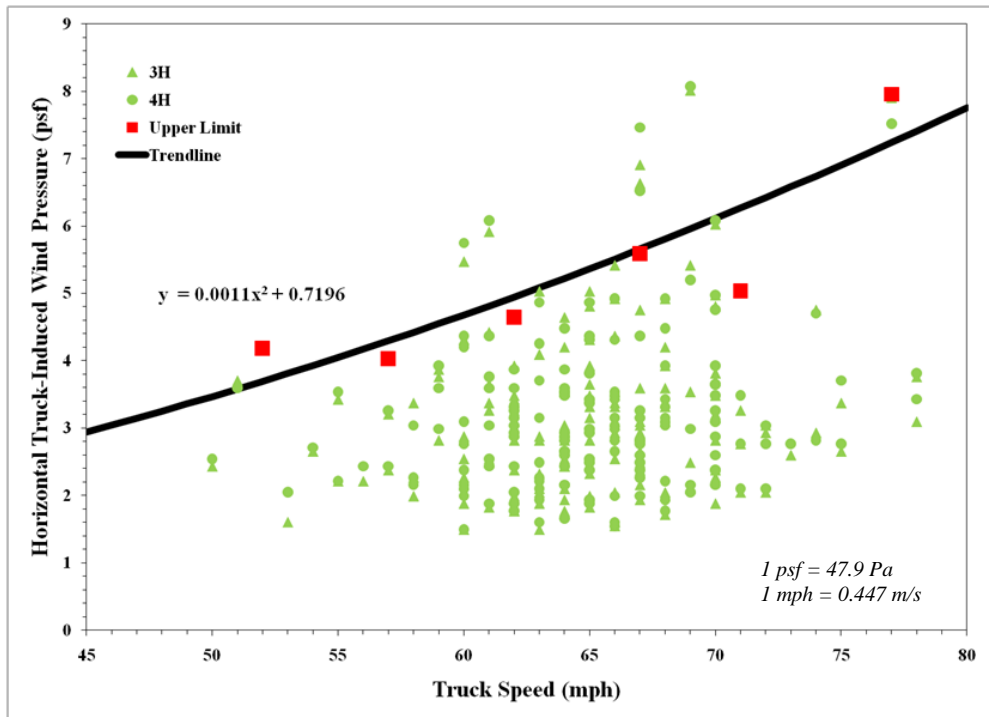


Figure 10-12. Parabolic curve fit obtained from the linear transformation for the horizontal component

In reference to Figure 10-11 and Figure 10-12 for the vertical and horizontal components of the truck-induced wind gust, the following fatigue loads was obtained:

For a truck traveling at 70 mph (31 m/s), the resulting fatigue load due to truck induced wind gust was found to be equal to 2.974 psf (142.4 Pa) for the vertical component, and 6.110 psf (292.5 Pa) for the horizontal component.

Section 11

Theoretical Calculation of the Fatigue Load due to Natural Wind Gust

Overview

A description of the theoretical program for evaluation of the fatigue load due to natural wind is presented in this chapter. The theoretical calculation of the fatigue load due to natural wind gust was developed to account for the variety of sign support structures in design, each with different configurations, materials, and dynamic behavioral properties. It makes use of the vibration response spectrum (VRS). The fatigue load is determined from the spectrum based on the dynamic characteristics of the specific structure being evaluated.

Specific Objectives of the Theoretical Program

There were three specific objectives with the theoretical program. The objectives are listed as follows:

1. Development of the Structural Excitation: simulation of the natural wind dynamic loading environment.
 - a) The structural excitation was developed using the Davenport excitation model. The model is based on a wind velocity power density spectrum (PDS) simulation model. The same model was used to develop the natural wind gust fatigue provisions in the *Supports Specifications*.
 - b) The wind velocity collected with this project was used to develop an additional experimental structural excitation PDS model.
 - c) A comparison was made between the Davenport model and the experimental model developed with the wind data collected with this project to assess the accuracy of the Davenport spectrum.
2. Development of the Structural Response: simulation of the dynamic response of the structure to the structural excitation developed in objective #1.
3. Development of the Vibration Response Spectrum (VRS): a spectrum developed that is used to determine the fatigue load due to natural wind gusts that is comprehensive to account for the variety of highway overhead support structure design types.

Significance of the Theoretical Program

The objective of the theoretical program was to provide a universal design method for fatigue loading on highway overhead support structures due to natural wind gust. Overhead support structures are highly flexible with low damping properties, which makes them susceptible to vibratory induced fatigue loading. The magnitude of this load is dependent on the dynamic behavior and characteristics of the structure. The objective of the theoretical program was to develop a relationship between fatigue loading and the dynamic response in terms of random vibration analysis as a single degree-of-freedom (SDOF) system. Examples include cantilever- and bridge-type overhead sign support structures, as well as variable message sign (VMS) structures (Figure 11-1). For analysis purposes, these structures were approximated as a SDOF system because their modes of vibration (as determined from modal analysis of experimental data collected on these structures) are significantly separated such that the vibration in response to randomly applied wind loading is controlled predominately by a single modal shape. For that reason, the modal shapes were estimated as vibrating independently from each other in single global directions (Creamer, *et al.* 1979, Foutch, *et al.* 2006).

The fatigue provisions for natural wind in the *Supports Specifications* are adequate within certain limitations. They were developed based on four particular categorized structural types. The structural response of one overhead signal support structure, one cantilever-type overhead sign support structure, and two luminaire support structures to natural wind excitation were analyzed. The transmitted stresses of each structure were averaged, and the fatigue provisions were developed from the averaged results (Kaczinski, *et al.* 1998). The *Supports Specifications* are therefore only applicable to the structures of the type mentioned, with the same dynamic properties equal to the averaged values determined, most importantly the natural frequency and critical damping percentage (a.k.a. damping ratio). The results of the theoretical analysis, and confirmed from the experimental study, show that profound differences exist in the dynamic properties of these structures, and therefore each structure behaves differently under wind-induced fatigue loading.

Differences in the dynamic properties, such as the case with bridge-type sign support structures and VMS support structures, are not accounted for nor addressed in the *Supports Specifications*. This study provides a detailed approach to handle cases that have different dynamic properties than those used to develop the *Supports Specifications*. Cantilever-type sign support structures can have different configurations and made with various materials and cross sectional shapes. These parameters will dramatically affect the magnitude of the fatigue load, and therefore a method that incorporates the specific dynamic properties of the structure is needed. Bridge-type sign support structures and VMS support structures, which are not covered by the *Supports Specifications*, can also be addressed with the proposed design method. The primary differences in these structures in comparison to conventional cantilever-type structures are related to stiffness and mass, which are directly related to the natural frequency and damping of the structure.



Figure 11-1. Highway overhead support structures with different configurations, sizes and shapes

Methodology

The development of the fatigue guidelines in the *Supports Specifications* utilized the Davenport excitation model based on a natural wind velocity power density spectrum (PDS) curve for simulating natural wind excitation in conjunction with the infinite-life approach for fatigue loading (Davenport 1961, Kaczinski, *et al.* 1998). The method presented employed the same Davenport excitation model and infinite-life approach. Importantly however, the response of the structure to the excitation was evaluated differently in this research than used in the development of the *Supports Specifications* fatigue provisions. The analysis of the response was based on principles of random vibration in utilization of the vibration response spectrum (VRS). This was done in order to account for the uniqueness and individuality of sign structures regarding their dynamic properties, which has significant affect on stresses generated from natural wind fatigue loading. The approach is equivalent to determining an equivalent static wind load, which produces the same response on the structure as a randomly applied dynamic wind load. The fatigue design equivalent static wind load is chosen from the VRS in terms of the natural

frequency and damping ratio of the structure. An additional experimental structural excitation model was developed from the wind data collected with this project. This was done in order to provide an assessment on the accuracy of the Davenport excitation model used in the theoretical program of this project. Because of the comprehensiveness of the VRS, the proposed method developed with the theoretical program of this project can be used as a tool to determine the appropriate design fatigue load due to natural wind gust for the particular structure in question.

Structural Excitation

Two excitation models were developed in the theoretical program of this project. The structural excitation models were as follows:

- Davenport excitation model, and
- Experimental excitation model.

The experimental excitation model was developed using the natural wind experimental data collected with this project. It was developed to assess the accuracy of the Davenport model. Based on the analysis presented in this chapter, the Davenport excitation model was found to be accurate and was used for the continuation of the development of the fatigue load in the manner specified with this theoretical program. A description of each model is provided in this section, along with the comparison between the two models, and the development of the fatigue load using the theoretical applications.

Davenport Excitation Model

The Davenport excitation model utilized a natural wind velocity power density spectrum (PDS) curve for simulating natural wind characteristics (Davenport 1961, Kaczinski, *et al.* 1998). The estimation of the structural excitation due to natural wind involved predicting the natural wind environment for which the structure was to be exposed. This was done using a spectral analysis based on A.G. Davenport's wind velocity power density spectrum shown in Eq. 11-1 (Davenport 1961):

$$S_v(f) = \frac{4\kappa\bar{V}_{10}^2 x^2}{f(1+x^2)^{\frac{4}{3}}} \quad [\text{Eq. 11-1}]$$

where

$S_v(f)$ = wind velocity power density spectrum at any height

f = frequency

\bar{V}_{10} = mean wind velocity at a standard height of 10 meters above ground level

κ = surface drag coefficient (Table 11-1)

$x = \frac{1200f}{\bar{V}_{10}^2}$ with $\frac{f}{\bar{V}_{10}^2}$ in cycles per meter.

Davenport developed the wind velocity PDS curve from 70 experimental wind velocity data collections from various locations around the world. His objective was to develop a model which simulated the turbulence and gustiness of wind velocity. He developed Eq. 11-1 from the 70 experimental data collections. The equation is a function of wind velocity frequency with respect to a mean wind velocity at a specified height. His formulation is shown in Figure 11-2 for frequencies ranging from 0 to 10 Hz, an open terrain (see Table 11-1), and an annual mean wind velocity of 11 mph (5 m/s).

Table 11-1. Terrain Coefficients developed for the wind velocity power density spectrum (Davenport 1961)

Type of Surface	κ	α
Open unobstructed country (e.g., prairie-type grassland, arctic tundra, desert)	0.005	0.15
Country broken by low clustered obstructions such as trees and houses (below 10 m high)	0.015 - 0.020	0.27 - 0.31
Heavily built-up urban centers with tall buildings	0.050	0.43

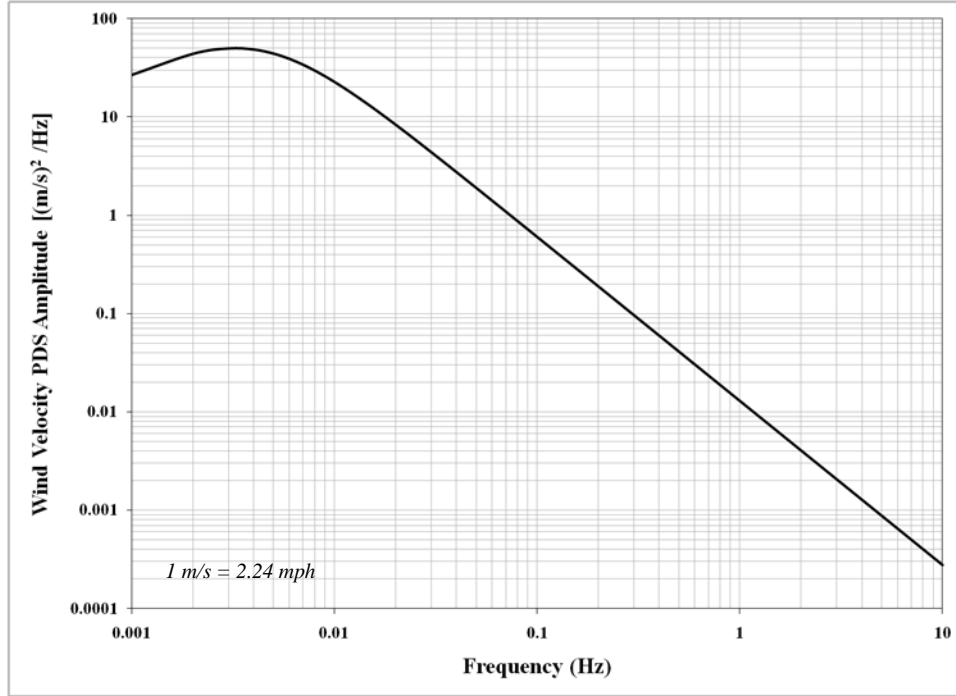


Figure 11-2. Wind velocity PDS for an annual mean wind velocity equal to 11 mph (5 m/s)

Once the behavior of the wind velocity environment was estimated, the PDS was transformed into a wind force PDS by using principles related to fluid mechanics. The drag force induced onto a structure due to natural wind is proportional to wind velocity squared, as shown by the Eq. 11-2:

$$F_D = \frac{1}{2} \rho C_d A V^2 \quad [\text{Eq. 11-2}]$$

where

F_D = drag force

ρ = density of air = $1.22 \frac{\text{kg}}{\text{m}^3}$

C_d = drag coefficient

A = area of exposed surface

V = wind velocity at any height.

By utilizing the proportionality between drag pressure and wind velocity, a wind pressure PDS was developed from Davenport's wind velocity PDS shown in Eq. 11-3. The plotted equation is shown in Figure 11-3 for an annual mean wind velocity of 11 mph (5 m/s) and normalized for exposed area and the drag coefficient.

$$S_F(f) = \rho^2 C_d^2 A^2 V^2 S_v(f) \quad [\text{Eq. 11-3}]$$

where

$S_F(f)$ = wind pressure power density spectrum at any height

ρ = density of air = $1.22 \frac{\text{kg}}{\text{m}^3}$

C_d = drag coefficient

A = area of exposed surface

V = wind velocity at any height

$S_v(f)$ = wind velocity power density spectrum at any height

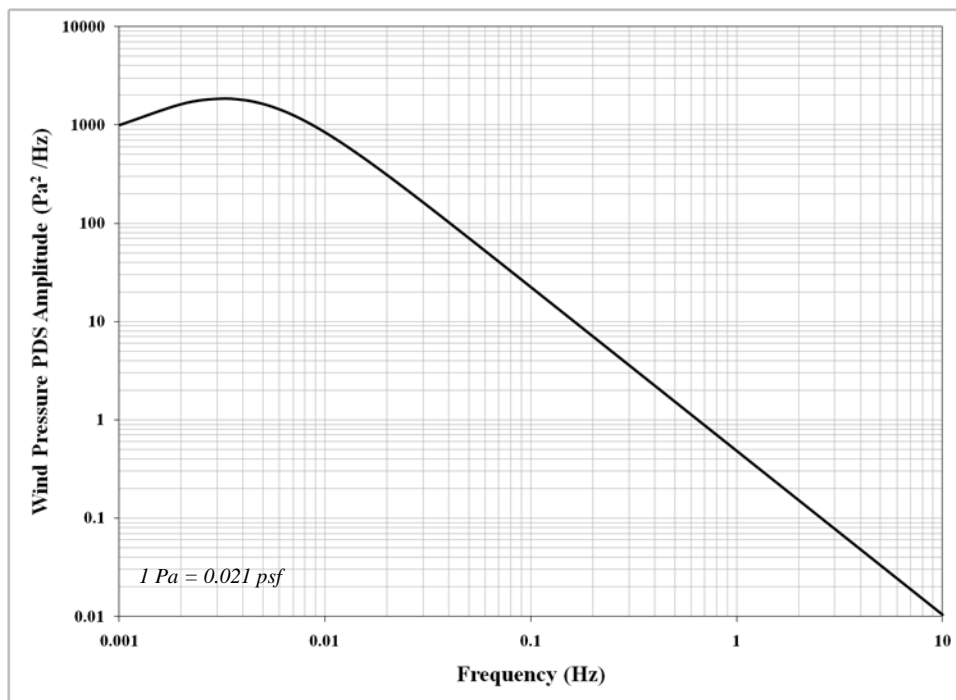


Figure 11-3. Wind pressure PDS for an annual mean wind velocity equal to 11 mph (5 m/s)

The PDS curve accounts for the gustiness and turbulence of wind velocity over a spectrum of frequencies, and was based on an averaged wind velocity taken at a specified height above ground level. Since most support structure are at or around 32 ft (10 m) in height, the PDS curve is well suited for these types of structures. Yet, the PDS can be used at any particular height by using the power law profile shown in Eq. 11-4 for approximating variation in wind velocity with height:

$$V = \bar{V}_{10} \alpha z^\alpha \quad [\text{Eq. 11-4}]$$

where

V = wind velocity at height z

α = surface coefficient in Table 11.1

z = height above ground.

For this case, where the objective was concentrated on formulating a design code for fatigue wind, the wind velocity variable in the pressure PDS equation was taken at the standard height of 32 ft (10 m) above ground level, and kept uniform across the wind exposed face of the structure. The purpose of which was to provide a simplified design equation for commercial use. Some conservative formulation exists as the wind velocity typically increases from the ground level upwards (Davenport 1961).

Infinite-Life Approach The infinite-life approach to fatigue design requires the wind pressure for a wind velocity that has a probability of exceedence equal to 0.01% to the annual mean wind velocity. This 0.01% exceedence probability wind velocity is referred to as the limit-state wind velocity, or fatigue wind. Once the natural wind environment was estimated, the next step was to apply the PDS to the infinite-life approach. Since the force spectrum was based primarily on the annual mean wind velocity, the wind velocity that was exceeded 0.01% of the time was found. The force spectrum was then calculated using the fatigue wind velocity.

Wind velocity is random in nature, but it can be predicted through statistical relationships. It has been found through many experiments that the magnitude of the wind velocity vector can be approximated to a reasonable degree of accuracy by the Rayleigh distribution (Liu 1991). By using the Rayleigh distribution, the wind velocity that has a probability of exceedence equal to 0.01% was found through the relationship in Eq. 11-5 as a function of the annual mean wind velocity.

$$P_E(v) = e^{\frac{-\pi v^2}{4\bar{V}^2}} \quad [\text{Eq. 11-5}]$$

where

$P_E(v)$ = probability

v = wind velocity corresponding to the probability

\bar{V} = mean wind velocity.

In the development of the fatigue provisions of the *Supports Specifications*, an analysis was conducted to determine which annual mean wind velocity to use in Eq. 11-5 to determine fatigue wind velocity (wind velocity with a 0.01% exceedence probability). The annual mean wind velocities of 59 major U.S. cities were analyzed. It was found that an annual mean wind velocity of 11 mph (5 m/s) was exceeded in only 19% of the U.S. cities analyzed and was therefore chosen. By plugging in 11 mph in Eq. 11-5, and solving for the wind velocity corresponding to the 0.01% probability, the fatigue wind velocity was found to be equal to 38 mph (17 m/s). The

force spectrum was then formed using the fatigue wind velocity (see Figure 11-4) and was used as the natural wind velocity prediction model.

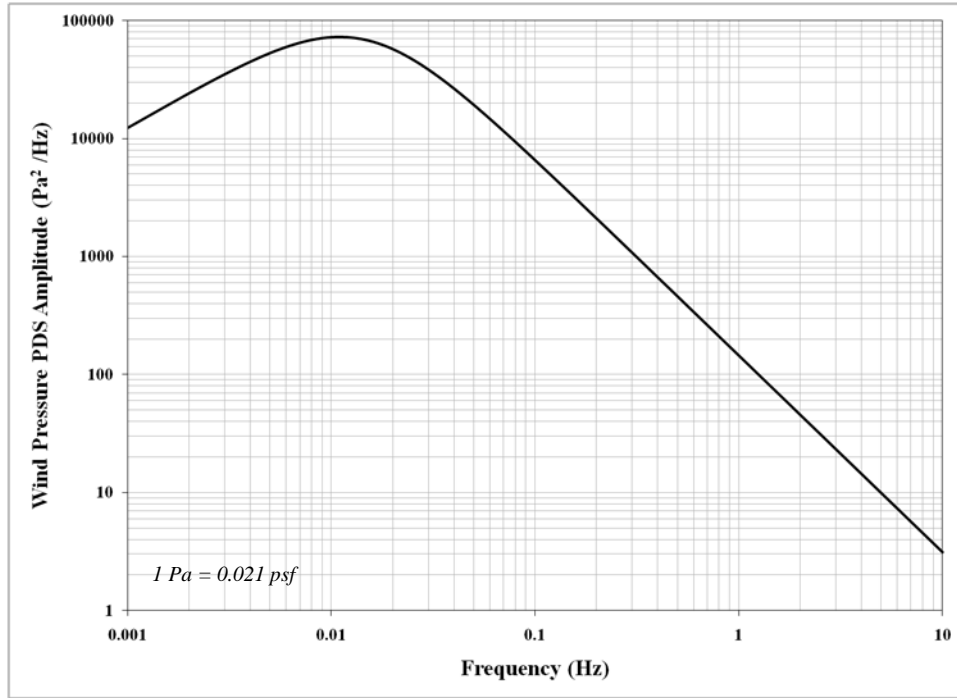


Figure 11-4. Wind pressure PDS of the fatigue wind velocity equal to 38 mph (17 m/s)

Experimentally Collected Wind Data Excitation Model

An experimental excitation model was developed using the wind velocity data collected with this research. Only the data considered usable (wind data directed on the front face of the structure) was used for the analysis. A velocity PDS of each data collection event was developed and a best fit trendline was created of the curves. The trendline was compared to the Davenport excitation model to assess the accuracy of the Davenport model.

Wind Velocity Power Density Spectrum Each wind velocity time history of the usable collected data was developed into a PDS. The time domain was transformed into the frequency domain through the Fourier transform (Eq. 11-6). The PDS was calculated by taking the Fourier transform and multiplying it by its conjugate, dividing by its period, and then taking the limit as the period approaches infinity (Eq. 11-7) (40, Irvine Mar. 2000).

$$X(f) = \int_{-\infty}^{\infty} x(t)e^{-j2\pi ft} dt \quad [\text{Eq. 11.6}]$$

where

$X(f)$ = Fourier transform

$x(t)$ = time history

f = frequency

t = time

j = imaginary

$$S(f) = \lim_{T \rightarrow \infty} \frac{1}{T} X(f)X^*(f) \quad [\text{Eq. 11-7}]$$

where

$S(f)$ = Power density spectrum

$X(f)$ = Fourier transform

f = frequency

T = Period

$X^*(f)$ = Complex conjugate of the Fourier transform

Power density spectrum curves are particularly useful for this application. They are ideal for random vibration analysis because of the inherent statistical properties of the time history that can be extracted in relation to the vibratory nature of the structure. The area under the PDS curve is equal to the mean square value. The square root of the mean square value is equal to the root-mean-square (RMS). For cases where the mean is equal to zero, the RMS is equal to the standard deviation (Harris 1996, Irvine Mar. 2000). The developed PDS curves using Eq. 11-6 and Eq. 11-7 are shown in Figure 11-5, along with the average PDS.

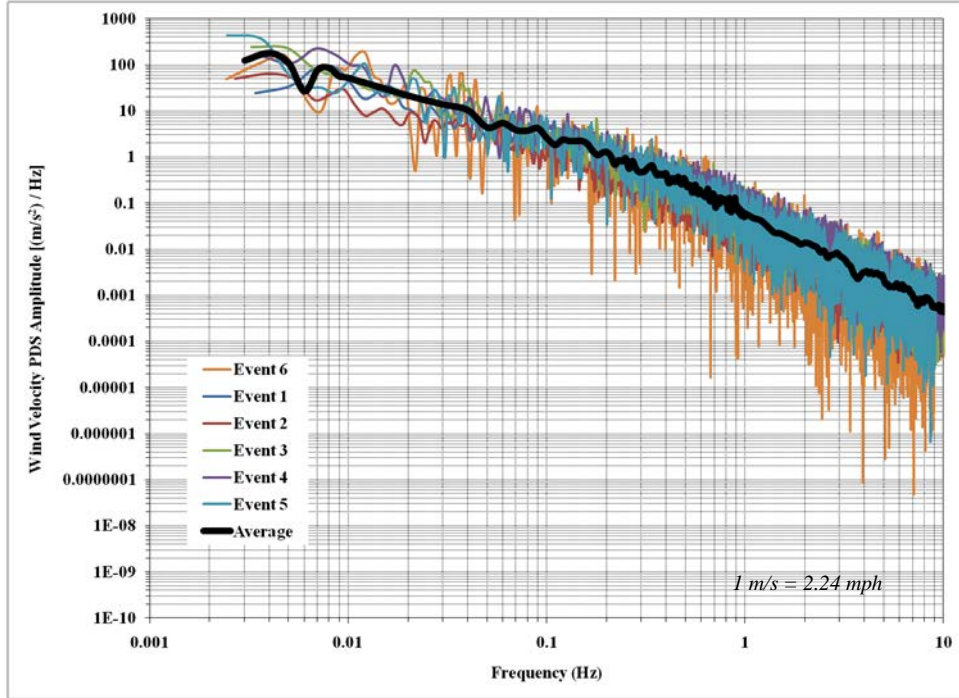


Figure 11-5. Experimental wind velocity PDS

Approximation of the Experimental Wind Velocity Power Density Spectrum A best fit line was developed that approximated the PDS average curve in Figure 11-5. A mathematical expression was needed that followed the curvature of the average PDS curve. On the log-to-log plot in Figure 11-5, the average PDS curve was viewed as bi-linear. The magnitude of the ordinate (y -axis) and abscissa (x -axis) data points were transformed into a log-to-log format so that the ordinate and abscissa axes would be a linear relationship on a standard linear plot without altering the curvature of the plot. This was done by taking the logarithm with a base 10 of the ordinate and abscissa values. The resulting plot is shown in Figure 11-6. The transformed plot (Figure 11-6) was subdivided into two sections that were observed to be linear. A linear trendline was fit to each section. The equation of the trendline was extracted and used as an approximation of the bi-linear curvature of the PDS plot. The logarithmic ordinate and abscissa axes were then transformed back to its original values using the logarithmic identity in Eq. 11-8.

$$y = \log_{10} x \quad \Leftrightarrow \quad x = 10^y \quad [\text{Eq. 11-8}]$$

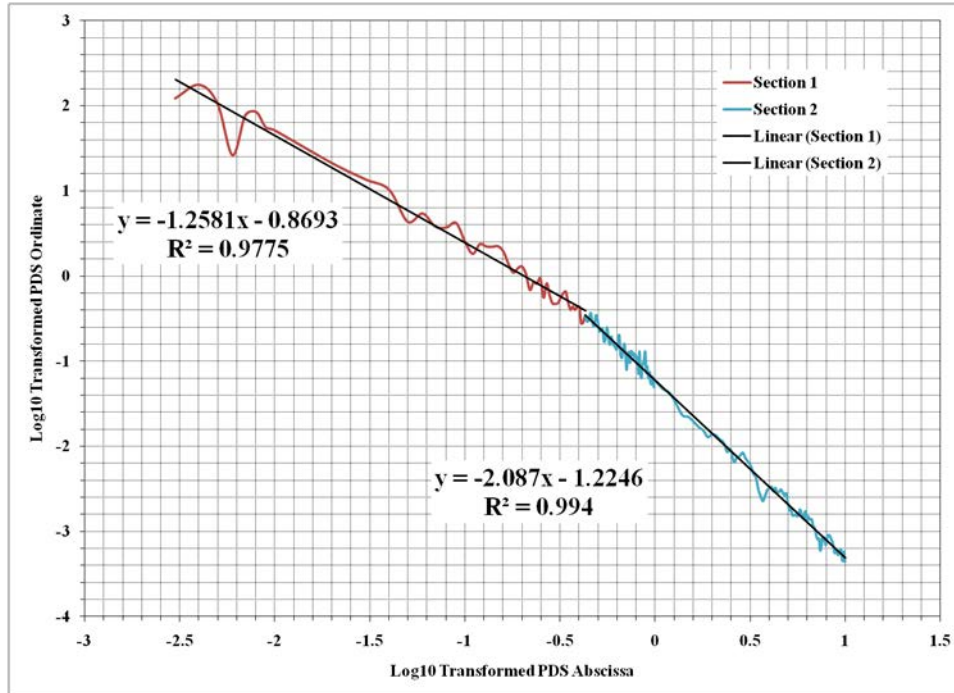


Figure 11-6 Logarithmic transformation of the average wind velocity PDS curvature

The next step was plotting the trendline equations onto logarithmic axes. Equivalent power equations, that represented the linear equations on a logarithmic axis, were developed of the two sectioned plot. The resulting plot is shown in Figure 11-7. The power equations in Figure 11-7 as a result describe the true curvature of the plot on both a logarithmic and linear axis, and can be used as a mathematical expression approximating the average wind velocity PDS. The approximation was capped at the lower frequencies by a constant distribution (see Figure 11-8) and used for the remainder of the analysis. As shown in the figure, the theoretical simulation of the experimental wind velocity PDS average closely followed the curvature and was viewed as a close approximation of the experimental curve.

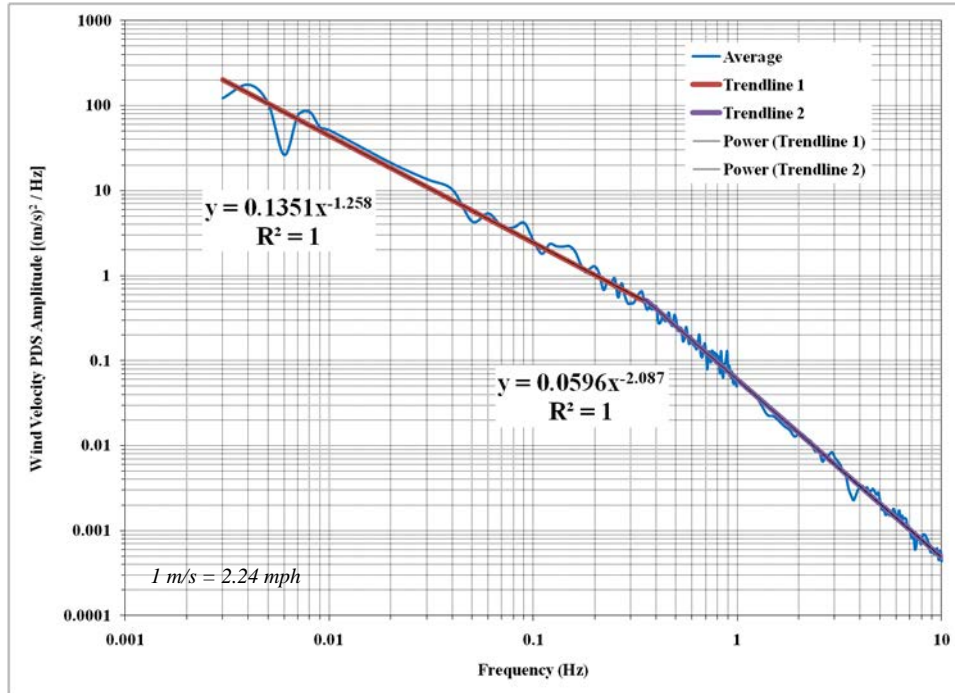


Figure 11-7. Best fit line for approximating the average wind velocity PDS curvature

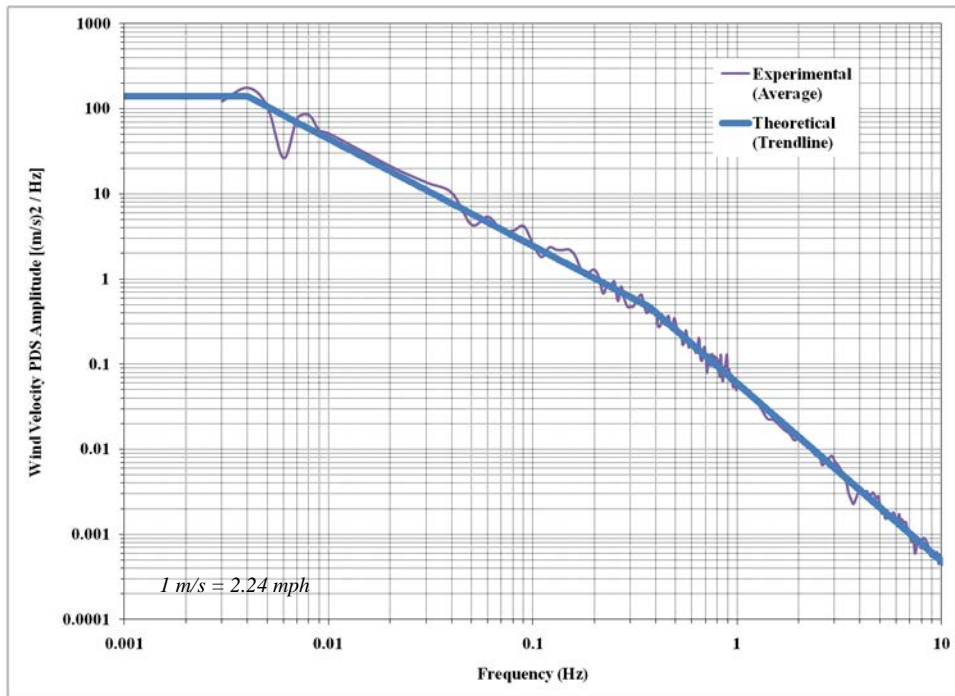


Figure 11-8. Theoretical plot of the experimental average wind velocity PDS of the best fit line process

Comparison between the Davenport and the Experimental Excitation Models

A comparison was made between the Davenport excitation model and the experimental excitation model developed from the wind data collected with this project. The average wind velocity was used for the comparison of both PDS excitations. The experimental excitation was based on an average wind velocity equal to 12.96 mph (5.79 m/s), and therefore this wind velocity was used in Eq. 11-1 for the Davenport model. A plot of the comparison is shown in Figure 11-9.

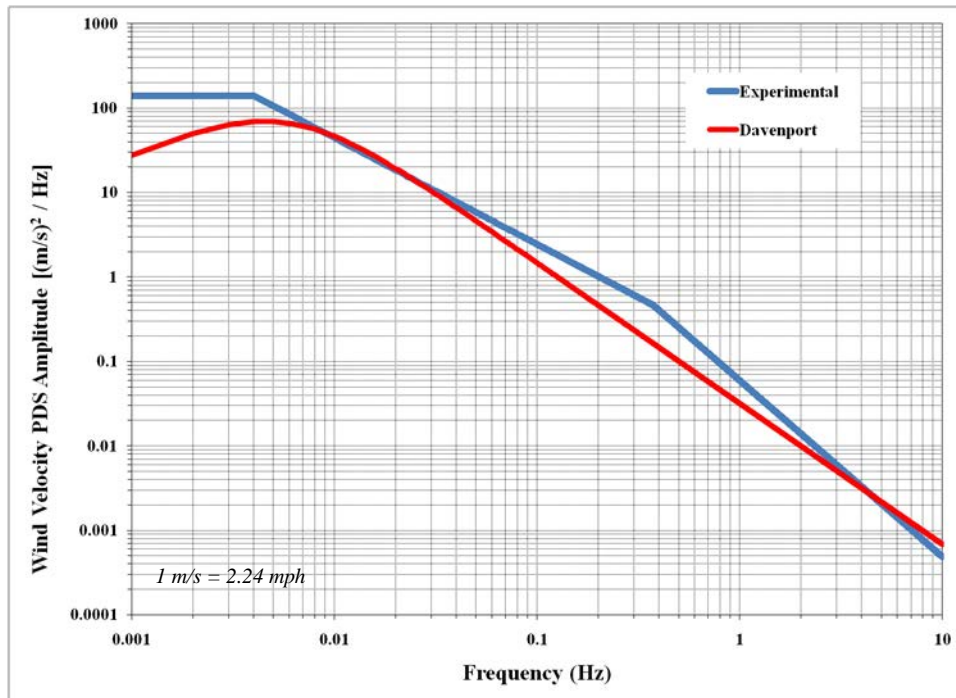


Figure 11-9. Comparison between the Davenport excitation model and the experimental excitation model

The plot indicates that the experimental PDS matched closely with the Davenport model. The experimental PDS was slightly greater than the Davenport model. The experimental PDS was based on an approximation, found through a fitted curve on limited experimental results gathered in a single location. The Davenport model was based on an equation that was developed from 70 experimentally collected wind records from around the world. The Davenport excitation model was used for the remainder of the analysis involved with the theoretical program for determining the fatigue load due to natural wind. This was decided based on the accuracy of the Davenport model found with this comparison as well as with the mathematical formulation of the Davenport model which allows it to be used with the continuation of the analysis required for the remainder of the theoretical approach.

Structural Response

Response Power Density Spectrum

Stresses are induced onto a structure when it vibrates, and because of the high flexibility and low damping properties of sign support structures, the vibratory stresses are enhanced as a direct result of the structure's dynamic characteristics. In the structural response analysis, the excitation on the structure from the randomly applied load, and the subsequent random vibration response of the structure, were approximated through basic principles of structural dynamics in utilization of the vibration response spectrum (VRS). The VRS in this context was a tool for determining the load transmitted onto the structure from the vibratory response created by the natural wind excitation described in the **Structural Excitation** section of this chapter.

The first step in the formulation of the VRS was determining the response of the structure from the wind pressure PDS excitation. The vibration behavior of sign support structures when excited were approximated as a single degree-of-freedom (SDOF) system in each of their major global directions. This was because the majority of vibration was controlled by single modal shapes. For the case with natural wind, the predominant mode of vibration with support structures was in the direction of the wind gust, exciting the horizontal modal shape.

The implication of developing the VRS was to account for the different types of sign support structures, each with differing configurations, sizes and shapes, and materials that have a direct influence on the dynamic characteristics of the structure. In the VRS development, the dynamic characteristics of the structure such as the natural frequency and damping ratio were kept variable in the calculation. In line with the directive needed in the VRS development, the response of a SDOF system from the wind pressure PDS excitation was calculated using Eq. 11-9 (Harris 1996, Irvine Jun. 2000).

$$\hat{U}_{PPSD}(f) = \frac{\left[1 + \left(2\xi \frac{f}{f_n}\right)^2\right]}{\left\{\left[1 - \left(\frac{f}{f_n}\right)^2\right]^2 + \left(2\xi \frac{f}{f_n}\right)^2\right\}} \hat{Y}_{PPSD}(f) \quad [\text{Eq. 11-9}]$$

where

$\hat{U}_{PPSD}(f)$ = response pressure PSD as a function of frequency, Pa²/Hz (psf²/Hz)

$\hat{Y}_{PPSD}(f)$ = excitation pressure PSD as a function of frequency, Pa²/Hz (psf²/Hz)

f = frequency, Hz

ξ = damping ratio

f_n = natural frequency of the structure, Hz

Equation 11-9 was used to calculate the response pressure PDS for individual natural frequencies and damping ratios of the particular structure of interest. It was formed using fundamental Structural Dynamics related to a SDOF system. The divisor term in Eq. 11-9 is referred to as the transfer function. It was multiplied by the excitation PDS equaling the response PDS. The units were in pressure. It represented the pressure load in the form of a PDS curve that was transmitted onto the structure resulting from the vibratory response created by the wind pressure PDS excitation. Dynamic amplification of the structure because of the applied loading was therefore inherent in Eq. 11-9, accounting for the dynamic properties that govern the response behavior.

An example of the excitation and response calculated using Eq. 11-9 is plotted in Figure 11-10. The example is for a structure with a natural frequency equal to 2.0 Hz and a critical damping percentage equal to 2.0%. The wind pressure PDS shown in Figure 11-4 was used as the excitation. This excitation represented the Davenport excitation model with the fatigue wind equal to 38 mph (17 m/s) in conformity with the infinite life approach to fatigue design.

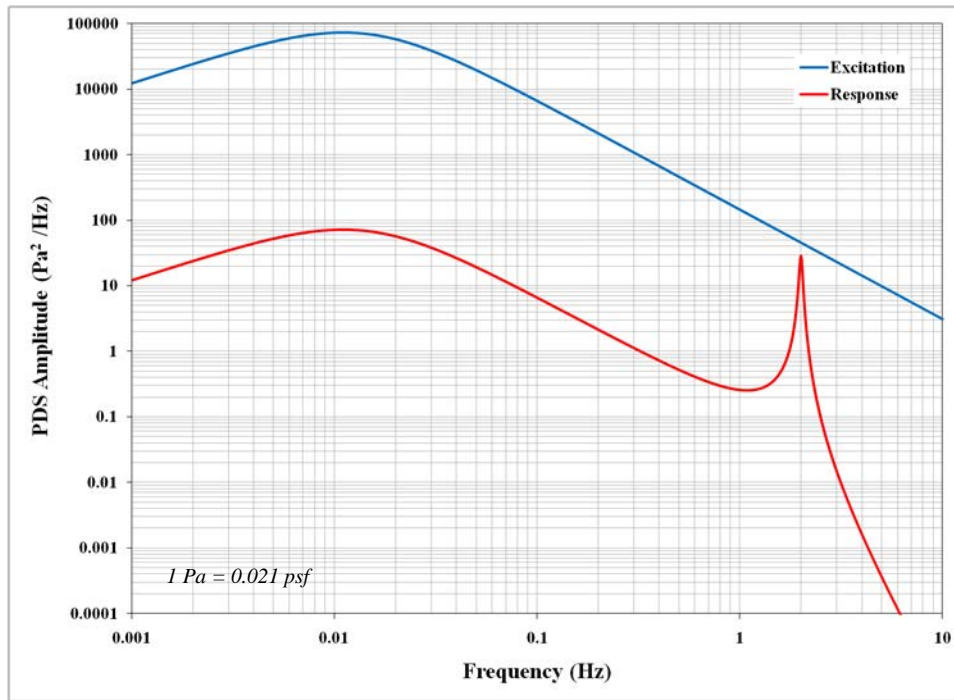


Figure 11-10. Response to wind pressure excitation PDS for 2.0% damping and 2.0 Hz natural frequency

The spike shown in the response curve of Figure 11-10 was located at the natural frequency used in the Eq. 11-9. Other frequency and damping values can be used in the equation to account for other support structures with differing dynamic properties. The results would have different spikes than the one depicted in Figure 11-10 of a 2.0 Hz natural frequency. In addition, the damping value influences the width and height of the spike. The spike would subsequently shrink for higher damping values, and increase for lower values, altering the area under the response curve.

Root Mean Square

The area under the response curve calculated using Eq. 11-9 is equal to the mean square value. The square root of the area curve is referred to as the root-mean-square (RMS). The RMS was a value used in this study for determining peak amplitudes within a random vibration structural response. It is representative of the variance of vibration amplitudes about a mean value in response to the turbulence and gustiness of the natural wind excitation. The RMS of the response pressure PDS for individual natural frequencies and damping ratios was determined by integrating the response pressure PDS over the frequency domain, and then taking the square root, as shown by Eq. 11-10 (Harris 1996, Irvine Jun. 2000).

$$U_{PRMS}(f_n, \xi) = \sqrt{\int_0^{\infty} \frac{\left[1 + \left(2\xi \frac{f}{f_n}\right)^2\right]}{\left\{\left[1 - \left(\frac{f}{f_n}\right)^2\right]^2 + \left(2\xi \frac{f}{f_n}\right)^2\right\}} \hat{Y}_{PPSD}(f) df} \quad [\text{Eq. 11-10}]$$

where

$U_{PRMS}(f_n, \xi)$ = overall response pressure RMS as a function of the natural frequency and damping ratio, Pa (psf)

For the response curve in Figure 11-10, using a natural frequency equal to 2.0 Hz and critical damping percentage equal to 2.0%, the square root of the area under the curve (RMS) calculated using Eq. 11-10, was equal to 1.78 psf (85.0 Pa). The calculated RMS value is commonly referred to as the overall level of the structural response PDS. The overall level was calculated for SDOF dynamic systems with individual natural frequencies and damping percentages and plotted to form the VRS that was used to calculate the fatigue load.

Vibration Response Spectrum

The VRS is a plot of the RMS of the response (Eq. 11-10) versus the range of natural frequencies used in the equation. The resulting VRS provides the transmitted pressure RMS onto the structure because of the dynamic amplification of the structure in relation to its specific dynamic characteristics. Take for example Figure 11-11. The same base input was applied to n number of structures. However, each structure had different mass and stiffness properties, which gave it different natural frequencies of vibration, f_n , and therefore each individual structural response to the base excitation was different, and subsequently, different response PDS curves. For each response curve, the RMS was determined using Eq. 11-11, and then plotted along with its corresponding natural frequency to form the pressure VRS shown in Figure 11-12.

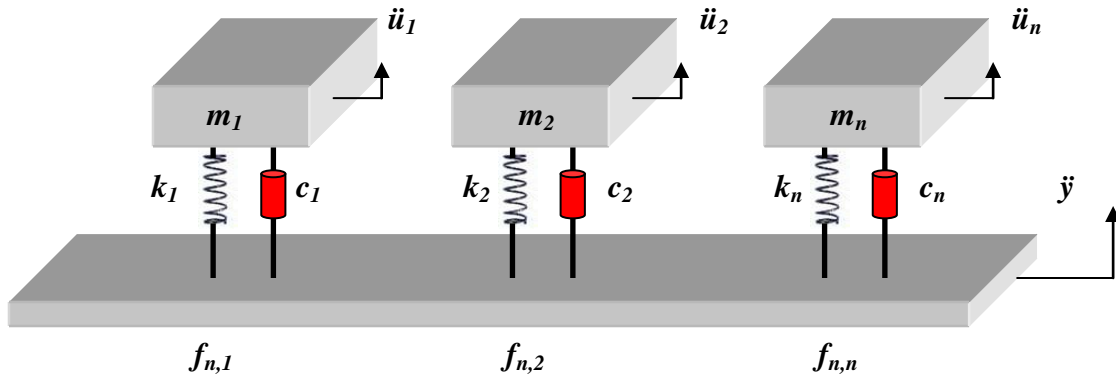


Figure 11-11. Dynamic response models of n SDOF systems to common excitation input

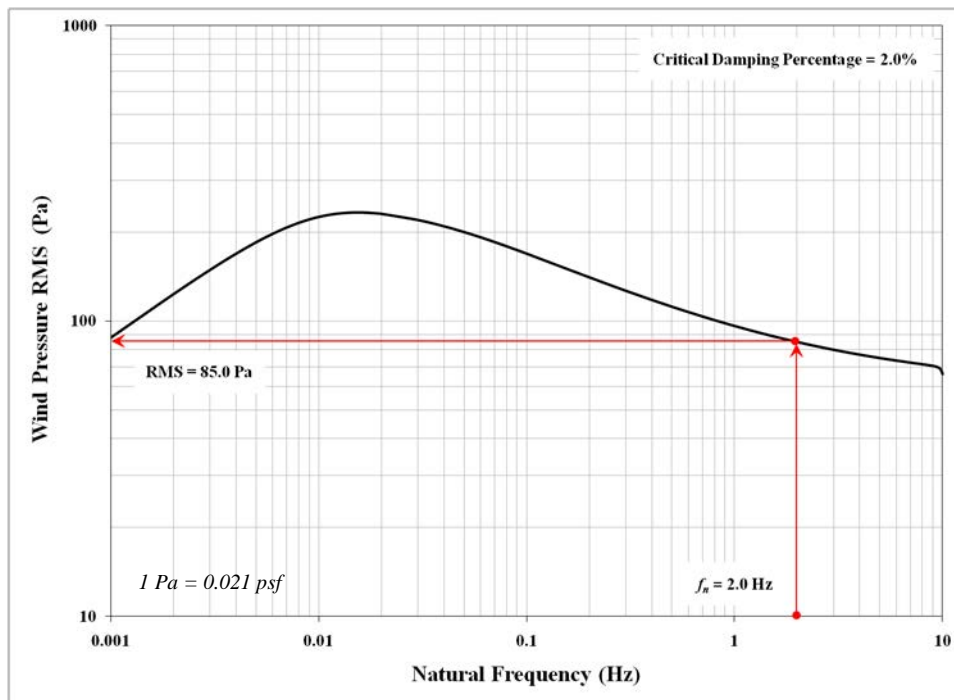


Figure 11-12. VRS wind pressure RMS for a structure with 2.0% damping and natural frequency of 2.0 Hz

The VRS in Figure 11-12 shows a decrease in RMS wind pressure as the natural frequency increase in large part because of the lessened proximity of the resonant frequency of the structure to the peak amplitude of the excitation PDS. The proper use of the VRS is to select the natural frequency of the structure of the predominant modal shape with vibratory motion in the direction of the wind gusts. For example, a structure with a horizontal modal frequency in the direction of the natural wind loading equal to 2.0 Hz would have a corresponding ordinate value equal to 1.78 psf (85.0 Pa) as calculated before and shown in Figure 11-12.

Natural Frequency

Highway overhead support structures have a variety of modal shapes, but because of the large separation between modes with vibration in the direction of the loading, they typically vibrate predominately independent from each other in distinct single directions. The appropriate natural frequency to use in the VRS must correspond to the modal shape that has motion in the direction of the natural wind loading. The most critical loading scenario for natural wind is directed normal to the plain of the sign (in the direction of traffic), most commonly referred to as the horizontal modal shape. An example of this is shown in Figure 11-13 illustrating the vibration behavior in response to the applied wind loading for the tested bridge-type VMS support structure. The appropriate frequency was equal to the earliest modal shape having horizontal vibratory motion, which was found to be equal to 2.81 Hz for the tested structure. For support structures, the horizontal modal shape is generally around 1 to 3 Hz, which typically corresponds to the first modal shape for cantilever-type structures, and the second modal shape for bridge-type structures.

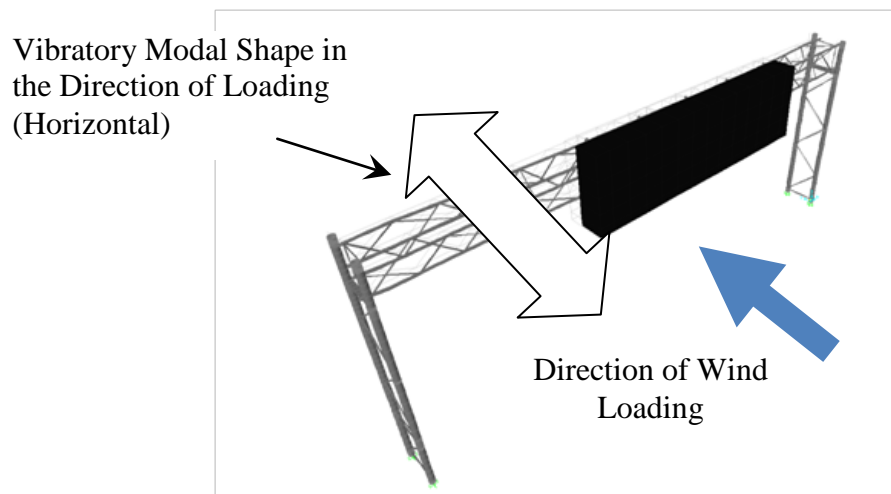


Figure 11-13. Horizontal vibratory motion in the direction of the wind loading

Finite element software (i.e., SAP2000, ANSYS, etc.) can be used to estimate the appropriate modal shapes and their associated natural frequencies to use with the VRS curves. If FEA software is not available, fundamental structural dynamics of a SDOF system (Eq. 11-11) can be used for estimating these values (AASHTO 2009, Creamer, *et al.* 1979, Harris 1996).

$$f_n = \frac{1}{2\pi} \sqrt{\frac{K}{M}} \quad [\text{Eq. 11-11}]$$

where

f_n = natural frequency, Hz

K = generalized stiffness, N/m (lb/ft)

M = generalized mass, kg (slug)

A recommended methodology in estimating natural frequencies and their associated modal shapes for overhead sign support structures using Eq. 11-11 can be found in the work performed by Creamer et al. (1979), which also contains useful calculation examples. It is understood that Eq. 11-11 would be predominately used by engineers in commercial applications, as FEA is not commonly exercised in industry.

Critical Damping Percentage

Damping also had an effect on the response of the structure as it vibrates. Take for example the VRS plot in Figure 11-14, with the same excitation but a damping value decreased to 0.5%. With a natural frequency equal to 2.0 Hz for example purposes, the RMS wind pressure would then be equal to 2.80 psf (134 Pa), a significant increase as compared to the 1.78 psf (85.0 Pa) value obtained with a damping value equal to 2.0%. This was true for any structural vibration frequency. As a result to a decreased damping value (worse case as opposed to an increased value), the spike in the response PDS increased in height and width, creating additional area under the curve as seen in Figure 11-15 as compared to Figure 11-10, and subsequently increasing the RMS.

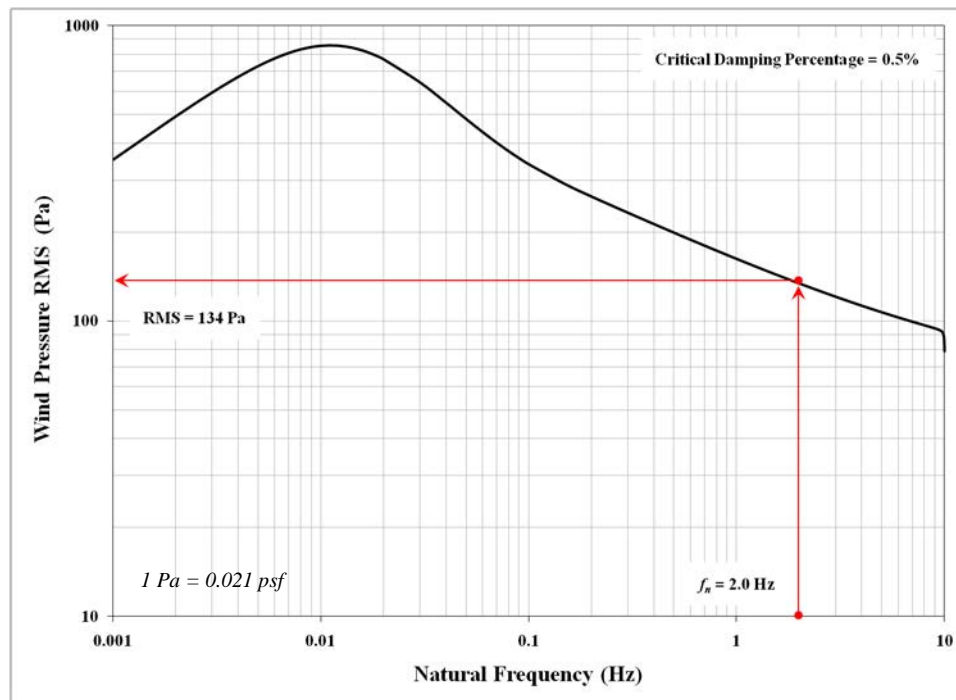


Figure 11-14. VRS wind pressure RMS with a critical damping percentage equal to 0.5%

A structure with no damping will theoretically vibrate forever. Apply damping, and the structure will slowly stop vibrating after a period of time. The length of time depends on the damping value, and the vibration frequency. During this time, stress is induced onto the structure. For structures with low damping ratios, longer periods of vibration at high amplitudes will result, during which time potentially damaging stress is transmitted onto the structure. If the stress is higher than the endurance limit of the connection detail, the fatigue life of the structure is decreased with each cycle of vibration. With higher natural frequencies of vibration, the transmitted load is decreased; but more importantly, damping becomes less important. Damping becomes more of a factor as the natural frequency of the structure decreases.

Damping is especially relevant to support structures because of their relatively high flexibility and subsequent low natural frequencies (1 to 3 Hz). What’s more, their damping ratios are mostly below 2.0%. A low damping will allow the structure to vibrate longer at high amplitudes, and thus produce more stress that could potentially cause fatigue damage. Damping ratios can vary depending on the structural material, and therefore actual values can be obtained from experimental data of comparable structures if available.

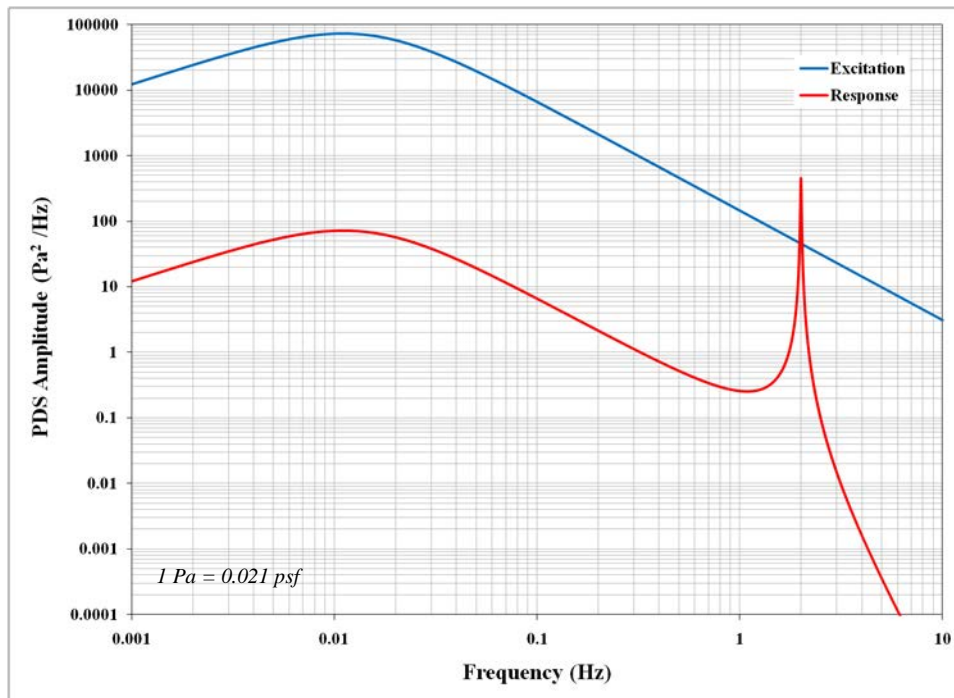


Figure 11-15. Response to wind pressure excitation PDS for 0.5% damping and 2.0 Hz natural frequency

Peak-to-Peak Stress Range

The design equation for fatigue due to natural wind loading must be representative of the amplitude peak-to-peak stress range that is induced on the structure during common everyday vibration. The majority of the structural vibration in response to natural wind excitation is controlled predominantly by a single modal frequency, the basis for which validates

approximating the response as a SDOF system. As a result, the response wind pressure PDS resembled a narrow-banded spectrum concentrated about the natural frequency. This is evident from Figure 11-10 and Figure 11-15, which is also true from experimental response spectrums of these structures. The RMS value of the spectrum embodies the variance of the vibration amplitudes from a mean, which symbolizes the response of the structure due to the turbulence and gustiness of natural wind. During a single transient event from a common everyday natural wind gust, the peak-to-peak ranges of the response will initiate at its largest value and then decay at rate indicative of the damping ratio. The design fatigue equation must exemplify the largest range created on the outset of this event. In view of this, given that the response is predominately controlled by a single modal frequency, and the gustiness and turbulence of natural wind is typified by the RMS value, the averaged initial peak-to-peak range of vibration was estimated as a constant-amplitude sinusoid (Kaczinski, *et al.* 1998). Therefore, the initial peak amplitude was approximated as the square root of two times the RMS value, and then doubled to form the initial peak-to-peak range, as shown by Eq. 11-12.

$$\begin{aligned} \text{Pressure Range} &= 2 \times \sqrt{2} \times U_{PRMS}(f_n, \xi) \\ &= 2.8U_{PRMS}(f_n, \xi) \end{aligned} \quad [\text{Eq. 11-12}]$$

where

Pressure Range = peak - to - peak pressure range, Pa (psf)

$U_{PRMS}(f_n, \xi)$ = overall response pressure RMS as a function of the natural frequency
and damping ratio calculated using Equation 3, Pa (psf)

The plots in Figure 11-12 and Figure 11-14 represent the wind pressure in terms of the RMS values only, and do not represent peak-to-peak ranges. To predict the peak-to-peak pressure range for design considerations, the VRS chart of RMS values was factored by 2.8 (Eq. 11-12). An example of the resulting plot is shown in Figure 11-16 for a critical damping percentage of 2.0%. As a result, a support structure with a natural frequency equal to 2.0 Hz and a critical damping percentage equal to 2.0% would require a wind pressure representing the peak-to-peak amplitude equal to 5.01 psf (240 Pa).

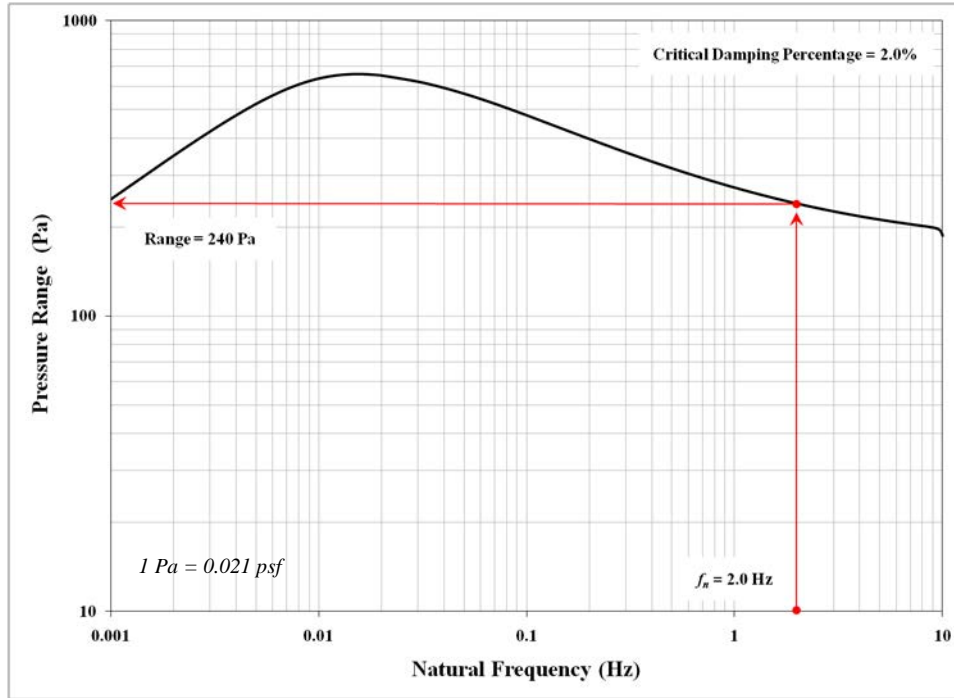


Figure 11-16. Peak-to-peak VRS for a support structure with 2.0 Hz natural frequency and 2.0% damping

Fatigue Load Vibration Response Spectrum

The fatigue load is extracted from the VRS plot in Figure 11-17 and used for design. The constant obtained from the plot and based on the dynamic characteristics of the structure is plugged into by Eq. 11-13 for each member along the facade of the structure exposed to natural wind.

$$P_{NW} = P_{VRS} C_d I_F \quad [\text{Eq. 11-13}]$$

where

P_{NW} = design fatigue load due to natural wind gust, psf (Pa)

P_{VRS} = transmitted pressure constant extracted from the VRS, psf (Pa)

C_d = drag coefficient

I_F = importance factor

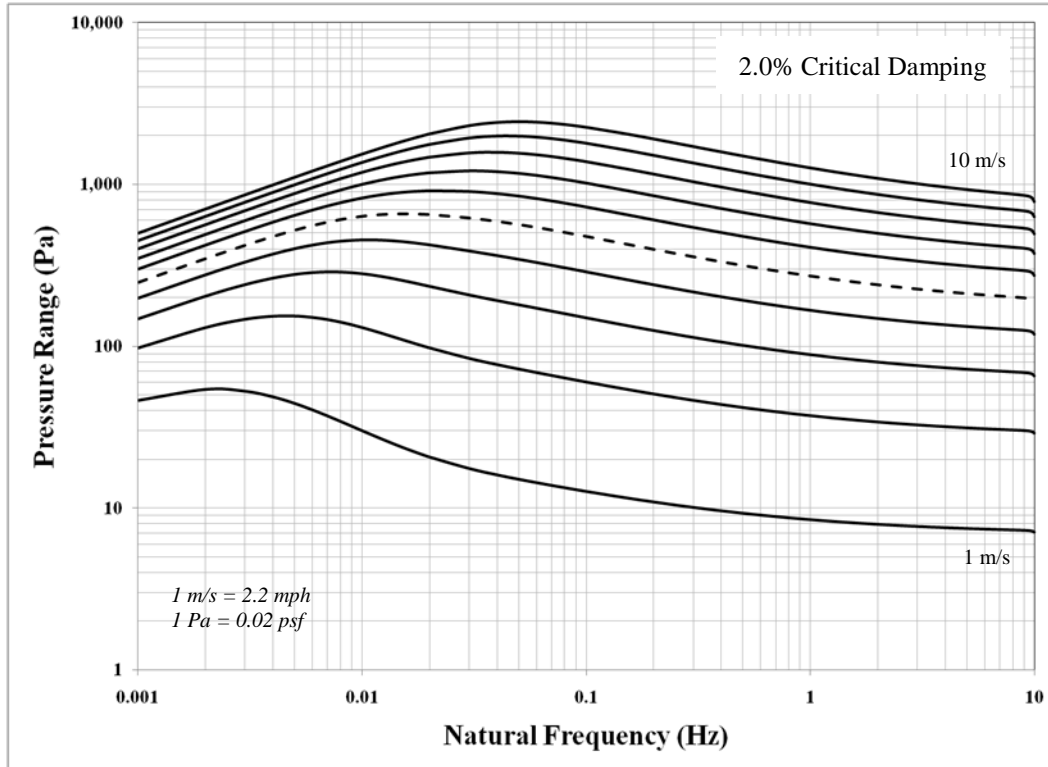


Figure 11-17. Fatigue load VRS using the Davenport excitation model

The fatigue load VRS was developed for a variety of 0.01% exceedence probabilities from annual mean wind velocities ranging from 2 mph (1 m/s) to 22 mph (10 m/s). The wind velocities based on the infinite-life approach were simply plugged into Eq. 11-1 and the structural excitation, structural response, and VRS development process was conducted. By using the infinite-life approach, and determining the peak-to-peak wind pressure range, the resulting VRS is referred to as the fatigue load VRS and is shown in Figure 11-17. The plot in Figure 11-17 was made for a 2.0% critical damping percentage. The x -axis depicts the natural frequency of the structure. The y -axis depicts the fatigue load referred to as the pressure range that is normalized for the drag coefficient. Vibration response spectrums for other damping values ranging from 0.1% to 1% were created and are shown in Figure 11-18. Plots for other critical damping percentages were also developed. The trend shows damping to become more influential as the natural frequency decreases. The wind pressure values vary greatly, which indicates the importance to obtain a true damping value in the fatigue analysis.

The plot also shows variation with annual mean wind velocity as depicted in the graph. It is important to note that the curves corresponding to the annual mean wind velocity are based on the 0.01% exceedence probability for that mean wind velocity. The fatigue provisions in the *Supports Specifications* specified an annual mean wind velocity based on an analysis of annual mean wind velocities of 59 major U.S. cities. It was found that an annual mean wind velocity of 11 mph (5 m/s) was exceeded in only 19% of the U.S. cities analyzed and was therefore chosen. The wind velocity with a 0.01% exceedence probability to the specified annual mean wind

velocity is equal to 38 mph (17 m/s) and is referred to as the fatigue wind. The curve in Figure 11-17 representing this specified fatigue wind is dashed for reference purposes. Other curves are provided if a different annual mean wind velocity is necessary based on the wind conditions of the site.

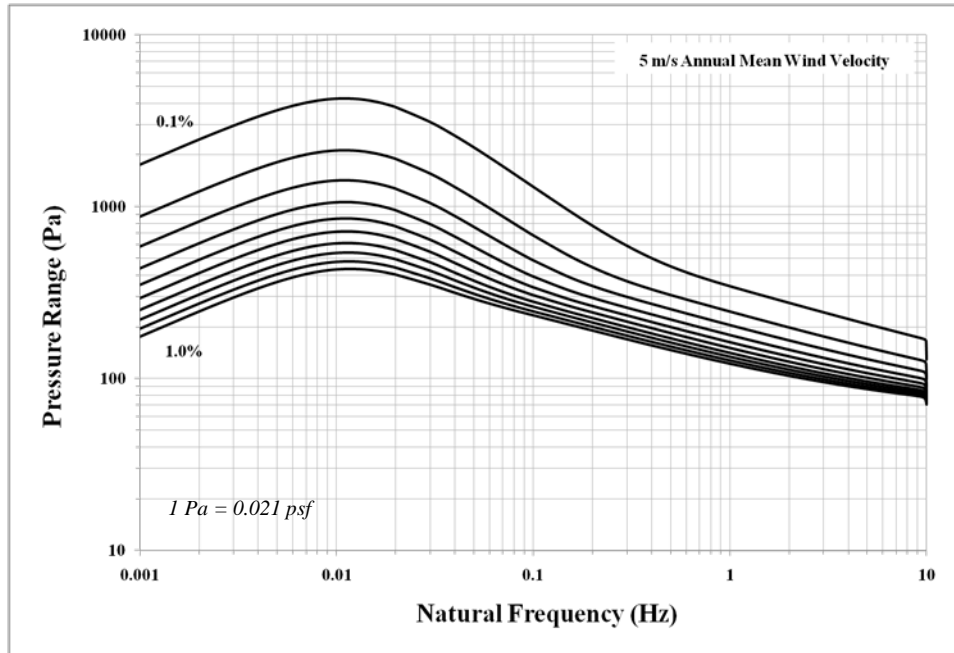


Figure 11-18. VRS plot showing increasing pressure ranges with decreasing critical damping percentages

Section 12

Theoretical Calculation of the Fatigue Load due to Truck-Induced Wind Gust

Overview

The developed theoretical procedure for determining the design fatigue load due to truck-induced wind gusts on highway overhead support structures is presented. Truck-induced wind gust is a loading generated on the structure from wind gust created when trucks travel underneath them at highway speeds. Semi-trailer commercial trucks were the focus of the research. It was considered a fatigue load because of the large number of trucks using the highway system, and the significant wind load generated on the overhead support structure with each passing truck. The theoretical study primarily involved analysis of support structures in relation to mechanical vibration and utilization of the shock response spectrum (SRS). The fatigue load due to truck gust was extracted from the SRS as an equivalent static wind load and used for design.

Research Significance

The fatigue load is determined primarily from the structural dynamic characteristics of the particular structure in question. Operational overhead support structures are highly flexible with low damping properties, which make them susceptible to vibratory induced fatigue loading caused by wind gust impulses generated from passing trucks. The magnitude of this load is dependent on the dynamic behavior and characteristics of the structure. The analysis becomes especially crucial when the frequency of the impulse matches the natural frequency of vibration of the structure. Frequencies of vibration and the frequencies of the truck gust impulses are similar, typically around 1 to 3 Hz, and therefore resonance issues are a major cause of fatigue damage. A method that incorporates the response of the structure based on its dynamic properties is needed for estimating the fatigue load. The intention of the study was to develop a relationship between fatigue loading and the structural dynamic response in terms of mechanical vibration as a single-degree-of-freedom (SDOF) system. Examples include cantilever- and bridge-type overhead sign support structures, as well as VMS support structures (Figure 12-1).

The fatigue provisions for truck gusts within the *Supports Specifications* were selected from the National Cooperative Highway Research Program (NCHRP) Report 412 (AASHTO 2009, DeSantis, *et al.* 1998, Kaczinski, *et al.* 1998), and later modified because of the research detailed in the NCHRP Report 469 (Dexter, *et al.* 2002, DeSantis, *et al.* 1998). It was stated in Report 412 that the design fatigue load in regards to truck gusts was based on the response of a single particular cantilever-type highway overhead variable message sign (VMS). The *Supports Specifications* are only applicable to highway signs with the same structural excitation and dynamic response characteristics reported. Differences in these characteristics, such as the case

with other cantilever- and bridge-type sign support structures, cannot be accounted for nor are addressed in the current *Supports Specifications*.



Figure 12-1. Highway overhead support structures with different configurations, sizes and shapes

This chapter details a universal approach to fatigue design to handle cases that have different structural dynamic properties than those used to develop the current *Supports Specifications*. Highway overhead support structures can have different configurations and are made with various materials and cross sectional shapes. These parameters will dramatically affect the dynamic behavior of the structure and subsequent magnitude of the fatigue load. A method for estimating the fatigue load that incorporates the specific dynamic properties of the structure can as a result account for the variety of sign structures in design. For that reason, the proposed method was considered universal. It is applicable to any type of support structure of varying configuration, material, strength, mass, and stiffness whereby its response can be approximated as a SDOF system. Bridge-type support structures, which are not covered by the *Supports Specifications*, can also be addressed with the proposed design method. The primary differences in these structures in comparisons to conventional cantilever-type structures are related to stiffness and mass. Since all of these dynamic features are directly related to the natural

frequency of the structure, the method described in this paper can be used to determine the design fatigue load due to truck gusts in specific reference to the dynamic characteristics of the particular structure in question.

Methodology

The framework of the developed method can be broken down into two major components: 1) the truck gust excitation of the structure, and 2) the dynamic response of the structure. Research data collected from the literature was used to simulate the truck gust excitation for this chapter. A typical truck gust pressure loading was developed in the form of a time history streamline. Different design truck speeds were employed in the time history simulation, resulting in truck gust impulses occurring at different frequencies, which in turn would excite different vibratory responses in the structure.

The response of the structure and consequent fatigue load due to the truck gust excitation was evaluated differently than the methods described in the literature. The proposed method was entirely new and unique with respect to support structures. The structural response was theoretically calculated based on principles of mechanical vibration, and the fatigue load was determined through utilization of the SRS. The load is extracted from the SRS in terms of the natural frequency of the structure to account for the variety of support structures in design, and the estimated speed of the truck to account for different loading impulses. The extracted value is in the form of an equivalent static wind load which produces the same response onto the structure as the dynamic impulse. Dynamic amplification was included within the fatigue load chosen from the SRS, since the SRS was developed based on the frequency of vibration of the structure in response to the loading event. The proposed method is used as a tool to easily determine the appropriate design fatigue load due to truck gust for the particular structure in question.

Structural Excitation

An accurate depiction of the truck gust wind excitation without influence from the type of structure and its dynamic behavior was needed in the development of the theoretical procedure. The research performed by Cook et al, in their collaboration with the Florida Department of Transportation (Cook, *et al.* 1996) was considered by the UAB research team as the best candidate. Cook's research involved experimentally determining the truck gust pressure load through direct measurement of wind pressure from passing trucks. The truck wind pressure was evaluated at varying heights above ground level using pressure transducers placed on a rigid road bridge spanning over the highway. Time history wind pressure impulses from 23 truck gust loading events were recorded. The findings in Cook's research were closely similar to other experimental research efforts on the subject performed by different investigators in other locations (Creamer, *et al.* 1979, Dexter, *et al.* 2002, Edwards, *et al.* 1984), and especially with NCHRP Report 469 that was used to develop the current *Supports Specifications*.

Cook's research indicated a biaxial fatigue loading event. The results indicated a horizontal and vertical component of the wind gust pressure impulses. This was also evident in the experimental data collected with by the UAB researchers of this project. The horizontal component was projected onto the face within the vertical plane that was oriented perpendicular to the ground. The vertical component was projected onto the face within the horizontal plane that was oriented parallel to the ground (Cook, *et al.* 1996). For some cases, the natural wind fatigue loading criteria in the horizontal direction controls over the horizontal truck-induced wind component, and therefore only the vertical component to the truck gust is used in design. For such cases, the stress values are significantly higher (nearly twice as much) with natural wind gusts than for the truck-induced wind gusts in the horizontal direction. However, this is not always the case and therefore a horizontal component and fatigue loading criteria associated with truck-induced wind gust was also developed with this research.

The pressure impulses recorded by Cook were simplified in order for them to be functional for numerical applications. The time history impulses were transformed into a linear composition by enveloping the samples by the triangular single cycle loading shown in Figure 12-2 for the vertical component, and Figure 12-3 for the horizontal component of the truck gust. This was done similar to the research performed by Ginal (2003), except impulses from trucks traveling at other speeds were also employed. The loading simulations in Figure 12-2 and Figure 12-3 represented a linear increase in wind pressure as the truck approaches, followed by an equivalent (in magnitude) suction as the truck passes and separates from the structure. For example, the vertical impulse is indicative a wind pressure directed upward onto the underside facade of the structure as the truck approached, followed by a suction pressure directed downward as the truck separated from the structure (Cook, *et al.* 1996, Ginal 2003). The same action is true for the horizontal impulse. The impulses in Figure 12-2 and Figure 12-3 represent the measured values taken at 17 ft (5.2 m) above ground level (Cook, *et al.* 1996).

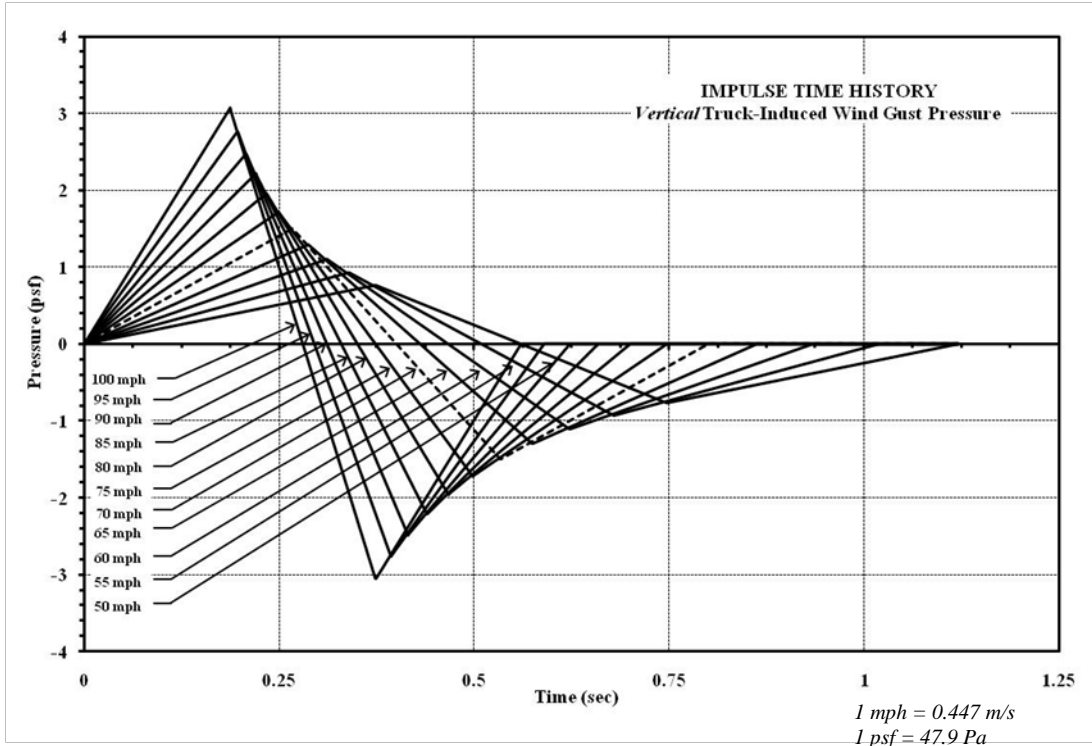


Figure 12-2. Vertical truck-induced wind gust impulses

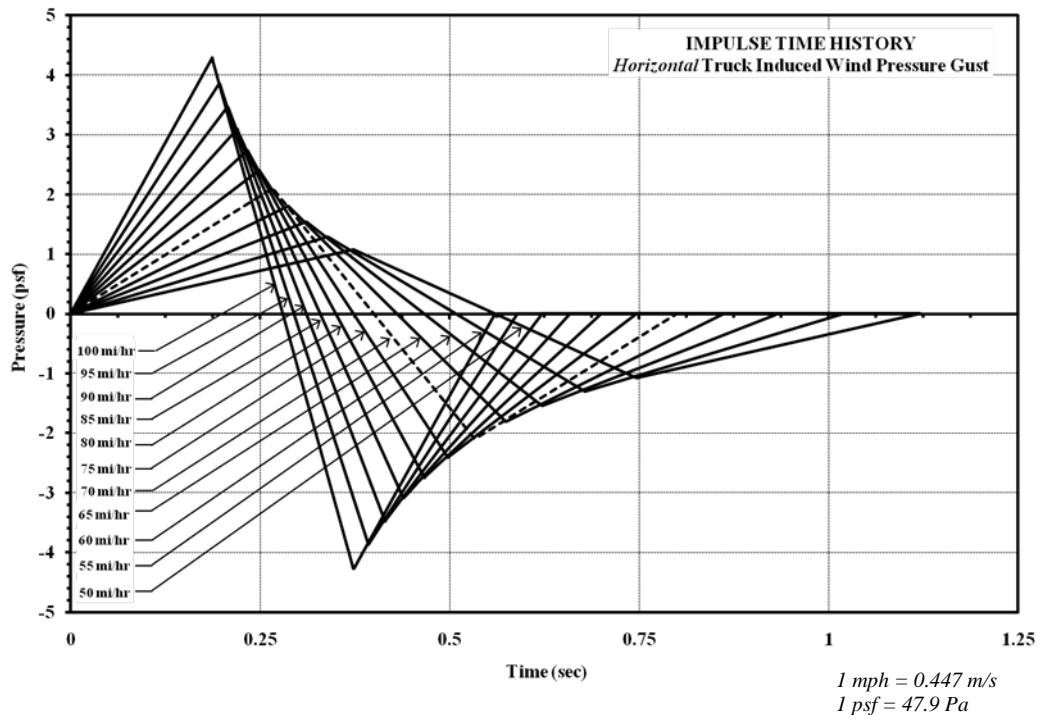


Figure 12-3. Horizontal truck-induced wind gust impulses

The wind pressure impulse resulting from a truck traveling at 70 mph (31.3 m/s) was used as an impulse Control (dashed line in Figure 12-2 and Figure 12-3). The Control reflects an envelopment procedure of the recorded time history samples of trucks that traveled at this speed. It was developed as a prediction model representative of the exposure environment from truck gusts defined at a 90% confidence level that the actual maximum absolute value of pressure and impulse duration will be equal to or below the Control at least 95% of the time (Cook, *et al.* 1996). The envelopment resulted in a linear increase and subsequent decrease to the maximum impulse pressures. These values were used for both the approach pressure and the separation pressure of the Control for symmetrical simplification of the simulated impulse. The duration of the Control determined by the envelopment procedure was approximately equal to 0.80 seconds.

Trucks traveling at other speeds generated wind gust impulses with different frequencies and durations than the Control, and would as a consequence excite different responses on the structure. Impulses generated at other truck speeds were identified and employed in this method to account for a variation in excitation frequencies. The impulses were normalized based on the Control impulse at 70 mph (31.3 m/s) using the mechanics of fluids relationships between wind pressure and the square of wind velocity, as well as Newtonian dynamic continuous motion kinematics of a particle with a constant acceleration.

Structural Response

The structural response from truck gust loads described in the previous section was approximated through basic principles of structural dynamics. For analysis purposes, the dynamic behavior of highway overhead sign support structures was approximated by a SDOF system. This was because their modes of vibration are significantly separated such that the vibration in response to transient loading is controlled predominately by a single modal shape in independent directions. For that reason, the modal shapes were estimated as vibrating independently from each other in single global directions (Creamer, *et al.* 1979 , Foutch, *et al.* 2006, Harris 1996). In this study, the structural response of a SDOF system from the truck gust load was calculated using Eq. 12-1 shown in index notation, i (Harris 1996, Irvine 2002):

$$\begin{aligned}
 P_i = & 2e^{-\xi\omega_n\Delta t} \cos(\omega_d\Delta t)P_{i-1} \\
 & - (e^{-2\xi\omega_n\Delta t})P_{i-2} \\
 & + 2\xi\omega_n\Delta tp_i \\
 & + \omega_n\Delta te^{-\xi\omega_n\Delta t} \left\{ \left[\frac{\omega_n}{\omega_d} (1 - 2\xi^2) \right] \sin(\omega_d\Delta t) - 2\xi \cos(\omega_d\Delta t) \right\} P_{i-1}
 \end{aligned}
 \tag{Eq. 12-1}$$

where

P_i = response pressure as a function of natural frequency and critical damping percentage, psf (Pa)

p_i = truck induced wind gust pressure impulse excitation, psf (Pa)

ω_n = undamped natural frequency of the structure, rad/sec

$\omega_d = \omega_n \sqrt{1 - \xi^2}$ = damped natural frequency of the structure, rad/sec

ξ = percent critical damping

t = time, sec

Equation 12-1 calculates the response pressure time history for individual natural frequencies and critical damping percentages of the particular structure of interest. It can be seen as an equivalent pressure load that is transmitted onto the structure from the vibration response created by the truck-induced excitation. The equation embodied full dynamic amplification based on the dynamic characteristics of the structure.

An example of the vibratory response time history of a typical sign support structure calculated using Eq. 12-1 is shown in Figure 12-4. The 70 mph (31.3 m/s) vertical Control impulse was used as the excitation for this example. The natural frequency with a modal shape in the direction of the vertical loading equal to 1.64 Hz was chosen for this example. This modal shape is best described as a rocking vibratory motion in the direction perpendicular to the ground (parallel to the vertical component loading). The plot shows response time histories of the structure for an undamped case, and for a critical damping percentage equal to 1.0%.

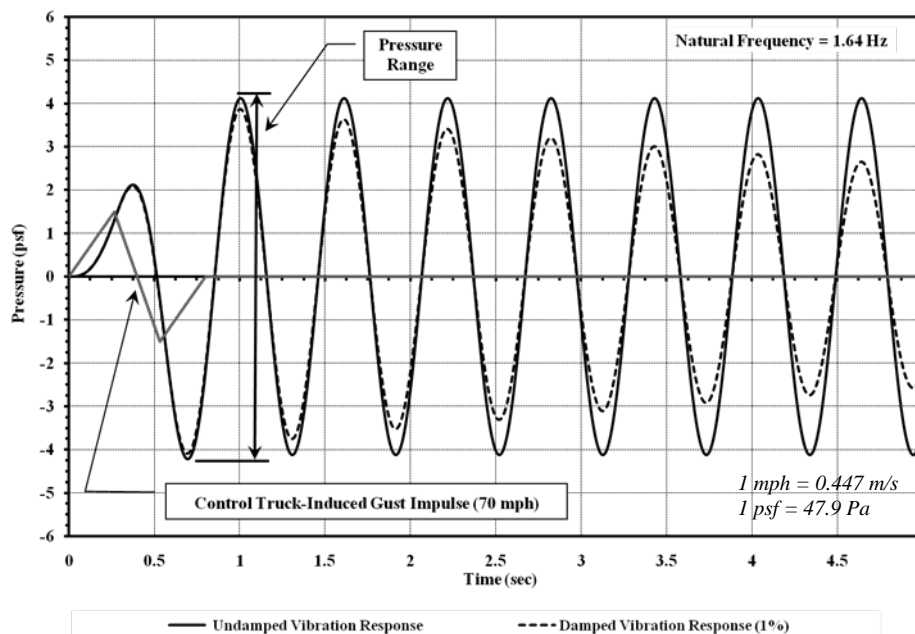


Figure 12-4. Structural response time history due to the vertical Control impulse

Highway overhead support structures typically have critical damping percentages around 2.0% and less. Even for 1.0% damping however, the difference in magnitude of the maximum pressure range observed between the two response cases (Figure 12-4) is very small, and significantly lessens as the damping percentage decreases. This reveals that the maximum peak response is not sensitive to structural damping, and therefore the undamped case was used in the SRS development, which adheres to other common SRS development case studies (Harris 1996, Irvine 2002). For such instances, the damped natural frequency parameter, ω_d , in Eq. 12-1 became equal to the undamped natural frequency, ω_n .

Shock Response Spectrum

The SRS in this context was a tool for determining the maximum load transmitted onto the structure from the vibration response created by truck gusts. The SRS was a plot of maximum peak values determined from the response time histories calculated using Eq. 12-1 for a range of SDOF systems (see Figure 12-5) with varying undamped natural frequencies under a common loading (Harris 1996, Irvine 2002). The SRS plot for the vertical component of the truck gust impulse is shown in Figure 12-6 and horizontal component shown in Figure 12-7. The SRS shown in these figures is a plot of the maximum response pressure ranges versus natural frequencies. The natural frequency domain extends from 0 to 10 Hz, and individual SRS curves for truck speeds ranging from 50 mph to 100 mph (22.4 m/s to 44.7 m/s) are plotted based on the impulses presented in Figure 12-2 and Figure 12-3.

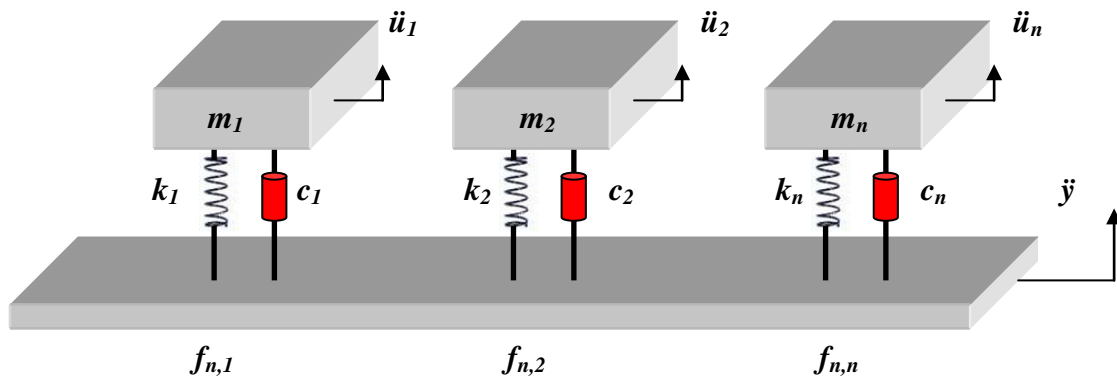


Figure 12-5. Dynamic response models of n SDOF systems to common excitation input

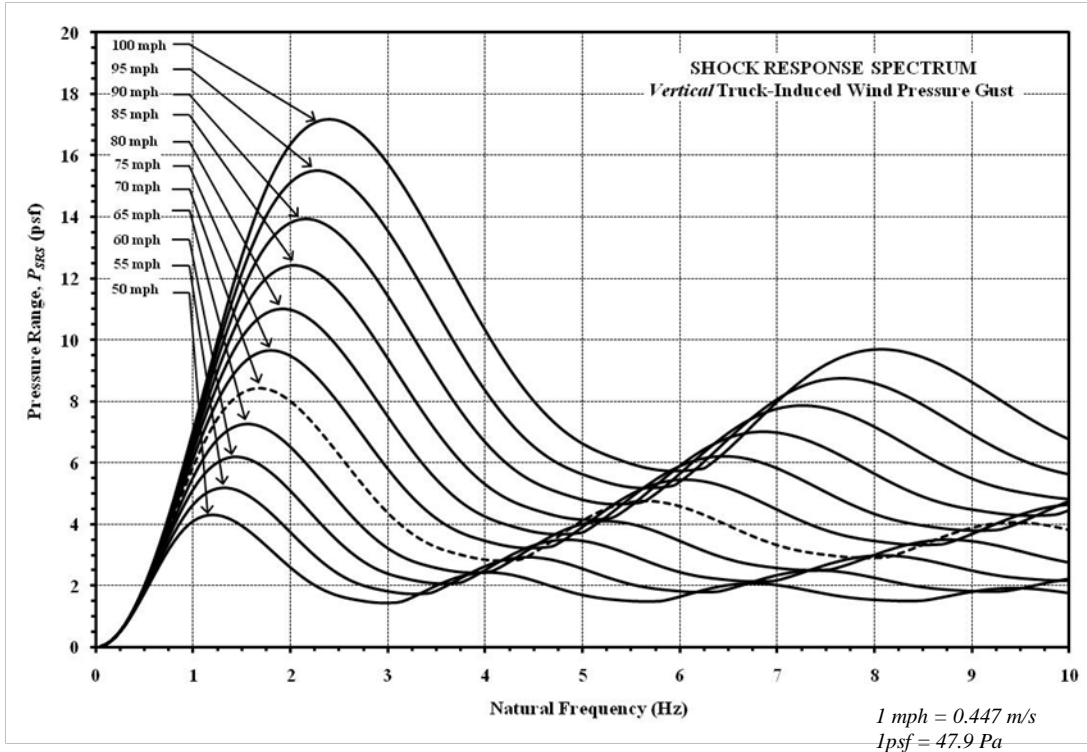


Figure 12-6. SRS for the vertical component of the truck-induced wind gust

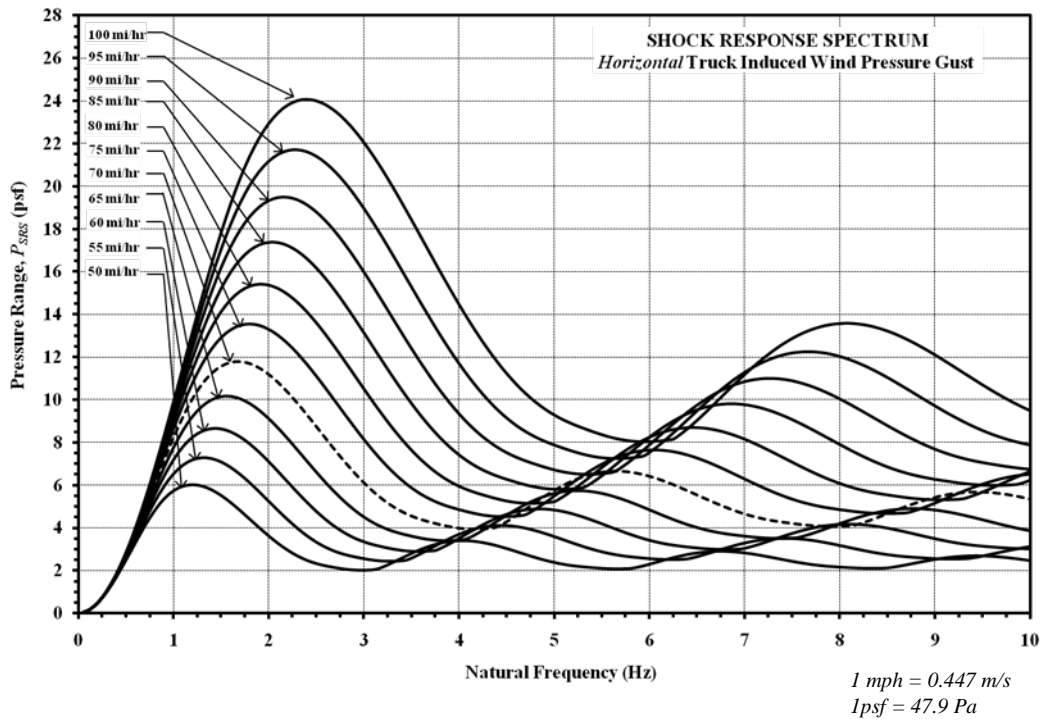


Figure 12-7. SRS for the horizontal component of the truck-induced wind gust

The pressure range, and subsequent stress range, was of interest when dealing with fatigue analysis. It is important to clarify the curves in Figure 12-6 and Figure 12-7 represent the initial range of the positive to negative peaks (see Figure 12-4) for each impulse. The stress generated from the vibration caused by this pressure range will be induced onto the structure with each passing truck, with little influence from the damping properties of the structure. The damping will allow the structure to slowly stop vibrating over a period of time by gradually decreasing the magnitude of this range, as shown in Figure 12-4 for the 1% damping case. However, if the initial pressure range occurring at the onslaught of the gust impulse generates a stress that is greater than the endurance limit of the material and connection detail, then the fatigue life of the structure is greatly decreased with each passing truck. And therefore, the design fatigue load must be representative of the initial range of values plotted in Figure 12-6 and Figure 12-7 in terms of the natural frequency of vibration of the structure which, as indicated in the figure, has a significant effect on the magnitude of the initial range.

Natural Frequency

The fatigue load is extracted from the SRS as the ordinate value corresponding to the natural frequency of vibration with a modal shape in the direction of the excitation. Sign support structures have a variety of modal shapes, but because of the large separation between modes with vibration in the direction of the loading, they vibrate predominately independent from each other in distinct single directions. The appropriate natural frequency to use in the SRS must correspond to the earliest modal shape that has motion in the direction of the truck-induced wind loading. For example, in the case for the vertically applied load, the truck-induced load was directed vertically onto the underneath facade of the structure. The appropriate modal shape would be a vertical vibratory motion (perpendicular to the direction of traffic) generally associated with the second modal shape of typical cantilever-type sign structures (see Figure 12-8), and the third modal shape of typical bridge-type support structures.

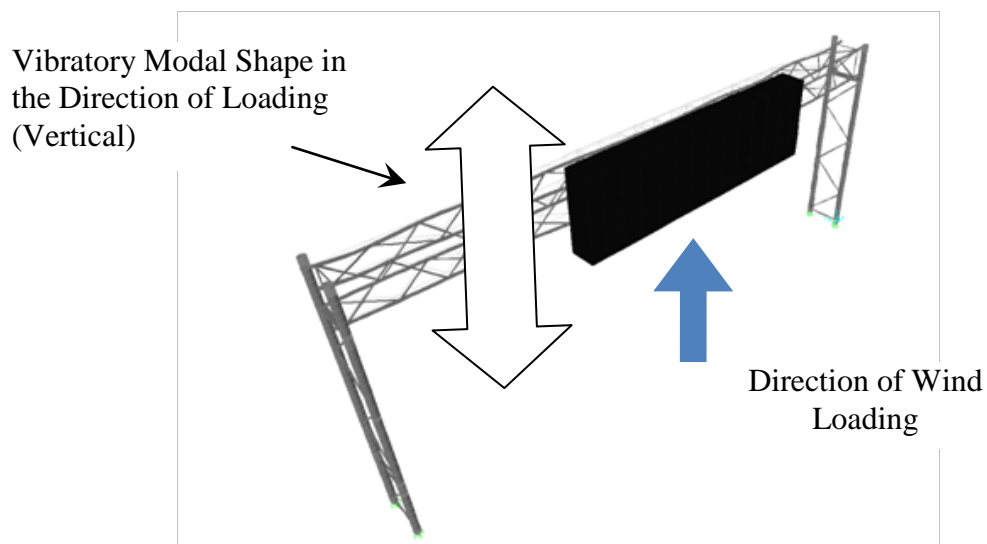


Figure 12-8. Vertical vibratory motion in the direction of loading

Finite element software (i.e., SAP2000) can be used to estimate the appropriate modal shapes and their associated natural frequencies to use with the VRS curves. If FEA software is not available, fundamental structural dynamics of a SDOF system (Eq. 12-2) can be used for estimating these values (AASHTO 2009, Edwards, *et al.* 1984, Fouad, *et al.* 1998).

$$f_n = \frac{1}{2\pi} \sqrt{\frac{K}{M}} \quad [\text{Eq. 12-2}]$$

where

f_n = natural frequency, Hz

K = generalized stiffness, N/m (lb/ft)

M = generalized mass, kg (slug)

A recommended methodology in estimating natural frequencies and their associated modal shapes for overhead sign support structures using Eq. 12-2 can be found in the work performed by Creamer *et al.* (1979), which also contains useful calculation examples.

Fatigue Load Shock Response Spectrum

The pressure range value extracted, P_{SRS} , from the SRS based on the dynamic characteristics of the structure is inputted into Eq. 12-3 for each member along the facade of the structure exposed to truck-induced wind gusts.

$$P_{TG} = P_{SRS} C_d I_F \quad [\text{Eq. 12-3}]$$

where

P_{TG} = design fatigue load due to truck - induced wind gust, psf (Pa)

P_{SRS} = transmitted pressure constant extracted from the SRS, psf (Pa)

C_d = drag coefficient

I_F = importance factor

The load is to be applied as a uniformly distributed load in the manner specified in the *Supports Specifications* (AASHTO 2009, Dexter, *et al.* 2002). Accommodation for height above ground level is also provided in the 2002 revisions. The height provisions conservatively match the findings in Cook's report (AASHTO 2009, Cook, *et al.* 1996, Dexter, *et al.* 2002). Whereas Cook's findings indicated a 10% reduction in wind pressure per foot increase starting from 17 ft (5.2 m) above ground level (Cook, *et al.* 1996), the *Supports Specifications* allow for a linear reduction in wind pressure starting from 19.7 ft (6 m) above ground level to zero at 32.8 ft (10 m) (AASHTO 2009, Dexter, *et al.* 2002). For that reason, the 2002 revisions on pressure reduction due to height above ground level were considered applicable to the method presented

in this chapter. Equation 12-4 can be used to calculate the wind pressure, P_h , at elevations higher than 19.7 ft (6.00 m) to be used in place of the P_{SRS} constant in Eq. 12-3:

$$P_h = -0.0763h + P_{SRS} \quad [\text{Eq. 12-4}]$$

where

P_h = truck - induced wind pressure at specified height above ground level, psf (Pa)

h = elevation increase from 19.7 ft (6.00 m) above the roadway, ft (m)

P_{SRS} = transmitted pressure constant extracted from the SRS, psf (Pa)

The design traveling speed of the truck to use in the SRS is generally taken as the speed limit. A Control speed of 70 mph (31.3 m/s) was chosen as an appropriate design recommendation. Other speeds are provided in the SRS plots for design choice, but also to illustrate the loading patterns.

The SRS plots have varying peaks which are dependent on the duration and frequency of the impulse excitation. It would be advisable to design structures that have natural frequencies outside of the frequencies plotted at these peaks. For example, referring to the 70 mph (31.3 m/s) vertically applied Control in Figure 12-6, the maximum possible structural response from this impulse would occur onto a structure that has a natural frequency with a vertical vibratory modal shape around 1.60 Hz. The transmitted pressure range from the response of the impulse for this particular example structure would be equal to 8.33 psf (399 Pa), taken as the ordinate value from the SRS in Figure 12-6.

Section 13

Discussion of the Results and Comparisons between the Theoretical and Experimental Programs

Overview

Comparisons between the theoretical and experimental calculations of the fatigue load due to natural wind and truck-induced wind gusts for the bridge-type VMS support structure are presented. Detailed discussions on the results of the comparison are provided.

Fatigue Load due to Natural Wind Gust

The theoretical and experimental results obtained from the analysis on the fatigue load due to natural wind gust were compared. The theoretical calculation involved the vibration response spectrum (VRS). The fatigue load was determined based on the structural dynamic properties of the structure, including the natural frequency and critical damping percentage. The experimental calculation was obtained through a back-calculation procedure from the experimentally obtained strain gauge measurements. The stress ranges that were developed using a combined loading analysis were plotted versus their corresponding three second average wind velocity. The fatigue load was determined at the fatigue wind found using the infinite-life approach. Importantly, the procedures used to obtain the fatigue load theoretically and experimentally were developed using the same principles in order for a direct comparison to be made.

Theoretical Calculation

The VRS was used to determine the theoretical fatigue load due to natural wind. It was developed independent of the structural type and is therefore applicable to the variety of support structures in design. The major assumption behind its design was that the structures behaved as single degree-of-freedom (SDOF) dynamic systems in each of their independent vibratory directions. This was because the majority of the vibration was found to be controlled by a single modal shape. The analysis was viewed and developed as a simplification, and the results of the analysis are a close approximation of the true value based on this fact.

The VRS was developed using the principles related to the infinite-life approach to fatigue design. The annual mean wind velocities provided in the VRS represent the wind velocity with a 0.01% exceedence probability. For instance, the 11 mph (5 m/s) annual mean wind velocity specified in the VRS represents a 38 mph (17 m/s) wind velocity, which has a 0.01% exceedence probability from the 11 mph (5 m/s) wind velocity. Therefore, the fatigue wind pressures specified for the 11 mph (5 m/s) wind velocity are values corresponding to a 38 mph (17 m/s) wind.

The dynamic characteristics of the bridge-type VMS support structure are needed in order to determine the fatigue load in accordance with the developed methodology. The annual mean wind velocity of the site location is also required. All the values needed to determine the load are provided in Table 13-1, where the dynamic properties were determined using the experimental data as described in **Section 8: Operational Modal Analysis**. The values represent the characteristics of the earliest modal shape in the direction of the loading. In this case, because the natural wind is directed onto the front face of the structure, the horizontal modal shape with vibratory motion in the direction of the load was used.

Table 13-1. Structural dynamic properties required to determine the fatigue load due to natural wind gust

Property	Value
Modal Shape	Horizontal Mode 2
Natural Frequency	2.81 Hz
Critical Damping Percentage	0.361%
Annual Mean Wind Velocity	11 mph

1 mph = 0.447 m/s

The fatigue load due to natural wind using the VRS based on the structural dynamic values listed in Table 13-1 was determined. For the specific bridge-type VMS support structure tested with this project, using an annual mean wind velocity equal to 11 mph (5 m/s), a 2.81 Hz natural frequency and 0.361% critical damping percentage, the fatigue wind pressure was found to be equal to 8.27 psf (396 Pa). The VRS used to determine this load is shown in Figure 13-1.

Experimental Calculation

The experimental calculation for the fatigue load due to natural wind gust for the bridge-type VMS support structure was determined using a back-calculation procedure. The fatigue load was found by back-calculating from the strain gauge measurements an equivalent static wind load that would produce the same readings. Dynamic amplification of the structure was therefore included in the calculated results. The developed fatigue load was based on the infinite-life approach to fatigue design. Based on the calculation for an annual mean wind velocity equal to 11 mph (5 m/s) [referred to as the fatigue wind with an 0.01% exceedence probability equal to 38 mph (17 m/s)], the fatigue load due to natural wind gust for the bridge-type support structure that was experimentally tested was found to be equal to 7.03 psf (336 Pa).

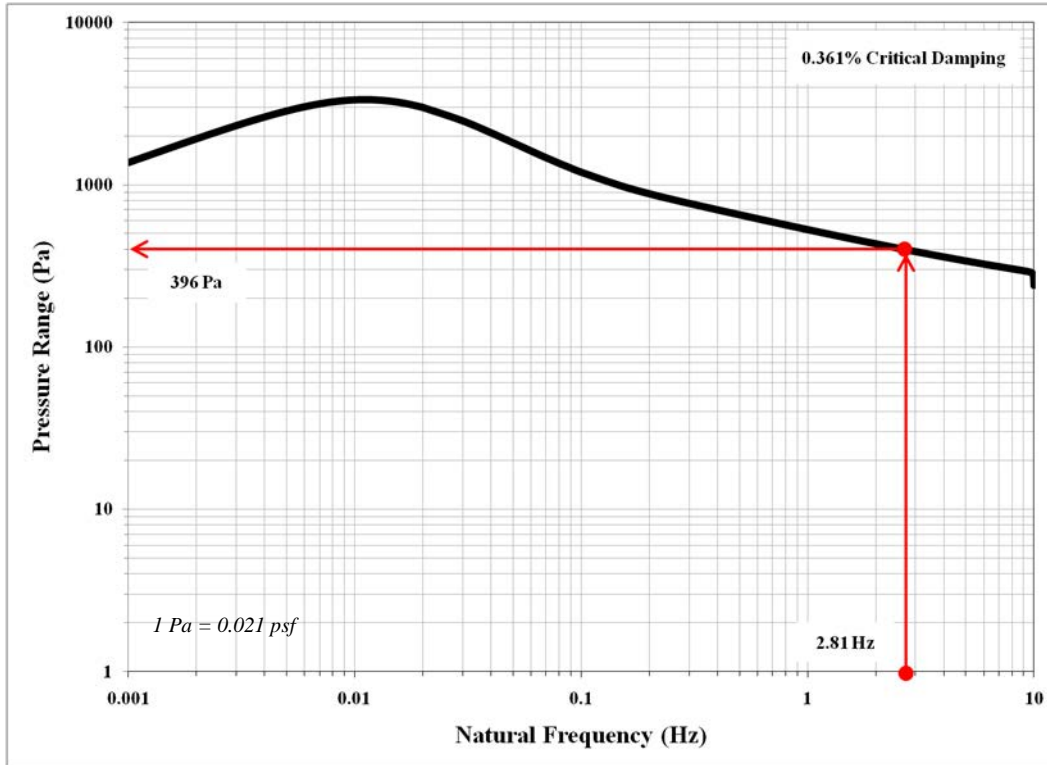


Figure 13-1. VRS for 0.361% damping, 2.81 frequency, and 11 mph (5 m/s) annual mean wind velocity

Comparison of the Results

The result of the theoretical study using the VRS was compared to the experimentally obtained value. A comparison of the results is listed in Table 13-2 and shown graphically in Figure 13-2. Also included in the bar graph of Figure 13-2 is the design pressure specified in the *Supports Specifications* for the fatigue loading due to natural wind gust.

Table 13-2. Comparison of the theoretical and experimental fatigue load due to natural wind gust

Theoretical Fatigue Load (psf)	Experimental Fatigue Load (psf)
8.27	7.03
Experimental / Theoretical = 0.850%	

1 psf = 47.9 Pa

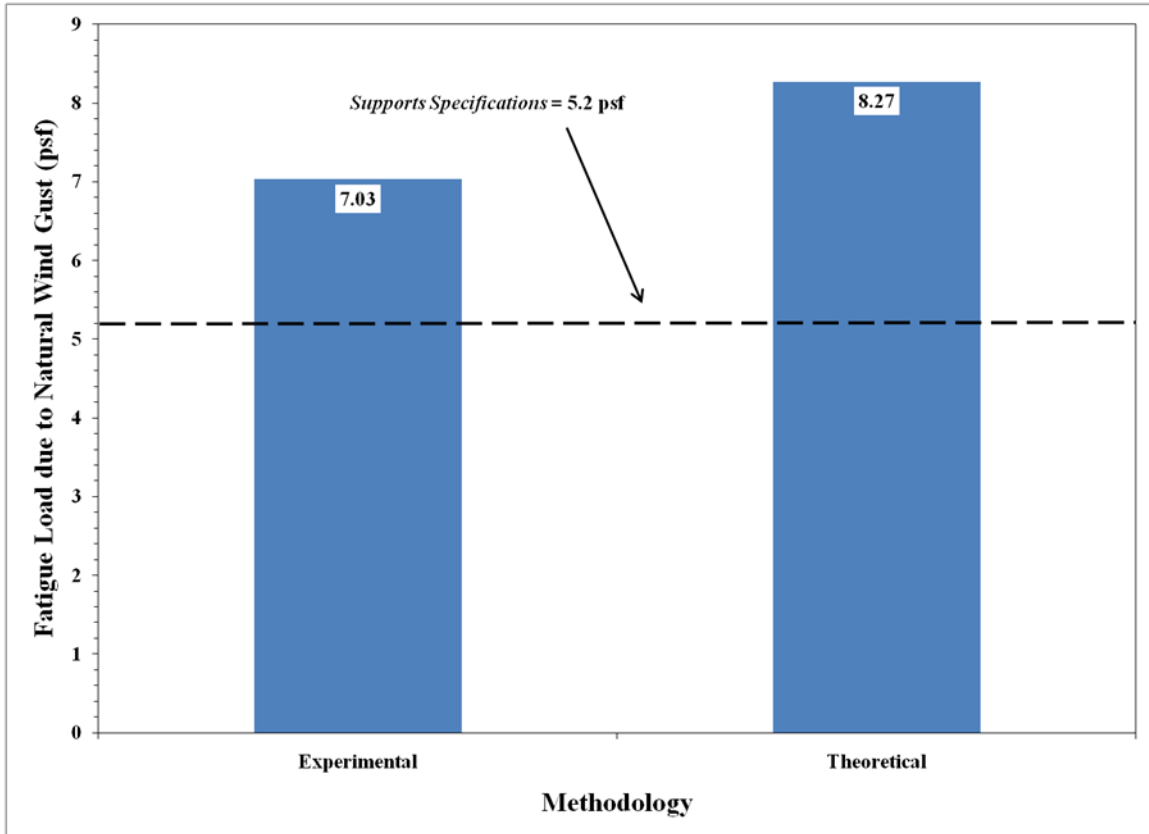


Figure 13-2. Comparison of the experimental and theoretical fatigue load due to natural wind gust

Discussion of the Comparison

The comparison indicates close agreement between the theoretical and experimental calculations. The fatigue load generated from the theoretical methodology was greater. This was because the excitation model used in the development of the VRS was contained slightly higher energy than that measured experimentally. The Davenport model was used in the development of the VRS, which was based on a larger sample size than the data collected with the experimental program, and encompassed wind behavior from a variety of locations around the world.

The comparison indicates that the VRS, which was developed independent of the structural type, accurately determined the fatigue load for the bridge-type VMS support structure. The VRS can be used for any type of structure than can be approximated as a single degree-of-freedom dynamic system. These structures are multiple degree-of-freedom systems, however since the majority of their vibration is controlled by a single modal shape, their dynamic behavior can be approximated as a single degree-of-freedom system. This is proven true based on the results of the comparison of the theoretical value with the experimentally derived value.

It is important to note that the *Supports Specifications* does not distinguish between structural types. The value used for the *Supports Specifications* was based structures with natural

frequencies of vibration at 2.0 Hz and critical damping percentages at 2.0%. The theoretical and experimental values were different than the *Supports Specifications*. This was because of their different vibration characteristics than those used to develop the specifications. The fatigue load experimental and theoretical results for the bridge structure used with this project were much greater, which proves the lack of comprehensiveness of *Supports Specifications*. The VRS however was able to account for the dynamic behavior of the structure, and accurately depict the correct fatigue load.

Fatigue Load due to Truck-Induced Wind Gust

The theoretical and experimental results obtained from the analysis of the fatigue load due to truck-induced wind gust were compared. The theoretical calculation involved the shock response spectrum (SRS). The fatigue load was determined based on the structural dynamic properties of the structure, including the natural frequency of vibration. The damping characteristics were not needed for this analysis since the wind pressure generated from the truck gust were transient events as compared to the continuous loading generated from natural wind,. The experimental calculation was obtained through a back-calculation procedure from the experimentally obtained accelerometer measurements. The maximum peak-to-peak amplitude response was used in a back-calculation procedure to determine an equivalent static wind load. Vertical and horizontal components of the truck-induced wind load were determined. Importantly, the procedures used to obtain the fatigue load theoretically and experimentally were developed using the same principles in order for a direct comparison to be made.

Theoretical Calculation

The SRS was used to determine the theoretical fatigue load due to truck-induced wind gust. It was developed independent of the structural type so that it could be used for any type of sign support structure. The major assumption behind its design was that the structures behaved as single degree-of-freedom dynamic systems in each of their independent vibratory directions. This was because the majority of the vibration was found to be controlled by a single modal shape. The analysis is viewed and developed as a simplification, and the results of the analysis are a close approximation of the true value based on this fact.

The dynamic characteristics of the bridge-type VMS support structure are needed in order to determine the fatigue load from the SRS. The speed of the traveling truck is also required. The structural dynamic values are provided in Table 13-3, and were determined using the experimental data as described in **Section 8: Operational Modal Analysis**. The values represent the characteristics of the modal shape in the direction of the loading. In this case, sense the truck gust is directed both underneath and onto the front face of the structures, the horizontal and vertical modal shapes with vibratory motion were used for each structure.

Table 13-3. Structural dynamic properties to determine the fatigue load due to truck-induced wind gust

Loading Component	Mode	Natural Frequency (Hz)
Vertical	3	3.79
Horizontal	2	2.81

The fatigue loads due to truck-induced wind gust using the SRS based on the structural dynamic values listed in Table 13-3 were determined. Importantly, the values obtained from the SRS are conservatively estimated for areas at a height 19.7 ft (6.00 m) above the roadway for a standard 14 ft (4.3 m) high semi-trailer, and reduces to zero at a height of 32.8 ft (10.0 m) above the roadway in accordance to the *Supports Specifications*. Equation 13-1 can be used to calculate the wind pressure at elevations higher than 19.7 ft (6.00 m):

$$P_h = -0.0763h + P_{SRS} \quad [\text{Eq. 13-1}]$$

where

P_h = truck - induced wind pressure at specified height above ground level, psf (Pa)

h = elevation increase from 19.7 ft (6.00 m) above the roadway, ft (m)

P_{SRS} = transmitted pressure constant extracted from the SRS, psf (Pa)

For the bridge-type VMS support structure of this project, using a truck speed of 70 mph (31 m/s), and using the vertical modal frequency equal to 3.79 Hz, the vertical component of the fatigue wind pressure extracted from the vertical component SRS (see Figure 13-3) was found to be equal to 2.961 psf (141.8 Pa) for an elevation of 19.7 ft (6.00 m) above the roadway. The underneath area of the VMS structure was at an elevation of 20 ft (6.1 m) above the roadway, and therefore using Eq. 14-1, the adjusted wind pressure for height was found to be equal to 2.938 psf (140.7 Pa). This pressure is to be applied as a uniformly distributed load onto the bottom portion of the VMS. Addition height adjustment is needed to find the pressure to be applied to the underneath portion of the truss span for the vertical load. For the horizontal component, using the same truck speed but for a horizontal modal frequency of 2.81 Hz, the wind pressure was found to be equal to 7.079 psf (338.9 Pa) extracted from the horizontal component SRS. The bottom of the sign is located at 20 ft (6.1 m) above the roadway. Using Eq. 14-1, the adjusted wind pressure for height was calculated to be equal to 7.056 psf (337.8 Pa). The horizontal load is to be applied as a triangular loading with a 7.63% reduction in wind pressure with each 1 ft (0.3 m) increase in elevation from 19.7 ft (6.00 m) above the roadway. The results of the vertical and horizontal wind pressures found using the SRS for the bridge-type VMS support structure are listed in Table 13-4.

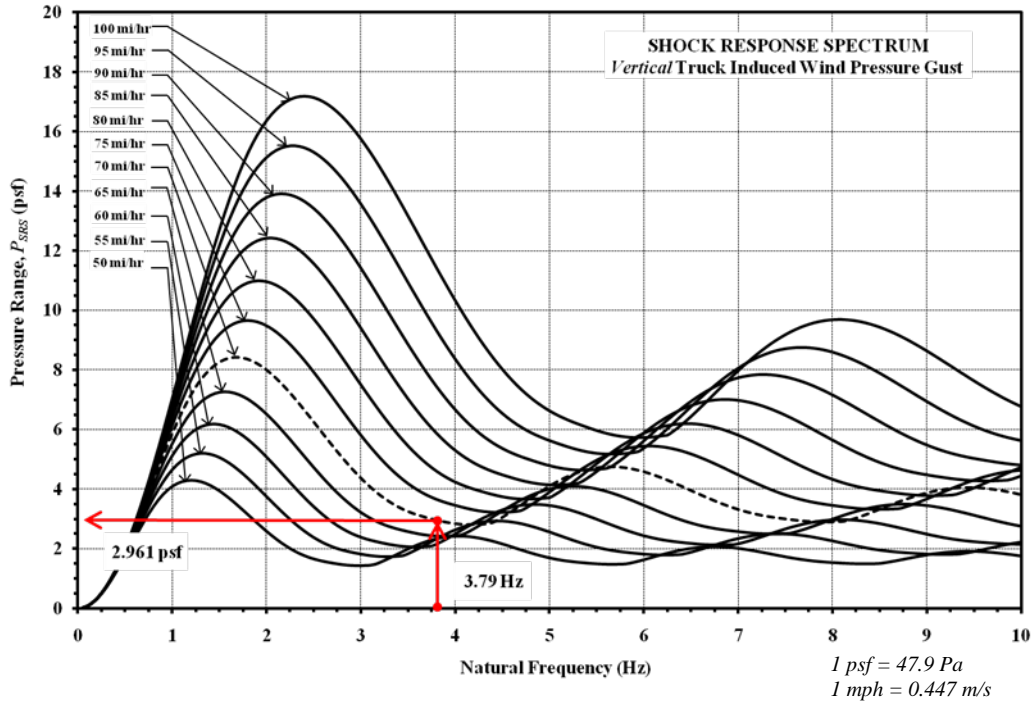


Figure 13-3. Vertical shock response spectrum used to determine the truck-induced wind pressure

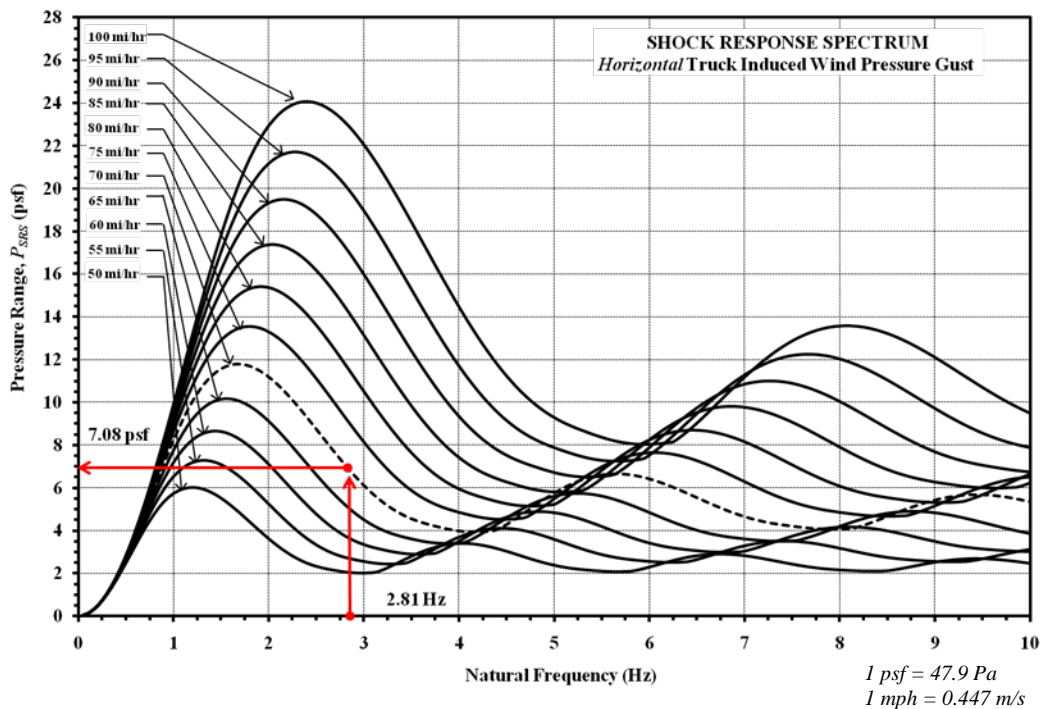


Figure 13-4. Horizontal shock response spectrum used to determine the truck-induced wind pressure

Comparison of the Results

The results of the theoretical study using the SRS were compared to the experimentally obtained values. A comparison of the results is listed in Table 13-4 and shown graphically in Figure 13-5. Also included in the bar graph of Figure 13-5 is the design pressure specified in the *Supports Specifications* for the fatigue loading due to truck-induced wind gust for a truck traveling at 70 mph (31 m/s).

Table 13-4. Comparison of the theoretical and experimental fatigue load due to truck-induced wind gust

Component	Theoretical Fatigue Load (psf)	Experimental Fatigue Load (psf)	Exp/Theo
Vertical	2.938	2.974	1.01
Horizontal	7.056	6.110	0.866

1 psf = 47.9 Pa

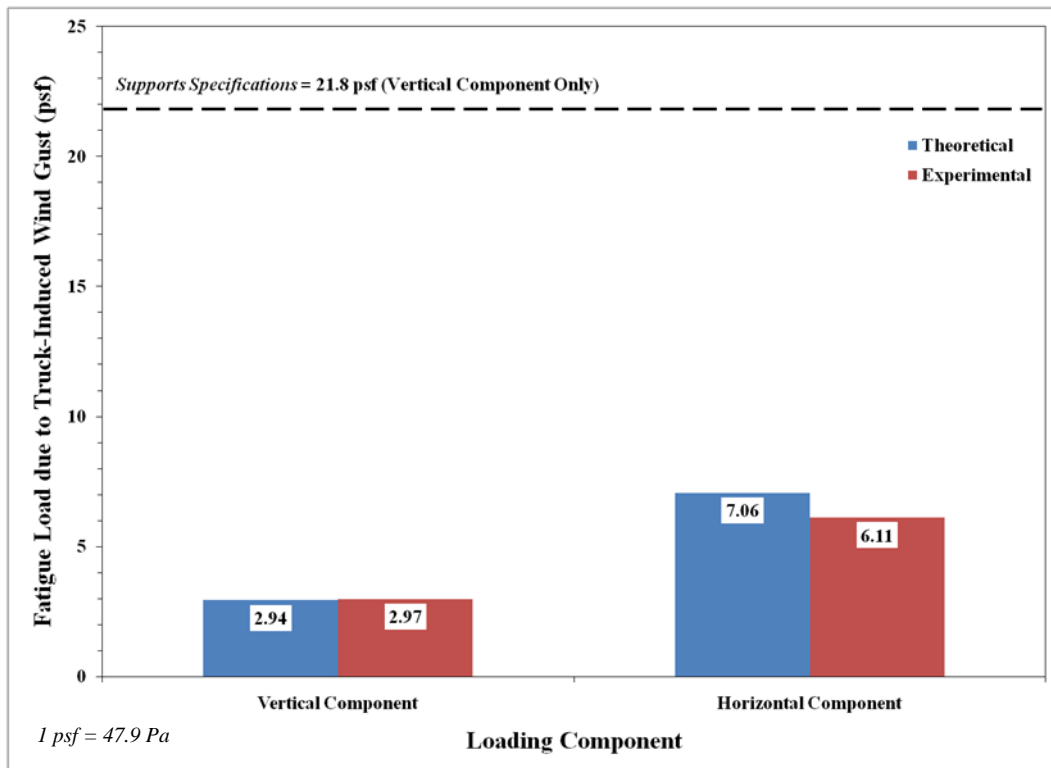


Figure 13-5. Comparison of the experimental and theoretical fatigue load due to truck-induced wind gust

Discussion of the Comparison

The comparison indicates close agreement between the theoretical and experimental calculations for each component. The SRS was able to accurately predict the fatigue load based on the structural dynamics. Although these structures are multiple degree-of-freedom systems, the SRS

based on a single degree-of-freedom system was able to approximate the fatigue load within a high degree of accuracy. This is because these structures exhibit independent vibration characteristics that can be simplified by simulating the behavior as a single degree-of-freedom dynamic system.

The SRS was able to account for differing behavior of the structure under the truck-induced wind gust vertical and horizontal loading to accurately predict the fatigue load. The close comparison to the experimental values is clear evidence of the SRS capabilities. The fatigue load criterion of the *Supports Specifications* does not have this capability, and provides a load to be used with all structures. The specification does not distinguish between structural types with different behavior under the loading condition, and therefore it is viewed to provide an inaccurate but highly conservative estimate of the fatigue load.

Section 14

Finite Element Analysis

Overview

Finite element analysis was performed on the bridge-type VMS support structure. The FEA software package SAP2000 v. 10 was used for the study (CSI 2007). The analysis was performed to address the behavior and stress of the structure to the theoretically and experimentally developed fatigue loads due to natural wind and truck-induced wind gusts. The results of the analysis were compared to the behavior of the structure due to the fatigue provisions of the *Supports Specifications*.

Model Development

A full scale, three-dimensional model was developed of the experimentally tested structure. The model was created from the shop drawings of the structure provided by the Alabama Department of Transportation (ALDOT). The drawings are provided in Appendix A of this report.

Geometry

The basic geometry of the model is shown in Figure 14-1. Body constraints were used to connect the VMS to the W-shape sections, and the W-shape sections to the truss span. The degrees-of-freedom assigned to the constraints were designed to simulate the U-bolts used at this location. Translational degrees-of-freedom were restrained whereas translational were unrestricted. A picture of the connection showing the back of the structure is provided in Figure 14-2.

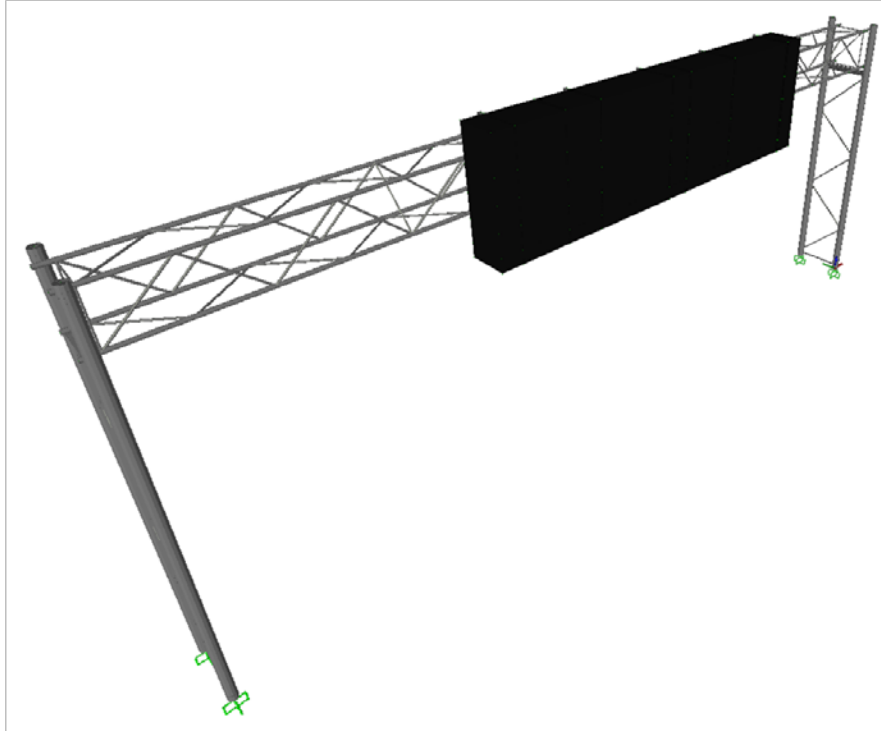


Figure 14-1. Basic geometry of the FEA model

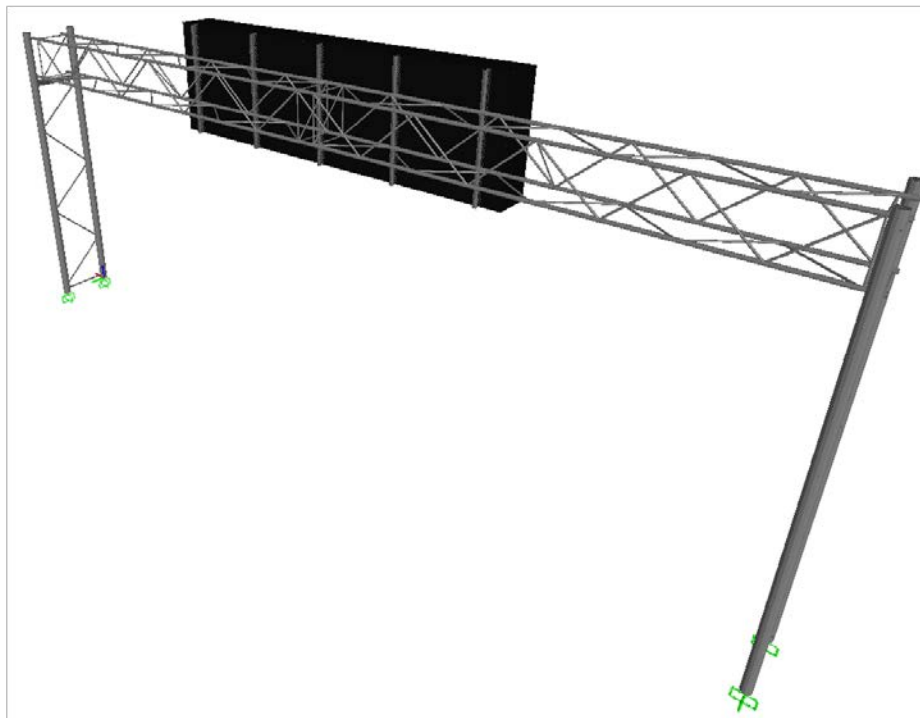


Figure 14-2. Sign-to-truss connection of the FEA model

The truss span-to-upright connection was more flexible than the same connection used for the cantilever structure. The connection for the bridge structure contained U-bolts for the top two chords and double U-bolts for the bottom chords. The connection was modeled using body constraints with restrained translational degrees-of-freedom and unrestrained rotational degrees-of-freedom for the top chords. The same constraints were used for the bottom chords, however because of the double U-bolt configuration, rotation about the y-axis (axis pointing in the direction of traffic) and rotation about the z-axis (axis pointing in the direction of gravity) were restrained. A close up of this connection is shown in Figure 14-3.

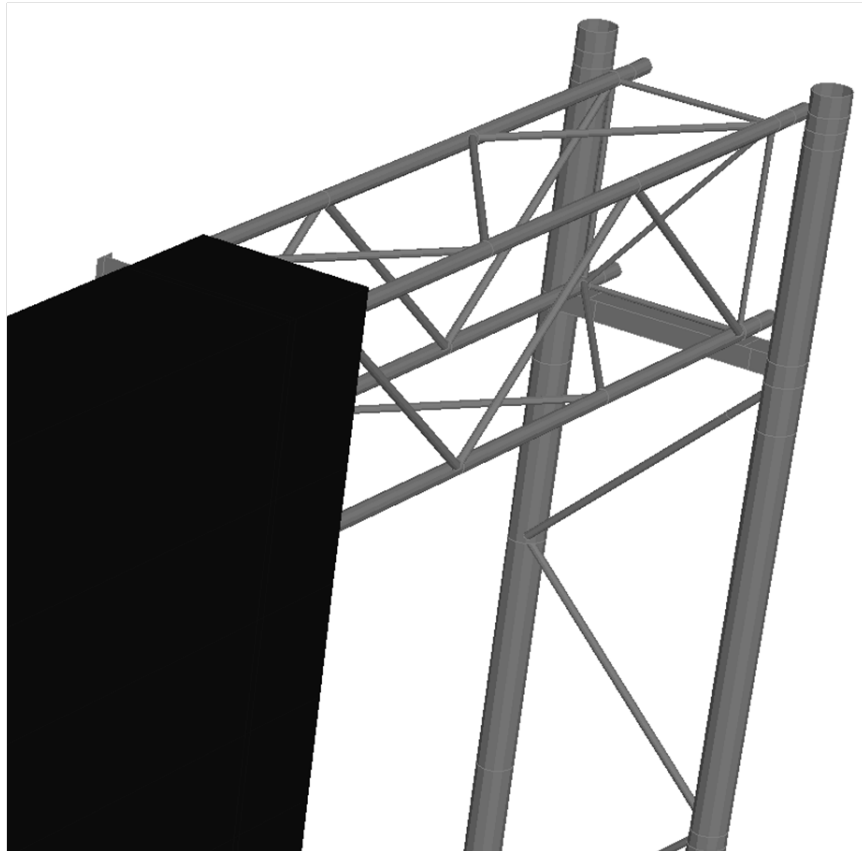


Figure 14-3. Truss-to-post connection of the FEA model

The base connection of the post support to the foundation had four anchor bolts per upright to attach the base plate to the concrete pile foundation. Because of the double upright configuration, and the bridge-type configuration of the support structure, simple fixed-end connections were used in the model. The structure was extremely rigid with little flexibility about the y-axis (pointing in the direction of traffic) and z-axis (pointing in the direction of gravity) directions. A close up of the connection is shown in Figure 14.8, showing the West upright which contained the addition extension detail to account for topography changes.

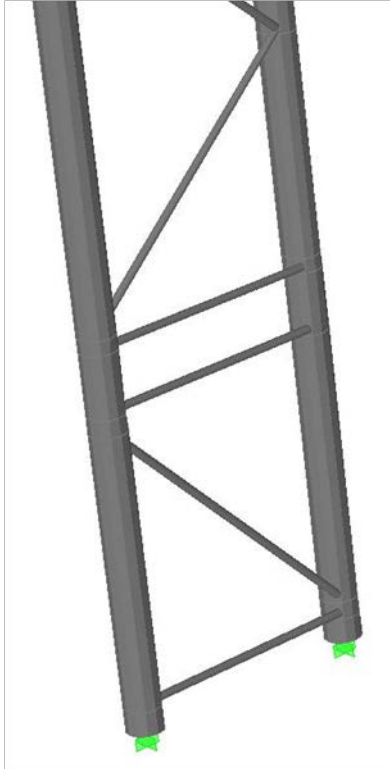


Figure 14-4. Fixed-end connection of the uprights for the FEA model

Element Type

Linear and hexahedral elements were used in the model. Linear elements were used for the truss and support post, as well as for the anchor bolts, pile foundation, and sign W-section connections. The elements consisted of two nodes and were each assigned a cross-sectional area that corresponded to the member they were simulating.

Hexahedral elements were used for the VMS. The elements were three dimensional six face “brick” elements with eight nodes located at the corners. Each side of the element was straight with no middle side nodes. Their basic function in the model was to transfer the wind loading to the truss span and upright members.

Material Definition

The primary material of the structure was steel. The primary materials used for the model are listed as follows:

- The uprights and truss section was made of API-5L-X52 steel pipe,
- The plates were made of structural steel ASTM A572 Gr. 50,
- The anchor bolts were made of AASHTO M314-90 Gr. 55 (essentially the same as ASTM F1554 Gr. 55), and

- The W-shape and T-shape sections used for the sign-to-truss connection were made of A572 Gr. 50 steel.

The strength properties of the materials previously listed and assigned to the structural members of the FEA model are listed in Table 14-1. Anchor bolts and the concrete foundation were not model with this structure.

Table 14-1. Material property definitions for the FEA model

Material	Assigned Elements	Material Designation	Modulus of Elasticity (psi)	Yield Stress (psi)	Tensile Stress (psi)
Steel Pipe	Truss, Post	API-5L-X52	29,000,000	52,000	66,000
Steel Plate	Truss and Base plates	ASTM A572 Gr. 50	29,000,000	50,000	65,000

1 psi = 6,891 Pa

The VMS was modeled in the structure with the purpose of transferring the wind loading to the support structure, and adding a mass on the truss span. The total weight assigned to the VMS was 3,900 lb (17,349 N). The weight was distributed uniformly throughout the VMS by assigning a mass per volume material definition equal to 0.136 slugs/ft³ (70.1 kg/m³) to the element properties assigned to the VMS.

Loading Designations

The fatigue loading developed theoretically and experimentally were applied to the structure. Loads developed for natural wind and truck-induced wind gusts were used. The loads represented equivalent static wind loads that would produce the same stress on the structure as the natural wind and truck-induced wind loading environments. The responses of the structure to these loading designations were evaluated and compared across experimental versus theoretical derivations. The loading obtained from the fatigue provision of the *Supports Specifications* were also applied to the FEA models for comparison. The three loading designations that were used for input into the FEA program are listed as follows:

1. Theoretically developed loading,
2. Experimentally developed loading, and
3. Loading obtained from the *Supports Specifications*.

Fatigue Loading Input for Natural Wind Gust

The fatigue loads due to natural wind gust derived experimentally and theoretically for the bridge-type VMS support structure were inputted into the FEA program. The fatigue provisions for natural wind gust obtained from the *Supports Specifications* were also inputted into the program. A listing of the loads determined from the theoretical and experimental research of this project is provided in Table 14-2. Descriptions and derivations of the experimental and

theoretical loads, and the natural wind fatigue provisions of the *Supports Specifications*, are provided in the following sections of this report:

- **Section 13: Discussion of the Results and Comparisons between the Theoretical and Experimental Programs**
- **Section 9: Experimental Calculation of the Fatigue Load Due to Natural Wind Gust**
- **Section 11: Theoretical Calculation of the Fatigue Load Due to Natural Wind Gust, and**
- **Section 3: Fatigue Provisions of the AASHTO *Supports Specifications*.**

Table 14-2. Fatigue loads due to natural wind gust

Methodology	Fatigue Load
Theoretical	8.27
Experimental	7.03
<i>Supports Specifications</i>	5.20

1 psf = 47.9 Pa

The loads were applied to the sign and truss members of the structure on the front of the structure that would be visible as if looking onto the elevation view of the shop drawings. This included the chords, vertical diagonals and struts, uprights, and VMS for the bridge structure. The loads in Table 14-2 were multiplied by the drag coefficient assigned to the member. For the truss members, the loading was in the form of a force per length because the members were modeled using linear elements. Therefore, the loading for these members were multiplied by their cross-sectional diameter. The loading input and values used for the input calculation for the bridge-structure according to the particular members exposed to natural wind are listed in Table 14-3.

Table 14-3. Fatigue loads due to natural wind gust used for the FEA input for each of the exposed members

Member	Drag Coefficient, C_d	Diameter (in)	FEA Loading Input		
			Theoretical	Experimental	<i>Supports Specifications</i>
Truss Chords	1.10	3.5	2.65 lb/ft	2.26 lb/ft	1.67 lb/ft
Truss Vertical Diagonals	1.10	1.90	1.44 lb/ft	1.22 lb/ft	0.906 lb/ft
Truss Vertical Struts	1.10	1.315	0.997 lb/ft	0.847 lb/ft	0.627 lb/ft
Uprights	1.10	8.625	6.54 lb/ft	5.56 lb/ft	4.11 lb/ft
VMS	1.70	/	14.1 psf	12.0 psf	8.84 psf

1 in = 2.54 cm

1 lb = 4.45 N

1 psf = 47.9 Pa

Fatigue Loading Input for Truck-Induced Wind Gust

The fatigue loads due to truck-induced wind gust derived experimentally and theoretically for the structure were inputted into the FEA program. Both the vertical and horizontal components were inputted representing a truck traveling at 70 mph (31 m/s). The fatigue provisions for truck-

induced wind gust obtained from the *Supports Specifications* were also inputted into the program. Importantly, the provisions only contain the vertical component of the truck gust and does not account for the horizontal component. A listing of the loads determined from the theoretical and experimental research of this project is provided in Table 14-4 for truck-induced wind gust. Descriptions and derivations of the experimental and theoretical loads, and the truck-induced wind gust fatigue provisions of the *Supports Specifications*, are provided in the following sections of this report:

- **Section 13 Discussion of the Results and Comparisons between the Theoretical and Experimental Programs,**
- **Section 10 Experimental Calculation of the Fatigue Load due to Truck-Induced Wind Gust,**
- **Section 12 Theoretical Calculation of the Fatigue Load due to Truck-Induced Wind Gust,** and
- **Section 3 Fatigue Provisions of the AASHTO *Supports Specifications*.**

Table 14-4. Fatigue loads due to truck-induced wind gust

Component	Theoretical Fatigue Load (psf)	Experimental Fatigue Load (psf)	<i>Supports Specifications</i>
Vertical	2.938	2.974	21.8
Horizontal	7.056	6.110	/

1 psf = 47.9 Pa

Vertical Component The vertical component of the truck-induced wind loads were applied to the underside of the support structures located directly above the highway traffic lane. The length of the load was 12 ft (3.7 m) corresponding to the length of the lane. The exposed members consisted of the bottom of the VMS, truss chords and horizontal diagonals and struts located within in the 12 ft (3.7 m) portion above the traffic lane.

The loads in Table 14-4 were multiplied by the drag coefficient assigned to the member. For the truss members, the loading was in the form of a force per length because the members were modeled using linear elements. Therefore, the loading for these members were multiplied by their cross-sectional diameter. The loading input and values used for the input calculation for the structure according to the particular members exposed to the vertical component of the truck-induced wind gust are listed in Table 14-5.

Table 14-5. Fatigue loads of the vertical component of the truck-induced wind gust used for the FEA input

Member	Drag Coefficient, C_d	Diameter (in)	FEA Loading Input		
			Theoretical	Experimental	Supports Specifications
Truss Chords	1.10	3.5	0.943 lb/ft	0.954 lb/ft	6.99 lb/ft
Truss Horizontal Diagonals	1.10	1.90	0.512 lb/ft	0.518 lb/ft	3.80 lb/ft
Truss Horizontal Struts	1.10	1.315	0.354 lb/ft	0.358 lb/ft	2.63 lb/ft
VMS	1.70	/	5.00 psf	5.06 psf	37.1 psf

$1 \text{ in} = 2.54 \text{ cm}$
 $1 \text{ lb} = 4.45 \text{ N}$
 $1 \text{ psf} = 47.9 \text{ Pa}$

Horizontal Component The horizontal component of the truck-induced wind loads were applied primarily to the exposed portion of the VMS located above the roadway. The length of the loading was 12 ft (3.7 m). The loading was applied as a triangular loading in the horizontal direction, with the maximum value (values provided in Table 14-4) assigned to the bottom section closest to the roadway, and decreased to zero at a height equal to 32.8 ft (10.0 m) above the roadway. The pressure loads listed in Table 14-4 were multiplied by the drag coefficient assigned to the member. The loading input and values used for the input calculation for the structure according to the particular members exposed to the horizontal component of the truck gust are listed in Table 14-6. Importantly, the fatigue provision of the *Supports Specifications* does not specify a horizontal component for the fatigue load due to truck-induced wind gust.

Table 14-6. Fatigue loads of the horizontal component of the truck-induced wind gust used for the FEA input

Member	Drag Coefficient, C_d	FEA Loading Input (psf)		
		Theoretical	Experimental	Supports Specifications
VMS	1.70	12.0	10.4	/

$1 \text{ psf} = 47.9 \text{ Pa}$
 / indicates no available fatigue load provided by the Supports Specifications for the horizontal component of the truck-induced wind gust

Solution

A nonlinear $P-\Delta$ solution was conducted first by the FEA program to determine the stiffness of the structure as a result of the dead load. Next, linear-static solutions using the loading previously listed in the tables for natural wind and truck-induced wind gust were conducted using the updated stiffness determined from the previous $P-\Delta$ analysis.

Internal reactions were extracted from the FEA linear static solutions. This included the following forces:

- Bending moment,
- Axial,

- Shear, and
- Torsion.

The reactions were evaluated at specific location on the structure that were found to contain the highest values. This included the following two locations:

1. Base plate-to-support post connection, and
2. Chord-to-support post connection.

Figure 14-5 shows the base-plate-to-support post connection circled in red. Both of the posts that made up the upright of the bridge-type VMS support structure were evaluated. Figure 14-6 shows the chord-to-support post connections. All four chords were evaluated.

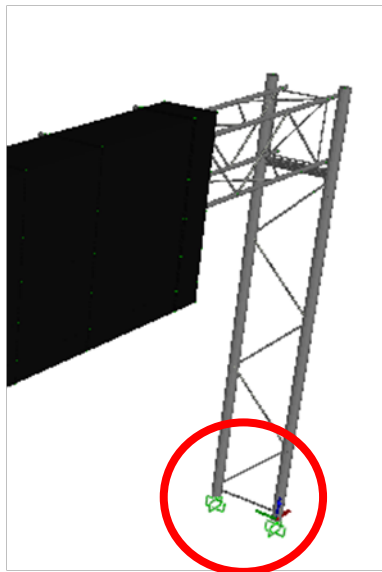


Figure 14-5. Base plate-to-support post connection used in the evaluation of the FEA solution results

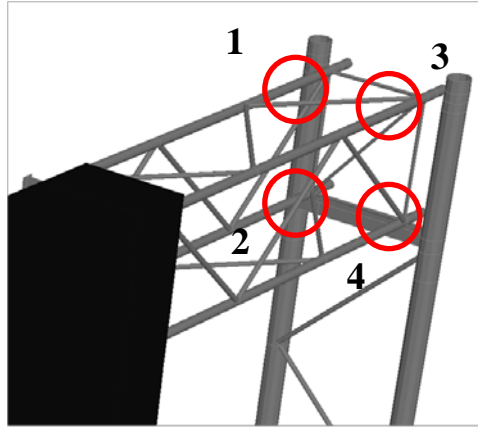


Figure 14-6. Base plate-to-support post connection used in the evaluation of the FEA solution results

Combined Loading Analysis

A combined loading stress analysis was performed using the internal reactions extracted from the FEA solution. The equations listed in Table 14-7 were used for this task. Stress elements were developed at these locations (see Figure 14-7) from the calculated stresses. Elements were developed along the perimeter of the cross sections at these locations, and the maximum normal and shear stresses were found. This was done for all loading designations. The results were compared to each other across loading designations. The results of the analyses are listed in Table 14-8 and represented graphically in Figure 14-8 for the fatigue loading due to natural wind gust. Table 14-9 lists the results for the fatigue loading due to truck-induced wind gusts. The values are shown graphically in Figure 14-9 for the normal stresses, and Figure 14-10 for the shear stresses.

Table 14-7. Relevant stress equations used for the combined loading analysis of the FEA results

Stress	Stress Equation
Axial	$\sigma_N = \frac{F_z}{A}$
Torsion	$\tau_T = \frac{M_z \rho}{J_{ZZ}}$
Unsymmetrical Bending	$\sigma_M = -\frac{M_x y}{I_{XX}} + \frac{M_y x}{I_{YY}}$
Transverse Shear*	$\tau_S = \frac{FQ}{It} = \frac{2F}{A}$

*for maximum transverse shear stress at neutral axis for thin walled pipes

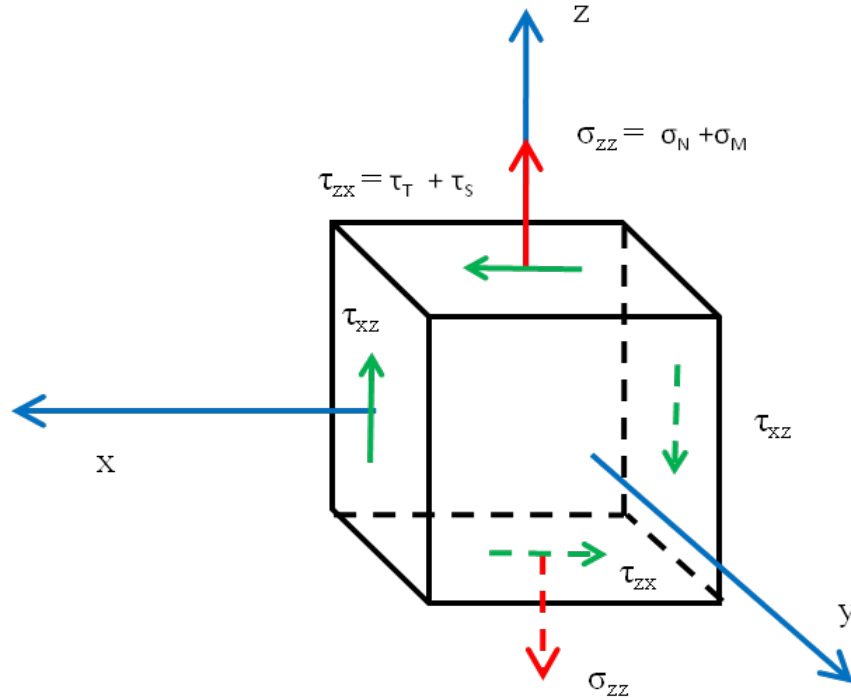


Figure 14-7. Typical stress element formed from the combined loading analysis of the FEA results

Table 14-8. FEA results of the combined loading analysis for fatigue loading due to natural wind gust

Connection	Load Input	Normal Stress (ksi)	Shear Stress (ksi)
Base Plate	Theoretical	3.569	0.705
	Experimental	3.034	0.600
	Supports Specifications	2.244	0.444
Chord	Theoretical	7.731	0.185
	Experimental	6.572	0.157
	Supports Specifications	4.861	0.116

1 ksi = 6.89 MPa

Table 14-9. FEA results of the combined loading analysis for fatigue loading due to truck-induced wind gust

Connection	Load Input	Stress due to Loading Component (ksi)					
		Vertical		Horizontal		Vertical & Horizontal	
		Normal	Shear	Normal	Shear	Normal	Shear
Base Plate	Theo.	0.010	0.000	0.504	0.099	0.514	0.099
	Exp.	0.011	0.000	0.437	0.086	0.447	0.086
	SS	0.079	0.001	0.000	0.000	0.079	0.001
Chord	Theo.	0.421	0.010	1.174	0.026	1.251	0.027
	Exp.	0.439	0.010	1.017	0.023	1.097	0.023
	SS	3.252	0.076	0.000	0.000	3.252	0.076

1 ksi = 6.89 MPa

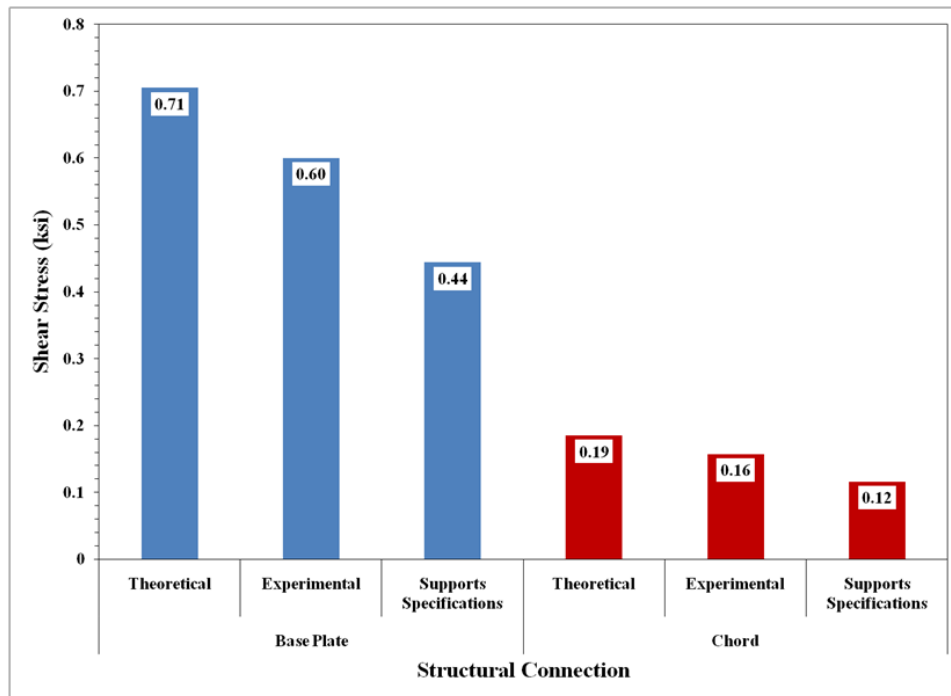
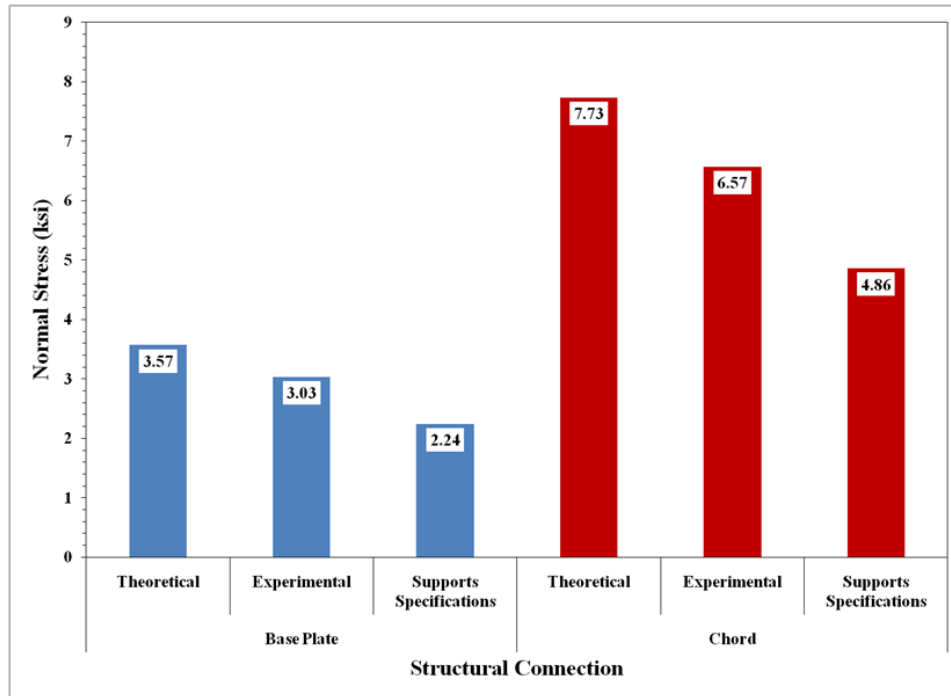


Figure 14-8. Graphical representation of the FEA results for fatigue loading due to natural wind gust

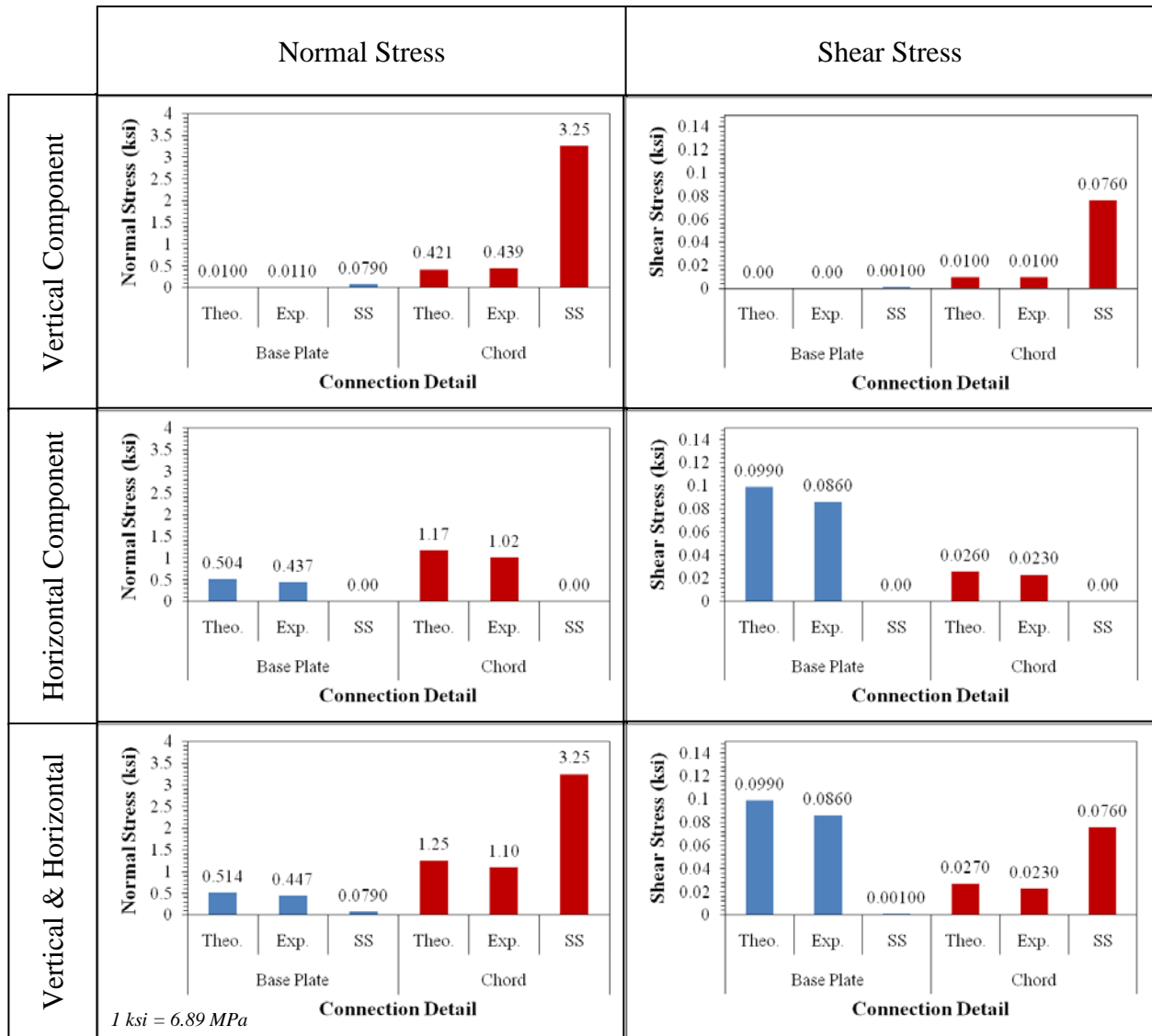


Figure 14-9. Graphical representation of the FEA results for fatigue due to truck-induced wind gust

Figure 14-9 of the FEA combined loading results contain bar graphs in a matrix formation. The normal stress results are in the first column for both of the connection details evaluated. The second column lists are the shear stress results. The first row of Figure 14-9 provides the normal and shear stresses for the vertical component of the truck-induced wind gust. The second row is the results for the horizontal component, and the third row is a combination of the vertical and horizontal components.

Discussion of the Results

Natural Wind Gust

The stresses resulting from the natural wind gust loading designations were evaluated and compared. The maximum normal stresses were located at the chord-to-support post connection. The maximum shear stresses were located at the base plate connections. The theoretical and experimental loading produced stresses that were in close agreement as compared to the stresses generated from the *Supports Specifications*. They were also larger than the *Supports Specifications* results, indicating that the *Supports Specifications* fatigue provisions for the bridge-type VMS support structure tested with this project underestimate the fatigue loading due to natural wind gust according to this analysis. The maximum values determined from the evaluation are provided in Table 14-10, listing the methodology that produced the maximum values with respect to the connection detail in consideration.

Table 14-10. Maximum stresses and locations from the FEA results for natural wind gust

Connection	Stress (ksi)		Loading Input
	Stress Type	Value	
Chord-to-Upright	Normal	7.731	Theoretical
Base Plate-to-Upright	Shear	0.705	Theoretical

1 ksi = 6.89 MPa

Truck-Induced Wind Gust

The stresses resulting from the vertical component, horizontal component, and a combination of the vertical and horizontal components of the truck-induced wind gust loading were evaluated. It was found for the vertical component that the fatigue provisions of the *Supports Specifications* for truck gust produced the highest normal stresses located at the chord-to-support post connection. The theoretical values controlled for the horizontal component, noting that the *Supports Specifications* does not contain fatigue provisions for the horizontal component of the truck gust. The normal stresses were highest at the chord connections, whereas the shear stresses were highest at the base plate. A listing of the maximum values for each structure along with the location of these stresses is provided in Table 14-11.

Table 14-11. Maximum stresses and locations from the FEA results for truck-induced wind gust

Component	Stress (ksi)		Connection	Loading Input
	Stress Type	Value		
Vertical	Normal	3.252	Chord-to-Upright	<i>Supports Specifications</i>
	Shear	0.076	Chord-to-Upright	<i>Supports Specifications</i>
Horizontal	Normal	1.174	Chord-to-Upright	Theoretical
	Shear	0.099	Base Plate-to-Upright	Theoretical
Vert. & Horz.	Normal	3.252	Chord-to-Upright	<i>Supports Specifications</i>
	Shear	0.099	Base Plate-to-Upright	Theoretical

1 ksi = 6.89 MPa

Maximum Horizontal Loading

For design, it is important to determine which stress values control between natural wind gust and truck-induced wind gust, noting that natural wind loading was applied in the horizontal direction. As shown in Table 14-12, it was found that the fatigue load due to natural wind gust predominately controlled at both of the connection details analyzed for this particular structure. The results in the table indicate that the fatigue load due to natural wind gust produced the highest normal and shear stresses than the horizontal and vertical components of the fatigue load due to truck-induced wind gusts.

Table 14-12. Controlling fatigue loads at the connection details

Loading Input	Connection	Normal Stress (ksi)		Shear Stress (ksi)	
		Value	Fatigue Load	Value	Fatigue Load
Theo.	Chord	7.731	NW	0.185	NW
	Base	3.569	NW	0.705	NW
Exp.	Chord	6.572	NW	0.157	NW
	Plate	3.034	NW	0.600	NW
SS	Chord	4.861	NW	0.116	NW
	Plate	2.244	NW	0.444	NW

1 ksi = 6.89 MPa

Section 15

Proposed Fatigue Provisions

Overview

The proposed fatigue design equations for natural wind and truck-induced wind gusts are presented in this section. The establishment of the proposed equations encompassed both the experimental and theoretical results from which the design methodologies were developed.

Design Fatigue Load due to Natural Wind Gust

The proposed fatigue design equations for natural wind gusts were developed from the experimental and theoretical programs with this project. The recommendations are presented in two forms as follows:

1. Generalized design equation, and
2. Detailed design equation.

The first form is a generalized design equation based on the experimental results of this project. It is applicable to the specific type of support structure that was analyzed with this project. The second equation is a more comprehensive design approach that accounts for the variety of highway overhead support structures in design. It was based on the theoretical program with this project. It requires a detailed structural analysis that accounts for the dynamic characteristics of the structure in determining the fatigue load.

General Fatigue Design Equation for Natural Wind Gust

The general fatigue design equation for natural wind gusts applicable for the bridge-type VMS support structures is shown as Eq. 15-1. It is to be applied horizontally to the exposed face of the structure as seen on an elevation view. The load is applied as a uniformly distributed load over the exposed areas. It is recommended for bridge-type VMS support structures with the following dynamic characteristics:

- Modal frequencies in the direction of the natural wind loading equal to 2.81 Hz or higher, and
- Critical damping percentage 0.341% or higher.

Equation 15-1 is considered un-conservative for structures with natural frequencies and damping percentages less than the values specified. For higher values, the equation is considered conservative.

$$P_{NW} = 7C_d I_F \left(\frac{\bar{v}}{11} \right)^2 \quad [\text{Eq. 15-1}]$$

where

P_{NW} = design fatigue load due to natural wind gust, psf (Pa)

C_d = drag coefficient

I_F = importance factor

\bar{v} = annual mean three second wind velocity, mph (m/s)

The proposed detailed equation described later in this section is recommended for structures with dynamic characteristics significantly different that the recommended values specified for Eq. 15-1.

The equation takes the form similar to the *Support Specifications* for easy implication. The drag coefficients and importance factors have not been altered, and are provided in the *Supports Specifications*. Accommodation for other annual mean wind velocities other than 11 mph (5 m/s) is also provided in the equation by a simplified ratio calculation.

Detailed Fatigue Design Equation for Natural Wind Gust

A detailed design equation was developed to account for the variety of highway overhead support structures in design, each with different configurations, cross sectional shapes, and material properties. Since these factors have significant influence on the dynamic characteristics of the structure, and because support structures are highly flexible with low damping properties, a method was needed in determining the fatigue load based on the vibration behavior of these structures. The following methodology is applicable to the bridge-type VMS support structure, as well as other support structures in design.

The fatigue design approach presented in this section accounts for the dynamic behavior of the structure in terms of the following structural dynamic characteristics:

- Natural frequency of the earliest horizontal modal shape with vibratory motion in the direction of traffic, and
- Critical damping percentage of the horizontal modal shape.

The fatigue load for natural wind is determined based on these properties. Based on the methodology used to determine the fatigue load, the detailed approach presented here is considered a unified design approach to fatigue design in that it accounts for the variety of support structures.

Natural Frequency Vibration response spectrums were developed that presented the fatigue load based on the dynamic properties of the structure. The load is extracted from the VRS in terms of the earliest modal frequency of the structure with a modal shape in the direction of the loading. The most critical loading scenario for natural wind is directed normal to the plain of the sign (in the direction of traffic), exciting the modal shape most commonly referred to as the horizontal modal shape. For support structures, the horizontal modal shape is generally around 1 to 3 Hz, which typically corresponds to the first modal shape for cantilever-type structures, and the second modal shape for bridge-type structures. Finite element software (i.e., SAP2000) can be used to estimate the appropriate modal shapes and their associated natural frequencies to use with the VRS curves. If FEA software is not available, fundamental structural dynamics of a single degree-of-freedom system (Eq. 15-2) can be used for estimating these values (AASHTO 2009, Creamer, *et al.* 1979, Harris 1996).

$$f_n = \frac{1}{2\pi} \sqrt{\frac{K}{M}} \quad [\text{Eq. 15-2}]$$

where

f_n = natural frequency, Hz

K = generalized stiffness, N/m (lb/ft)

M = generalized mass, kg (slug)

A conservative estimate would be to assume a modal frequency of 1.0 Hz for cantilever-type sign support structures and 2.0 Hz for bridge-type VMS support structures to use with the VRS. This is because the equivalent static wind load increases as the modal frequency decreases. The resonant frequencies of natural wind gust occupies a very broadband spectrum, and are relatively low, typically at and around 0.1 Hz. Therefore, with structural natural frequencies that approach the frequencies of the wind excitation, higher dynamic amplification is induced onto the structure because of resonance. The equivalent static wind load that is extracted from the VRS is subsequently higher to account for the increase in stresses that are generated onto the structure as a result of the intensified dynamic amplification to natural wind loading.

Critical Damping Percentage The critical damping percentage is especially relevant to support structures. Support structures have relatively high flexibility and subsequently low natural frequencies (1 to 3 Hz). Their damping ratios are mostly below 2.0%. A low damping will allow the structure to vibrate longer at high amplitudes when exposed to natural wind, and thus produce more stresses that could potentially cause fatigue damage. The following assumptions for the critical damping percentage are recommended for design purposes:

- 0.015 (1.5%) for cantilever sign support structures, and
- 0.0035 (0.35%) for bridge-type VMS support structures.

However, damping ratios can vary depending on the structural material, and therefore actual values can be obtained from experimental data of comparable structures if available.

Fatigue Design Procedure A systematic procedure for determining the design fatigue load due to natural wind based on the proposed detailed approach is presented. The procedure is applicable to bridge-type VMS support structures, as well as other support structures in design.

Step 1: Annual Mean Wind Velocity

The annual mean wind velocity is acquired at the site where the support structure is located. The National Weather Service Offices near the site can be used to determine this value. It is recommended to use a value of 11 mph (5 m/s), however other values can be used based on meteorological data.

Step 2: Modal Analysis

A modal analysis to determine the dynamic characteristics of the support structure is performed. The earliest modal frequency of the modal shape in the direction of the natural wind loading as well as the critical damping percentage are required for this procedure. Finite element analysis software can be helpful with this step. If FEA is not available, the modal frequency and modal shape can be estimated using Eq. 15-2. The values listed in Table 15-1 can be used for conservative estimates. It is important to note that these estimates were based on the experimental data collected with cantilever sign and bridge VMS support structures.

Table 15-1. Conservative estimates of the natural frequency and critical damping percentages

Support Structure	Natural Frequency	Critical Damping Percentages
Cantilever-Type Sign Support Structure	1.0 Hz	1.5%
Bridge-Type VMS Support Structure	2.0 Hz	0.35%

Step 3: Vibration Response Spectrum

A VRS constant, P_{VRS} , is extracted from the spectrum as the ordinate value corresponding to the natural frequency and damping ratio selected in Step 2, and the annual mean wind velocity selected in Step 1. For instance, the VRS in Figure 15-1 is applicable if using a damping ratio of 1.5% (recommended for cantilever-type sign support structures). If using a damping ratio of 0.35% (recommended for bridge-type VMS support structures), the VRS in Figure 15-2 would be applicable. The VRS in Figure 15-3 is provided for other damping ratios if necessary.

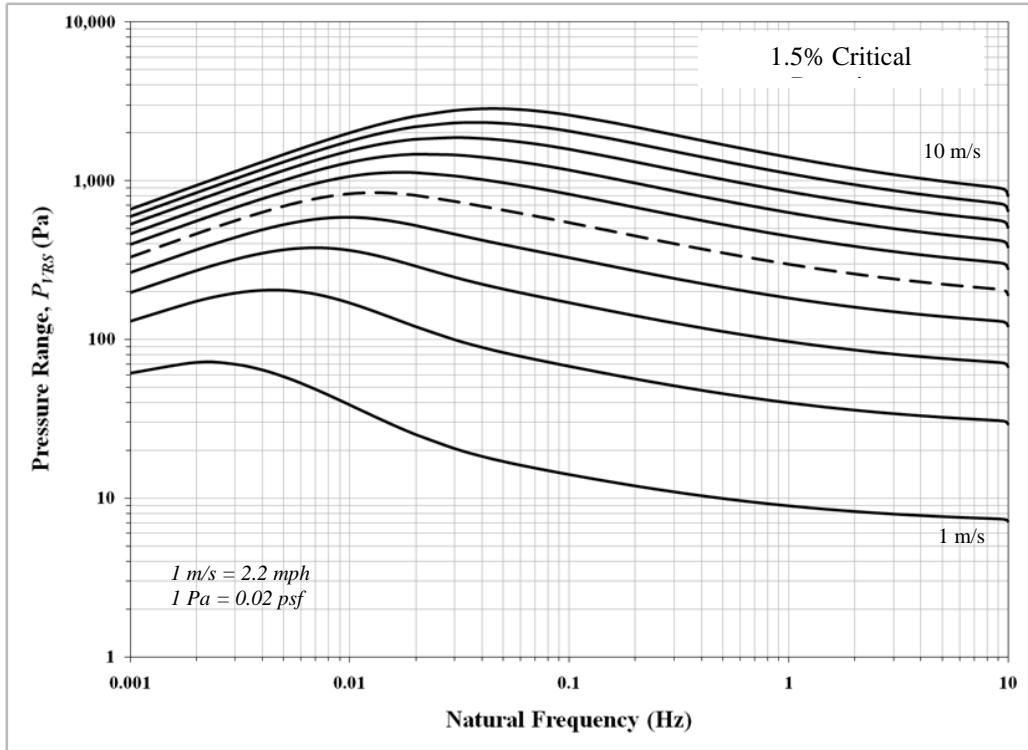


Figure 15-1. Fatigue load VRS for a critical damping percentage equal to 1.5%

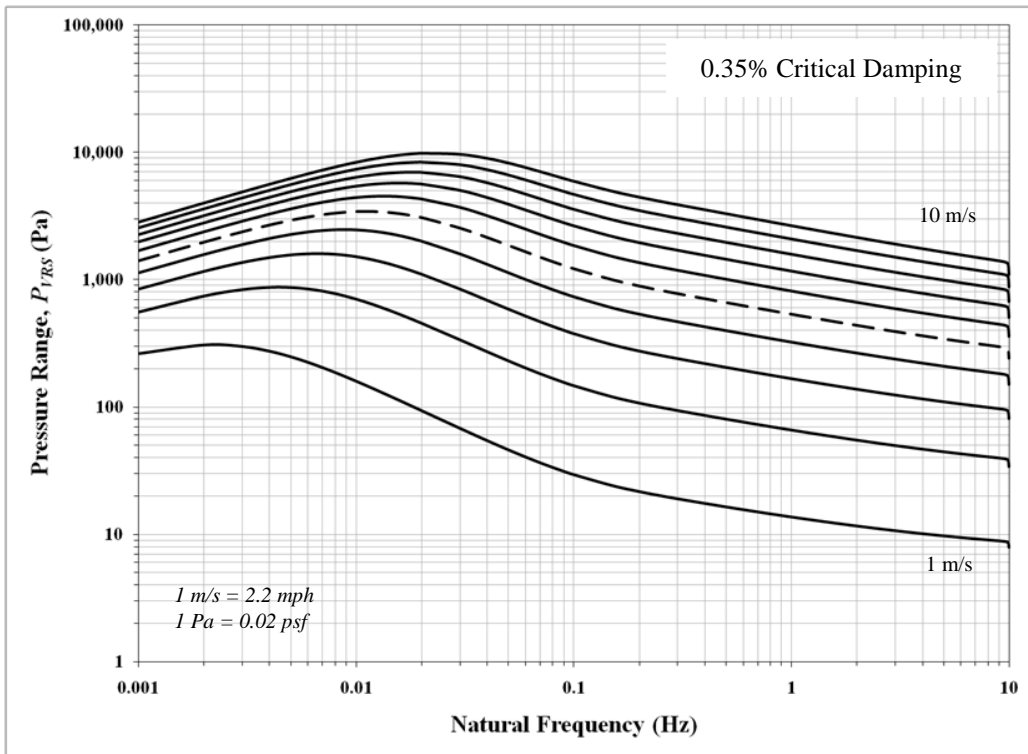


Figure 15-2. Fatigue load VRS for a critical damping percentage equal to 0.35%

Step 4: Fatigue Design Equation

Input the VRS constant, P_{VRS} , determined from Step 3 into Eq. 15-3 and apply as a uniformly distributed load for each member along the face of the structure that is exposed to natural wind.

$$P_{NW} = P_{VRS} C_d I_F \quad [\text{Eq. 15-3}]$$

where

P_{NW} = design fatigue load due to natural wind gust, psf (Pa)

P_{VRS} = transmitted pressure constant extracted from the VRS, psf (Pa)

C_d = drag coefficient

I_F = importance factor

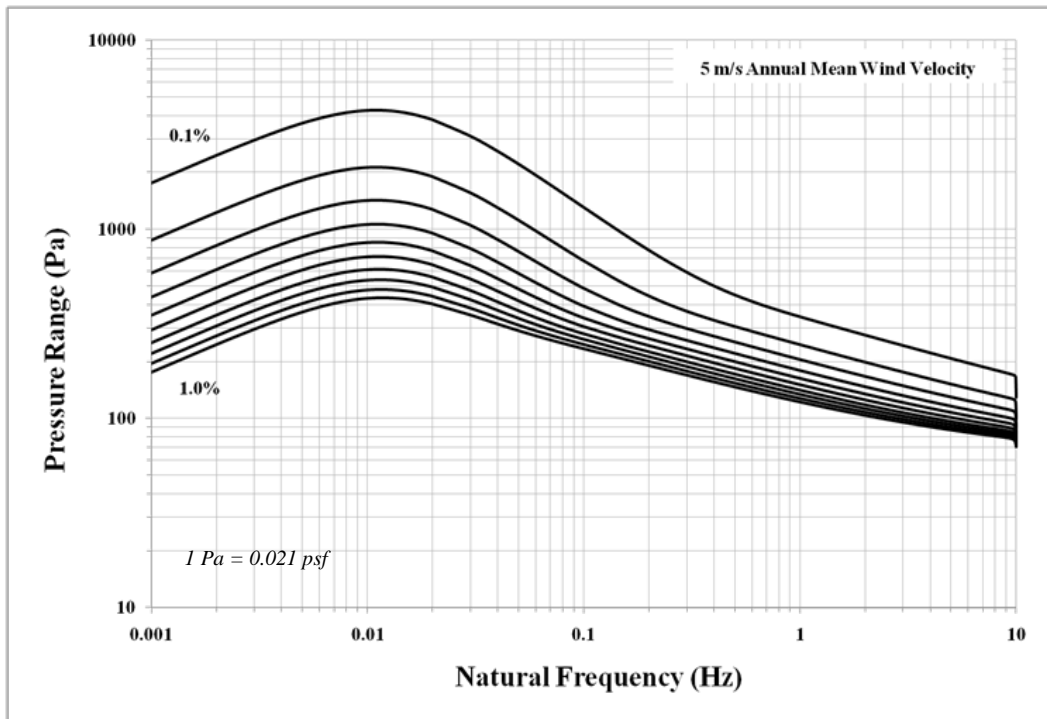


Figure 15-3. VRS plot of critical damping percentages ranging from 1.0% to 0.1%

Design Fatigue Load due to Truck-Induced Wind Gust

The proposed fatigue design equations for truck-induced wind gusts were developed from the experimental and theoretical programs with this project. The recommendations are presented in two forms as follows:

1. Generalized design equation, and
2. Detailed design equation.

Vertical and horizontal components of the truck gust were developed for the generalized and detailed fatigue design methodologies. The first methodology is a generalized design equation based on the experimental results of this project. It is applicable to the specific type of support structure that was analyzed with this project. The second equation is a more comprehensive design approach that accounts for the variety of highway overhead support structures in design. It was based on the theoretical program with this project. It requires detailed structural analysis that accounts for the dynamic characteristics of the structure in determining the fatigue load.

General Fatigue Design Equation for Truck-Induced Wind Gust

The proposed general design equation for truck-induced wind gust was developed from the experimental results of this project. It is applicable to the type of structure analyzed. Separate equations were developed for the cantilever-type sign support structure and the bridge-type VMS support structure.

Vertical Component The general fatigue design equation for the vertical component of the truck-induced wind gusts is shown as Eq. 15-4. It is to be applied vertically to the exposed underneath area of the structure onto a 12 ft (3.66 m) length portion (or width of the traffic lane, whichever is greater) located directly over the traffic lane. The load is applied as a uniformly distributed load. It is at maximum at a height of 19.7 ft (6.00 m) above the roadway, and decreases linearly to zero at a height of 32.8 ft (10 m). Equation 15-4 is recommended for bridge-type VMS support structures; specifically for support structures with a modal frequency of 3.79 Hz for vertical modal shapes in-plane with the vertically applied load.

$$P_{TG} = 3C_d I_F \left(\frac{v}{70} \right)^2 \quad [\text{Eq. 15-4}]$$

where

P_{TG} = design fatigue load due to truck - induced wind gust, psf (Pa)

C_d = drag coefficient

I_F = importance factor

v = traveling speed of the truck, mph (m/s)

The equation takes the form similar to the *Support Specifications* for easy implication. The drag coefficients and importance factors have not been altered, and are provided in the *Supports Specifications*. Accommodation for other traveling speeds other than 70 mph (31.3 m/s) is provided in the equation if necessary.

Horizontal Component The general fatigue design equation for the horizontal component of the truck-induced wind gusts is shown as Eq. 15-5. It is to be applied horizontally to the exposed

area on the front face of the structure onto a 12 ft (3.66 m) length portion (or width of the traffic lane, whichever is greater) located directly over the traffic lane. The load is applied as a triangularly distributed load. It is at maximum at a height of 19.7 ft (6.00 m) above the roadway, and decreases linearly to zero at a height of 32.8 ft (10 m). Equation 15-5 is recommended for bridge-type VMS support structures; specifically for support structures with a modal frequency of 2.81 Hz for horizontal modal shapes in-plane with the horizontally applied load.

$$P_{TG} = 6.1C_d I_F \left(\frac{v}{70} \right)^2 \quad [\text{Eq. 15-5}]$$

where

P_{TG} = design fatigue load due to truck - induced wind gust, psf (Pa)

C_d = drag coefficient

I_F = importance factor

v = traveling speed of the truck, mph (m/s)

The equation takes the form similar to the *Support Specifications* for easy implication. The drag coefficients and importance factors have not been altered, and are provided in the *Supports Specifications*. Accommodation for other traveling speeds other than 70 mph (31.3 m/s) is provided in the equation if necessary.

Detailed Fatigue Design Equation for Truck-Induced Wind Gusts

A detailed design equation was developed to account for the variety of sign support structures in design, each with different configurations, cross sectional shapes, and material properties. Since these factors have significant influence on the dynamic characteristics of the structure, and because supports structures are highly flexible, a method was needed in determining the fatigue load based on the vibration behavior of these structures. The approach presented in this section accounts for the dynamic behavior of the structure in terms of the modal frequency. The fatigue load is determined based on these properties. The approach was considered a unified design approach to fatigue design for support structures in that it accounts for the variety of structures. It is applicable to both the cantilever-type sign and the bridge-type VMS support structures of this project, as well as other support structures in design. Design methodologies for the vertical and horizontal components of the truck-induced wind gust are presented.

Natural Frequency Shock response spectrums (SRS) were developed that presents the fatigue load based on the dynamic properties of the structure. The load is extracted from the SRS in terms of the earliest modal frequency of the structure with a modal shape in the direction of the loading. This would include modal shapes with vertical vibratory motion for the vertical component and the modal shapes with horizontal vibratory motion for the horizontal component. For sign support structures, the vertical and horizontal modal shapes are generally around 1 to 4 Hz. Finite element software (i.e., SAP2000) can be used to estimate the appropriate modal shapes and their associated natural frequencies to use with the SRS curves. If FEA software is

not available, fundamental structural dynamics of a SDOF system (Eq. 15-6) can be used for estimating these values (AASHTO 2009, Creamer, *et al.* 1979, Harris 1996) A conservative approach would be to use the peak amplitude from the SRS that corresponds to the truck speed regardless of the natural frequency of the structure.

$$f_n = \frac{1}{2\pi} \sqrt{\frac{K}{M}} \quad [\text{Eq. 15-6}]$$

where

f_n = natural frequency, Hz

K = generalized stiffness, N/m (lb/ft)

M = generalized mass, kg (slug)

Fatigue Design Procedure A systematic procedure based on the proposed detailed approach for determining the vertically and horizontally applied fatigue design load due to truck-induced wind gusts may be given as follows.

Step 1: Design Speed of the Truck

The first step involves determining the design speed of the truck. A speed of 70 mph (31.3 m/s) is recommended however other speeds can be used if necessary.

Step 2: Modal Analysis

The second step involves a modal analysis of the support structure. The earliest modal frequency with a modal shape in the direction of the truck gust loading is needed. This would include modal shapes with vertical vibratory motion for the vertical component and the modal shapes with horizontal vibratory motion for the horizontal component. The damping ratio is not required for truck-induced gusts and therefore not considered in the methodology. Finite element analysis software can be helpful with this step in determining the necessary modal frequencies. If FEA is not available, the modal frequency and modal shape can be estimated using Eq. 15-6.

Step 3: Shock Response Spectrum

The third step involves the SRS shown in Figure 15-4 for the vertical component Figure 15-5 for the horizontal component. A SRS constant, P_{SRS} , is extracted from the spectrum as the ordinate value corresponding to the natural frequency determined Step 2.

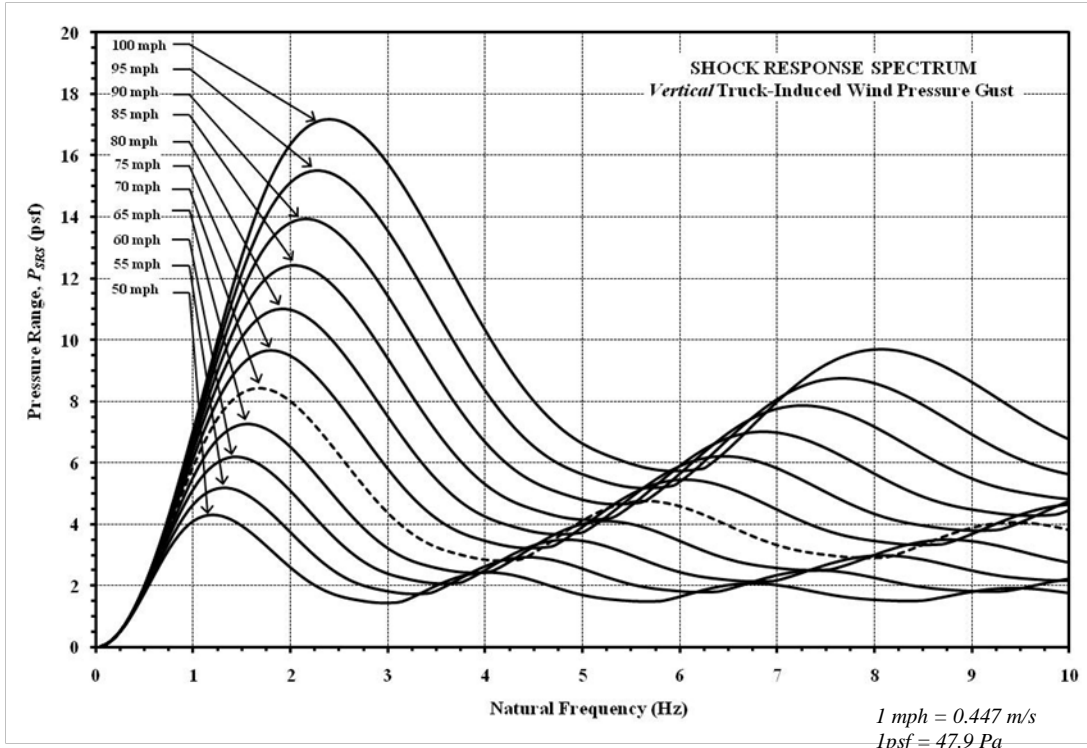


Figure 15-4. SRS for the vertical component of the truck-induced wind gust

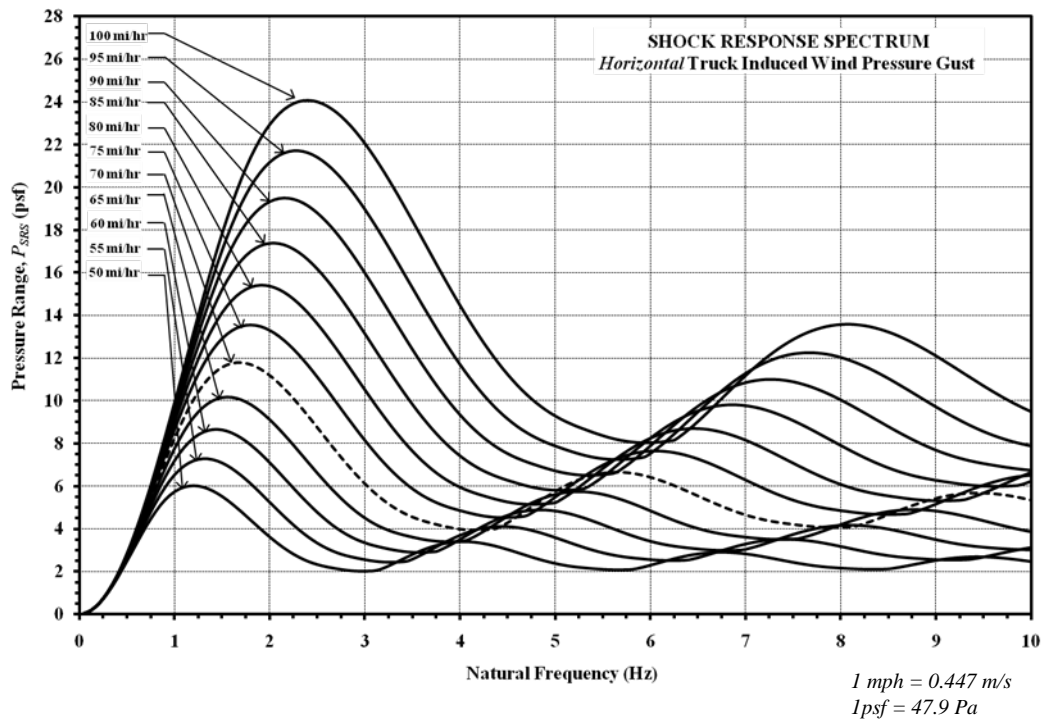


Figure 15-5. SRS for the horizontal component of the truck-induced wind gust

Step 4: Fatigue Design Equation

The next step is plugging all information gathered from Steps 1-3 into the fatigue design equation for truck-induced gusts based on the detailed approach. Input the SRS constant, P_{SRS} , determined from Step 3 into Eq. 15-7 for each member along the face of the structure exposed to truck-induced wind gusts. It is to be applied in the same fashion as the general design equation for truck-induced gusts for the horizontal and vertical components.

$$P_{TG} = P_{SRS} C_d I_F \quad [\text{Eq. 15-7}]$$

where

P_{TG} = design fatigue load due to truck - induced wind gust, psf (Pa)

P_{SRS} = transmitted pressure constant extracted from the SRS, psf (Pa)

C_d = drag coefficient

I_F = importance factor

Step 5: Height Accommodation

Accommodations for height can be made to the values determined from Eq. 15-7. In terms of the vertical component, this can be performed for structures with exposed areas higher than 19.7 ft (6.00 m). The truck gust pressure is assumed maximum at a height of 19.7 ft (6.00 m) above the roadway, and decreases linearly to zero at a height of 32.8 ft (10 m) according to Eq. 15-8.

$$P_h = -0.0763h + P_{SRS} \quad [\text{Eq. 15-8}]$$

where

P_h = truck - induced wind pressure at specified height above ground level, psf (Pa)

h = elevation increase from 19.7 ft (6.00 m) above the roadway, ft (m)

P_{SRS} = transmitted pressure constant extracted from the SRS, psf (Pa)

Equation 15-8 applies to the triangular distributed loading of the horizontal component. The distributed load decreases from its maximum value to zero at a rate equal to 0.0763 psf/ft (1.113 Pa/m).

Section 16

Design Fatigue Load Example Calculations

Overview

Examples demonstrating the determination of the design fatigue load using the developed methodology for natural wind and truck-induced wind gusts are presented. The general and detail approaches were used and compared to each other as well as to the design fatigue equation in the *Supports Specifications*. The comparison tested the accuracy of the *Supports Specifications* with respect to the experimentally determined values, as well as the theoretical approaches developed with this project.

A variety of case studies of different types of structures were included in the example comparisons. Each of the structures contained different structural dynamic properties based on case studies obtained from previous research (Creamer, *et al.* 1979, Foutch, *et al.* 2006, Kaczinski, *et al.* 1998). The fatigue load due to natural wind gust and truck-induced wind gust are calculated for three bridge-type VMS support structures. Each of the bridge-type support structures evaluated in the contained varying span lengths. The design cases are presented to detail accuracy issues encountered when using the fatigue provisions of the *Supports Specifications* and the methodologies developed with this research.

Fatigue Provisions of the AASHTO *Supports Specifications*

The fatigue design equations for natural wind and truck-induced gusts are provided in Eq. 16-1 and Eq. 16-2 (AASHTO 2009). The fatigue load was calculated using these equations for the case studies presented, and the results were compared to the fatigue design equations developed with this project.

Natural Wind Gust

$$P_{NW} = 5.2C_d I_F \left(\frac{\bar{v}}{11} \right)^2 \quad [\text{Eq. 16-1}]$$

where

P_{NW} = design fatigue load due to natural wind, psf (Pa)

C_d = drag coefficient

I_F = importance factor

\bar{v} = annual mean wind velocity other than 11 mph (5 m/s)

Truck-Induced Wind Gust

$$P_{TG} = 18.8C_d I_F \left(\frac{V}{65} \right)^2 \quad [\text{Eq. 16-2}]$$

where

P_{TG} = design fatigue load due to truck gust, psf (Pa)

C_d = drag coefficient

I_F = importance factor

V = truck speed, mph (m/s)

The above equations were used for the comparison, and were applied in the manner specified in the *Supports Specifications* fatigue provisions.

Design Case Scenarios

The fatigue load due to natural wind and truck-induced wind gusts were determined for three bridge-type VMS support structures. Each structure had different spans which affected their structural dynamic properties. The dynamic properties were based on bridge-type VMS support structures that were evaluated in previous studies (Foutch, *et al.* 2006, McLean, *et al.* 2004). They were chosen to illustrate the potential for underestimation or overestimation of the fatigue provisions in the *Supports Specifications*. This was done primarily by altering the natural frequencies, which represents a practical scenario as these structures are not exact in size, shape, configuration, stiffness, mass, and material. The fatigue loads are calculated using the proposed general and detailed equations that were developed with this research and presented in **Section 15: Proposed Fatigue Provisions**. The results of the calculations are compared with the fatigue provisions provided by the AASHTO *Supports Specifications*. It is important to note that the provisions in the *Supports Specifications* are specified for cantilever-type sign support structures. Provisions for bridge-type structures are not available. However, a comparison is provided to show the relevance of the provisions, and the need for the developed of new provisions.

A listing of the design cases along with the specific dynamic properties required for calculating the fatigue loads are provided in Table 16-1. The natural frequencies of vibration and span lengths are included in the table. The span lengths are included in the case descriptions because of their influence on the natural frequency of vibration and ultimately the design fatigue load as determined from this research. Critical damping percentages of these structures were not provided in the literature. Therefore, a value of 0.35% was used for all three structures, which was based on the experimentally tested VMS structure with this project.

Table 16-1. Bridge-type VMS support structure design cases

Support Structure	Design Case Description					
	Span Length	Horizontal Natural Frequency	Vertical Natural Frequency	Critical Damping Percentage	Annual Mean Wind Velocity	Traveling Truck Speed
Structure 1	89 ft	3.01	3.10			
Structure 2	94 ft	2.88	3.38	0.35%	11 mph	70 mph
Structure 3	145 ft	1.35	2.02			

1 ft = 0.3048 m
1 mph = 0.44704 m/s

The natural frequencies listed in the table represent the earliest modal frequency with vibratory motion in the direction of the loading. This is illustrated in Figure 16-1 and Figure 16-2 for the bridge structure. For natural wind, the earliest modal frequency in the direction of the loading would be the horizontal modal frequency as shown in Figure 16-1. This would also include the horizontal component of the truck-induced wind gust. For the vertical component of the truck-induced wind gust, the earliest modal frequency in the direction of the loading would be the vertical modal frequency as shown in Figure 16-2.

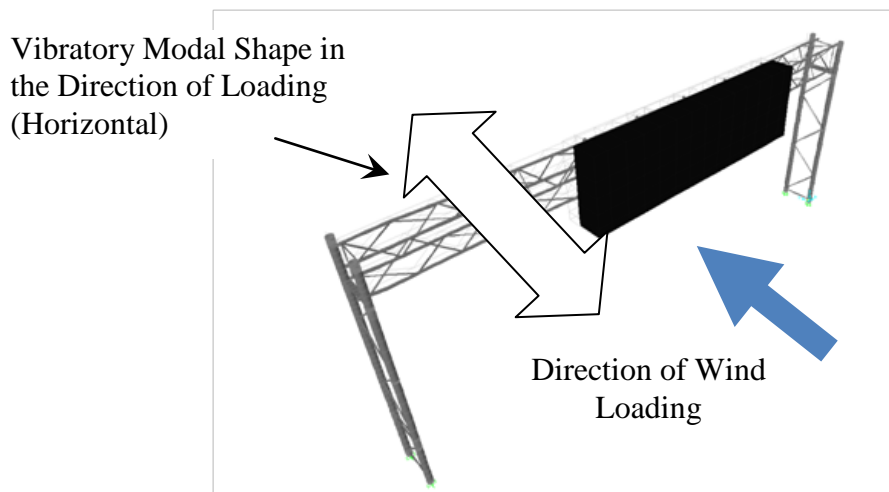


Figure 16-1. Horizontal vibratory motion in the direction of loading

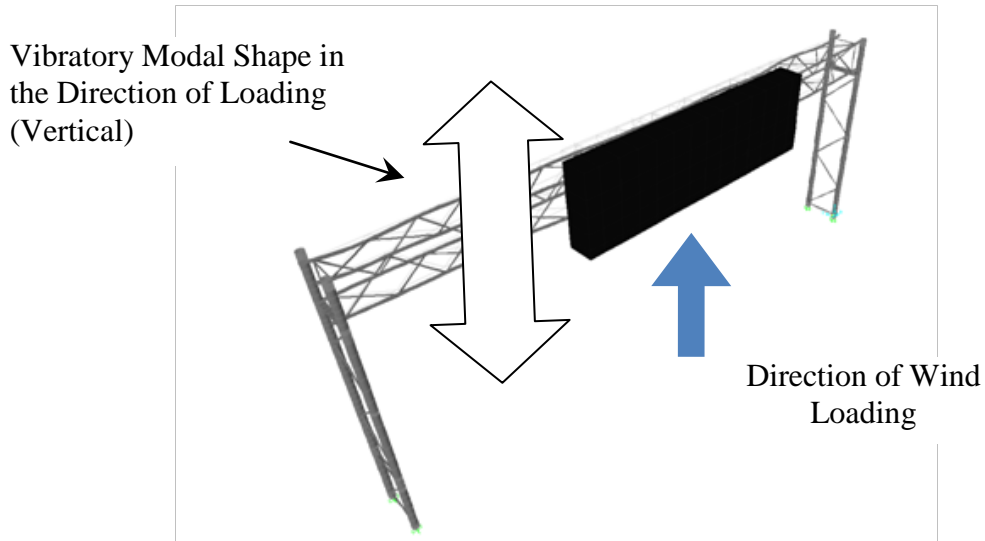


Figure 16-2. Vertical vibratory motion in the direction of loading

Design Fatigue Load due to Natural Wind Gust

The natural wind loading for the three design cases was directed onto the exposed area on the front face of the structures (normal to the front plain of the sign and support members, in the direction of traffic). An example of this direction is shown in Figure 16-1 for typical bridge-type VMS support structures. The results of the analysis using the general and detailed design equations Eq. 15-1 and Eq. 15-3 provided in **Section 15: Proposed Fatigue Provisions** and the *Supports Specifications* (Eq. 16-1) are given in Table 16-2. The VRS used for each case with the detailed equation is provided in Figure 16-3 through Figure 16-5. A bar chart illustrating the comparison between the fatigue load calculation approaches is provided in Figure 16-6.

Table 16-2. Design case results with the evaluation of the design fatigue load due to natural wind gust

Support Structure	AASHTO Eq. 16-1 (psf)	Design Methodology (psf)			Methodology AASHTO	
		General (Eq. 15-1)	Detailed (Eq. 15-3)	General / Detailed	General	Detailed
Structure 1	5.20	7.00	8.22	0.852	1.35	1.58
Structure 2	5.20	7.00	8.30	0.843	1.35	1.60
Structure 3	5.20	7.00	10.3	0.680	1.35	1.98

1psf = 47.873 Pa

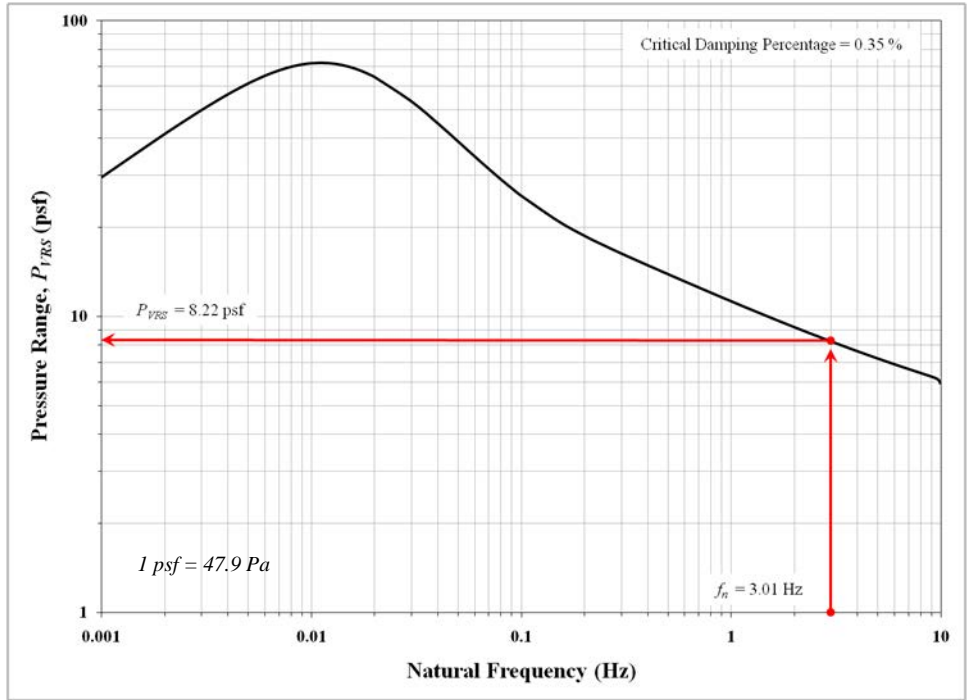


Figure 16-3. VRS of structure 1 design case scenario

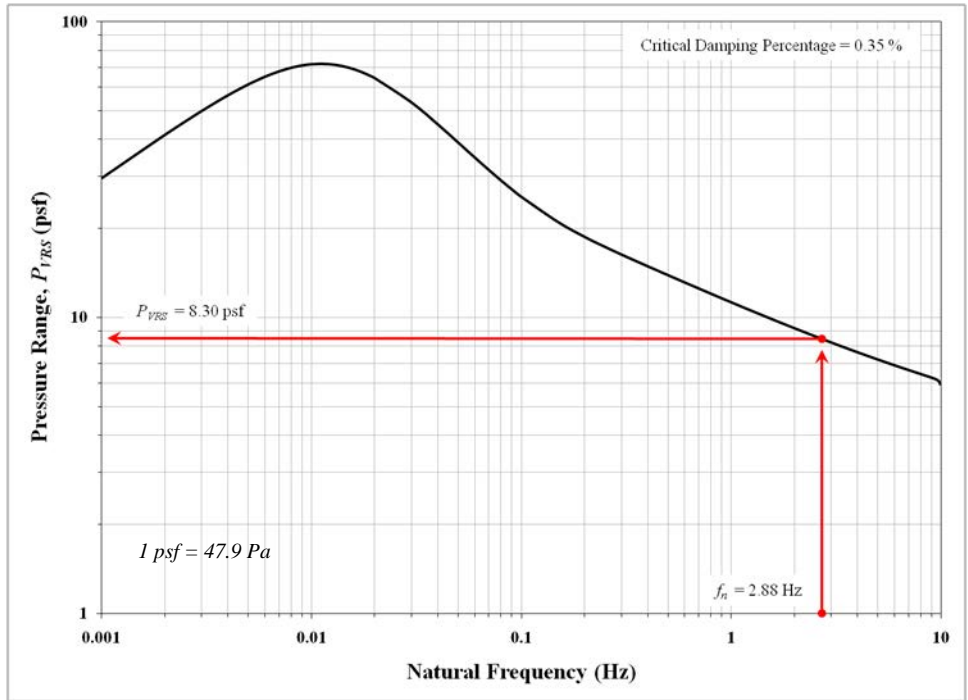


Figure 16-4. VRS of structure 2 design case scenario

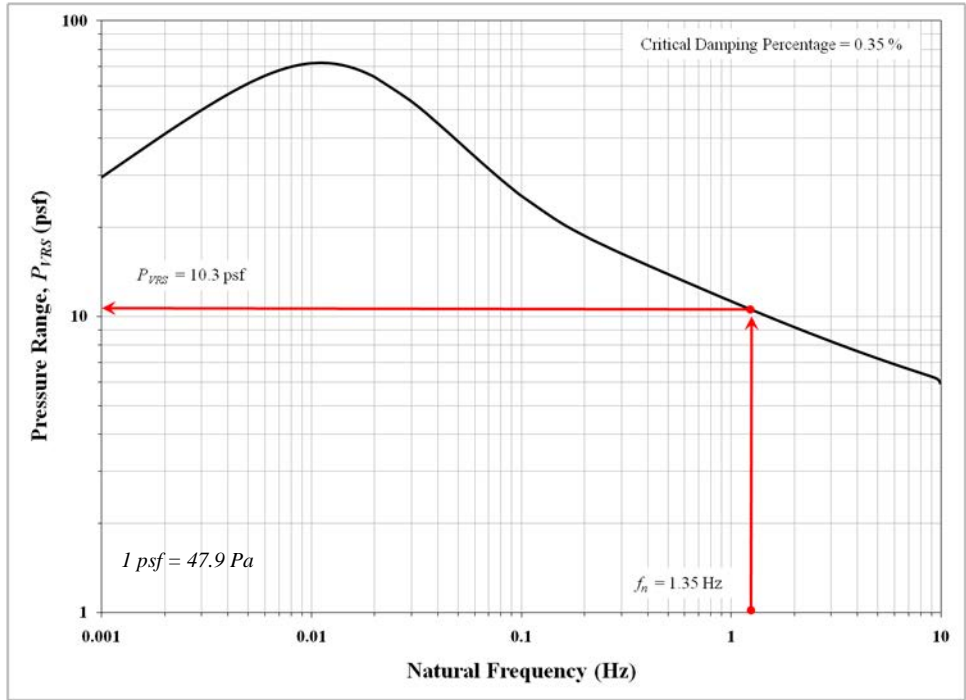


Figure 16-5. VRS of structure 3 design case scenario

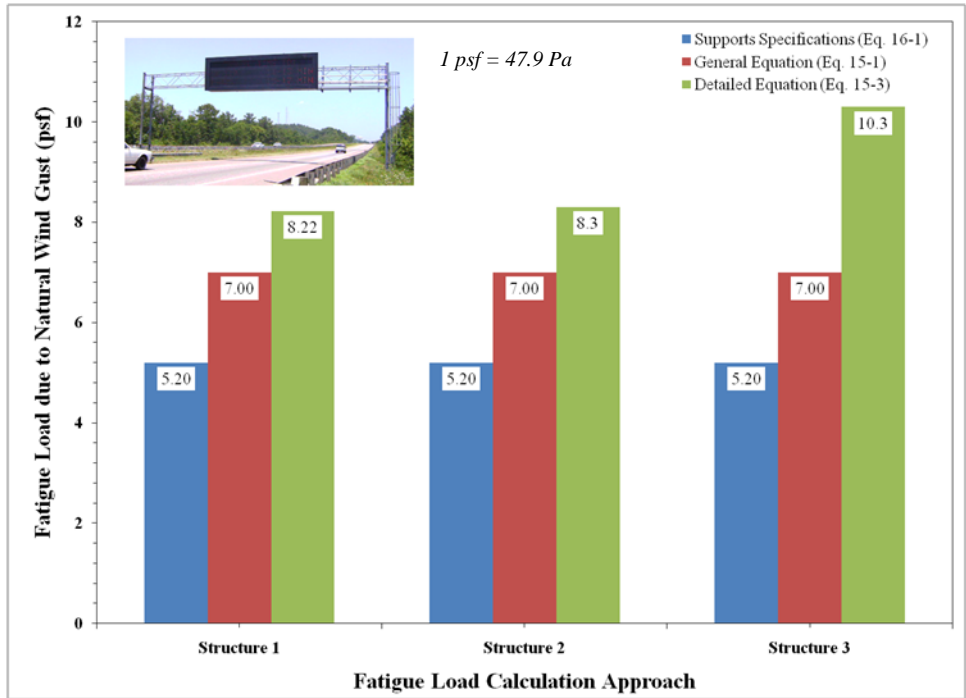


Figure 16-6. Comparisons between the fatigue load due to natural wind calculation approaches

Discussion of the Results

Comparisons between the general and detail fatigue design equation were performed, as well as a comparison with the *Supports Specifications*. Structure 4 had the closest dynamic properties to the tested VMS support structure with this project, which had a 71 ft (21.6 m) span. As the span of the bridge structures increased, the natural frequencies of vibration became lower. As a result, the fatigue loads according to the detailed equation increased. This was due to the change in flexibility and increase in dynamic amplification from the wind load because the natural frequency of the structures came in close proximity to the resonant frequencies of the wind. Therefore, it can be concluded that the fatigue load must be higher for longer bridge spans in the order listed in Table 16.6 of the calculated results.

Design Fatigue Load due to Truck-Induced Wind Gust

Evaluation of the design case scenarios listed in Table 16.5 were performed to illustrate the proposed design approach for calculating fatigue loads due to truck gusts, and to compare the results to the *Supports Specifications*. The vertical and horizontal components of the design fatigue load were calculated using the general design equation as well as the detailed design equation developed with this research. For the general methodology with bridge-type VMS support structures, Eq. 15-4 was used to calculate the vertical component loading, and Eq. 15-5 was used to calculate the horizontal component loading. Equation 15-7 was used calculate the vertical and horizontal component of the fatigue load for the detailed methodology.

The calculations reflect the design fatigue load to be applied to the structure. For the vertical component, the load is to be applied vertically to the horizontal exposed area on the underneath portion of the overhead truss above the traffic lane (see Figure 16-2). The earliest modal shape with a vibratory motion in the direction of the vertical loading is required for the calculation. The exposed area was located approximately 19.7 ft (6.00 m) above the roadway for all structures, and therefore no adjustment for height was required. For the horizontal component, the load is to be applied horizontally onto the vertical exposed area located on the front of the structure (see Figure 16-1). The earliest modal shape with a vibratory motion in the direction of the horizontal loading is required for the calculation. The load is to be applied as a triangular distributed load. The values calculated represent the maximum value at a height equal to 19.7 ft (6.00 m) above the roadway, and decreases linearly to zero at a height of 32.8 ft (10 m) according to Eq. 15-8.

A summary of the results of the comparison are listed in Table 16-3 for the vertical component and Table 16-4 for the horizontal component. The *Supports Specifications* does not contain provisions for the horizontal component of the truck gust, and is listed as a “/” in the results. The provisions indicate that the fatigue load due to natural wind gust is generally the controlling factor in design for fatigue loading in the horizontal direction. The SRS used for the detailed equation are found in Figure 16-7 through Figure 16.-12. Bar charts illustrating the comparisons are provided in Figure 16-13 for the vertical component of the fatigue load, and Figure 16-14 for the horizontal component of the fatigue load.

Table 16-3. Design case results with the evaluation of the vertical component

Support Structure	AASHTO Eq. 16-2 (psf)	Design Methodology (psf)			Methodology AASHTO	
		General (Eq. 15-4)	Detailed (Eq. 15-7)	General Detailed	General	Detailed
Structure 2	21.8	3.00	3.39	0.885	0.138	0.156
Structure 3	21.8	3.00	7.99	0.375	0.138	0.367

1psf = 47.873 Pa

Table 16-4. Design case results with the evaluation of the horizontal component

Support Structure	AASHTO (psf)	Design Methodology (psf)		
		General (Eq. 15-5)	Detailed (Eq. 15-7)	General Detailed
Structure 1	/	6.10	6.11	0.998
Structure 2	/	6.10	6.57	0.928
Structure 3	/	6.10	11.0	0.555

1psf = 47.873 Pa

/ indicates no fatigue load provision are specified in the Supports Specification for the horizontal component of the truck-induced wind gust

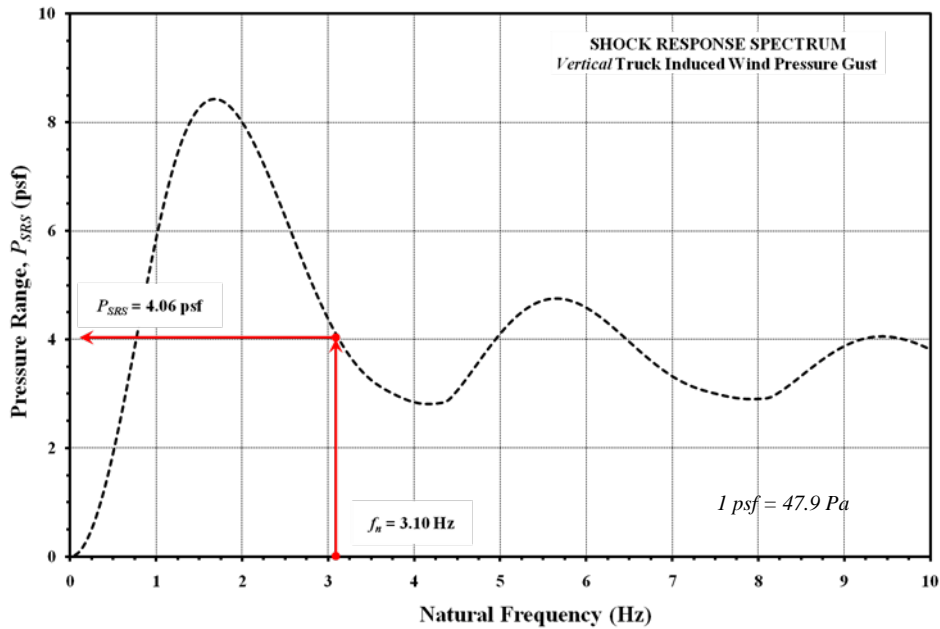


Figure 16-7. Vertical SRS of Structure 1 design case scenario

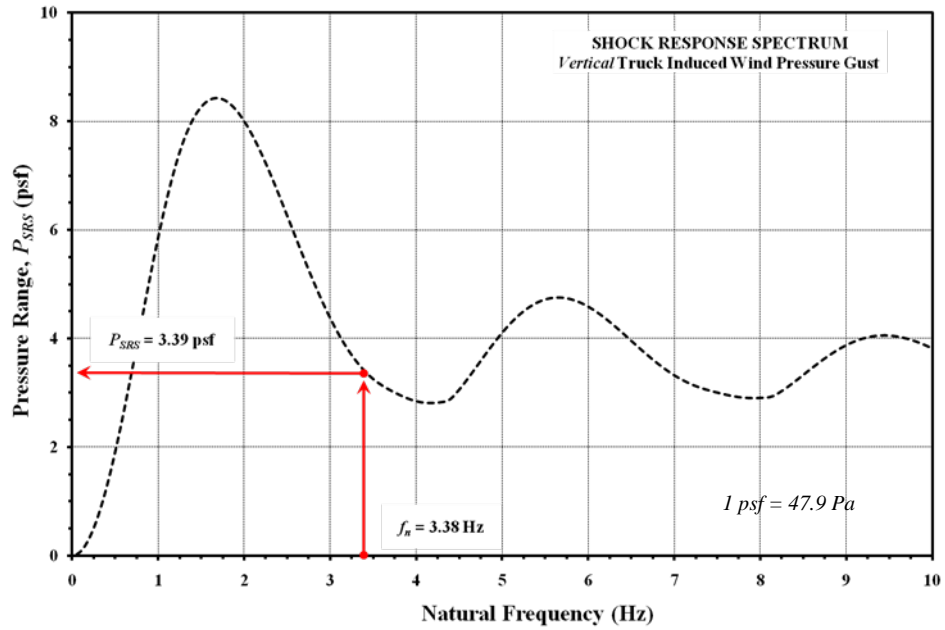


Figure 16-8. Vertical SRS of Structure 2 design case scenario

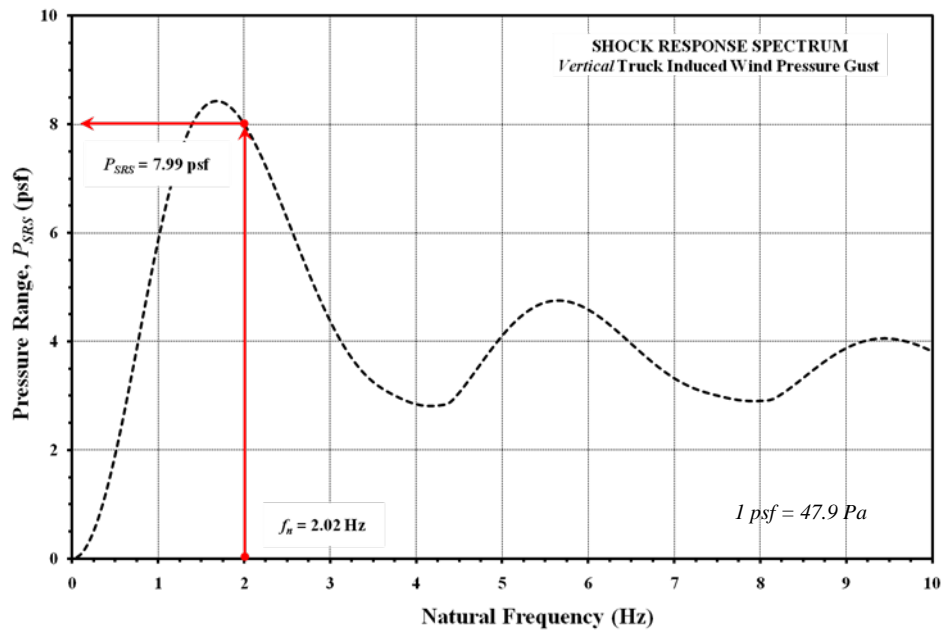


Figure 16-9. Vertical SRS of Structure 3 design case scenario

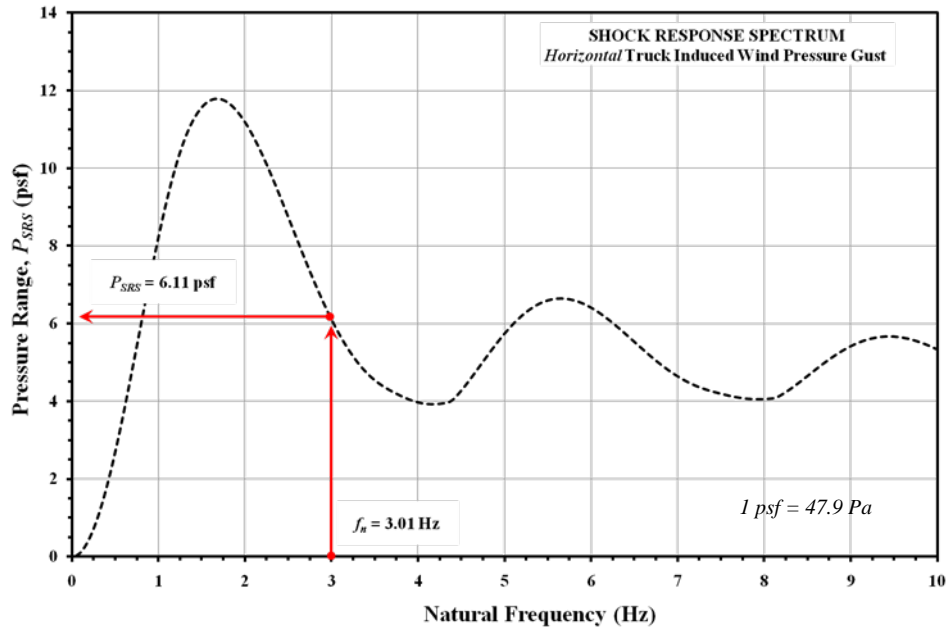


Figure 16-10. Horizontal SRS of Structure 1 design case scenario

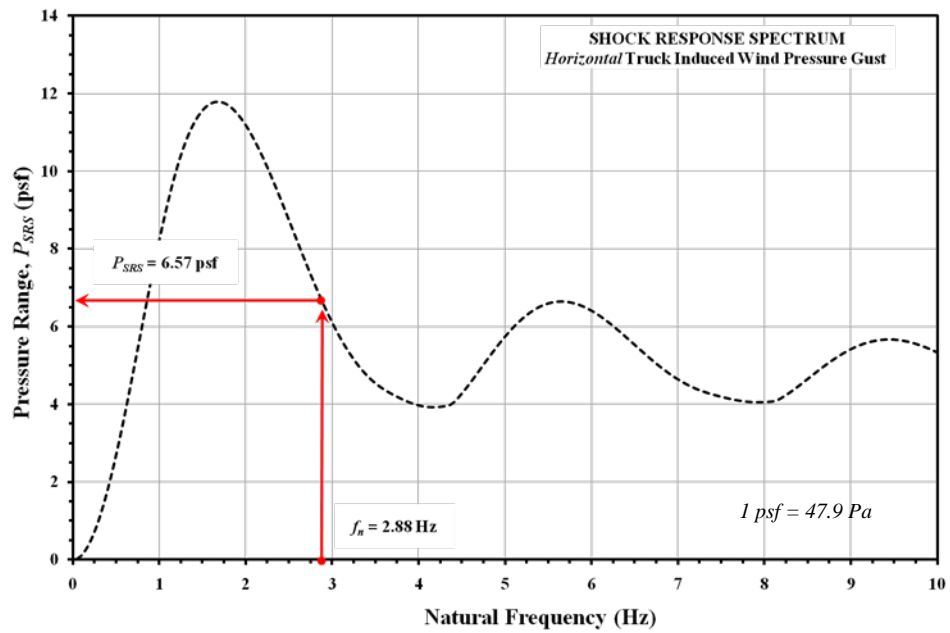


Figure 16-11. Horizontal SRS of Structure 2 design case scenario

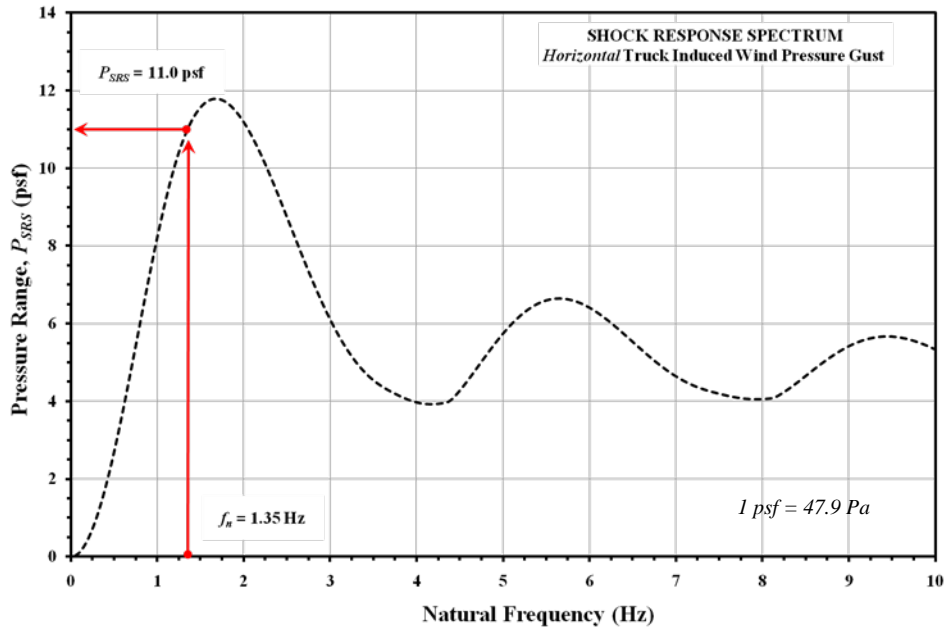


Figure 16-12. Horizontal SRS of Structure 3 design case scenario

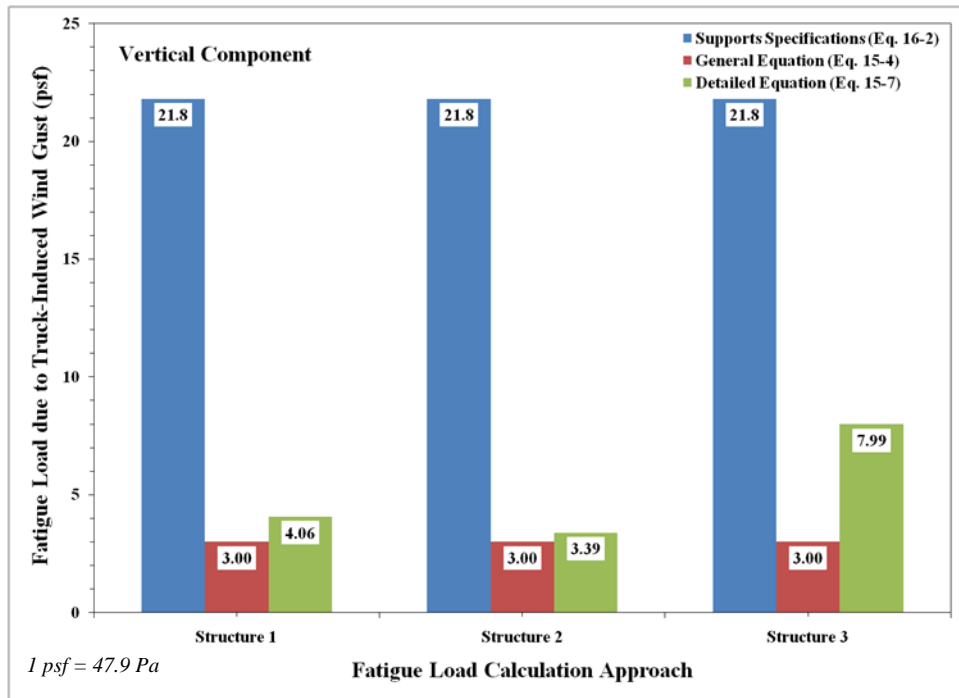


Figure 16-13 Comparisons between the vertical component calculation approaches

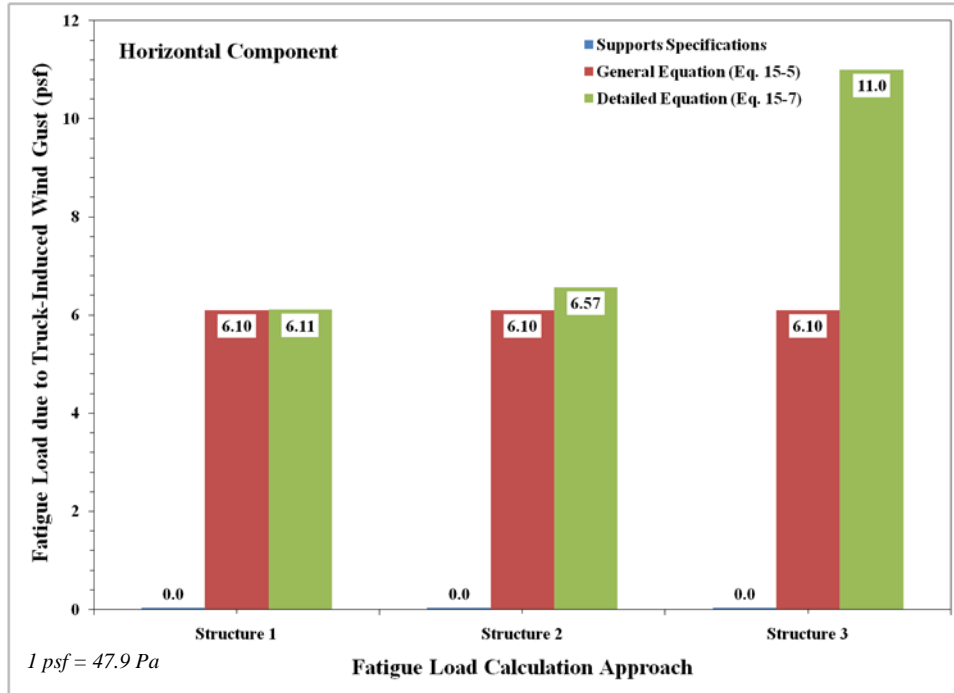


Figure 16-14 Comparisons between the horizontal component calculation approaches

Discussion of the Results

The results from both the general and detailed design equations were significantly less than the *Supports Specifications*. The equations were developed from experimental and theoretical evaluation of the bridge-type VMS support structure used with this research. For the vertical component, the general and detailed equations are very similar for Structures 1 and 2. This is because their natural frequencies of vibration in the vertical direction were similar to the bridge-type VMS support structure used to develop the general equation. However, the vertical component of Structure 3 was much higher than the general equation. The natural frequency was lessened because of the much larger bridge span of Structure 3, and therefore dynamic amplification was increased because of the proximity of the structural natural frequency to the spectral peak of the truck gust.

Similar trends are observed with the horizontal component of the truck gust. Importantly, the *Supports Specifications* does not contain provisions for the horizontal component and therefore no comparison can be made. Structures 1 and 2 have similar results because they have similar dynamic properties to the tested structure. Structure 3, with the larger span, is much larger than the other two for the same reasons as the vertical component. The large differences indicated that the general equation has certain limitations as expressed in **Section 15: Proposed Fatigue Provisions**. The detailed approach, however, is applicable to any structure based on their dynamic behavior under the loading scenarios.

Section 17

Summary and Conclusions

Overview

The fatigue load due to natural wind gust and truck-induced wind gust were developed from experimental and theoretical programs. The results were compared to the fatigue provisions of the *Supports Specifications*. General and detailed equations were developed. The general equation was developed based on the experimental data collected and evaluated on the specific structural type that was tested with this research. The detailed equation was developed based on the theoretical methodology developed with this project. It was developed as a universal and comprehensive approach to be applicable to any type of support structure, each with different configurations, material properties, member sizes and shapes.

Summary of the findings and conclusions of this project are presented in this section. The section is divided into subsections corresponding to the major tasks performed in this project. The tasks were conducted to develop the fatigue loads as well as to provide comparisons to ascertain the accuracy of the fatigue provisions provided in the *Supports Specifications*, which included the following ten items:

1. Bridge-type VMS support structure specimen,
2. Structural instrumentation,
3. Testing procedures,
4. Data collection samples,
5. Operational modal analysis,
6. Design fatigue load due to natural wind gust,
7. Design fatigue load due to truck-induced wind gust,
8. Comparisons between the experimental and theoretical results,
9. Finite element analysis, and
10. Design fatigue load examples showing comparisons with the *Supports Specifications*.

Project Summary

Highway Overhead Support Structure Specimen

One bridge-type VMS support structure was tested with this project. The bridge-type VMS was located on highway I-65 Northbound near Alabaster, AL. The structure was made of steel and had a four-chord truss that spanned 71 ft (22 m) over two highway traveling lanes.

Structural Instrumentation

The highway overhead support structure was instrumented with the following transducers:

- Strain gauges,
- Accelerometers, and
- Anemometers.

Strain gauges were placed on the supporting posts and chords of the tested structure. They were used to evaluate the stress ranges developed at these locations. Accelerometers were placed strategically at specific locations on the structure to measure vibratory motion of each degree-of-freedom. They were used to measure the dynamic characteristics of the structure. Anemometers were used to measure the ambient natural wind environment to develop three-dimensional wind velocity vectors.

Each transducer was wired into a data acquisition system. The sampling frequencies were set at 60 Hz, well above the highest modal frequency of the structure. The allocation of the assigned channels used for instrumentation and maximum number were as follows:

- Strain Gauges: 12 channels
- Anemometers: 4 channels
- Accelerometers: 4 channels
- Total Channels = 20

Testing Procedures

A van containing the data acquisition system was driven to the testing site and the instrumentation was wired into the system for all testing procedures. Data collected for the natural wind gust experimentation were collected at 45 minute intervals and saved onto a disk for data analysis back in the lab. A random procedure was used for the data collection for the truck-induced wind gust experimentation. The structure was located on the highway in between exits where traffic was operating at normal highway speeds. Trucks were selected randomly and the time of truck passing and truck speed (measured from a radar gun) were documented.

Data Collection Samples

A total of 23.25 hours of natural wind data were collected on the support structure. The data were reduced for velocities greater than 9 mph (4 m/s) and oriented on the front face of the structure. This was because significant vibration was not evident for wind velocities less than 9 mph (4 m/s), and the drag coefficients used with this research are only applicable for winds oriented normal to the face of the structures. Winds onto the back face of the structure were not used because of the support truss span oriented in front of the VMS. The average usable wind velocity that was used in the development of the fatigue load for natural wind gust was found to be 10.99 mph (4.913 m/s).

A total of 157 truck tests were performed. Trucks of all types that commonly use the highway system were used in the tests. Truck speeds ranging from 50 mph (22 m/s) to 80 mph (36 m/s) were measured. Trucks traveling on the inside and outside lanes were also measured. The test procedures conducted with this test was comprehensive because of the range of truck types and speeds recorded, as well as the large sample size.

Operational Modal Analysis

An operational modal analysis was performed on the support structure to determine the dynamic behavior during the loading events. This was done for both natural wind gust and truck-induced wind gust. The modal shapes, modal frequencies, and modal damping were determined under the loading scenarios.

The information gathered from this task was used in the determination of the fatigue loads using the theoretical approaches developed with this project. The fatigue load was determined based on the structure's dynamic characteristics using the vibration response spectrum (VRS) for natural wind gust, and the shock response spectrum (SRS) for truck-induced wind gust. For these approaches, it was important to know the shape of vibration and the frequency of vibration. It was also necessary to find the critical damping percentages of the structures for determining the fatigue load due to natural wind gust.

Design Fatigue Load due to Natural Wind Gust

The design fatigue load due to natural wind gust was determined. Experimental and theoretical programs were developed to determine the design fatigue loads. General and detailed design fatigue equations were developed for the structure. Recommendations, limitations, and application procedures were presented.

The general equation is applicable for structures with similar dynamic characteristics as the bridge-type VMS support structure tested with this project. The equation was developed using a back-calculation procedure from the experimental data collected. It is in the form of an equivalent static wind load that would produce an equivalent stress range on the structure as the dynamic loading environment measured during the testing.

The general equation was developed for structures with dynamic characteristics different than the structures tested with this project. The equation utilizes the VRS. The spectrum provides the fatigue load based on the natural frequency of vibration of the structure, the critical damping percentage, and the annual mean wind velocity. The approach is considered comprehensive in that it is applicable to any support structure with different configurations, material properties, sizes and shapes. The fatigue load is based on the dynamic properties of the structure, which included dynamic amplification due to the proximity of the natural frequencies of these structures to the resonant frequencies of natural wind.

Design Fatigue Load due to Truck-Induced Wind Gust

The design fatigue load due to truck-induced wind gust was determined. Vertical and horizontal components of the loading were evaluated. Experimental and theoretical programs were developed to determine the design fatigue loads in which general and detailed design fatigue equations were developed. Recommendations, limitations, and application procedures were presented.

Equations for the vertical component and the horizontal component of the fatigue loading were presented. The equations are applicable for structures with similar dynamic characteristics as the bridge-type VMS support structure tested with this project. The equations were developed using a back-calculation procedure from the experimental data collected. They are in the form of an equivalent static wind load that would produce an equivalent stress range on the structure as the dynamic loading environment measured during the testing.

The general equation was developed for structures with dynamic characteristics different than the structures tested with this project. The equation utilizes the SRS. The spectrum provides the fatigue load based on the natural frequency of vibration of the structure. The approach is considered comprehensive in that it is applicable to any support structure with different configurations, material properties, sizes and shapes. The fatigue load is based on the dynamic properties of the structure, which included dynamic amplification due to the proximity of the natural frequencies of these structures to the resonant frequencies of truck-induced wind gusts.

Comparisons between the Theoretical and Experimental Programs

The fatigue load due to natural wind and truck-induced wind gusts developed from the theoretical and experimental programs were compared to each other. The comparison was performed to ascertain the accuracy of the theoretical approach for both loading scenarios. The theoretical approach was developed independent of the type of support structure. It is based primarily on the dynamic characteristics of the structure. The experimental results were based primarily on the type of structure with the specific dynamic characteristics of the structures tested. A successful comparison indicates that the theoretical approach is applicable and universal in that it can be used to determine the fatigue loads based on the dynamic vibration characteristics for any type of support structure.

Finite Element Analysis

Finite element analysis (FEA) was performed using the SAP2000 FEA program. Models were developed for the bridge-type VMS support structure tested with this project. The analysis was conducted to provide an accurate model that can be used for fatigue stress evaluation at important and specific areas of the structures that are prone to fatigue damage. The developed fatigue loads were inputted into the software program as equivalent static wind loads, and the stress generated at the base plate and chords-to-support locations were analyzed. Certain properties of the structures, material and geometric, can be altered with the FEA models that cannot be done experimentally. For this reason, the FEA model was considered an important aspect of the study, and for future studies concerning highway overhead sign support structures.

Design Examples and Comparisons with the Supports Specifications

Examples on how to determine the fatigue load using the general and theoretical equations developed with this research were presented. The results were compared to the fatigue provisions provided in the AASHTO *Supports Specifications*. Bridge-type VMS structures with different dynamic characteristics were used for the design examples to demonstrate how to determine the appropriate loading, but also to explain the limitations of the general equations and the *Support Specifications*.

Project Conclusions

Specific conclusions drawn from the tasks and objectives accomplished with this project are listed as follows. The conclusions are specifically related to the design of highway overhead sign support structures for fatigue loading due to natural wind and truck-induced wind gusts. Recommendations along with important and significant observations made during the work performed are presented.

Structural Instrumentation

Only a few instruments were not working properly with the tested structure. The large number of instrumentation was placed for redundancy reasons. The measurements for natural wind were recorded in three-dimensions by measuring wind velocity and direction in the vertical and horizontal planes. The data indicated that the wind was primarily directed normal to the elevation face of the structure with a small degree change of +/- 5 degrees. Therefore, only the anemometer measuring the horizontal plane is required for this type of testing.

Testing Procedure

The data collection procedures for natural wind were successful, with no problems observed with the testing procedures. The testing procedure for the truck-induced gust. The testing procedure used with the bridge structure allowed for the measurement of many different truck types that

use the highway system. The results represented the response of the structure to a variety of truck types rather than a single truck type..

Operational Modal Analysis

The experimental data collected with the support structure indicated significant vibration for wind speeds greater than 9 mph (4 m/s). Vibration was observed to minimal for lower speeds, and inconsequential to wind induced fatigue stresses.

- The major frequencies of vibration ranged from 1.41 Hz to 3.79 Hz.
- No significant torsional vibration was observed of the truss span supporting the VMS.
- The predominant modal frequency of vibration with the largest vibration magnitudes due to natural wind gust was in the horizontal direction equal to 1.81 Hz, indicating horizontal bending of the truss span in this direction and significant axial loading in the uprights.
- The predominant modal shape of vibration with the largest vibration magnitudes due to truck-induced wind gust was in the horizontal direction parallel to the direction of traffic. Significant vertical vibration was also observed with this loading, but with vibration magnitudes less than the magnitudes in the horizontal direction.
- The critical damping percentage in the horizontal direction was equal to 0.361%, and 0.119% in the vertical direction.

Experimental Calculation of the Fatigue Load due to Natural Wind Gust

The fatigue load was determined from the experimental data collected using the infinite-life approach to fatigue design. The determined fatigue load represented the wind pressure resulting from a 38 mph (17 m/s) wind velocity, which was equal to the 0.01% exceedence probability from an annual mean wind velocity of 11 mph (5 m/s).

- The fatigue load due to natural wind gust determined from the experimental investigation was found to be equal to **7.03 psf (337 Pa)**.
- The fatigue load was determined using the strain gauges placed on the north and south labeled uprights.

Experimental Calculation of the Fatigue Load due to Truck-Induced Wind Gust

A horizontal and vertical component of the fatigue load due to truck-induced wind gust was determined from the experimental data. All of the developed loads represent a semi-trailer traveling at a speed equal to 70 mph (31 m/s).

- The maximum vertical component of the truck-induced wind gust pressure was found to be equal to **2.97 psf (142 Pa)**.

- The maximum horizontal component of the truck-induced wind gust pressure was found to be **6.11 psf (293 Pa)**.

Theoretical Calculation of the Fatigue Load due to Natural Wind Gust

The fatigue load due to natural wind gust was determined theoretically utilizing the vibration response spectrum (VRS). The VRS was developed based on the structural dynamic characteristics of the structure. All values that formulated the spectrum were based on the infinite-life approach to fatigue design. The fatigue load extracted from the VRS represented the wind pressure resulting from a 38 mph (17 m/s) wind velocity, which was equal to the 0.01% exceedence probability from an annual mean wind velocity of 11 mph (5 m/s).

The Davenport wind velocity power density spectrum (PDS) was used as the excitation model to simulate the behavioral characteristics of natural wind, which closely match the PDS developed from the experimental wind velocity data collected with this project. The Davenport PDS had a slightly larger level because of the amount of data used in its development versus the limit amount of data used to develop the experimental PDS with this project. However, because of the closeness between the two spectrums, the Davenport model was considered accurate and applicable with this approach.

- The fatigue load extracted from the VRS for the support structure was based on the dynamic properties obtained from the operational modal analysis. Specifically, the natural frequency of the structure with the earliest modal shape of vibration in the direction of the natural wind loading was equal to 2.81 Hz, and the critical damping percentage in this direction was equal to 0.361%.
- The fatigue load due to natural wind gust determined from the experimental investigation was found to be equal to **8.27 psf (396 Pa)**.

Theoretical Calculation of the Fatigue Load due to Truck-Induced Wind Gust

A horizontal and vertical component of the fatigue load due to truck-induced wind gust was determined from the theoretical investigation. The fatigue load was extracted from the shock response spectrum (SRS) based on the dynamic properties of the structure. All of the developed loads represent a semi-trailer traveling at a speed equal to 70 mph (31 m/s).

- The fatigue load extracted from the SRS for the support structure was based on the dynamic properties obtained from the operational modal analysis. Specifically, the natural frequency of the structure with the earliest modal shape of vibration in the direction of the vertical component of the truck-induced wind gust was equal to 3.79 Hz, and the natural frequency of the structure with the earliest modal shape of vibration in the direction of the horizontal component of the truck-induced wind gust was equal to 2.81 Hz.
- The theoretical vertical component of the truck-induced wind gust pressure was found to be equal to **2.94 psf (141 Pa)**.

- The theoretical horizontal component of the truck-induced wind gust pressure was found to be equal to **7.06 psf (338 Pa)**.

Comparison between the Theoretical and Experimental Results

Fatigue Load due to Natural Wind Gust

- The loads determined experimentally and theoretically were closely matched, indicating that the VRS is an accurate approach in determining the fatigue load due to natural wind gust.
- Because of the close comparisons, the VRS is considered comprehensive. It was developed independent of the structural type.
- The close comparisons indicate that the dynamic behavior of these structures can be approximated by a single degree-of-freedom dynamic system because their behavior is predominately controlled by a single modal shape.
- The theoretical load was slightly larger than the experimental load. This was because of the wind velocity excitation model used in the theoretical approach to simulate the behavior of natural wind represented a larger sample size than the data samples used to develop the experimental fatigue load.

Fatigue Load due to Truck-Induced Wind Gust

- The vertical and horizontal loads determined experimentally and theoretically were closely matched, indicating that the SRS is an accurate approach in determining the fatigue load due to truck-induced wind gust.
- Because of the close comparisons, the SRS is considered comprehensive. It was developed independent of the structural type.
- The close comparisons indicate that the dynamic behavior of these structures can be approximated by a single degree-of-freedom dynamic system because their behavior is predominately controlled by a single modal shape.

Finite Element Analysis

- The finite element analysis (FEA) indicated that in the natural wind gust controls in the horizontal direction. The largest stresses at the base plate and chord-to-post support connections were produced by natural wind gust as compared to the horizontal component of the truck-induced wind gust.
- Normal stresses were highest near the chord-to-post support, whereas shear stresses were highest near the base plate. This was evident with both the natural wind gust and truck-induced wind gust scenarios.

Proposed Fatigue Provisions

- The drag coefficients, height coefficients, and importance factors specified in the *Supports Specifications* are applicable with the proposed design fatigue equations.
- The proposed general equations are applicable for structures with similar properties to the structure tested with this project and used in the development of the equations. The detailed equations are universal and comprehensive, applicable for any type of support structure.

Design Fatigue Equation due to Natural Wind Gust

General Equation The general fatigue design equation for natural wind gusts applicable for the bridge-type VMS support structures is shown as Eq. 17-1. It is to be applied horizontally to the exposed façade of the structure as seen on an elevation view. The load is applied as a uniformly distributed load over the exposed areas. It is recommended for bridge-type VMS support structures with the following dynamic characteristics:

- Modal frequencies in the direction of the natural wind loading equal to 2.81 Hz or higher, and
- Critical damping percentage 0.341% or higher.

Equation 17-1 is considered un-conservative for structures with natural frequencies and damping percentages less than the values specified. For higher values, the equation is considered conservative.

$$P_{NW} = 7C_d I_F \left(\frac{\bar{v}}{11} \right)^2 \quad [\text{Eq. 17-1}]$$

where

P_{NW} = design fatigue load due to natural wind gust, psf (Pa)

C_d = drag coefficient

I_F = importance factor

\bar{v} = annual mean three second wind velocity, mph (m/s)

Detailed Equation A systematic procedure for determining the design fatigue load due to natural wind based on the proposed detailed approach is presented. The procedure is applicable to cantilever-type sign support structures, and bridge-type VMS support structures, as well as other support structures in design.

Step 1: Annual Mean Wind Velocity

The annual mean wind velocity is acquired at the site where the support structure is located. The National Weather Service Offices near the site can be used to determine this value. It is recommended to use a value of 11 mph (5 m/s), however other values can be used based on meteorological data.

Step 2: Modal Analysis

A modal analysis to determine the dynamic characteristics of the support structure is performed. The earliest modal frequency of the modal shape in the direction of the natural wind loading as well as the critical damping percentage are required for this procedure. Finite element analysis software can be helpful with this step. If FEA is not available, the modal frequency and modal shape can be estimated using Eq. 15-2. The values listed in Table 17-1 can be used for conservative estimates. It is important to note that these estimates were based on the experimental data collected with cantilever sign and bridge VMS support structures.

Table 17-1. Conservative estimates of the natural frequency and critical damping percentages

Support Structure	Natural Frequency	Critical Damping Percentages
Cantilever-Type Sign Support Structure	1.0 Hz	1.5%
Bridge-Type VMS Support Structure	2.0 Hz	0.35%

Step 3: Vibration Response Spectrum

A VRS constant, P_{VRS} , is extracted from the spectrum as the ordinate value corresponding to the natural frequency and damping ratio selected in Step 2, and the annual mean wind velocity selected in Step 1. For instance, if using a damping ratio of 1.5% (recommended for cantilever-type sign support structures), the VRS in Figure 17-1 is applicable. If using a damping ratio of 0.35% (recommended for bridge-type VMS support structures), the VRS in Figure 17-2 would be applicable. The VRS in Figure 17-3 is provided for other damping ratios if necessary.

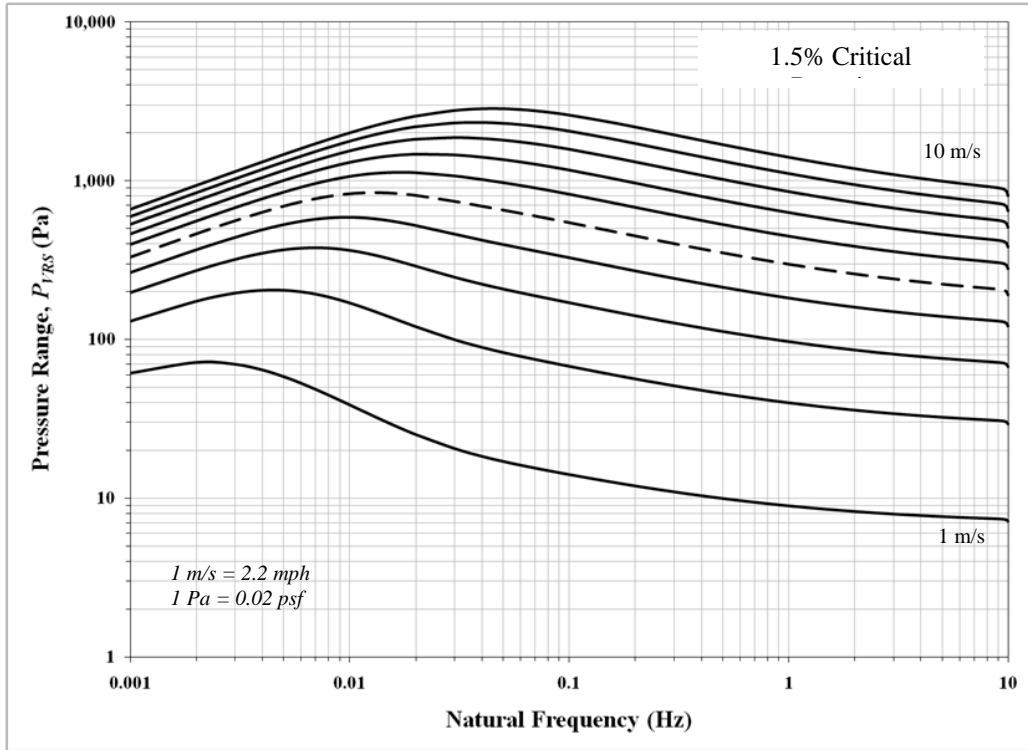


Figure 17-1. Fatigue load VRS for a critical damping percentage equal to 1.5%

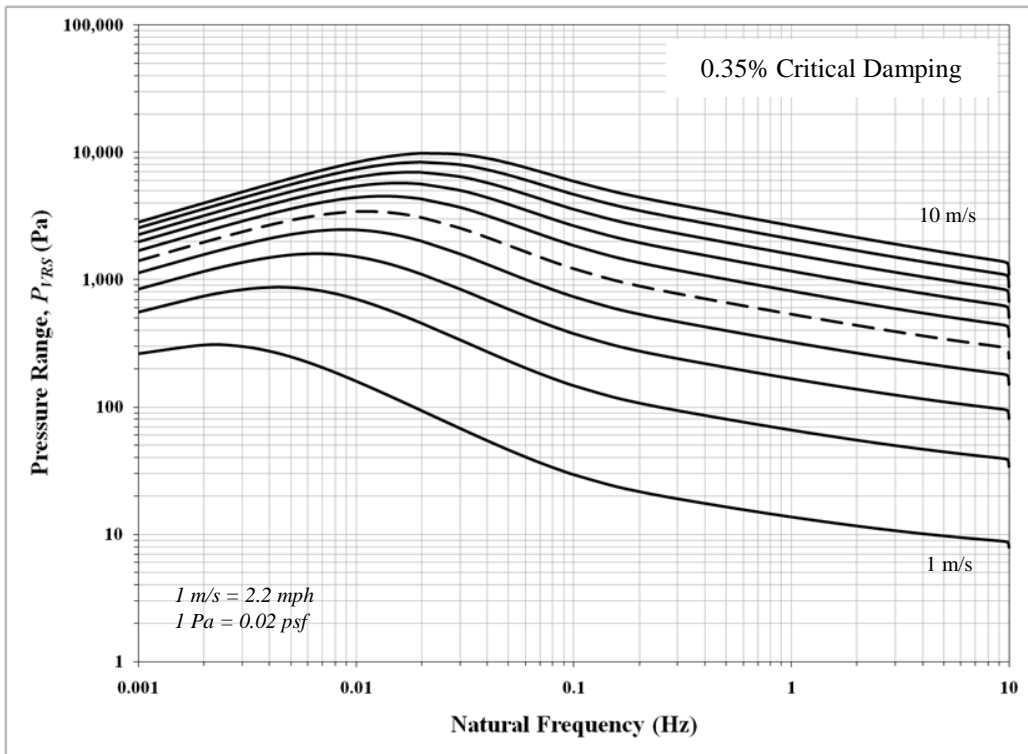


Figure 17-2. Fatigue load VRS for a critical damping percentage equal to 0.35%

Step 4: Fatigue Design Equation

Input the VRS constant, P_{VRS} , determined from Step 3 into Eq. 17-2 and apply as a uniformly distributed load for each member along the face of the structure that is exposed to natural wind.

$$P_{NW} = P_{VRS} C_d I_F \quad [\text{Eq. 17-2}]$$

where

P_{NW} = design fatigue load due to natural wind gust, psf (Pa)

P_{VRS} = transmitted pressure constant extracted from the VRS, psf (Pa)

C_d = drag coefficient

I_F = importance factor

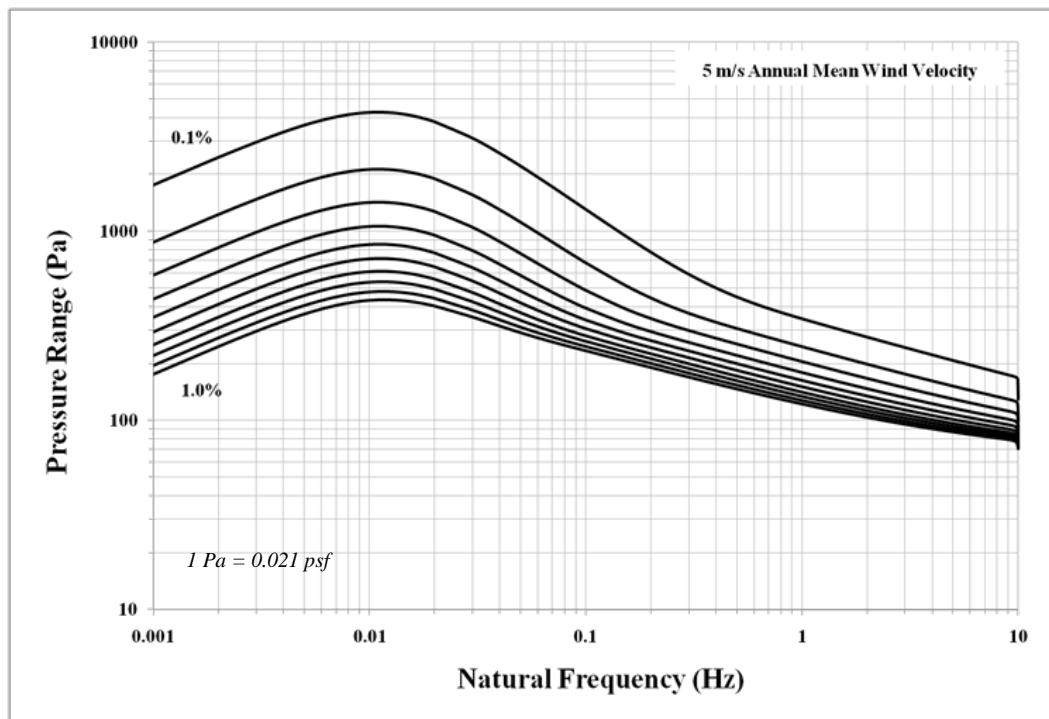


Figure 17-3. VRS plot of critical damping percentages ranging from 1.0% to 0.1%

Design Fatigue Load due to Truck-Induced Wind Gust

General Equation for the Vertical Component. The general fatigue design equation for the vertical component of the truck-induced wind gusts is shown as Eq. 17-3. It is to be applied vertically to the exposed underneath area of the structure onto a 12 ft (3.66 m) length portion (or width of the traffic lane, whichever is greater) located directly over the traffic lane. The load is applied as a uniformly distributed load. It is at maximum at a height of 19.7 ft (6.00 m) above the roadway, and decreases linearly to zero at a height of 32.8 ft (10 m). Equation 17-3 is

recommended for bridge-type VMS support structures; specifically for support structures with a modal frequency of 3.79 Hz for vertical modal shapes in-plane with the vertically applied load.

$$P_{TG} = 3C_d I_F \left(\frac{v}{70} \right)^2 \quad [\text{Eq. 17-3}]$$

where

P_{TG} = design fatigue load due to truck - induced wind gust, psf (Pa)

C_d = drag coefficient

I_F = importance factor

v = traveling speed of the truck, mph (m/s)

General Equation for the Horizontal Component. The general fatigue design equation for the horizontal component of the truck-induced wind gusts is shown as Eq. 17-4. It is to be applied horizontally to the exposed area on the front face of the structure onto a 12 ft (3.66 m) length portion (or width of the traffic lane, whichever is greater) located directly over the traffic lane. The load is applied as a triangularly distributed load. It is at maximum at a height of 19.7 ft (6.00 m) above the roadway, and decreases linearly to zero at a height of 32.8 ft (10 m). Equation 17-4 is recommended for bridge-type VMS support structures; specifically for support structures with a modal frequency of 2.81 Hz for horizontal modal shapes in-plane with the horizontally applied load.

$$P_{TG} = 6.1C_d I_F \left(\frac{v}{70} \right)^2 \quad [\text{Eq. 17-4}]$$

where

P_{TG} = design fatigue load due to truck - induced wind gust, psf (Pa)

C_d = drag coefficient

I_F = importance factor

v = traveling speed of the truck, mph (m/s)

Detailed Equation. A systematic procedure based on the proposed detailed approach for determining the vertically and horizontally applied fatigue design load due to truck-induced wind gusts may be given as follows.

Step 1: Design Speed of the Truck

The first step involves determining the design speed of the truck. A speed of 70 mph (31.3 m/s) is recommended however other speeds can be used if necessary.

Step 2: Modal Analysis

The second step involves a modal analysis of the support structure. The earliest modal frequency with a modal shape in the direction of the truck gust loading is needed. This would include modal shapes with vertical vibratory motion for the vertical component and the modal shapes with horizontal vibratory motion for the horizontal component. The damping ratio is not required for truck-induced gusts and therefore not considered in the methodology. Finite element analysis software can be helpful with this step in determining the necessary modal frequencies. If FEA is not available, the modal frequency and modal shape can be estimated using Eq. 15-6.

Step 3: Shock Response Spectrum

The third step involves the SRS shown in Figure 17-4 for the vertical component Figure 17-5 for the horizontal component. A SRS constant, P_{SRS} , is extracted from the spectrum as the ordinate value corresponding to the natural frequency determined Step 2.

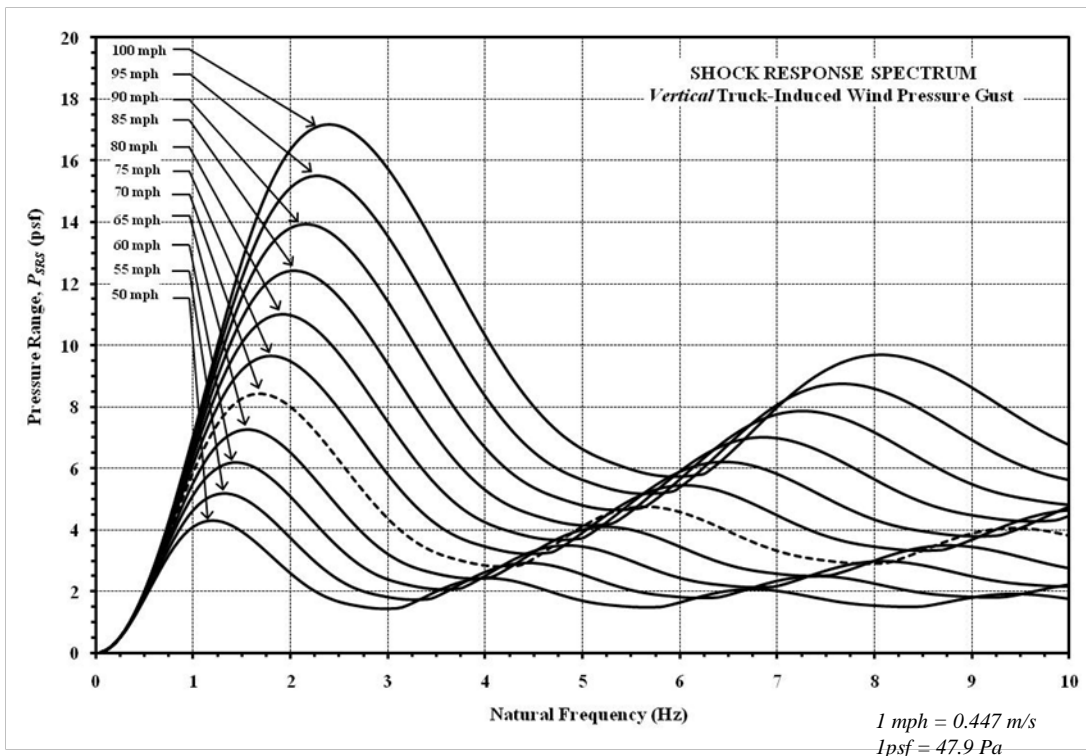


Figure 17-4. SRS for the vertical component of the truck-induced wind gust

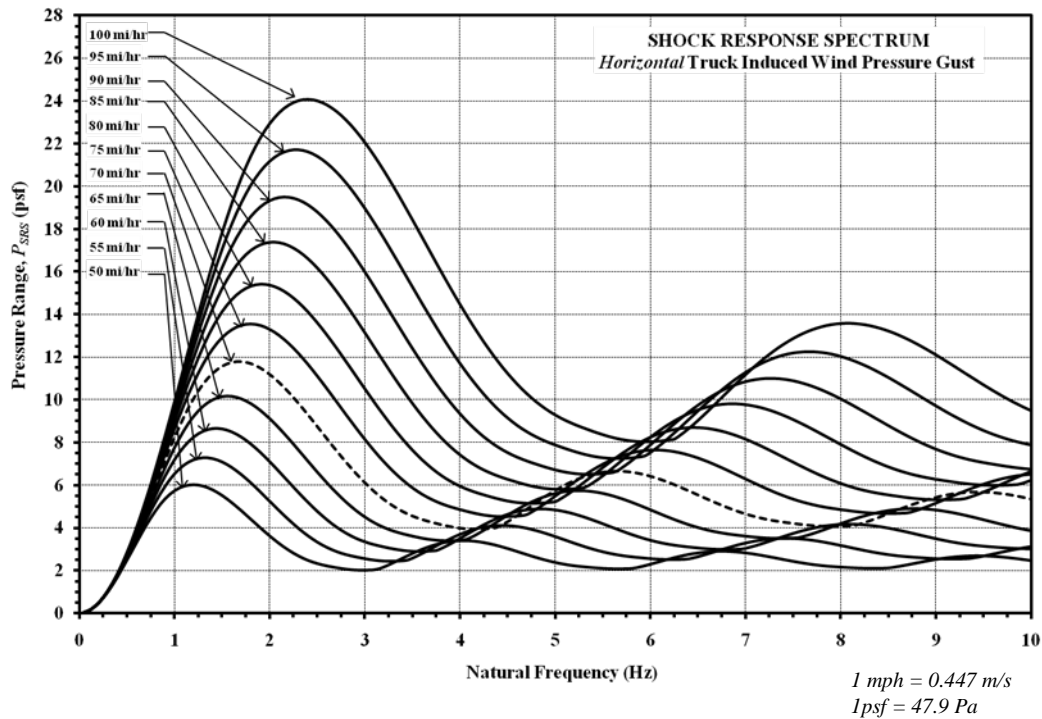


Figure 17-5. SRS for the horizontal component of the truck-induced wind gust

Step 4: Fatigue Design Equation

The next step is plugging all information gathered from Steps 1-3 into the fatigue design equation for truck-induced gusts based on the detailed approach. Input the SRS constant, P_{SRS} , determined from Step 3 into Eq. 17-5 for each member along the face of the structure exposed to truck-induced wind gusts. It is to be applied in the same fashion as the general design equation for truck-induced gusts for the horizontal and vertical components.

$$P_{TG} = P_{SRS} C_d I_F \quad [\text{Eq. 17-5}]$$

where

P_{TG} = design fatigue load due to truck - induced wind gust, psf (Pa)

P_{SRS} = transmitted pressure constant extracted from the SRS, psf (Pa)

C_d = drag coefficient

I_F = importance factor

Step 5: Height Accommodation

Accommodations for height can be made to the values determined from Eq. 17-5. In terms of the vertical component, this can be performed for structures with exposed areas higher than 19.7 ft

(6.00 m). The truck gust pressure is assumed maximum at a height of 19.7 ft (6.00 m) above the roadway, and decreases linearly to zero at a height of 32.8 ft (10 m) according to Eq. 17-6.

$$P_h = -0.0763h + P_{SRS} \quad [\text{Eq. 17-6}]$$

where

P_h = truck - induced wind pressure at specified height above ground level, psf (Pa)

h = elevation increase from 19.7 ft (6.00 m) above the roadway, ft (m)

P_{SRS} = transmitted pressure constant extracted from the SRS, psf (Pa)

Equation 17-6 applies to the triangular distributed loading of the horizontal component. The distributed load decreases from its maximum value to zero at a rate equal to 0.0763 psf/ft (1.113 Pa/m).

Design Fatigue Load Examples and Comparisons with the AASHTO Supports Specifications

Fatigue Load due to Natural Wind Gust

- Support structures with natural frequencies greater than 2.00 Hz are less vulnerable to fatigue loading. The higher the natural frequency of the structure, the less susceptible the structure becomes to wind induced fatigue loads.
- The fatigue load provisions of the *Supports Specifications* are not applicable to bridge-type VMS support structures, and significantly underestimates the fatigue load.

Fatigue Load due to Truck-Induced Wind Gust

- The fatigue load provisions of the *Supports Specifications* when compared to the developed equations for truck-induced gust were highly conservative.

Section 18

Future Investigations and Research

Overview

Future research initiatives are presented in this section. A large amount of data was collected with this project and therefore the recommendations and proposed research presented will utilize this data collection. This data represents the behavior of cantilever-type sign as well as bridge-type VMS support structures under wind induced loading. The objectives of this research was primarily to use the data to develop design fatigue loads for these structures and assess the accuracy of the new provisions and criteria on fatigue design in the AASHTO 2001 *Supports Specifications*, which differ considerably from those in previous editions. However, other investigations can be launched using the large data collection that was obtained with this research.

The following topics listed as follows represent proposed investigations and research to accomplish future objectives:

- Operational Modal Analysis of Highway Overhead Sign Support Structures,
- Fatigue Design of Bridge-Type Sign Support Structures,
- Fatigue Design of Anchor Bolt Connections of Highway Overhead Support Structures,
- Application of the Vibration Response Spectrum for Traffic Signals, Luminaires, and High Mast Support Structures, and
- Design of Highway Overhead Support Structures to Mitigate Fatigue Stresses.

Brief descriptions on each of the initiatives listed above are presented in the following sections.

Operational Modal Analysis of Highway Overhead Sign Support Structures

Highway overhead support structures are vulnerable to wind induced loading primarily because their modes of vibration are in proximity to the resonant frequencies of the wind induced loading. The majority of the fatigue damage is a direct result of dynamic vibration of these structures to the wind loading events. This makes the fatigue issue with these structures as structural dynamic problem. The research performed with this project on cantilever-type sign and bridge-type VMS support structures indicated that the structural dynamic behavior of these structures are primarily controlled by single modal shapes that are dependent on the wind loading scenario. It was proven that the structures can be approximated as single degree-of-freedom

systems, however these structures, as with all structures, are multiple degree-of-freedom systems.

The modal analysis on the support structural types performed with this project is well established. A study is needed to perform a complete modal analysis on the full range and types of highway overhead support structures in order to obtain a large database of information that can be used for fatigue design. The proposed study will focus on the operational modal characteristics of the structures including natural frequencies, modal shapes, and critical damping percentages. As indicated with the theoretical program of this project, the natural frequency of vibration and critical damping percentage as a large and significant influence on the wind induced fatigue load. Importantly, the natural frequency and modal shapes are properties that can be approximated through mathematical configurations. The critical damping percentage however is a value that can only be obtained through experimental data collection.

The results of the proposed project can be used to develop accurate dynamic models. The models will represent the structural dynamic characteristics for the many types of highway overhead support structures currently in design. Methodologies on calculating the natural frequency of vibration and determination of the modal shapes of support structures will be investigated. Natural frequency and critical damping percentage tables and matrix type design aids can be developed based on cantilever overhang lengths and bridge spans.

Fatigue Design of Bridge-Type Sign Support Structures

The highway overhead support structures investigated in this project involved the cantilever-type sign support structure and the bridge-type VMS support structure. The dynamic behavior of these structures was evaluated and fatigue loads were developed from the results. The bridge-type VMS support structure is very similar to the bridge-type sign support structure. The only difference is the additional mass of the VMS as compared to a typical aluminum sign. As proven with this research, the magnitude of the fatigue load is primarily based on the dynamic properties of the structure. The objective of the proposed research is to investigate the dynamic properties of these structures and develop fatigue loads specific to bridge-type sign support structures.

Fatigue Design of Anchor Bolt Connections of Highway Overhead Support Structures

The instrumentation of this research involved strain gauges placed on the anchor bolts of the cantilever-type sign support structure. A large amount of data was collected under various wind induced loading scenarios. High stresses were observed due to a combined bending moment and axial tension and compression action on the bolts. This information can be used to specifically investigate the fatigue performance of the anchor bolts. Fatigue life estimations can be made based on the configuration of the anchor bolt layout of the cantilever structure. This information, and the knowledge and understanding gained from the investigation, can be used to develop improved layouts and base plate design to better perform under the wind-induced fatigue loading events.

Application of the Vibration Response Spectrum for Traffic Signals, Luminaires, and High Mast Support Structures

The theoretical program developed with this research involved the determination of the fatigue load due to natural wind through the use of the vibration response spectrum (VRS). The fatigue load is extracted from the spectrum based on the natural frequency and critical damping percentage of the structure. It is applicable to any structure that can be approximated as a single degree-of-freedom system and is exposed to natural wind loading. The methodology is considered universal and comprehensive in that it can be applicable to the many different types of support structures with different configurations, sizes, shapes, and material properties. Application of the VRS to traffic signals, luminaires, and high mast would be beneficial to the design community. A universal approach can be used to ease design issues associated with fatigue due to natural wind loads. It can be applied to the many different types of traffic signals, luminaires, and high mast support structures.

Design of Highway Overhead Support Structures to Mitigate Fatigue Stresses

Fatigue loading on overhead highway sign support structures comes in many different varieties. Whether it is in the form of naturally occurring wind gusts or truck-induced wind gusts, fatigue loading can seriously damage support structures over time. Research projects have focused on determining and evaluating the accuracy of design fatigue loads, but little focus has been directed towards improving the design of these structures to be less vulnerable to this type of loading. Recent experimental projects have indicated that sign support structures are vulnerable to fatigue loading because their natural frequencies of vibration are near the wind gust frequencies of the loading environment. The structures operate in this environment in a continuous near resonant condition with very low critical damping percentages to impede the vibration. The goal of this project is to develop new innovative designs for sign support structures to mitigate stresses generated from wind-induced fatigue loads. This will be done through altering the arrangement and configuration of structural components to ultimately shift the structural dynamic behavior of the structure further away from potential resonant conditions associated with fatigue. Theoretical approaches involving FEA will be applied, and experimentally collected structural dynamic behavior collected from past experimental projects will be utilized for fatigue loading simulations. Optimization techniques including factorial analysis will be used to develop the new designs to function at their most efficient capability during fatigue exposure. The study will encompass bridge-type and cantilever-type structures supporting conventional aluminum signs and heavy variable message signs. The project will result in standardized and comprehensive designs of support structures that are not prone to fatigue induced wind loads.

The main objective of this study is to develop new innovative designs for highway overhead sign support structures to mitigate stresses generated from wind-induced fatigue loads. The designs will be developed using a theoretical approach involving extensive finite element analyses (FEA). Experimental data collected from the ALDOT and UAB Project # 930-683, Design of Overhead Sign Structures for Fatigue Loads, will be used to simulate the fatigue loading.

Optimization techniques will be applied to develop the new design to function at its most efficient capability during fatigue exposure. The completion of the project will result in standardized and comprehensive designs of support structures that are not prone to fatigue induced wind loads and that can ultimately be adopted by ALDOT.

In light of recent experimental fatigue studies on sign support structures performed with Project # 930-683, the primary factors that contributed to the fatigue damage were vibratory stresses generated from wind-induced loading. It was revealed that an extensive evaluation into the design of sign support structures that focuses on their structural dynamic behavior can mitigate these stresses. New fatigue based designs would improve the fatigue life of the structure and lesson overall maintenance costs. The project will result in comprehensive designs with increased resistance to fatigue loads, and would provide standard designs for ALDOT's review. The optimization techniques and factorial analyses performed with this study will produce the most effective design within measures of practicality and applicability. It is anticipated that these standard designs will result in significant cost savings and streamlining of construction operations for ALDOT.

Section 19

References

AASHTO, *Standard Specifications for Structural Supports for Highway Signs, Luminaires and Traffic Signals*, 5th Edition, American Association of State Highway and Transportation Officials, Washington, D.C., 288 pp., 2009.

AASHTO, *Standard Specifications for Structural Supports for Highway Signs, Luminaires and Traffic Signals*. Fourth Edition, American Association of State Highway and Transportation Officials, Washington, D.C., 270 pp., 2001.

AASHTO, *Standard Specifications for Structural Supports for Highway Signs, Luminaires and Traffic Signals*. Third Edition, American Association of State Highway and Transportation Officials, Washington, D.C., 78 pp., 1994.

AASHTO (American Association of State Highway and Transportation Officials). *Standard Specifications for Structural Supports for Highway Signs, Luminaires and Traffic Signals*. Washington, D.C. 69 pp., 1985.

AASHTO, *AASHTO LRFD Bridge Design Specifications*, Customary U.S. Units, 4th Edition with 2008 and 2009 U.S. Edition Interims, and *AASHTO LRFD Bridge Design Specifications, SI Units*, 4th Edition, American Association of State Highway and Transportation Officials, Washington, D.C., 2007.

AASHTO, *Standard Specifications for Transportation Materials and Methods of Sampling and Testing*, 29th Edition and AASHTO Provisional Standards, 2009 Edition, American Association of State Highway and Transportation Officials, Washington, D.C., 2009.

Agosta, A. M., Bloomquist, D., Cook, R. A., Taylor, K. F. *Wind Load Data for Variable Message Signs*. Report Number 0728-9488. Florida Department of Transportation, Research Management Center, April, 1996.

Albert, M.N., Manuel, L., Frank, K.H., and Wood, S.L., Field Testing of Cantilevered Traffic Signal Structures under Truck-Induced Gust Loads. Report No. FHWA/TX-08/0-4586-2, Center for Transportation Research, University of Texas at Austin, 2007.

Azzam, D.; Fatigue Behavior of Highway Welded Aluminum Light Pole Support Structures. Dissertation, University of Akron, May 2006.

- Cali, P., and Covert, E.E., On the Loads on Overhead Sign Structures in Still Air by Truck Induced Gusts. Wright Brothers Facility Report 8-97, Massachusetts Institute of Technology.
- Creamer, B. M., Frank, K. H., Klingner, R. E. *Fatigue Loading on Cantilever Sign Support Structures From Truck Wind Gusts*. Research Report Number 209-1F. Texas State Department of Highways and Public Transportation, Transportation Planning Division, April, 1979.
- CSI Analysis Reference Manual*. Computers and Structures, Inc., Berkeley, California, January, 2007.
- Cook, Ronald A., Bloomquist, D., Agosta, A.M., Taylor, K.F., Wind Load Data for Variable Message Signs. Report Number 0728-9488. Florida Department of Transportation, Research Management Center, April, 1996.
- Davenport, A. G. The Spectrum of Horizontal Gustiness Near the Ground in High Winds. *Quarterly Journal, Royal Meteorological Society*, Vol. 87, London 1961.
- Dexter, R. J., and Ricker, M. J. *Fatigue-Resistant Design of Cantilevered Signal, Signs, and Light Supports*. NCHRP Report 469, The Transportation Research Board, Washington, DC, 2002.
- Dexter, R. J., Johns, K. W. Development of Fatigue Design Load Ranges for Cantilevered Sign and Signal Support Structures, *Journal of Wind Engineering and Industrial Aerodynamics*, 77&78, 1998, pp. 315-326.
- DeSantis, P.V., and Haig, P.E., Unanticipated Loading Causes Highway Sign Failure. Proceedings of ANSYS Convention, 1996.
- Edwards, J.A., and Bingham, W.L. Deflection Criteria for Wind Induced Vibrations in Cantilever Highway Sign Structures. Report No. FHWA/NC/84-001, Center for Transportation Engineering Studies, North Carolina State University, 1984.
- Fackler, W.C., Pusey, H.C., Volin, R.H., Schell, E.H. *Equivalence Techniques for Vibration Testing*. The Shock and Vibration Information Center, Naval Research laboratory, Code 6020, Washington D.C., 1972.
- Fisher, J. W., Keating, P. B., Nussbaumer, A., Yen, B. T. *Resistance of Welded Details Under Variable Amplitude Long-Life Fatigue Loading*. NCHRP Report 354, Transportation Research Board, Washington D. C., 1993.
- Foutch, D. A., Kim, T. W., LaFave, J. M., Rice, J. A. *Evaluation of Aluminum Highway Sign Truss Designs and Standards for Wind and Truck Gust Loadings*. Research Report Number 153. Illinois Department of Transportation, Bureau of Materials and Physical Research, Physical, December, 2006.

Fouad, Fouad H.; and Calvert, Elizabeth A., New Wind Design Criteria for Traffic Signal Support Structures, *UTCA Report Number 04219*, University Transportation Center for Alabama, Tuscaloosa, AL (August 31, 2005) 49pp.,
http://utca.eng.ua.edu/projects/final_reports/04219fnl.pdf.

Fouad, Fouad H., and Calvert, Elizabeth. "Design of Cantilevered Overhead Sign Supports," *Transportation Research Record*, Issue No. 1928, Transportation Research Board, Washington, D.C., 2005.

Fouad, Fouad H.; and Calvert, Elizabeth A., AASHTO 2001 Design of Overhead Cantilevered Sign Supports, *UTCA Report Number 02216*, University Transportation Center for Alabama, Tuscaloosa, AL (March 30, 2004) 91 pp.,
http://utca.eng.ua.edu/projects/final_reports/02216fnl.pdf.

Fouad, Fouad H.; Calvert, Elizabeth; Davidson, James S.; and Delatte, Norbert. "Proposed Revisions to AASTHO 2001 Supports Specifications," *Compendium of Papers CD-ROM*, Transportation Research Board, 83rd Annual Meeting, Washington, DC, Jan. 11-15, 2004.

Fouad, Fouad H., and Calvert, Elizabeth. "Wind Load Provisions in the 2001 AASHTO Supports Specifications," *Transportation Research Record*, Issue No. 1845, Transportation Research Board, Washington, D.C., 2003.

Fouad, Fouad H.; Davidson, James S.; Delatte, Norbert; Calvert, Elizabeth A.; Chen, Shen-En; Nunez, Edgar; and Abdalla, Ramy, "Structural Supports for Highway Signs, Luminaires, and Traffic Signals." *NCHRP Report 494*, Transportation Research Board, Washington, D.C. (2003) 49 pp.

Fouad, Fouad H.; Davidson, James S.; Delatte, Norbert; Calvert, Elizabeth A.; Chen, Shen-En; Nunez, Edgar; and Abdalla, Ramy, *Structural Supports for Highway Signs, Luminaires, and Traffic Signals: Draft Final Report*, NCHRP Project 17-10(2), Prepared for National Cooperative Highway Research Program, Transportation Research Board, National Research Council, The University of Alabama at Birmingham, Birmingham, AL (May 2002) 116 pp.

Fouad, Fouad H. and Elizabeth Calvert. "Impact Of The New Wind Load Provisions On The Design Of Structural Supports," *Compendium of Papers CD-ROM*, Transportation Research Board, 82nd Annual Meeting, Washington, DC, Jan. 12-16, 2003.

Fouad, Fouad H. and Elizabeth Calvert. "Wind Load Provisions in the 2001 Supports Specifications," *Compendium of Papers CD-ROM*, Transportation Research Board, 82nd Annual Meeting, Jan. 12-16, 2003.

- Fouad, Fouad H.; and Calvert, Elizabeth A., Evaluating the Design Safety of Highway Structural Supports, *UTCA Report Number 00218*, University Transportation Center for Alabama, Tuscaloosa, AL (August 2001) 65 pp., http://utca.eng.ua.edu/projects/final_reports/00218report.htm.
- Fouad, Fouad H.; Nunez, Edgar; and Calvert, Elizabeth A. “Proposed Revisions to AASHTO Standard Specifications for Structural Supports for Highway Signs, Luminaires, and Traffic Signals,” *Transportation Research Record*, Issue No. 1656, Transportation Research Board, Washington, D.C., 1999.
- Fouad, Fouad H.; Mehta, Kishor C.; and Calvert, Elizabeth A., *Wind Loads Report: Final Draft*. NCHRP Project 17-10(2), Prepared for National Cooperative Highway Research Program, Transportation Research Board, National Research Council, The University of Alabama at Birmingham, Birmingham, AL (Sept. 1999) 168 pp.
- Fouad, Fouad H.; Calvert, Elizabeth A.; and Nunez, Edgar, “Structural Supports for Highway Signs, Luminaires and Traffic Signals.” *NCHRP Report 411*, Transportation Research Board, Washington, D.C. (1998) 114 pp.
- Fouad, Fouad H.; Calvert, Elizabeth A.; and Nunez, Edgar, *Structural Supports for Highway Signs, Luminaires, and Traffic Signals: Draft Final Report*. NCHRP Project No. 17-10, Department of Civil and Environmental Engineering, The University of Alabama at Birmingham, Birmingham, Alabama (Sept. 1997) 254 pp.
- Fouad, Fouad H.; Calvert, Elizabeth A.; and Nunez, Edgar, *Structural Supports for Highway Signs, Luminaires, and Traffic Signals: Draft Final Specification*. NCHRP Project No. 17-10, Department of Civil and Environmental Engineering, The University of Alabama at Birmingham, Birmingham, Alabama (Sept. 1997) 252 pp.
- Gilani, A., and Whittaker, A., “Fatigue-Life Evaluation of Steel Post Structures I: Background and Analysis.” *Journal of Structural Engineering*, ASCE, New York, NY (2000).
- Ginal, S. Fatigue Performance of Full-Span Sign Support Structures Considering Truck-Induced Gust and Natural Wind Pressures. Thesis, Marquette University, December, 2003.
- Gray, B.D., Fatigue Effects on Traffic Signal Structures. Thesis, University of Wyoming, December, 1999.
- Harris, C. M. *Shock and Vibration Handbook*, 4th Ed. McGraw-Hill Companies, Inc., 1996.
- Irvine, T. An Introduction to Random Vibration. Vibration Data Publications, October 26, 2000. www.vibrationdata.com.

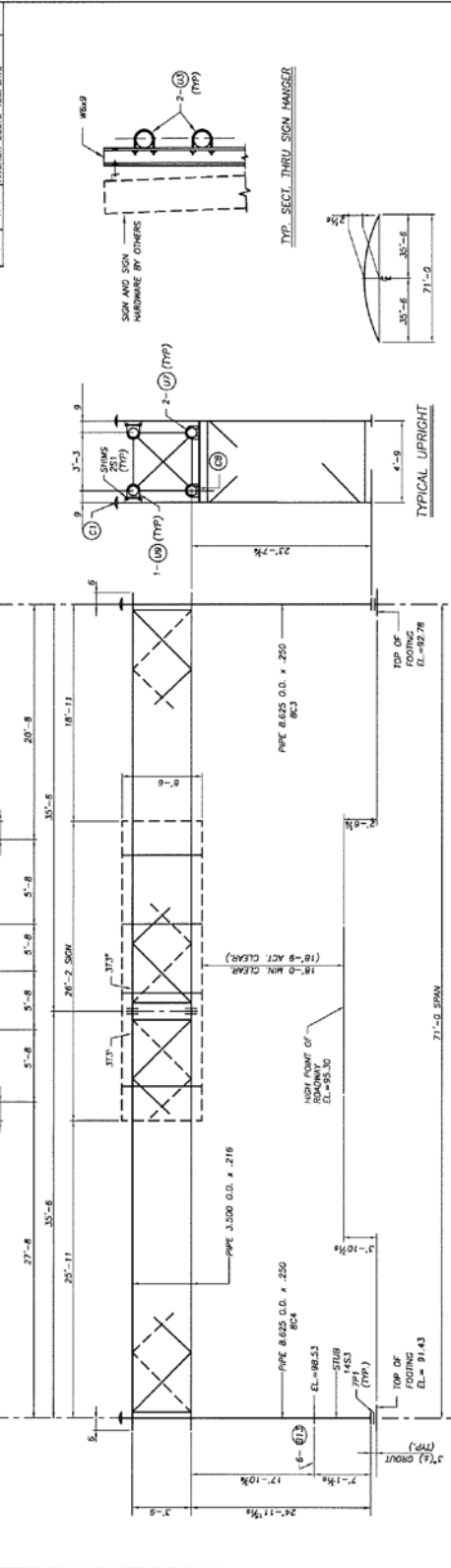
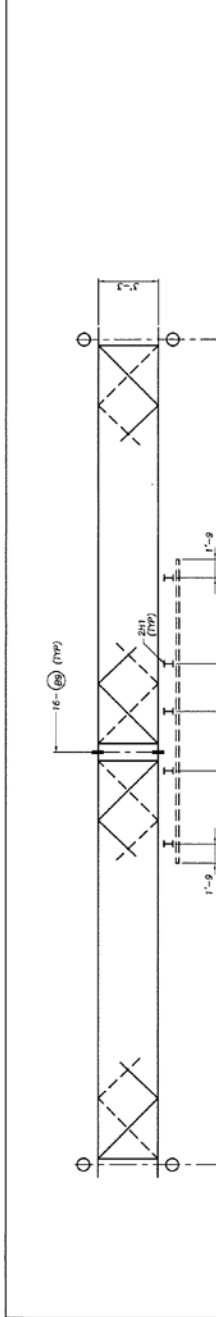
- Irvine, T. An Introduction to the Vibration Response Spectrum. Vibration Data Publications, June 14, 2000. www.vibrationdata.com.
- Irvine, T. An Introduction to Spectral Functions. Vibration Data Publications, March 3, 2000. www.vibrationdata.com.
- Irvine, T. P95/50 Rule—Theory and Applications. Vibration Data Publications, June 20, 1996. www.vibrationdata.com.
- Irvine, T. Methods for Converting a Power Spectral Density to a Shock Response Spectrum. Vibration Data Publications, November 16, 2007. www.vibrationdata.com.
- Irvine, T. Sine Function Identification and Removal. Vibration Data Publications, August 14, 2000. www.vibrationdata.com.
- Irvine, T. Enveloping Data Via the Vibration Response Spectrum. Vibration Data Publications, October 11, 1999. www.vibrationdata.com.
- Irvine, T. An Introduction to the Shock Response Spectrum. Vibration Data Publications, May 24, 2002. www.vibrationdata.com.
- Irvine, T. Equivalent Static Loads for Random Vibration. Vibration Data Publications, March 13, 2008. www.vibrationdata.com.
- Irvine, T. Random Vibration Fatigue. Vibration Data Publications, August 29, 2003. www.vibrationdata.com.
- Irvine, T. Bending Frequencies of Beams, Rods, and Pipes, Revision K, June 24, 2004. www.vibrationdata.com.
- Irwin, H.P., and Peeters, M. An Investigation of the Aerodynamic Stability of Slender Sign Bridges, Calgary. LTR-LA-246, national Research Council Canada-Aeronautical Establishment, 1980.
- James, M.L., Smith, G.M., Wolford, J.C., Whaley, P.W., *Vibration of Mechanical and Structural Systems: With Microcomputer Applications*. Harper & Row, Publishers, Inc., 1989.
- Kaczinski, M. R., Dexter, R. J., and Van Dien, J. P. *Fatigue Resistant Design of Cantilevered Sign, Signal and Light Supports*, NCHRP Report 412, Transportation Research Board, Washington, D.C., 1998.

- Kashar, L., Nester, M.R., Johns, J.W., Hariri, M., and Freizner, S., Analysis of the Catastrophic Failure of the Support Structure of a Changeable Message Sign. Structural Engineering in the 21st Century, Proceedings of the 1999 Structures Congress, New Orleans, LA, 1115-118, 1999.
- Liu, H. *Wind Engineering: A Handbook for Structural Engineers*. Prentice-Hall, Inc., 1991.
- McDonald, J.R., Mehta, K.C., Oler, W., and Pulipaka, N., Wind Load Effects on Signs, Luminaires and Traffic Signal Structures. Texas Department of Transportation Report No. 1303-1F, Wind Engineering Research Center-Texas Tech University, Lubbock, TX, 1995.
- McLean, W.T., Park, J.S., Stallings, J.M., Fatigue Evaluation of Two Variable Message Sign Structures, Research Report No. 930-431, Alabama Department of Transportation, July 2004.
- Paz, M. *Structural Dynamics: Theory and Computation*, 4th Ed. Chapman & Hall, 1997.
- Scanlan, R. H., Simiu, E. *Wind Effects on Structures: An Introduction to Wind Engineering*. John Wiley & Sons, Inc., 1978.
- Sheskin, D. J. *Handbook of Parametric and Nonparametric Statistical Procedures*, 4th Ed. Taylor & Francis Group, LLC, 2007.
- South, S. M. *Fatigue Analysis of Overhead Sign and Signal Structures*. Report Number 115. Illinois Department of Transportation, Bureau of Materials and Physical Research, Physical, May, 1994.
- Ramy, A.S., Fatigue Resistant Design of Non-Cantilevered Sign Support Structures. Thesis, University of Alabama at Birmingham, 2000.
- Rao, S.S. *Mechanical Vibrations*, 3rd Ed. Addison-Wesley Publishing Company, Inc., 1995.
- Walpole, R.E., Myers, R.H., Myers, S.L., Ye, K., *Probability & Statistics for Engineers & Scientists*, 7th Ed. Prentice Hall, Inc., 2002.
- Yang, C. Y. *Random Vibration of Structures*. John Wiley & Sons, Inc., 1986.
- Zalewski, B., Huckelbridge, A., Dynamic Load Environment of Bridge-Mounted Sign Support Structures. Report No. ST/SS/05-002. Ohio Department of Transportation, Office of Research and Development, September 2005.

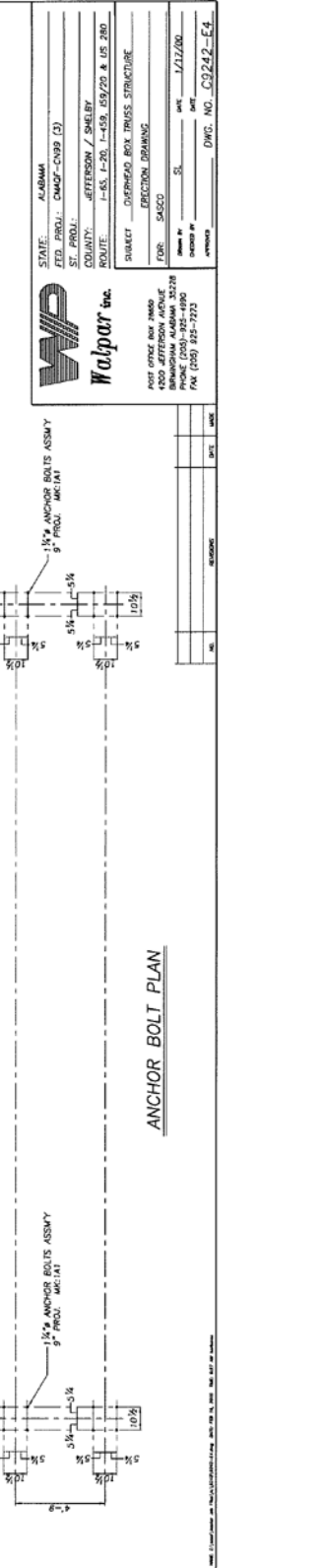
Appendix A

Shop Drawings of the Tested Bridge-Type VMS Support Structure

QTY.	MARK	DESCRIPTION
1	8C4	UPRIGHT
1	8C3	UPRIGHT
2	313X	SHIMS
4	1A1	ANCHOR BOLTS ASSY
5	2H1	SIGN HANGERS
4	313	PIPE 8.625 O.D. x .250
4	313	PIPE 3.500 O.D. x .216
20	6	1/4" ANCHOR BOLTS ASSY
8	10	1/2" ANCHOR BOLTS ASSY
16	8	1/2" ANCHOR BOLTS ASSY
12	10	1/2" ANCHOR BOLTS ASSY
4	251	SHIMS
4	741	UPRIGHT SIGN TEMPLATE



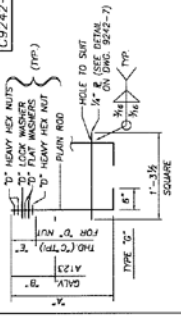
ELEVATION
 STR. NO. DMS-N237
 MILE POST: 133
 (LOOKING IN DIRECTION OF TRAFFIC)
 NOTE: STRUCTURES SHALL NOT BE ERECTED WITHOUT SIGNS AND/OR A SUITABLE REVISION CAMBER.



STATE: ALABAMA
 FED. PROJ.: DAMP-CV93 (2)
 ST. PROJ.:
 COUNTY: JEFFERSON / SHELBY
 ROUTE: I-65, I-20, I-69, 59/20 & US 280
 SUBJECT: OVERHEAD BOX TRUSS STRUCTURE
 DRAWN BY: SAECO
 CHECKED BY: SAECO
 DATE: 1/17/20
 DWG. NO. C9242-E4

Wolpar Inc.
 1000 10th Ave. NE
 Birmingham, AL 35208
 PHONE: (205) 992-4990
 FAX: (205) 992-7212

C9242-1



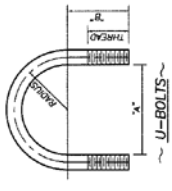
ANCHOR BOLTS ASSYS ~

NOTE: (225) INGVAL A.B. ROD (INCLUDES 1 TEST SAMPLE)
 (225) SPEC. CHAMP V-NOTCH TESTING 15FT LBS.
 @ 40°F REDD.

MARK QTY	1"	1 1/4"	1 1/2"	2"	2 1/2"	3"	REMARKS
1A1	58	4	3	7	1 1/4	10	10"

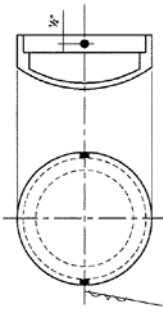
NOTE: (225) INGVAL A.B. ROD (INCLUDES 1 TEST SAMPLE)
 (225) SPEC. CHAMP V-NOTCH TESTING 15FT LBS.
 @ 40°F REDD.

ALUM 356-F	1	
ALUM 356-F	1	



U-BOLTS ~

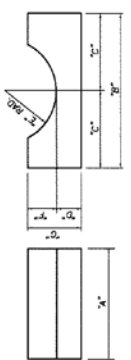
MARK QTY	DIA.	1"	1 1/4"	1 1/2"	2"	2 1/2"	3"	RADIUS	THD	MATERIAL	ADV	RELL
U3	1/2	3/8	3/4	2 1/4	2					A307	3 1/2	1 1/4
U4	1/2	3/8	3/4	2 1/4	2					6061	3 1/2	1 1/4
U5	1/2	3/8	3/4	2 1/4	2					6061	3 1/2	1 1/4
U7	3/2	3/8	3/4	2 1/4	2					A307	3 1/2	1 1/4
U8	1 1/2	3/8	3/4	2 1/4	2					A307	3 1/2	1 1/4
U10	1 1/2	3/8	3/4	2 1/4	2					A307	3 1/2	1 1/4
U11	1 1/2	3/8	3/4	2 1/4	2					6061	3 1/2	1 1/4
U12	1 1/2	3/8	3/4	2 1/4	2					6061	3 1/2	1 1/4
U13	1 1/2	3/8	3/4	2 1/4	2					6061	3 1/2	1 1/4



POLE CAPS ~
 (ALUM 356-F)

DRILL & TAP FOR
 2 - 1/2 SET SCREWS
 @ 180° APART

PART NO	REMARKS	QTY	ADV	RELL
00388	6% O.D. PIPE	58	1/2	



SADDLE SHIM DETAIL ~
 (ALUM 356-F)

PART NO	1"	1 1/4"	1 1/2"	2"	2 1/2"	3"	REMARKS	QTY	ADV	RELL
00390	4	2	1/2	1 1/2	1 1/2	1 1/2	1 1/2 O.D. 30	12	1/2	
00391	6	3	1 1/4	1 1/2	1 1/2	1 1/2	1 1/2 O.D. 18	12	1/2	
00392	6	3	1 1/4	1 1/2	1 1/2	1 1/2	1 1/2 O.D. 18	12	1/2	
00393	6	3	1 1/4	1 1/2	1 1/2	1 1/2	1 1/2 O.D. 18	12	1/2	

REF DIMS: E1-E14
 MTL. SPECS. AS NOTED
 WELD SPECS. AWS D1.1-1982 & AWS D1.1-1982



Wolpar Inc.
 POST OFFICE BOX 21860
 HOUSTON, TEXAS 77228
 PHONE (281) 995-1900
 FAX (281) 995-7273

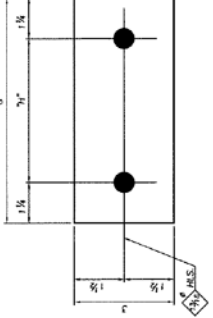
STATE: ALABAMA
 FED. PROJ.: CMGR-CM89 (3)
 ST. PROJ.:
 COUNTY: JEFFERSON/SHELBY
 ROUTE: 1-631-201-631-597/29 & US 289

SUBJECT: SIGN STRUCTURES
 MISC. DETAILS

FOR: SACCO
 DRAWN BY: MIF
 CHECKED BY:
 DATE: 1/18/90
 DWG. NO.: C9242-1

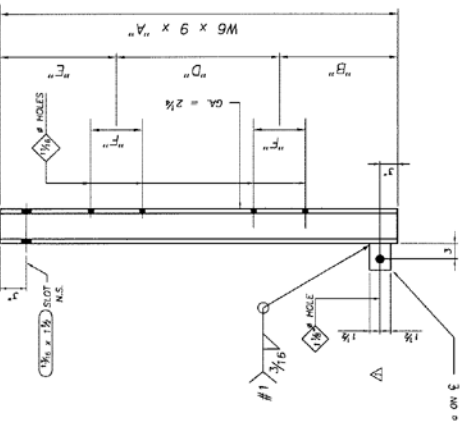
C9242-2

MARK	QTY	DESCRIPTION OF MATERIAL	UNIT	DATE	BY
ZH1	20	W	W	5	
ZH2	40	6 x 9		5	
ZH3	5			5	
ZH4	5			5	
ZH5	5			5	
ZH6	5			5	
ZH7	5			5	
ZH8	5			5	
ZH9	5			5	
ZH10	5			5	
ZH11	5			5	
ZH12	5			5	
ZH13	5			5	
ZH14	5			5	
ZH15	5			5	
ZH16	5			5	
ZH17	5			5	
ZH18	5			5	
ZH19	5			5	
ZH20	5			5	
ZH21	5			5	
ZH22	5			5	
ZH23	5			5	
ZH24	5			5	
ZH25	5			5	
ZH26	5			5	
ZH27	5			5	
ZH28	5			5	
ZH29	5			5	
ZH30	5			5	
ZH31	5			5	
ZH32	5			5	
ZH33	5			5	
ZH34	5			5	
ZH35	5			5	
ZH36	5			5	
ZH37	5			5	
ZH38	5			5	
ZH39	5			5	
ZH40	5			5	
ZH41	5			5	
ZH42	5			5	
ZH43	5			5	
ZH44	5			5	
ZH45	5			5	
ZH46	5			5	
ZH47	5			5	
ZH48	5			5	
ZH49	5			5	
ZH50	5			5	
ZH51	5			5	
ZH52	5			5	
ZH53	5			5	
ZH54	5			5	
ZH55	5			5	
ZH56	5			5	
ZH57	5			5	
ZH58	5			5	
ZH59	5			5	
ZH60	5			5	
ZH61	5			5	
ZH62	5			5	
ZH63	5			5	
ZH64	5			5	
ZH65	5			5	
ZH66	5			5	
ZH67	5			5	
ZH68	5			5	
ZH69	5			5	
ZH70	5			5	
ZH71	5			5	
ZH72	5			5	
ZH73	5			5	
ZH74	5			5	
ZH75	5			5	
ZH76	5			5	
ZH77	5			5	
ZH78	5			5	
ZH79	5			5	
ZH80	5			5	
ZH81	5			5	
ZH82	5			5	
ZH83	5			5	
ZH84	5			5	
ZH85	5			5	
ZH86	5			5	
ZH87	5			5	
ZH88	5			5	
ZH89	5			5	
ZH90	5			5	
ZH91	5			5	
ZH92	5			5	
ZH93	5			5	
ZH94	5			5	
ZH95	5			5	
ZH96	5			5	
ZH97	5			5	
ZH98	5			5	
ZH99	5			5	
ZH100	5			5	



SHIM PLATES

MARK	QTY	SIZE	THICKNESS
ZS1	16	6x6	1/4"
ZS2	32	7x4	5/16"
ZS3	8	8 1/2 x 6	6/16"



SIGN HANGER

MARK	QTY	SIZE	LENGTH	THICKNESS
ZH1	20	8'-6"	3'-9"	4/8"
ZH2	40	8'-6"	3'-9"	5/8"
ZH3	5	8'-6"	4'-0"	6/16"
ZH4	5	8'-6"	5'-0"	6/16"

MATERIAL SPECS.
 ALL MAT'L - ASTM A15
 ONLY AFTER FAB PER ASTM A123
 HANGERS PER ASTM D11 - 1980 & A510 1981
 HOLES SHALL BE 1/16"

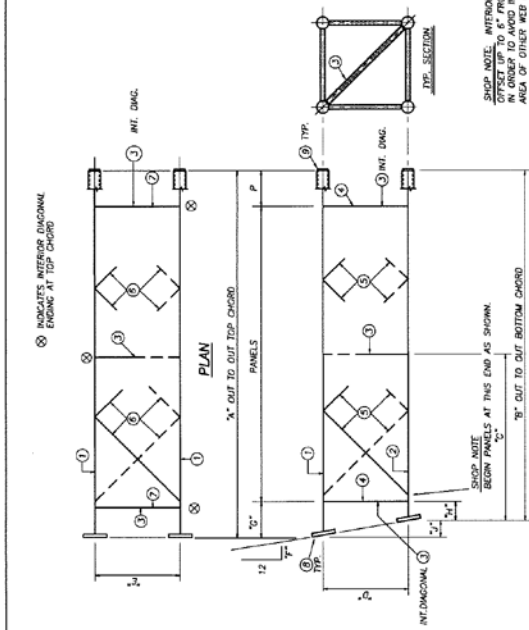


POST OFFICE BOX 3900
 100 JEFFERSON AVENUE
 MOBILE, ALABAMA 36688
 PHONE (305) 925-4000
 FAX (305) 925-7273

STATE: ALABAMA
 FED. PROJ.: CMDF-CN99 (3)
 ST. PROJ.: JEFFERSON/SHELBY
 COUNTY: JEFFERSON/SHELBY
 ROUTE: I-65-201-491-5979 & US 289

SUBJECT: SIGN STRUCTURE
 DETAIL OF SIGN HANGERS & SHIMS

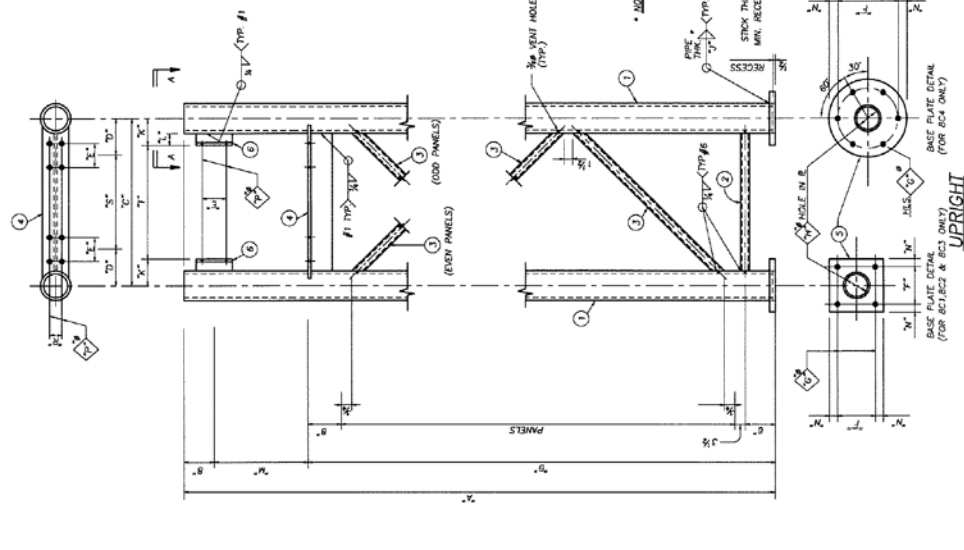
DATE: 1/13/00
 DRAWN BY: JEP
 CHECKED BY: JEP
 DWG. NO.: C9242-2



C9242-8

MARK	QTY	DESCRIPTION OF MATERIAL	UNIT	AMOUNT
8C1	2	PIPE 8.625 x 250	UPRIGHT	26.0%
8C2	1	PIPE 1.900 x 145		4.0%
8C3	1	PIPE 1.900 x 145		4.0%
8C4	1	PIPE 1.900 x 145		4.0%
8C5	1	PIPE 1.900 x 145		4.0%
8C6	1	PIPE 1.900 x 145		4.0%
8C7	1	PIPE 1.900 x 145		4.0%
8C8	1	PIPE 1.900 x 145		4.0%
8C9	1	PIPE 1.900 x 145		4.0%
8C10	1	PIPE 1.900 x 145		4.0%
8C11	1	PIPE 1.900 x 145		4.0%
8C12	1	PIPE 1.900 x 145		4.0%
8C13	1	PIPE 1.900 x 145		4.0%
8C14	1	PIPE 1.900 x 145		4.0%
8C15	1	PIPE 1.900 x 145		4.0%
8C16	1	PIPE 1.900 x 145		4.0%
8C17	1	PIPE 1.900 x 145		4.0%
8C18	1	PIPE 1.900 x 145		4.0%
8C19	1	PIPE 1.900 x 145		4.0%
8C20	1	PIPE 1.900 x 145		4.0%
8C21	1	PIPE 1.900 x 145		4.0%
8C22	1	PIPE 1.900 x 145		4.0%
8C23	1	PIPE 1.900 x 145		4.0%
8C24	1	PIPE 1.900 x 145		4.0%
8C25	1	PIPE 1.900 x 145		4.0%
8C26	1	PIPE 1.900 x 145		4.0%
8C27	1	PIPE 1.900 x 145		4.0%
8C28	1	PIPE 1.900 x 145		4.0%
8C29	1	PIPE 1.900 x 145		4.0%
8C30	1	PIPE 1.900 x 145		4.0%
8C31	1	PIPE 1.900 x 145		4.0%
8C32	1	PIPE 1.900 x 145		4.0%
8C33	1	PIPE 1.900 x 145		4.0%
8C34	1	PIPE 1.900 x 145		4.0%
8C35	1	PIPE 1.900 x 145		4.0%
8C36	1	PIPE 1.900 x 145		4.0%
8C37	1	PIPE 1.900 x 145		4.0%
8C38	1	PIPE 1.900 x 145		4.0%
8C39	1	PIPE 1.900 x 145		4.0%
8C40	1	PIPE 1.900 x 145		4.0%
8C41	1	PIPE 1.900 x 145		4.0%
8C42	1	PIPE 1.900 x 145		4.0%
8C43	1	PIPE 1.900 x 145		4.0%
8C44	1	PIPE 1.900 x 145		4.0%
8C45	1	PIPE 1.900 x 145		4.0%
8C46	1	PIPE 1.900 x 145		4.0%
8C47	1	PIPE 1.900 x 145		4.0%
8C48	1	PIPE 1.900 x 145		4.0%
8C49	1	PIPE 1.900 x 145		4.0%
8C50	1	PIPE 1.900 x 145		4.0%
8C51	1	PIPE 1.900 x 145		4.0%
8C52	1	PIPE 1.900 x 145		4.0%
8C53	1	PIPE 1.900 x 145		4.0%
8C54	1	PIPE 1.900 x 145		4.0%
8C55	1	PIPE 1.900 x 145		4.0%
8C56	1	PIPE 1.900 x 145		4.0%
8C57	1	PIPE 1.900 x 145		4.0%
8C58	1	PIPE 1.900 x 145		4.0%
8C59	1	PIPE 1.900 x 145		4.0%
8C60	1	PIPE 1.900 x 145		4.0%
8C61	1	PIPE 1.900 x 145		4.0%
8C62	1	PIPE 1.900 x 145		4.0%
8C63	1	PIPE 1.900 x 145		4.0%
8C64	1	PIPE 1.900 x 145		4.0%
8C65	1	PIPE 1.900 x 145		4.0%
8C66	1	PIPE 1.900 x 145		4.0%
8C67	1	PIPE 1.900 x 145		4.0%
8C68	1	PIPE 1.900 x 145		4.0%
8C69	1	PIPE 1.900 x 145		4.0%
8C70	1	PIPE 1.900 x 145		4.0%
8C71	1	PIPE 1.900 x 145		4.0%
8C72	1	PIPE 1.900 x 145		4.0%
8C73	1	PIPE 1.900 x 145		4.0%
8C74	1	PIPE 1.900 x 145		4.0%
8C75	1	PIPE 1.900 x 145		4.0%
8C76	1	PIPE 1.900 x 145		4.0%
8C77	1	PIPE 1.900 x 145		4.0%
8C78	1	PIPE 1.900 x 145		4.0%
8C79	1	PIPE 1.900 x 145		4.0%
8C80	1	PIPE 1.900 x 145		4.0%
8C81	1	PIPE 1.900 x 145		4.0%
8C82	1	PIPE 1.900 x 145		4.0%
8C83	1	PIPE 1.900 x 145		4.0%
8C84	1	PIPE 1.900 x 145		4.0%
8C85	1	PIPE 1.900 x 145		4.0%
8C86	1	PIPE 1.900 x 145		4.0%
8C87	1	PIPE 1.900 x 145		4.0%
8C88	1	PIPE 1.900 x 145		4.0%
8C89	1	PIPE 1.900 x 145		4.0%
8C90	1	PIPE 1.900 x 145		4.0%
8C91	1	PIPE 1.900 x 145		4.0%
8C92	1	PIPE 1.900 x 145		4.0%
8C93	1	PIPE 1.900 x 145		4.0%
8C94	1	PIPE 1.900 x 145		4.0%
8C95	1	PIPE 1.900 x 145		4.0%
8C96	1	PIPE 1.900 x 145		4.0%
8C97	1	PIPE 1.900 x 145		4.0%
8C98	1	PIPE 1.900 x 145		4.0%
8C99	1	PIPE 1.900 x 145		4.0%
8C100	1	PIPE 1.900 x 145		4.0%

MARK	QTY	W"	H"	T"	C"	PANELS	U"	V"	W"	H"	T"	C"	U"	V"
8C1	1	28'-0 3/4"	22'-1 1/2"	4'-9"	5 @ 4'-1 1/2" (-) = 20'-8"	9	4 1/2"	10 1/2"	1 1/2"					
8C2	1	28'-0 3/4"	21'-6"	4'-9"	5 @ 4'-0 3/4" (-) = 20'-0 3/4"	9	4 1/2"	10 1/2"	1 1/2"					
8C3	1	28'-0 3/4"	21'-5 1/2"	4'-9"	5 @ 4'-1 1/4" (-) = 22'-0"	9	4 1/2"	10 1/2"	1 1/2"					
8C4	1	22'-3 3/4"	17'-8 3/4"	4'-9"	4 @ 4'-2 3/4" (-) = 16'-3"	9	4 1/2"	11 1/2"	1 1/2"					



STATE: ALABAMA
 FED. PROJ.: CMOP-C099 (3)
 COUNTY: JEFFERSON / SHELBY
 ROUTE: 1-65, 1-26, 1-452, 89/20 & US 285
 SUBJECT: OVERHEAD SIGN SUPPORT

FOR: SAKCO
 DRAWN BY: MRF
 DATE: 1/17/00
 DWG. NO.: C9242-8

POST OFFICE BOX 3800
 BRUNNICH ALABAMA 35208
 PHONE (205) 925-4990
 FAX (205) 925-7173

CS242-14

MARK	QTY	SIZE	DESCRIPTION OF MATERIAL	UNIT	PRICE	TOTAL
1451	1	2"	UPRIGHT STUB	6.2%		
1452	2	PIPE 8.625 X .250	UPRIGHT STUB	6.2%		
1453	1	2"	UPRIGHT STUB	6.2%		
1454	1	PIPE 8.625 X .250	UPRIGHT STUB	6.2%		
1455	1	2"	UPRIGHT STUB	6.2%		
1456	1	PIPE 8.625 X .250	UPRIGHT STUB	6.2%		
1457	1	2"	UPRIGHT STUB	6.2%		
1458	1	PIPE 8.625 X .250	UPRIGHT STUB	6.2%		
1459	1	2"	UPRIGHT STUB	6.2%		
1460	1	PIPE 8.625 X .250	UPRIGHT STUB	6.2%		
1461	1	2"	UPRIGHT STUB	6.2%		
1462	1	PIPE 8.625 X .250	UPRIGHT STUB	6.2%		
1463	1	2"	UPRIGHT STUB	6.2%		
1464	1	PIPE 8.625 X .250	UPRIGHT STUB	6.2%		
1465	1	2"	UPRIGHT STUB	6.2%		
1466	1	PIPE 8.625 X .250	UPRIGHT STUB	6.2%		
1467	1	2"	UPRIGHT STUB	6.2%		
1468	1	PIPE 8.625 X .250	UPRIGHT STUB	6.2%		
1469	1	2"	UPRIGHT STUB	6.2%		
1470	1	PIPE 8.625 X .250	UPRIGHT STUB	6.2%		
1471	1	2"	UPRIGHT STUB	6.2%		
1472	1	PIPE 8.625 X .250	UPRIGHT STUB	6.2%		
1473	1	2"	UPRIGHT STUB	6.2%		
1474	1	PIPE 8.625 X .250	UPRIGHT STUB	6.2%		
1475	1	2"	UPRIGHT STUB	6.2%		
1476	1	PIPE 8.625 X .250	UPRIGHT STUB	6.2%		
1477	1	2"	UPRIGHT STUB	6.2%		
1478	1	PIPE 8.625 X .250	UPRIGHT STUB	6.2%		
1479	1	2"	UPRIGHT STUB	6.2%		
1480	1	PIPE 8.625 X .250	UPRIGHT STUB	6.2%		
1481	1	2"	UPRIGHT STUB	6.2%		
1482	1	PIPE 8.625 X .250	UPRIGHT STUB	6.2%		
1483	1	2"	UPRIGHT STUB	6.2%		
1484	1	PIPE 8.625 X .250	UPRIGHT STUB	6.2%		
1485	1	2"	UPRIGHT STUB	6.2%		
1486	1	PIPE 8.625 X .250	UPRIGHT STUB	6.2%		
1487	1	2"	UPRIGHT STUB	6.2%		
1488	1	PIPE 8.625 X .250	UPRIGHT STUB	6.2%		
1489	1	2"	UPRIGHT STUB	6.2%		
1490	1	PIPE 8.625 X .250	UPRIGHT STUB	6.2%		
1491	1	2"	UPRIGHT STUB	6.2%		
1492	1	PIPE 8.625 X .250	UPRIGHT STUB	6.2%		
1493	1	2"	UPRIGHT STUB	6.2%		
1494	1	PIPE 8.625 X .250	UPRIGHT STUB	6.2%		
1495	1	2"	UPRIGHT STUB	6.2%		
1496	1	PIPE 8.625 X .250	UPRIGHT STUB	6.2%		
1497	1	2"	UPRIGHT STUB	6.2%		
1498	1	PIPE 8.625 X .250	UPRIGHT STUB	6.2%		
1499	1	2"	UPRIGHT STUB	6.2%		
1500	1	PIPE 8.625 X .250	UPRIGHT STUB	6.2%		

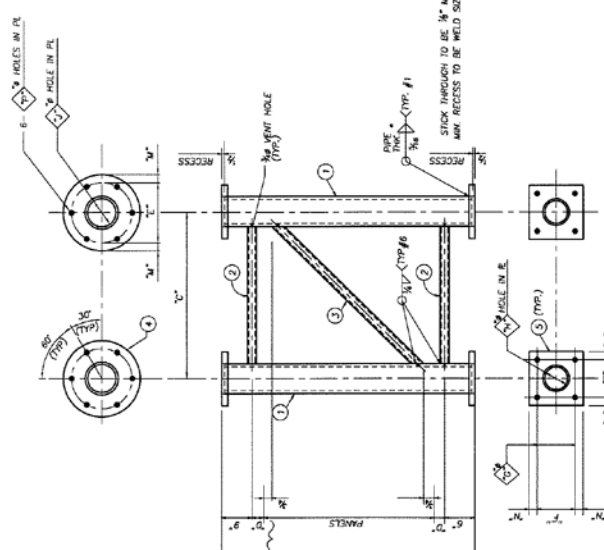
MATL. SPECS.
 UPRIGHTS-STEEL, PIPE-A136, A53, A57 (32 KSI MIN. YIELD)
 PLATES, STEEL, PIPE-A57 OR B (35 KSI MIN. YIELD)
 GALV. ASTM-A136
 ALL DIMENSIONS UNLESS OTHERWISE SPECIFIED
 ALL PIPE SIZES ARE OUTSIDE DIAMETER.
 GALVANIZING VENT HOLES TO BE REAMED SMOOTH

WALPAR INC.
 1000 W. UNIVERSITY BLVD.
 MOBILE, ALABAMA 36688
 PHONE (205)-922-4990
 FAX (205) 925-2723

STATE: ALABAMA
 FED. PROJ.: QM09-089 (3)
 ST. PROJ.:
 COUNTY: SETTERSON/SHELBY
 ROUTE: 1-651-201-4591-5971-20 & US 289

SUBJECT: OVERHEAD SIGN SUPPORT
 DETAIL OF UPRIGHT STUB

DATE: 1/17/00
 DRAWN BY: MJP
 CHECKED BY: []
 APPROVED: []



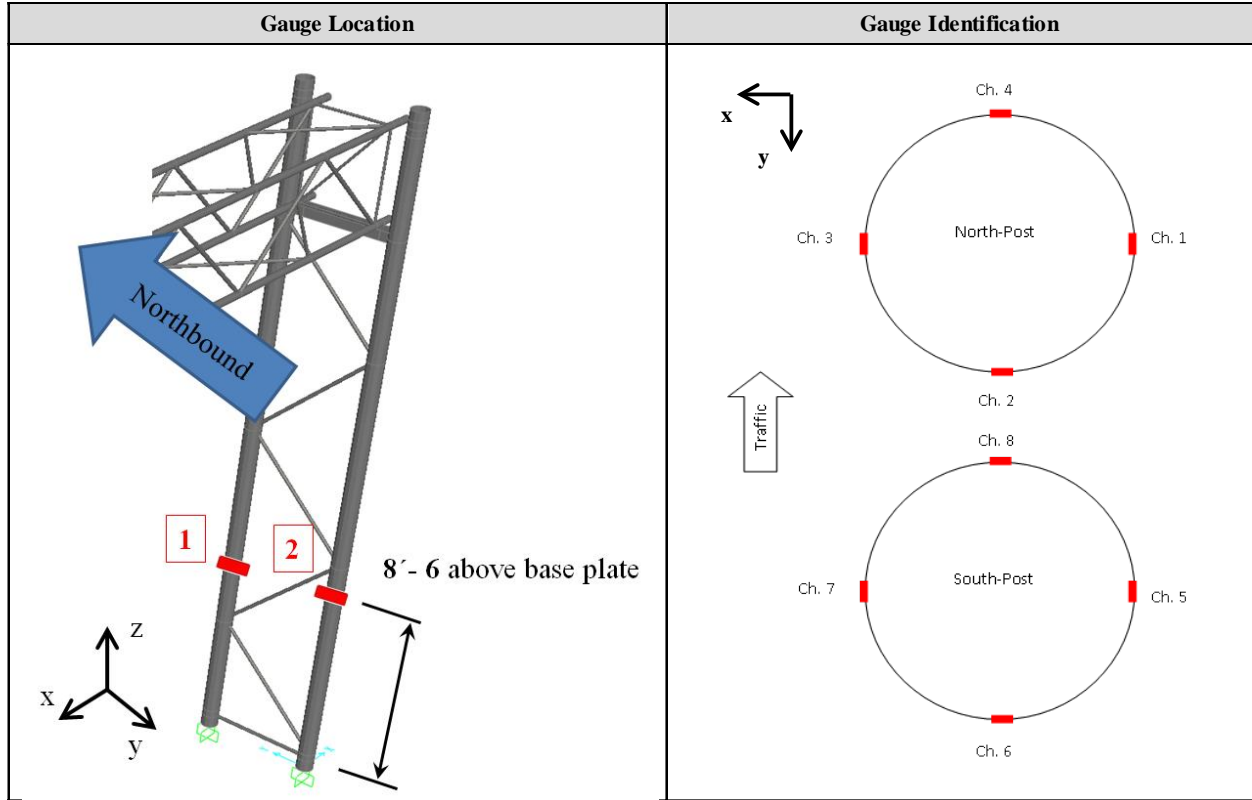
UPRIGHT STUB

MARK	QTY	SIZE	PANELS	1"	2"	3"	4"	5"	6"	7"	8"	9"	10"	11"	12"	13"	14"	15"	16"	17"	18"	19"	20"	
1451	1	8'-3 1/2"	104'-5 1/2" x 4'-5 1/2"																					
1452	1	4'-9"	104'-5 1/2" x 4'-5 1/2"																					
1453	1	7'-1 1/2"	104'-5 1/2" x 4'-5 1/2"																					

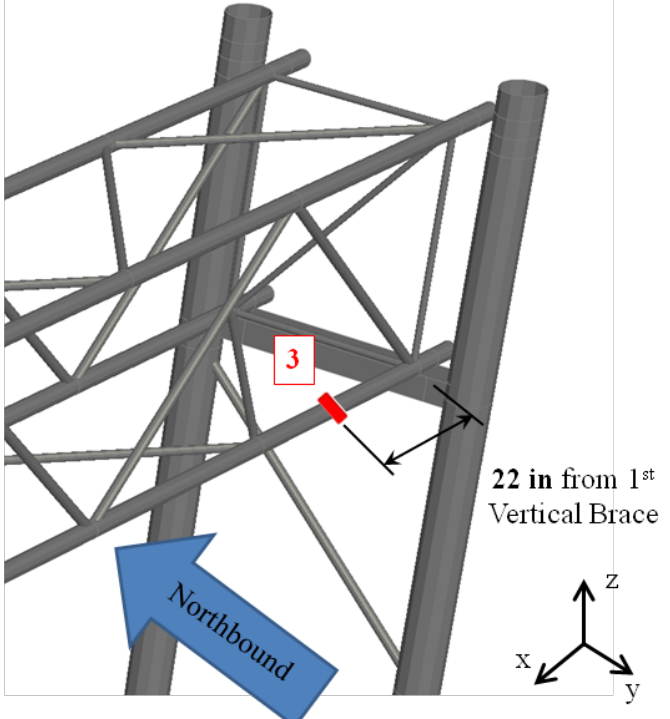
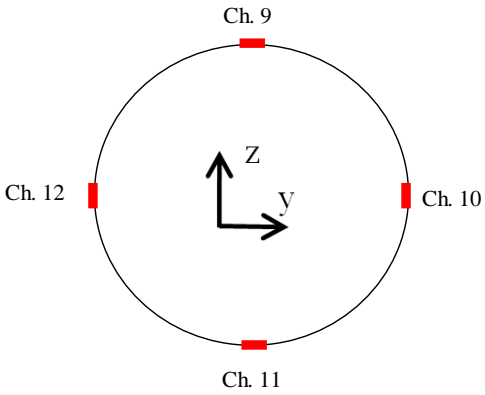
Appendix B

Instrumentation and Layout of the Bridge-Type VMS Support Structure

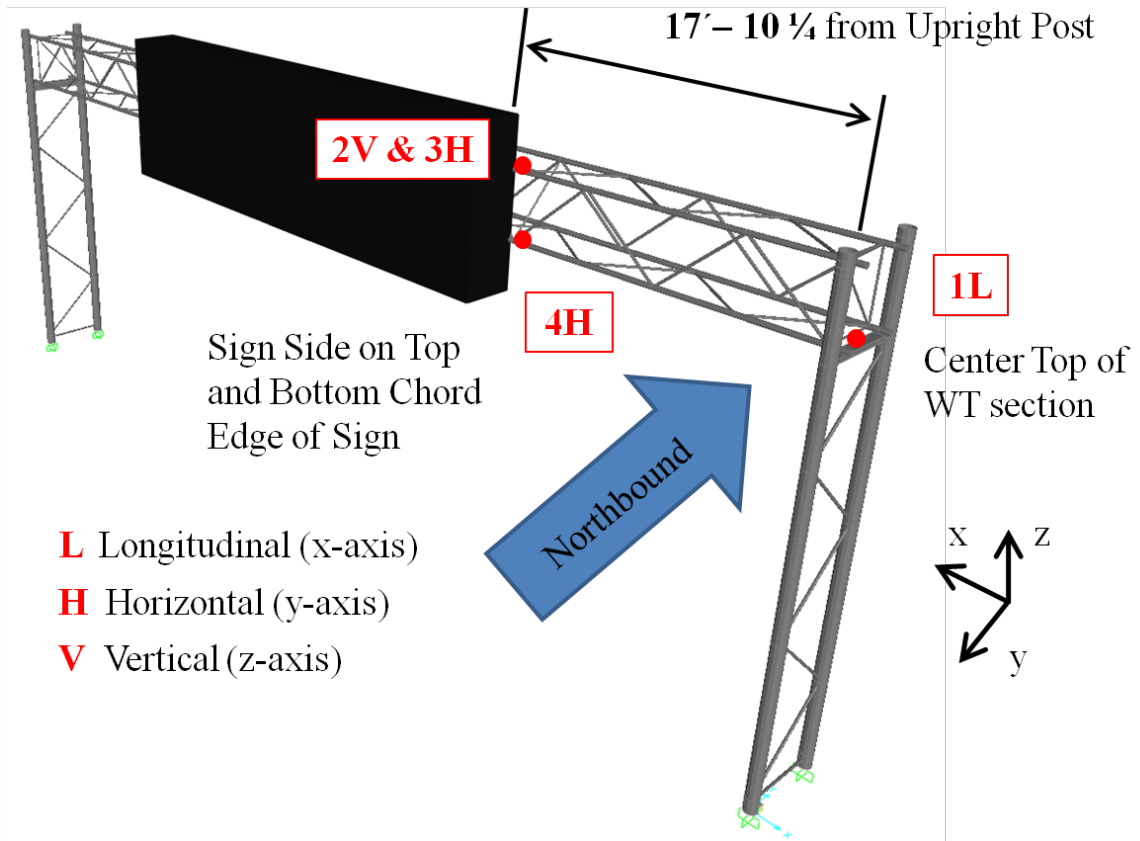
Post Strain Gauge Identification



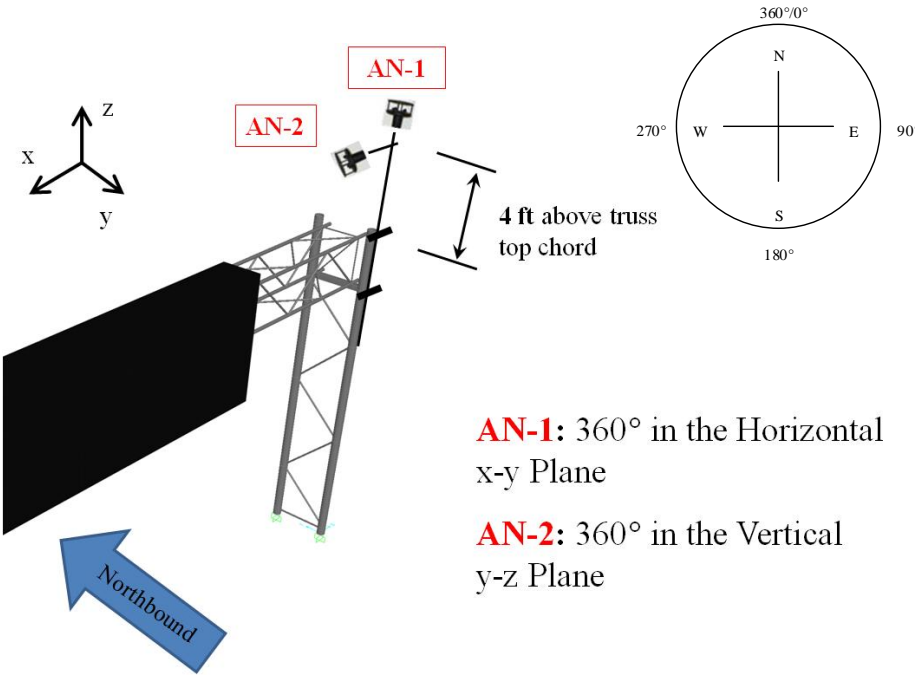
Chord Strain Gauge Identification

Gauge Location	Gauge Identification
 <p>A 3D perspective view of a truss chord. A red square with the number '3' is placed on a chord. A blue arrow labeled 'Northbound' points to the left. A coordinate system with x, y, and z axes is shown at the bottom right. A dimension line indicates the gauge is '22 in from 1st Vertical Brace'.</p>	 <p>A circular cross-section of a chord with four strain gauges labeled Ch. 9, Ch. 10, Ch. 11, and Ch. 12. A coordinate system with x, y, and z axes is shown in the center.</p>

Accelerometer Identification



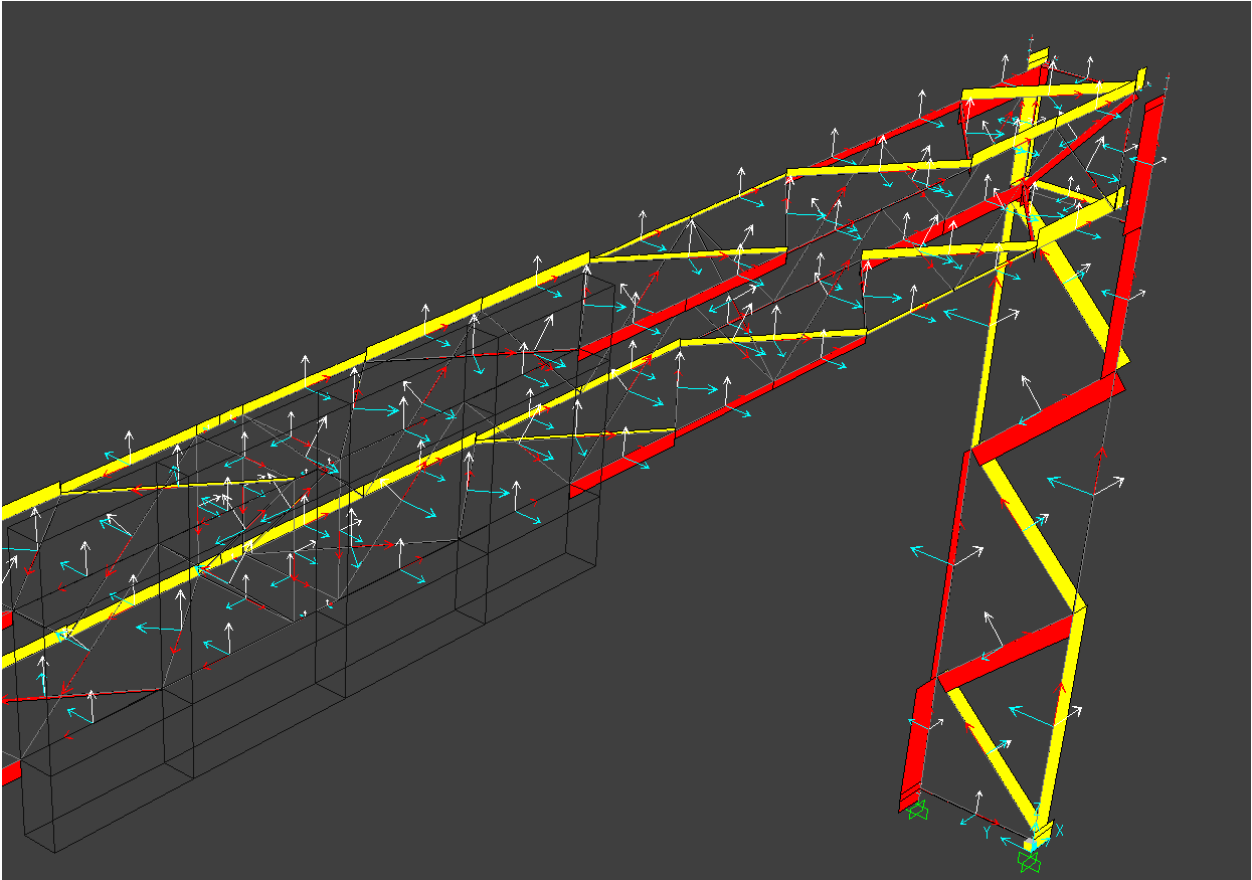
Anemometer Identification

Location		Identification		
 <p>AN-1: 360° in the Horizontal x-y Plane</p> <p>AN-2: 360° in the Vertical y-z Plane</p>		AN	Channel	
		AN-1	mph	17
			Degree	18
		AN-2	Mph	19
Degree	20			
<p><u>Comments</u></p> <p>South bearing (180°) for both anemometers are pointing out from the front face of the sign, against the direction of traffic.</p>				

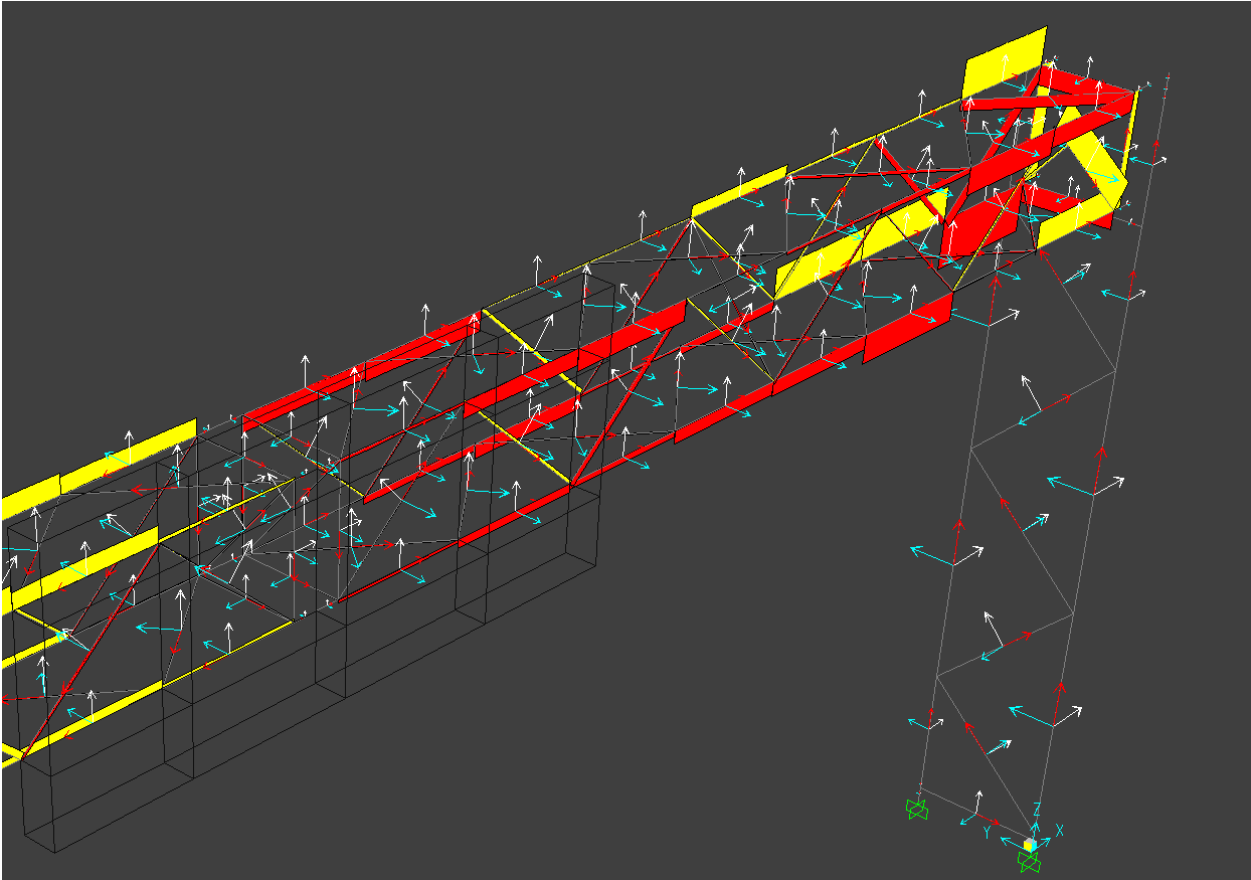
Appendix C

Finite Element Analysis Results for Optimal Placement of the Upright Strain Gauges on the Bridge-Type VMS Support Structure

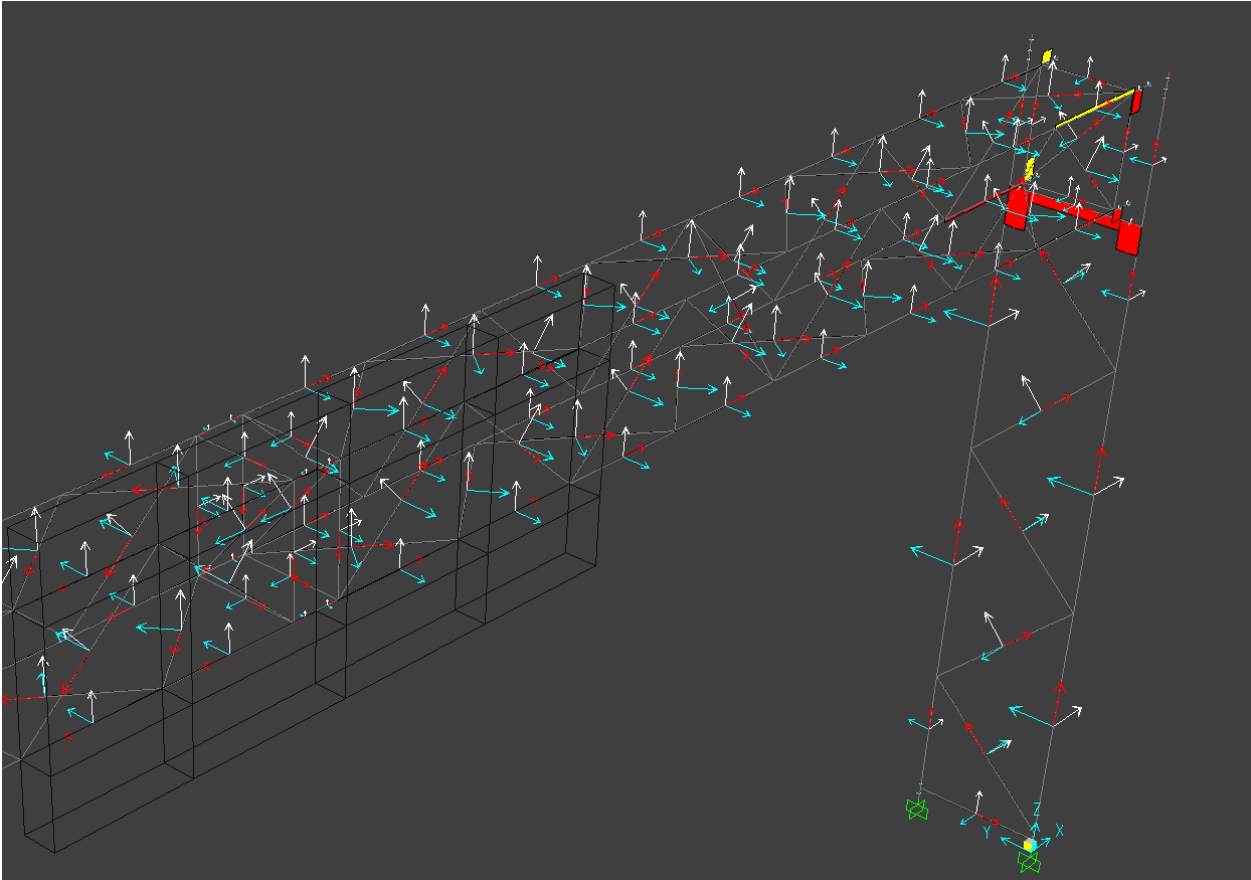
Horizontal Load: Axial



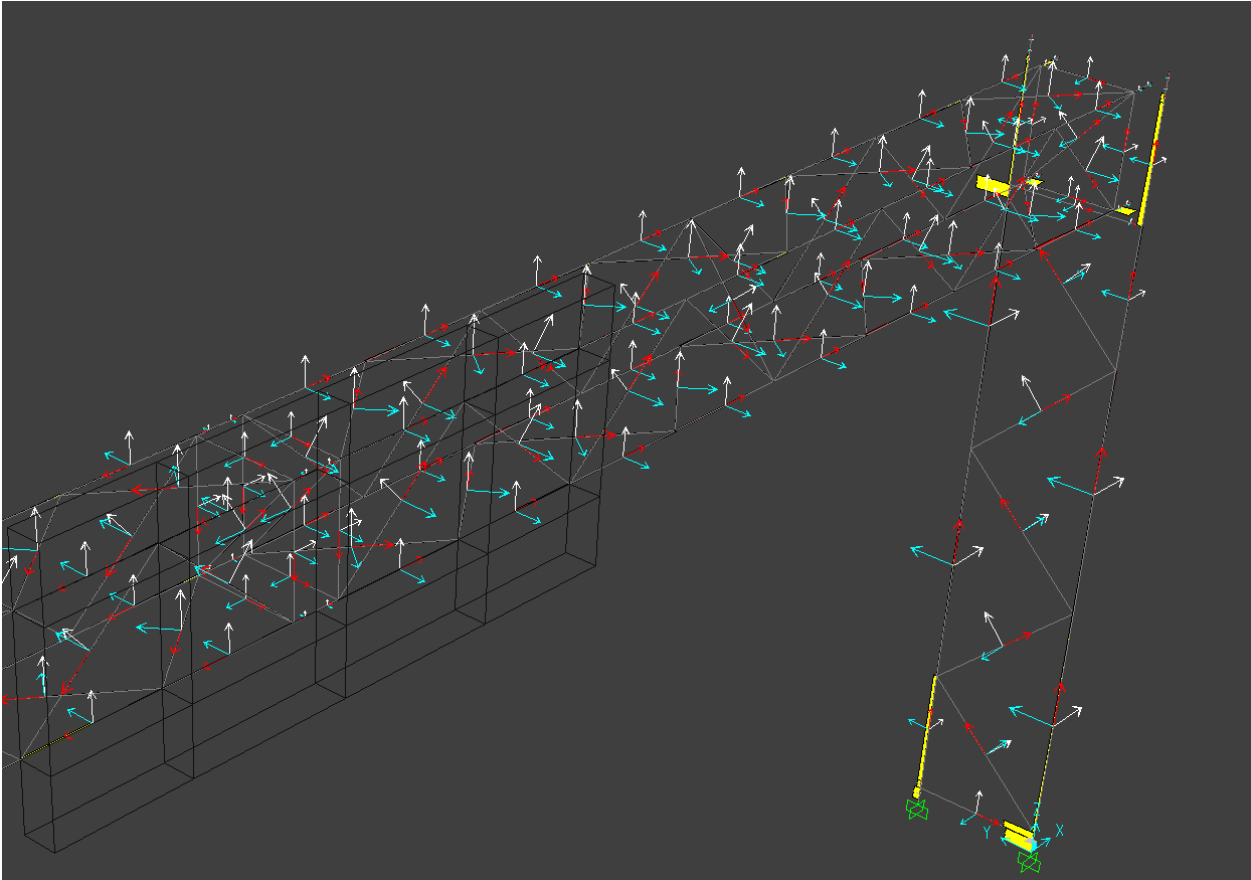
Horizontal Load: Torsion



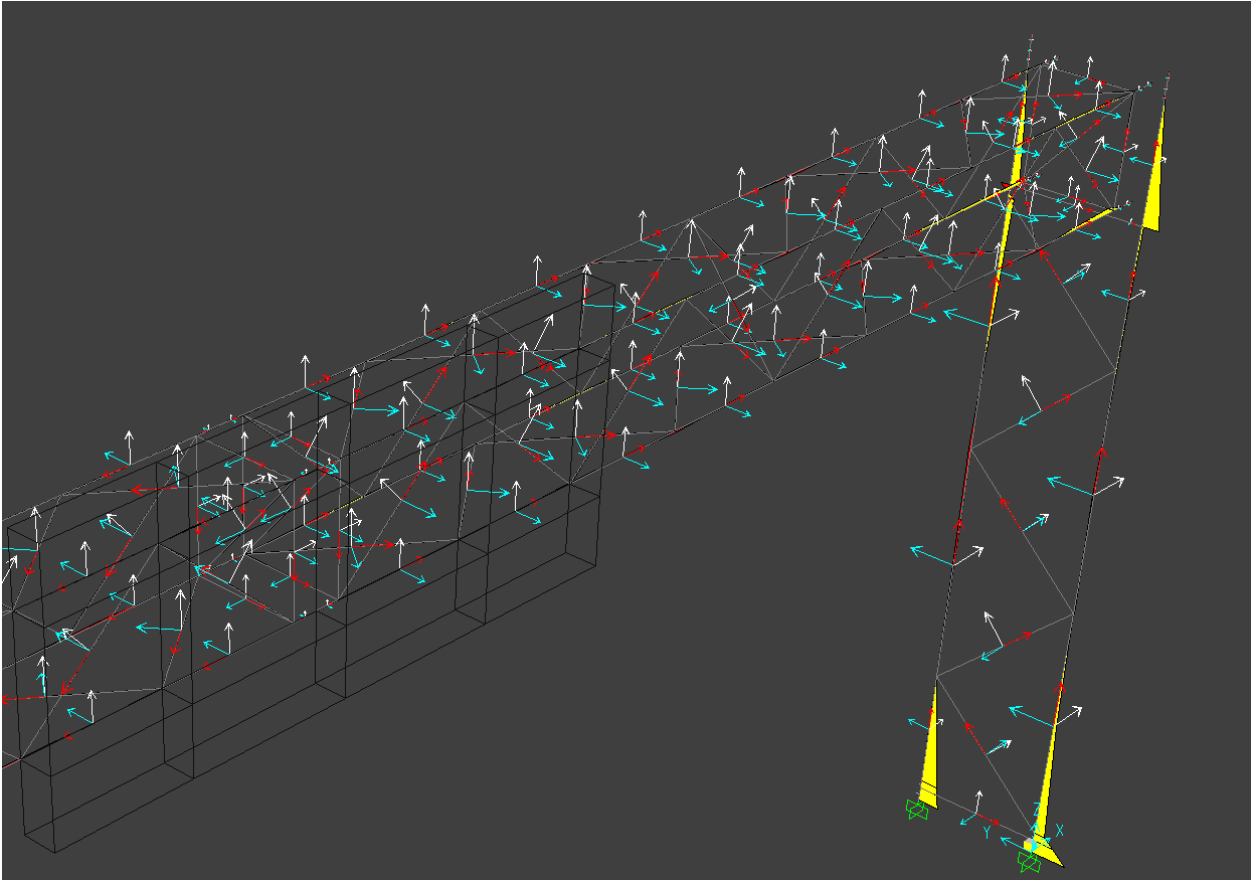
Horizontal Load: Shear 2-2



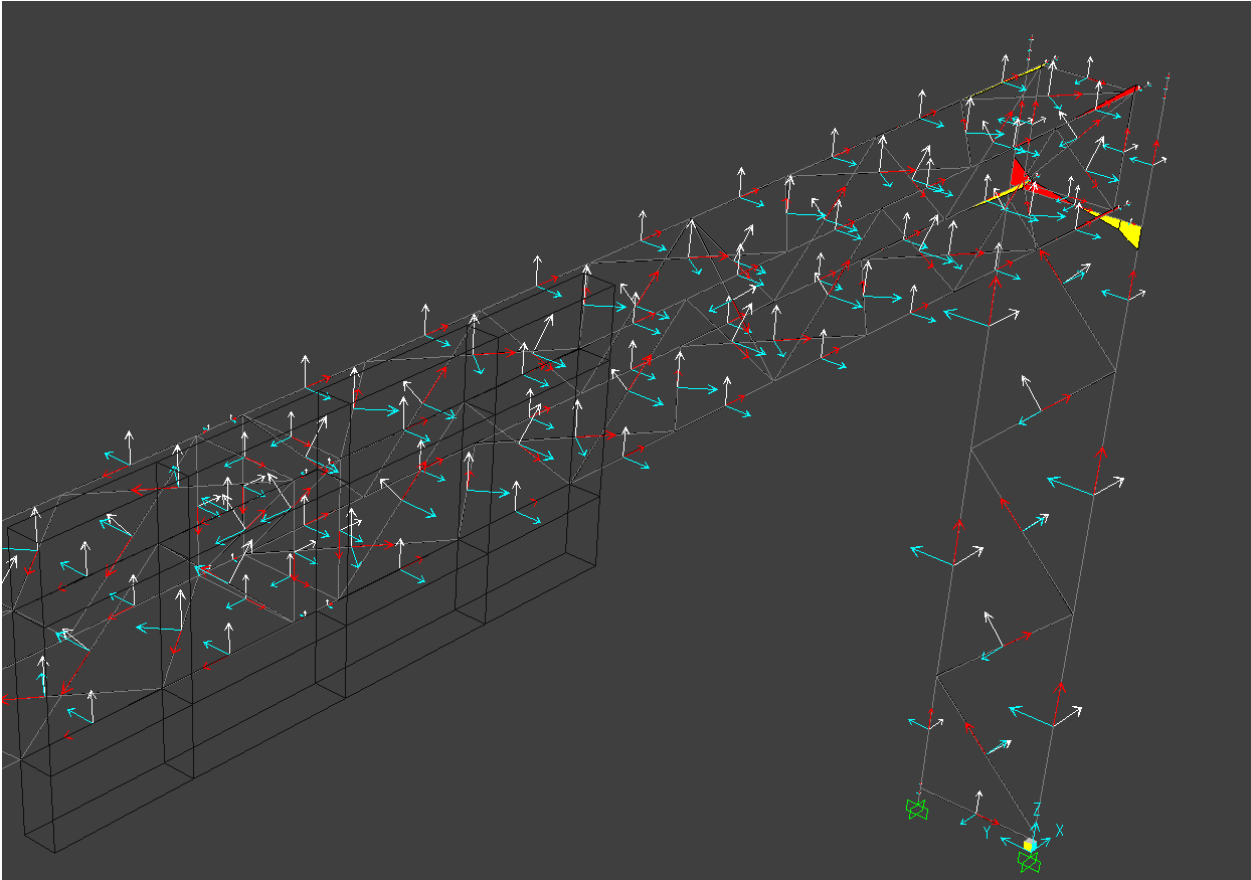
Horizontal Load: Shear 3-3



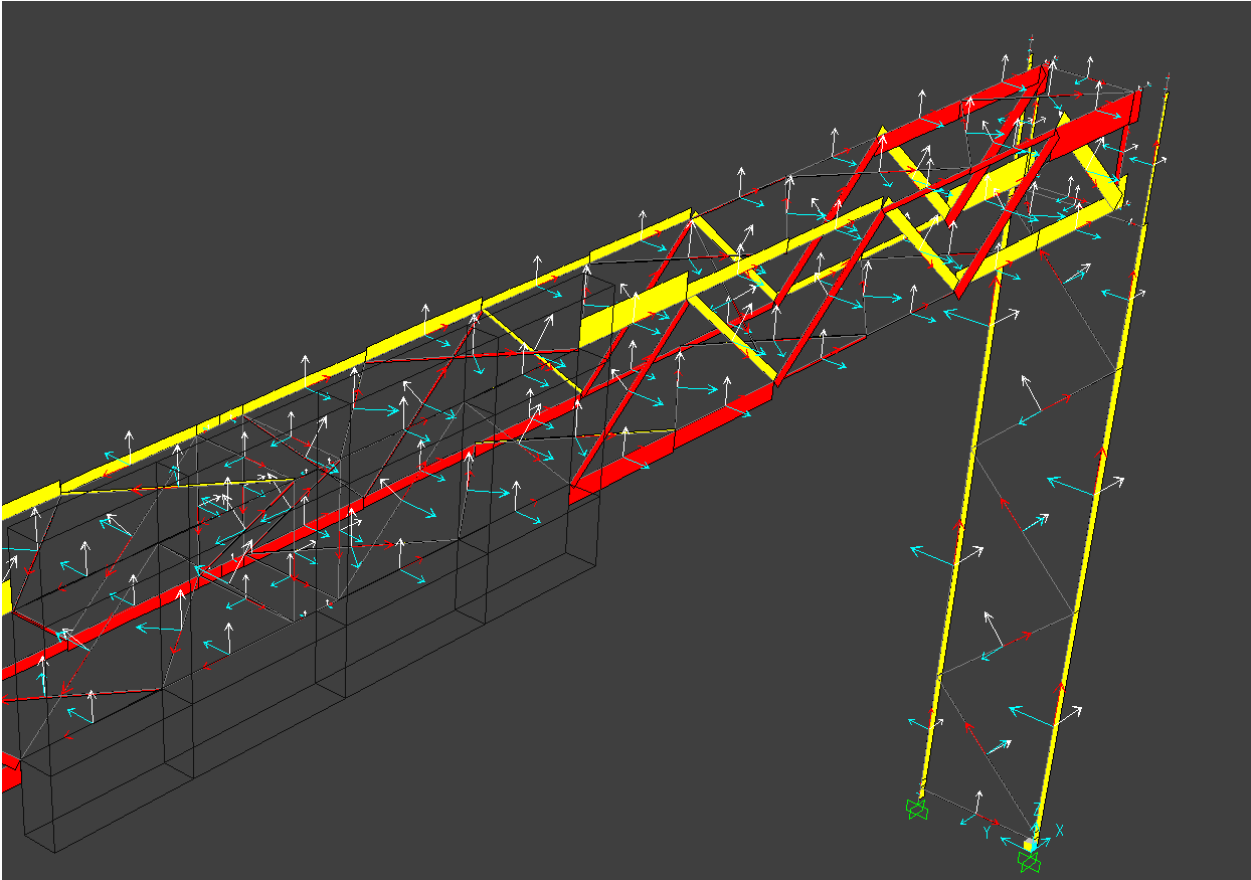
Horizontal Load: Moment 2-2



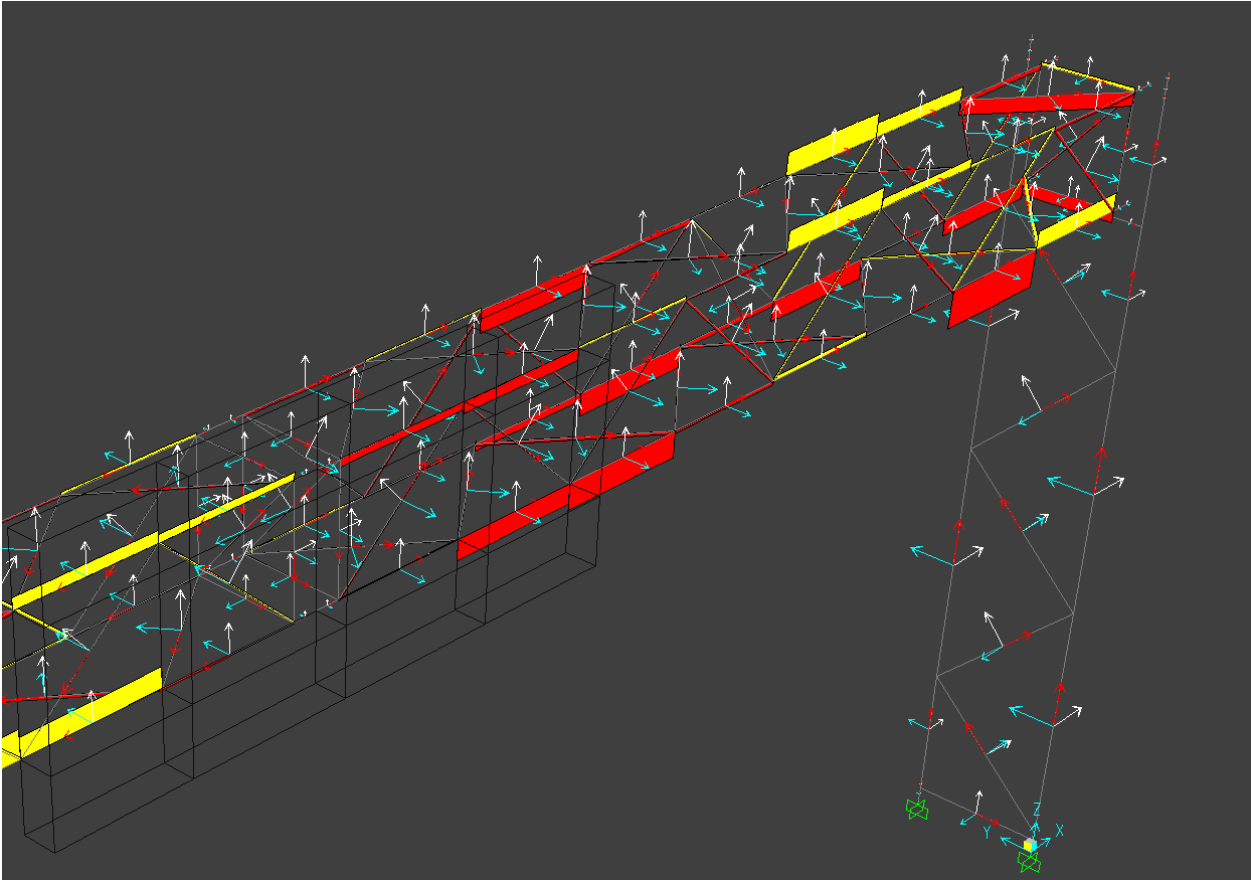
Horizontal Load: Moment 3-3



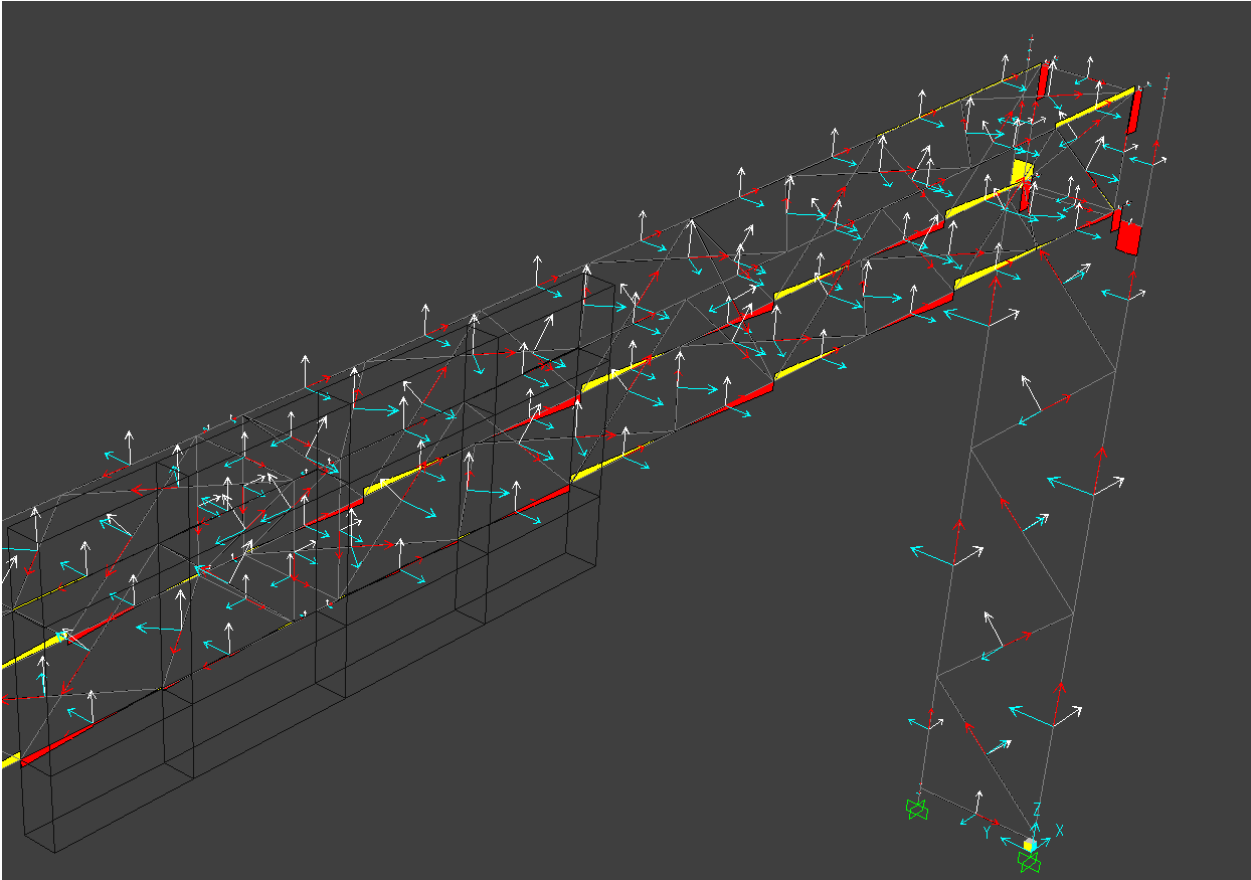
Vertical Load: Axial



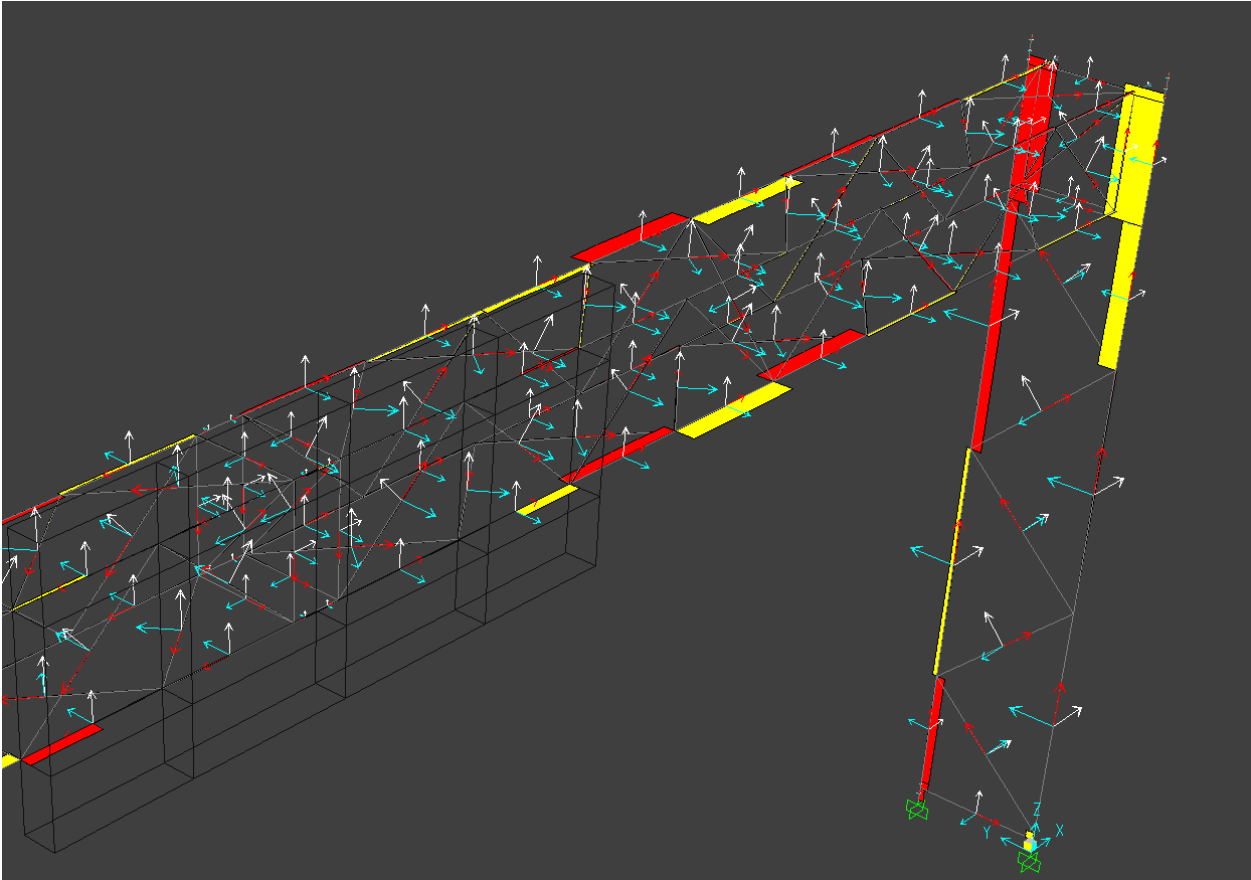
Vertical Load: Torsion



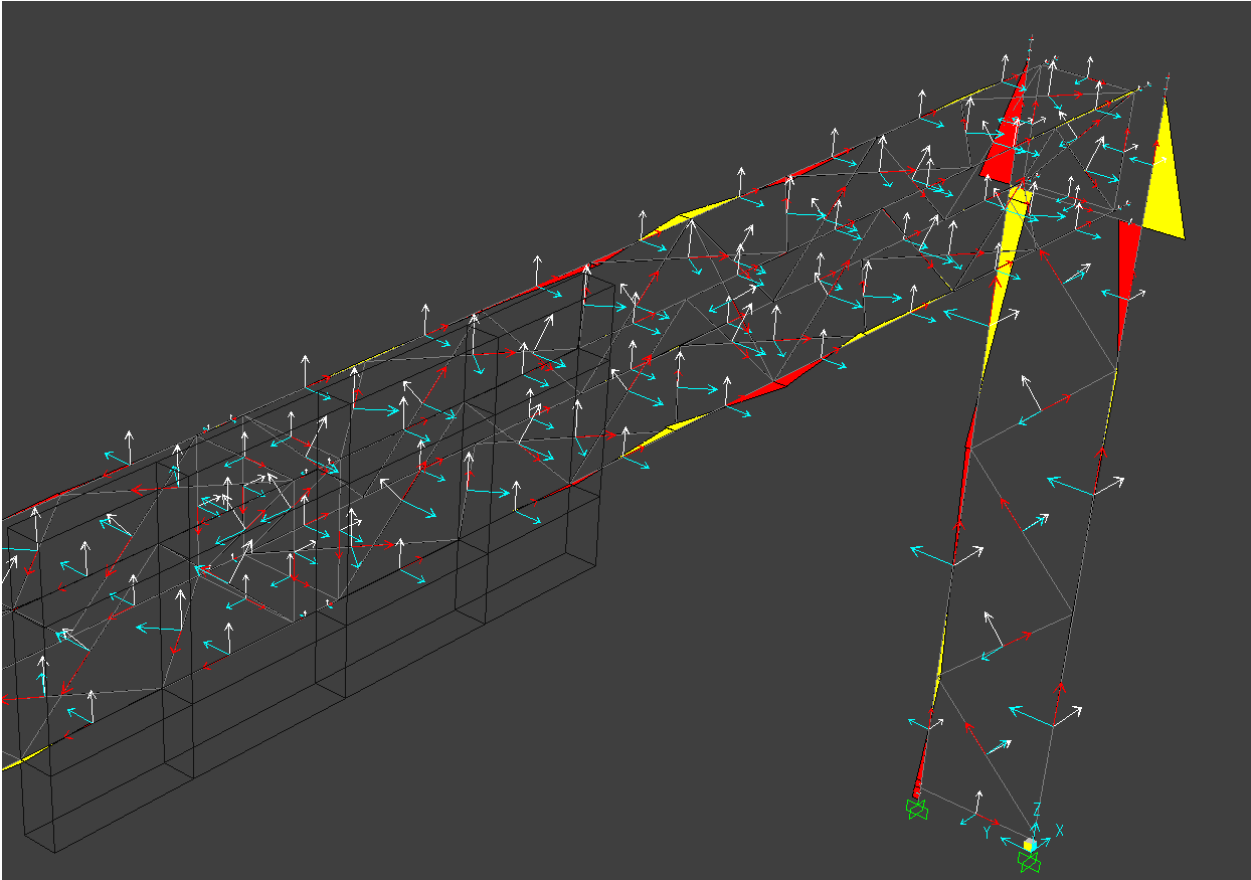
Vertical Load: Shear 2-2



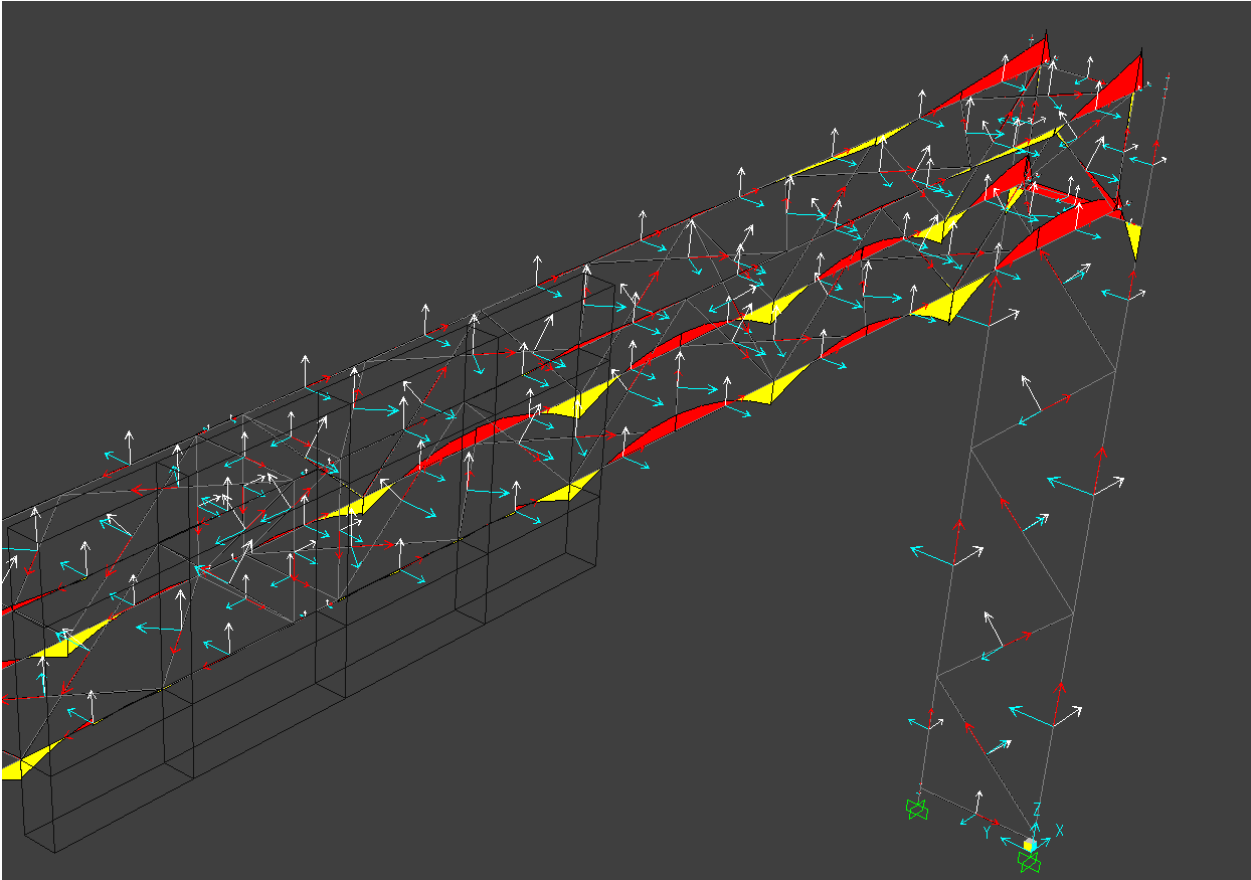
Vertical Load: Shear 3-3



Vertical Load: Moment 2-2



Vertical Load: Moment 3-3



Appendix D

Radar Speed Gun used to Measure Truck Speed for Truck-Induced Wind Gust Testing on the Bridge-Type VMS Support Structure

Bushnell Speedster II Radar Speed Gun - Handheld Cordless 101900



URL: <http://www.radarguns.com/bushnell-radar-guns-101900.html>

Code: BU-RG-101900

SKU: 101900

UPC:

Copyright © 2004 – 2009 RadarGuns.com

Home > Bushnell > Bushnell Speedster II Radar Speed Gun - Handheld Cordless 101900

Bushnell Speedster II Radar Speed Gun - Handheld Cordless 101900

Bushnell Speedster Series II Radar Gun - Bushnell Speedster Series 2 Radar Guns 101900 is the latest model of **Bushnell Radar gun** - exclusively from the biggest and best **radar guns** store you'll find anywhere! **Bushnell Speedster II speed gun** takes the simplicity of the best-selling **Bushnell Velocity Radar Gun**, and adds a new advanced digital processor that allows you to switch between MPH and KPH any time you need! Finally, a more affordable **sport radar gun** in a configuration to fit your needs and budget! The **Bushnell Speedster II Radar Gun 10-1900** is a handy, multi-functional **speed gun** for all kinds of sports enthusiasts. **Bushnell Speedster 2 Speed Gun** tracks miles per hour of everything from pitching speeds, tennis serves and downhill skiers to cars on the racetrack.

This **Bushnell Radar Gun** can measure the speed of a baseball at 10-110 mph from over 75 feet away, and can measure the speed of a race car from 10-200 mph at over 1300 feet away. This radar gun features a highly legible 4-row LCD graphics display, trigger and 2-way button pad. The **Bushnell Speedster II Speed Gun** uses proven digital technology and DSP (Digital Signal Processing) to provide instantaneous and **real time** speed measurements of +/- 1.0 mph speed accuracy. **Bushnell Speedster Radar Gun Series II** supports both MPH and KPH speed modes. On the **Bushnell Speedster II**, to change from MPH to KPH or vice versa, make sure the unit is "ON". Next, pull the trigger and leave engaged, and quickly press the button underneath the LCD display (quick presses of the button will toggle between MPH and KPH. When you are satisfied with the desired measurement unit, simply release the buttons.

The following KIT packages are available with the Bushnell Speedster2 Radar Gun:

- **Bushnell Speedster II MEGA Kit 2** includes **Bushnell Speedster II Radar Speed Gun 101900**, **S3 Waterproof Dry Protective Box T-6500-3 Black** and **Free Batteries**.
- **Bushnell Speedster II VALUE Kit 2** comes with **Bushnell Speedster II Radar Speed Gun 101900** and **Free Batteries**.

Do you want to play a cop, busting speeding cars on your street with your **radar-gun**, but do not want to spend the money on a **police radar gun** or a laser LIDAR? Or you like going fast in your car and want your friends to check your car's exit speed from a difficult slalom on a race course? Or maybe you just want to track speeds of baseballs, softballs, or tennis balls, and see various statistics and averages right there in real time. You do not have to go to a baseball store to find a perfect **baseball gift!** We have one of the **best radar guns** at a price you can afford! **Bushnell Speedster II radar gun** makes a great gift for anyone who loves speed in one form or another. Accept no cheap **radargun** imitations - this model comes with the full two year warranty from **Bushnell**. We are an Authorized US Distributor of all **Bushnell Performance Optics** products. For a wide selection of **Bushnell Radarguns** please visit our **Bushnell Radar Guns Page**.

Want to learn how **radar guns** work? Make sure to read our **Bushnell Speedster FAQ**.

Specifications for Bushnell Speedster II Speed Gun:

Baseball, softball, tennis range: 110 mph / 100 Feet Away
 Cars, boats, karts, auto racing: 10-200 mph / 1300+ Feet Away
 Size (in. / mm): 4.3 x 8.4 x 6 / 109 x 213 x 152
 Weight: 19 / 539

Features of Bushnell Speedster II Radar Gun 101900:

- Easy-to-use speed gun - accurately measures speed of cars, baseballs, softballs, RC cars, RC boats, etc..
- Compact & Ergonomic Radar gun design - comfortable Bushnell point-and-shoot pistol grip
- Displays Speed on an LCD Graphics Display
- Displays fastest speed once trigger is released
- RF Radar gun with +/- 1 mph /1 kph accuracy
- Two C batteries (please see our options above for optional alkaline and rechargeable C-batteries)







Appendix E

Truck-Induced Wind Gusts Data Collection for the Bridge-Type VMS Support Structure

Legend

I = Inside Lane (closest to northbound upright)

O = Outside Lane (closest to southbound upright)

Identification	Truck Type	Identification	Truck Type
1	<p>Cab Only</p> 	4	<p>Tandem</p> 
2	<p>Typical Deflector</p> 	5	<p>Flat Bed</p> 
3	<p>No Deflector</p> 	6	<p>Tanker</p> 

Truck Event	Time	Type	Lane	Speed
1	10:36:36 AM	2	I	65
2	10:37:30 AM	2	I	75
3	10:38:06 AM	2	I	68
4	10:38:45 AM	2	I	62
5	10:39:45 AM	2	I	78
6	10:40:06 AM	2	I	70
7	10:41:12 AM	2	I	71
8	10:42:09 AM	5	I	64
9	10:42:39 AM	6	O	57
10	10:42:57 AM	1	I	65
11	10:43:15 AM	5	O	74
12	10:44:09 AM	2	I	65
13	10:45:18 AM	2	I	68
14	10:45:30 AM	6	O	64
15	10:46:06 AM	2	I	69
16	10:46:42 AM	2	I	66
17	10:47:27 AM	5	I	68
18	10:49:18 AM	3	I	70
19	10:50:24 AM	2	I	66
20	10:51:33 AM	5	I	70
21	10:52:27 AM	2	I	67
22	10:53:57 AM	1	I	61
23	10:55:48 AM	2	O	67
24	10:56:12 AM	5	O	62
25	10:57:03 AM	2	I	65
26	10:57:45 AM	5	I	69
27	10:58:33 AM	5	I	65
28	11:00:45 AM	6	O	63
29	11:02:33 AM	2/6	I/O	65
30	11:03:21 AM	6	I	62
31	11:07:27 AM	2	I	53
32	11:08:21 AM	6	O	68
33	11:09:15 AM	2	I	65
34	11:11:39 AM	2	I	64
35	11:12:03 AM	3	I	64
36	11:12:45 AM	2	O	66
37	11:14:18 AM	2	I	66
38	11:15:33 AM	5	I	58
39	11:16:39 AM	2	I	60
40	11:41:57 AM	2	I	71
41	11:43:03 AM	2	O	63
42	11:45:36 AM	2	I	60
43	11:46:24 AM	1	I	62
44	11:47:39 AM	2	O	60
45	11:48:33 AM	5	O	75
46	11:51:12 AM	2	I	68
47	11:51:27 AM	2	I	59
48	11:52:54 AM	2	I	67
49	11:54:18 AM	3	I	66
50	11:54:54 AM	4	I	65
51	11:57:45 AM	6	I	65
52	11:59:15 AM	3	I	60
53	12:00:03 PM	2	I	51
54	12:00:18 PM	5	I	66
55	12:01:18 PM	2	I	62

Truck Event	Time	Type	Lane	Speed
56	12:02:33 PM	4	I	68
57	12:04:18 PM	2	I	67
58	12:06:21 PM	2	I	62
59	12:06:48 PM	3	I	70
60	12:09:27 PM	2	I	64
61	12:10:30 PM	2	I	62
62	12:12:18 PM	2	I	65
63	12:13:03 PM	2	I	56
64	12:13:18 PM	2	I	63
65	12:15:39 PM	5	O	61
66	12:16:24 PM	2	I	66
67	12:16:33 PM	2	I	64
68	12:16:57 PM	2	I	66
69	12:17:24 PM	2	I	64
70	12:18:42 PM	3	O	58
71	12:19:45 PM	5	I	67
72	12:20:24 PM	2	I	67
73	12:21:24 PM	4	I	61
74	12:22:06 PM	2	I	67
75	12:22:45 PM	2	I	65
76	12:23:03 PM	1	O	70
77	12:23:25 PM	2	O	66
78	12:24:06 PM	6	I	66
79	12:24:06 PM	2	I	69
80	1:56:36 AM	5	O	63
81	1:57:51 AM	2	I	62
82	1:59:06 AM	2	I	64
83	1:59:09 AM	2	O	67
84	2:00:18 AM	2	I	64
85	2:01:12 AM	2	I	69
86	2:01:36 AM	2	I	64
87	2:02:27 AM	3	O	66
88	2:04:03 AM	2	I	72
89	2:05:09 AM	3	I	61
90	2:05:48 AM	5	I	66
91	2:06:30 AM	1	O	61
92	2:07:06 AM	2	I	63
93	2:07:21 AM	5	I	78
94	2:07:57 AM	2	I	61
95	2:09:09 AM	2	I	67
96	2:09:24 AM	2	I	61
97	2:09:27 AM	2	O	69
98	2:10:54 AM	2	O	70
99	2:12:48 AM	3	I	70
100	2:14:30 AM	2	O	74
101	2:14:42 AM	2	I	65
102	2:14:54 AM	2	I	70
103	2:15:18 AM	3	I	63
104	2:16:12 AM	2	I	62
105	2:17:42 AM	5	I	68
106	2:18:09 AM	3	I	70
107	2:20:33 AM	2	I	62
108	2:20:51 AM	2	O	67
109	2:22:06 AM	2	I	70
110	2:22:36 AM	2	O	68
111	2:22:54 AM	2	I	62

Truck Event	Time	Type	Lane	Speed
112	2:23:18 AM	6	I	67
113	2:24:03 AM	5	O	60
114	2:25:06 AM	2	I	64
115	2:26:24 AM	2	I	62
116	2:30:42 AM	2	I	63
117	2:31:03 AM	2	I	54
118	2:31:39 AM	2	I	60
119	2:31:57 AM	2	O	64
120	2:32:18 AM	2	O/I	59
121	2:33:12 AM	3	I	67
122	2:34:09 AM	2	I	66
123	2:35:12 AM	2	I	60
124	2:35:27 AM	1	I	63
125	2:40:19 AM	3	I	59
126	2:40:28 AM	2	I	55
127	2:40:37 AM	2	O	77
128	2:43:07 AM	2	I	60
129	2:43:31 AM	2	I	73
130	2:44:19 AM	3	O	70
131	2:45:16 AM	2	I	64
132	2:46:52 AM	2	I	70
133	2:49:22 AM	2	I	61
134	2:50:10 AM	2	I	60
135	2:51:13 AM	2	I	58
136	2:51:58 AM	2	I	57
137	2:52:16 AM	2	I	68
138	2:53:40 AM	2	O	70
139	2:54:25 AM	2	I	64
140	2:56:49 AM	2	O	72
141	2:57:16 AM	5	I	64
142	2:59:13 AM	2	O	68
143	2:59:31 AM	6	O	70
144	3:00:22 AM	2	O	63
145	3:01:10 AM	2	O	65
146	3:01:46 AM	6	O	68
147	3:02:34 AM	2	I	69
148	3:03:07 AM	2	I	66
149	3:03:52 AM	2	I	64
150	3:05:46 AM	2	O	67
151	3:06:04 AM	2	I	66
152	3:07:01 AM	2	O	72
153	3:08:16 AM	CAR LOAD	I	50
154	3:09:49 AM	2	O	71
155	3:10:31 AM	3	I	63
156	3:10:55 AM	5	I	60
157	3:11:13 AM	2	I	55